

A TOPOGRAPHICAL ANALYSIS OF HIPPOCAMPAL  
FIELD CONNECTIVITY ~~IN THE RAT~~

Dennis Chan

A thesis submitted for the degree of Doctor of Philosophy

Department of Anatomy and Developmental Biology,  
University College London

March 1992

ProQuest Number: 10797636

All rights reserved

INFORMATION TO ALL USERS

The quality of this reproduction is dependent upon the quality of the copy submitted.

In the unlikely event that the author did not send a complete manuscript and there are missing pages, these will be noted. Also, if material had to be removed, a note will indicate the deletion.



ProQuest 10797636

Published by ProQuest LLC (2018). Copyright of the Dissertation is held by the Author.

All rights reserved.

This work is protected against unauthorized copying under Title 17, United States Code  
Microform Edition © ProQuest LLC.

ProQuest LLC.  
789 East Eisenhower Parkway  
P.O. Box 1346  
Ann Arbor, MI 48106 – 1346

**This dissertation is dedicated to my parents, Rudy and Anna Chan**

## ACKNOWLEDGEMENTS

The author would like to thank John O'Keefe for all the time, patience and resources devoted to me during the course of my Ph.D., as well as for his encouragement and criticisms. Thanks also to my colleague David Al Dulaimi, and to Alan and Penny Ainsworth for their respective technical and histological assistance. Special thanks to Andrew Speakman, Michael Recce and Ugur Bilge for their help and advice in general and computing expertise in particular. Also, I would like to acknowledge everyone on the 4th floor, in whose company it has been a pleasure to spend three highly enjoyable years.

This work was sponsored by a scholarship from the Medical Research Council.

# CONTENTS

Acknowledgements	3
Contents	4
Abstract	6
Introduction	9

## **Section 1 A review of the anatomy of the hippocampal formation**

1. The hippocampus proper	14
1.1. Structure	
1.2. The dentate gyrus	
1.3. The hilus	
1.4. Field CA3	
1.5. Field CA1	
1.6. Interneurons in Ammon's horn	
2. The subicular complex	50
2.1. The subiculum	
2.2. The pre- and parasubiculum	
3. The entorhinal cortex	57
3.1. Structure and neuronal types	
3.2. Intrinsic connections of the entorhinal cortex	
3.3. Extrinsic afferents to the entorhinal cortex	
3.4. The projection from the entorhinal cortex to the hippocampus	
4. Subcortical afferents to the hippocampal formation	74
5. Extrinsic efferents of the hippocampal formation	80
5.1. Neocortical projections	
5.2. The precommissural fornix	

## Section 2

Materials and Methods	88
Results	94
Control experiments	
I    A double-labelling study of the bilateral organization of the CA3-CA1 projection	105
Ii   A study of the topographical organization of the CA3-CA1 projection	118
Iii  A study of the topographical organization of the CA3-CA3 association	160
Iiii A preliminary study of the organization of the projection from CA3 to the lateral septal nucleus	170
Iiv  A preliminary anterograde study of the organization of the projection from the dentate gyrus to CA3	177
III  A double-labelling study of the projections from the entorhinal cortex to Ammon's horn	191
Discussion	213
References	246

## ABSTRACT

The intrinsic connectivity of the hippocampus in the rat was studied using the retrograde tracers Fast Blue and rhodamine microspheres. In an initial double-labelling study the bilateral labelling within the CA3 field was observed following injection of the two dyes into homologous regions in the two CA1 fields. The labelling in the contralateral CA3 field was found to be identical both in distribution and in density to that observed in ipsilateral CA3, suggesting that the CA3-CA1 projection is bilaterally symmetrical. The observation that nearly 100% of backfilled cells were double-labelled indicates that homologous regions in the two CA1 fields receive information from the same cells in CA3, which indicates that the two CA1 fields act as one functional unit. Evidence for the existence of a sparse association/commissural system within CA1 was provided by the presence of a small number of labelled cells in the contralateral CA1 field.

The topographic organization of the CA3-CA1 projection was studied following a series of injections of the two dyes into different locations across the extent of the CA1 field. In this experiment a new technique for the injections of tracers into the hippocampus was introduced, in which a microelectrode positioned adjacent to the tip of the injection pipette was used to record neuronal activity during the operation. This allowed the complex spike firing of hippocampal cells to be used as a marker for the dorsoventral location of the injection, thus greatly improving the accuracy of the injections.

An analysis of the labelling in the extended hippocampus reveals that projections to CA1 arise from bands of cells organized diagonally across the CA3 field. The CA3-CA1 projection was topographically organized in the septotemporal plane, with progressively more temporal parts of CA1 receiving inputs from bands located

more temporally in CA3. Further analysis showed that cells positioned along a diagonal axis in CA1 were found to receive fibres from the same band of cells in CA3, and that this "CA1 axis" is similar to the axis of the diagonal bands in CA3. It therefore appears that the CA3-CA1 projection is organized in a diagonal fashion across the septotemporal length of the hippocampus both in terms of projecting and recipient cells.

A number of injections was also placed into the CA3 field in order to study the CA3 association projection. In these cases the pattern of labelling in the CA3 field in the extended hippocampus was organized parallel to the septotemporal axis, and was topographically organized such that any given region in CA3 preferentially received fibres from cells located along the same transverse segment of CA3. These findings support the notion that the CA3 association pathway interconnects cells spread over a large fraction of the septotemporal extent of CA3.

Preliminary data concerning the organization of the projection from the dentate gyrus to CA3 were collected following an injection of biocytin into the dentate gyrus. Additional data was taken from 3 animals in which rhodamine microspheres were found to be transported anterogradely along the mossy fibres in a previously unreported fashion. In all cases the projection was organized orthogonal to the septotemporal axis for most of its length, with a shift in trajectory in proximal CA3 in the temporal direction.

These results show that these three intrahippocampal pathways are angled with respect to each other, thus forming a lattice framework of connections similar to the "crossing fibre arrays" described by Tamamaki and Nojyo (1991a). Each pathway displays a specific directionality which, in contrast to the original lamellar hypothesis, allows the spread of information across all parts of the hippocampus.

A double-labelling technique was used to assess the nature of the projections

from the entorhinal cortex to the CA3 and CA1 fields. The entorhinal-CA3 pathway is topographically organized such that caudal parts of the entorhinal cortex project preferentially to septal parts of the CA3 field, whereas rostral parts innervate cells in temporal CA3. Labelling was almost exclusively restricted to cells in layer II. The projections from medial and lateral parts of the entorhinal cortex are organized separately, confirming the subdivision of the entorhinal projection into two components. A comparison of these results with those of Ruth *et al.* (1982, 1988) reveals a marked similarity with the organization of the perforant path input to the dentate gyrus, which suggests that the entorhinal projections to the dentate gyrus and to CA3 may in fact represent a single pathway.

In contrast, the projection to CA1 does not appear to show any form of topographical organization. Injections across the CA1 field invariably produced labelling which was restricted to the region around the rhinal fissure at the dorsolateral edge of the entorhinal cortex. This labelling extended along the entire rostrocaudal extent of the entorhinal cortex and mainly involved layer III cells. The specificity of this projection provides some argument for the consideration of this region as a separate functional entity from the remainder of the entorhinal cortex.

## INTRODUCTION

*"At the base of these ventricles, which face inward toward the median line, an elevation of white substances rises up and, as it were, grows there. This is raised up from the inferior surface like an appendage, and is continuous with the psaloid body, or lyra. In its length it extends toward the anterior parts and the front of the brain, and is provided with a flexuous figure of varying thickness. This recalls the image of a Hippocampus, that is, of a little sea-horse."*

Arantius 1587

The end of the nineteenth century and the beginning of the twentieth witnessed the release of a number of studies on the anatomy of the hippocampus based on the Golgi technique, culminating in the publication in 1934 of a paper by Lorente de No, in which he expanded on the work of his predecessors to produce a treatise containing details of hippocampal structure, cell types and pathways, in addition to a proposal for the division of the hippocampus into various anatomically distinct fields.

The implication of a role for the hippocampus in memory function, as suggested by the findings of Scoville and Milner in 1957, prompted further research into the anatomy of this structure, which resulted in the generation of a considerable body of data describing the various extra- and intrahippocampal pathways. In 1971, using electrophysiological techniques to assess connectivity, Andersen and his co-workers put forward a lamellar hypothesis of the functional anatomy of the hippocampus, in which the hippocampus is portrayed as being composed of a series of individually functioning units oriented perpendicular, or "transverse", to the septotemporal axis of the hippocampus. Incoming information from the entorhinal cortex is believed to be segregated into the various units or "lamellae", which subsequently relays the

information to the subicular complex after processing through the intrahippocampal trisynaptic pathway, the individual components of which are uniformly arranged along the transverse axis of the hippocampus.

A number of subsequent anatomical studies, including those of Hjorth-Simonsen (1973), Swanson *et al.* (1978) and Laurberg (1979), revealed a degree of septotemporal divergence within the intrahippocampal projections which was not concurrent with the lamellar hypothesis. In 1989, Amaral and Witter published a critique of the theory in which the findings of these earlier studies, along with data from their own experiments using the anterograde tracer PHA-L, were marshalled as evidence that the intrahippocampal pathways, with the exception of the mossy fibre projection, are not organized in a lamellar fashion.

Two recent papers also addressed this issue: in the first of these, Ishizuka *et al.* (1990) used both extracellular and intracellular anterograde tracing techniques to assess the CA3-CA1 and CA3-CA3 projections. Both projections were topographically organized in the three dimensions of the hippocampus, and exhibited a degree of divergence which conflicted with the concept of lamellar organization within these pathways. In direct contrast, the report of Tamamaki and Nojyo (1991a), in which the trajectories of the various intrahippocampal projections were reconstructed in three dimensions following intracellular injections of HRP, concluded that each projection was indeed organized in a lamellar fashion, although in a manner different to that suggested by Andersen *et al.* (1971) in that the lamellae of the various pathways were aligned at angles to one another, to create an array of crossing fibres within the hippocampus.

Other studies have called into question the validity of the "trisynaptic circuit" as a model of information processing within the hippocampal formation. Two key principles underpin this theory of hippocampal circuitry. The first emphasises the serial

nature of the connections: information is transmitted from the entorhinal cortex to the dentate gyrus, and thence to the CA3 field, which in turn projects to CA1. The integrity of this circuit is maintained by the absence of any additional functional connections: for example, the dentate gyrus is held to be the sole recipient of inputs from the entorhinal cortex, and in turn projects only to CA3. The second principle concerns the unidirectionality of the circuitry: no feedback connections, either excitatory or inhibitory in nature, are believed to exist between the fields of the hippocampus.

While the latter principle has received confirmation from subsequent studies, some evidence exists to suggest that additional "bypass" connections may influence the pattern of processing in the hippocampus. Several studies have demonstrated the presence of direct projections from the entorhinal cortex to CA3 and to CA1, bypassing the mossy fibre and Schaffer collateral systems respectively (Steward 1976; Steward and Scoville 1976; Witter *et al.* 1988).

In this dissertation the retrogradely-transported fluorescent tracers, Fast Blue and rhodamine microspheres, are used to assess the intrahippocampal pathways in three separate experiments. Experiment I addresses the issue of interhemispheric connectivity between the two hippocampi by examining the relative natures of the ipsilateral and contralateral projections from CA3 to CA1 and by comparing the distribution of projections to homologous regions in the two CA1 fields.

In Experiment II the lamellar theory of hippocampal organization is examined, with a particular emphasis on the topographical organization of the CA3-CA1 pathway. In this experiment, the hippocampus is dissected and extended in order to allow visualization of the pattern of projection along the septotemporal axis of the hippocampus. These data are supplemented by additional information taken from injections into the CA3 field itself (providing information on the CA3 association projection) and into the lateral septal nucleus, thus enabling a comparison of the

organizations of three major efferent systems of the CA3 field. In the final section of Experiment II, the CA3-CA1 and CA3-CA3 projections are compared with the results of anterograde tracing studies on the mossy fibre projection from the dentate gyrus to CA3.

Experiment III assesses the validity of the trisynaptic circuit as a suitable model following an exploration of the nature of the projections from the entorhinal cortex to the CA3 and CA1 fields. In addition to examining the topographic organizations of the two projections, the double labelling technique employed in this study provides a means of comparing the distributions in the entorhinal cortex of the cells of origin of the two pathways.

In order to provide a background to the experiments performed in this study, a review of the current understanding of the anatomy of the hippocampal formation is provided in Section 1 of this dissertation. A description of each of the subdivisions of the hippocampal formation, and of the connections between the subdivisions, is included in this review. In addition Section 1 provides an overview of the various afferent and efferent connections between the hippocampal formation and other brain structures.

The experiments themselves are described in detail in Section 2 of this dissertation. Following an account of the *Materials and Methods* employed, the results of each experiment are outlined separately, and precede in turn a general discussion of the findings from this study.

## SECTION 1

# 1. THE HIPPOCAMPUS PROPER

## 1.1. STRUCTURE

Within the brain, the hippocampus lies as a sausage-shaped structure beneath the cortical mantle. Developmentally, the hippocampus ranks alongside the allocortical olfactory cortex, periallocortical entorhinal and cingulate cortex, and the septal nuclei as the phlogenetically oldest structures in the mammalian telencephalon.

The hippocampus proper consists of the three-layered dentate gyrus and the Cornu Ammonis (Ammon's horn), which is described as three- or four-layered (some authors choose to treat the distal portion of the apical dendritic field, the stratum moleculare, as a separate layer).

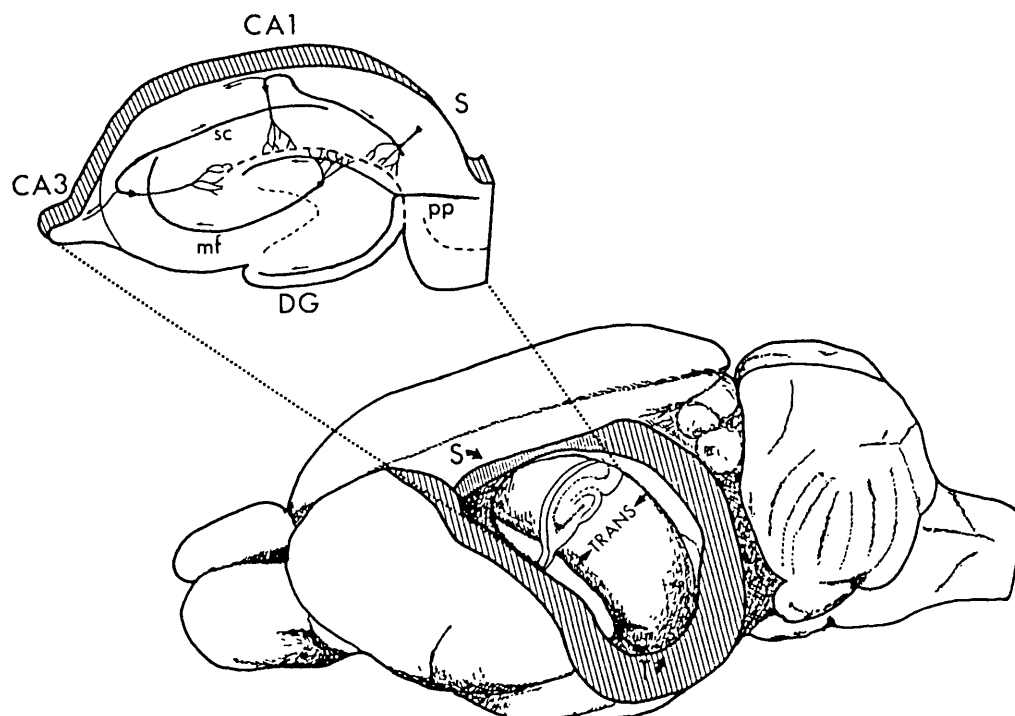
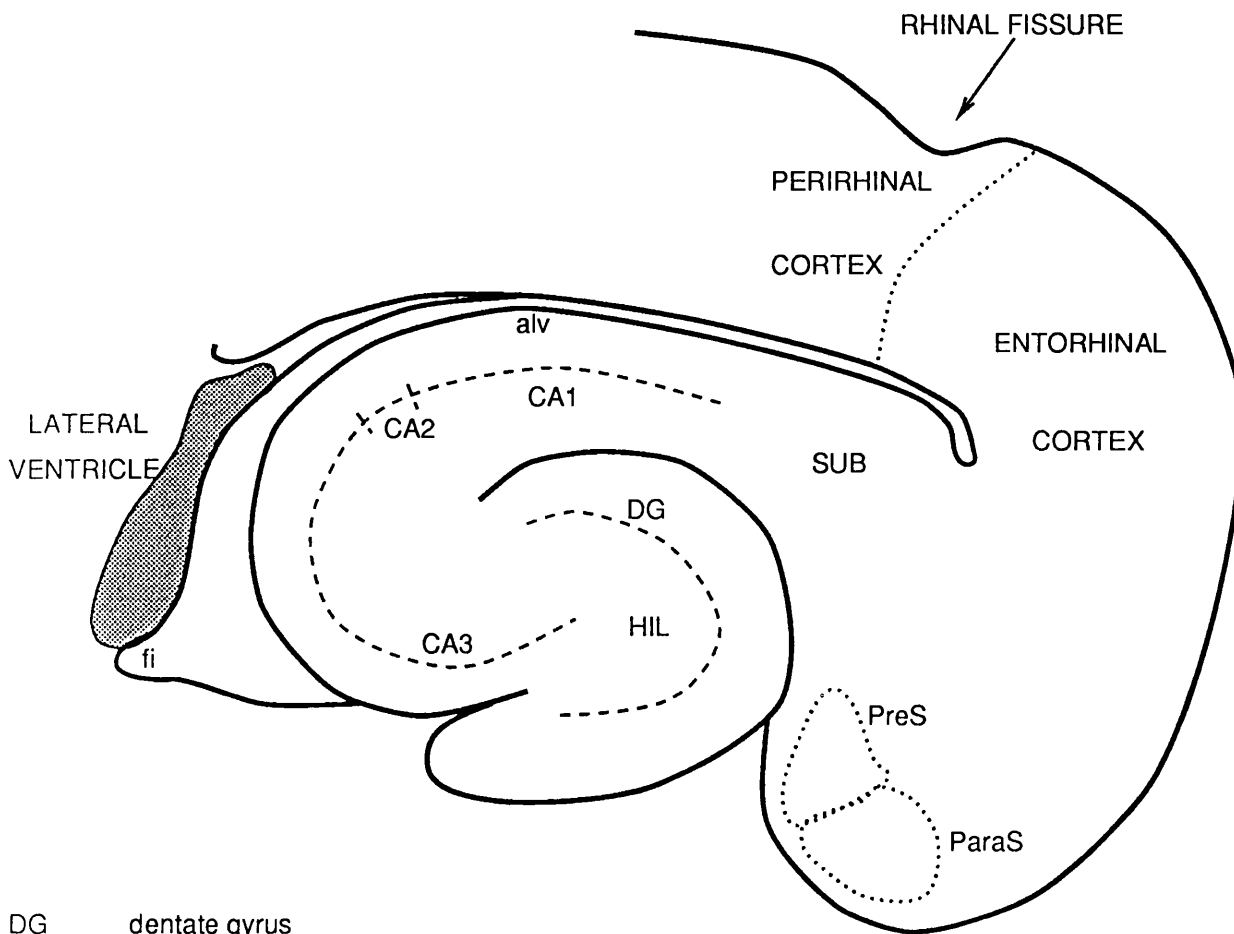


Fig.1 The above diagram (taken from Amaral and Witter 1989) shows the position of the hippocampus in the rat brain. The hippocampus is curved such that its longitudinal, or septotemporal, axis runs from the septal nuclei (S) at its rostradorsal end to the temporal cortex (T) at its caudoventral end. The transverse axis is oriented perpendicular to the septotemporal axis.

DG dentate gyrus; mf mossy fibres; pp perforant path; sc Schaffer collaterals



DG	dentate gyrus
HIL	hilus
SUB	subiculum
PreS	presubiculum
ParaS	parasubiculum
alv	alveus
fi	fimbria

**Fig.1b** A diagram of a horizontal section through the brain which depicts the physical relationship of the various fields of the hippocampal formation.

The dentate gyrus is composed of a molecular layer, constituting the dendritic field of the granule cells, the granule cell layer, and the polymorph layer (the hilar region or hilus in the rat) which contains the axons of the granule cells and a number of neurons of differing morphological aspect. The granule cell layer is often parcellated into two blades separated by a crest region: the blades are variously described as

infrapyramidal/suprapyramidal [*the terminology which will be adopted in this dissertation*], exposed/buried, and medial/lateral.

Lorente de No (1934) divided the Cornu Ammonis into four fields, CA1-4, with field CA1 corresponding approximately to the regio superior of Ramon y Cajal (1911) and field CA3 to the regio inferior. CA2 is a narrow transition zone between CA1 and CA3 which contains both large and small pyramidal cells. Field CA4 comprises the end zone of Ammon's Horn, with the CA3/CA4 boundary "found approximately at the point where the stratum pyramidale enters the hilus of the F.D. and bends itself". The remainder of CA4 consists of the scattered pyramidal cells located in the hilus of the dentate gyrus. Fields CA1 and CA3 were further partitioned into 3 subfields, such that CA1a and CA3a were those parts situated most proximal to the subiculum, while CA1c and CA3c were most proximal to the dentate gyrus. Differences in cell morphology between the subfields were described, with greater variation in the CA3 subfields than in those of CA1.

The peculiar nature of the hilar region, which contains the initial components of the granule cell axons, scattered pyramidal cells of CA4 in addition to a collection of non-pyramidal neurons of divergent morphology (Amaral 1978), has created debate as to the inclusion of this region within the dentate gyrus (Blackstad 1956) or Ammon's horn (Lorente de No 1934). Consideration of the cell types has led to the belief that the hilus is more closely related to the dentate gyrus, and that the region is an area of emergence of the polymorphic zones of the dentate gyrus and Ammon's horn.

## 1.2. THE DENTATE GYRUS

### 1.2.1. The granule cells

In contrast to the pyramidal cells of Ammon's horn in the rat, most of which develop prenatally, 85% of granule cells form after birth (Angevine 1965; Bayer and Altman 1974). Three gradients in development are observed: the infrapyramidal blade forms before the suprapyramidal blade, the dorsal extent of the dentate gyrus develops before the ventral extent, while the pattern of neuroblast migration creates a gradient such that the superficial granule cells are joined by cells situated progressively deeper into the cell layer.

Granule cells exhibit two types of dendritic morphology: cells located superficially give rise to 2-5 primary dendrites from the apex of the cell body, while cells deeper in the layer have a single primary dendrite (Desmond and Levy 1982). In addition, the former type of granule cell is characterised by a greater dendritic length and a larger span of dendritic field.

The dendritic field of the granule cells can be divided into three components on the basis of afferent termination: inputs from the lateral and medial entorhinal areas form asymmetric synapses on the spines located respectively in the outer and middle thirds of the molecular layer (Nafstad 1967), while the inner third is the recipient of fibres from subcortical regions and from cells in the hilus.

Studies using extended hippocampi (Gaarskjaer 1978a,b) have shown a variation in the cell density in the granule cell layer, such that the density is highest at the septal extent of the hippocampus, with a gradual decrease in the middle region and a sharp decline in numbers at the temporal pole. This granule cell distribution is inversely correlated with the density of CA3 pyramidal cells (low at the septal end and highest

in the temporal regions), so that the ratio of the number of granule cells to that of CA3 pyramids at any given level along the septotemporal axis fell in a near-linear fashion from 10:1 septally to 2:3 at the temporal pole.

### **1.2.2. The mossy fibre projection**

#### *The projection to CA3*

A single axon arises from the base of the granule cell body. The irregular excrescences along its length caused Ramon y Cajal (1893) to attribute to it the term "mossy fibre", while Golgi (1886) showed that these fibres formed a dense plexus of axon collaterals in the hilus before reaching the CA3 field, where they were found (Schaffer 1892) to run in a demarcated portion of the apical dendritic field close to the pyramidal cell layer - the stratum lucidum. The fact that mossy fibres do not penetrate CA2 is utilized in the definition of this field as separate from CA3.

Ultrastructural studies (Laatsch and Cowan 1966; Amaral and Dent 1981) have revealed the mossy fibres to be thin, unmyelinated axons of diameter 0.1-0.7 $\mu\text{m}$ , along which giant boutons (up to 10 $\mu\text{m}$  in diameter) are distributed. These boutons are invaginated by the spines of CA3 pyramidal cells, on which asymmetric contacts are established (Blackstad and Kjarheim 1961; Claiborne *et al.* 1986). Up to five spines are seen to invaginate one mossy fibre bouton (Amaral and Dent 1981), although it is unclear whether these spines belong to one, or several, CA3 pyramidal cells. There is also an input onto the dendritic shafts of pyramidal basket cells in the CA3 region (Frotscher 1985), which may provide a means for feedforward inhibition of the CA3 projection cells. Claiborne *et al.* (1986) noted that, upon reaching the CA3 field, the giant boutons were found at approximately every 135 $\mu\text{m}$  along the length of the mossy

fibre, so that each fibre would have about 14 such expansions over a typical 2mm transverse extent of CA3. Each granule cell would appear therefore to provide an input to 14-70 CA3 pyramidal cells, and since there are estimated (West and Andersen 1980; Boss *et al.* 1985) to be approximately  $10^6$  granule cells and  $1.5 \times 10^5$  CA3 pyramids in the hippocampus of one side, each CA3 cell would appear to receive an input from 90 to 450 granule cells.

### *Mossy fibre trajectories*

Early Golgi studies (Golgi 1886; Koelliker 1896; Lorente de No 1934) described an infrapyramidal bundle of mossy fibres which was shorter in length than the suprapyramidal bundle, although more recently it has been found that very few mossy fibre boutons are located deep to the CA3 layer, which suggests that this infrapyramidal projection is very sparse (Gaarskjaer 1986). Furthermore, the fact that the suprapyramidal bundle is situated infrapyramidally around the part of CA3 most proximal to the hilus, and that the "infrapyramidal bundle" shows considerable variation in extent across the septotemporal extent of the hippocampus, has led to some dispute over the validity of this parcellation of the mossy fibre projection, and over the usage of the infrapyramidal bundle by Lorente de No (1934) as a relevant marker for the subdivision of the CA3 field, although there remains the possibility that the termination of "infrapyramidal bundle" synapses upon the basal dendrites of proximal CA3 cells, when considered in addition to the input from the suprapyramidal bundle upon the apical dendrites, may confer a unique functional specificity upon the affected CA3 cells.

Different subregions of the dentate gyrus give rise to different mossy fibre trajectories which in turn terminate in different regions of the CA3 field: axons from

the tip of the suprapyramidal blade run through the stratum radiatum to reach the stratum lucidum and therefore do not synapse on the region of CA3 proximal to the hilus, while fibres arising from the infrapyramidal blade synapse on the basal dendrites of proximal CA3 cells before running through the pyramidal layer to attain the stratum lucidum. In addition, the septotemporal spread of the mossy fibres varies according to the position of the cells of origin within the dentate gyrus (Gaarskjaer 1981): fibres originating from superficial and lateral granule cells run for a greater distance in septal and temporal distances than those arising from deep and medial cells. This reflects the gradients in the development of the dentate gyrus, with the oldest cells possessing the most extensive axonal spread.

At any level along the septotemporal extent of the hippocampus in the rat, the mossy fibres are found to run approximately at right angles to the septotemporal axis in the region of CA3 proximal to the hilus, with an abrupt change in direction in distal CA3 towards the temporal pole (Blackstad *et al.* 1970; Swanson *et al.* 1978; Gaarskjaer 1978b, 1981, 1986). This deviation has been interpreted by Blackstad *et al.* (1970) as indicative of the lack of availability of sites for synaptic connection in CA3 septal to the level of origin of the fibres, thus causing a movement temporally in search of free sites, while the sharp termination at the CA3/CA2 border would suggest the presence of an inhibitory trophic factor in the CA2/CA1 region which prevents the mossy fibres from further advance. The increase in the ratio of CA3 pyramidal cells to granule cells towards the temporal pole would appear to provide some backing for this concept of axonal migration.

The mossy fibres diverge no more than 400 $\mu$ m in the septotemporal plane from their level of origin (Gaarskjaer 1981) before they turn in a temporal direction at the CA3/CA2 border. This strict delimitation of the granule cell projection has given rise to the belief that the dentate gyrus is composed of a series of septotemporally-arranged

lamellae, following a pattern of organization for the intrahippocampal circuitry initially voiced by Andersen *et al.* (1971). The argument for the consideration of the dentate gyrus as a set of independently-functioning units is reinforced further by the absence of any associative pathway: no intradentate projection between granule cells is believed to exist either ipsilaterally or contralaterally, in contrast to the extensive intrinsic circuitry within the entorhinal cortex (the major source of afferents to the dentate gyrus) and field CA3 (the target of the mossy fibre projection).

### *Putative neurotransmitters*

The neurotransmitters utilized in the mossy fibre pathway remain a matter of debate, although a number of studies have found that the mossy fibre nerve terminals contain glutamate (Crawford and Connor 1972; Storm-Mathisen 1983), GABA (Ottersen and Storm-Mathisen 1984), enkephalin (Gall *et al.* 1981), dynorphin (McGinty *et al.* 1983, Chavkin *et al.* 1985), cholecystokinin (Stengaard-Pedersen *et al.* 1983; Gall *et al.* 1986), chromogranin (Somogyi *et al.* 1984) and zinc (Stengaard-Pedersen *et al.* 1983). The degree of co-existence of these substances in the same nerve terminals is at present unknown, although a recent ultrastructural study in the monkey (Sandler and Smith 1991) has discovered the co-existence of glutamate and GABA in the mossy fibre terminals, suggesting that the inhibitory postsynaptic potential (IPSP) which is seen to follow the excitatory postsynaptic potential (EPSP) evoked in CA3 by granule cell stimulation (Yamamoto 1972) may be in part due to a release of GABA by the mossy fibres (which are commonly attributed to provoke the EPSP by way of an excitatory neurotransmitter), although temporal considerations of the EPSP-IPSP sequence hint that the GABAergic IPSP is mediated primarily by interneurons following either feedforward inhibition from the granule cells (Buzsaki 1984) and/or feedback inhibition

from CA3 pyramidal cells (Andersen *et al.* 1964).

The existence of excitatory amino acid receptors (Cotman *et al.* 1986; Andreasen *et al.* 1989) on the postsynaptic CA3 pyramidal cells indicates that the excitatory effect of the mossy fibre projection is mediated at least in part by glutamate, with the possibility of complex regulation of activity by way of the other putative neurotransmitters and neuromodulators substances located in the terminals.

### *The projection to the hilus*

In his Golgi preparations, Ramon y Cajal (1911) observed that the mossy fibres gave rise to a number of collaterals which ramified just below the granule cell layer, creating a plexus which later work (Soriano *et al.* 1983) has shown to be highly extensive in nature. Using the technique of intracellular HRP filling, which allows a complete visualisation of the axonal plexus, Claiborne *et al.* (1983) have found that each mossy fibre gives off about seven collaterals which ramify mainly within the hilar region. The collateral spread along the septotemporal plane is similar (up to 400  $\mu$ m) to that noted for the projection to CA3, while the spread transverse to this plane is dependent on the location of the projecting granule cell: those near the tip of the suprapyramidal layer have a restricted plexus which lies just beneath the cell layer, while the cells around the crest of the dentate and in the infrapyramidal blade have extensive collateral plexuses which are often found to cover the entire central region of the hilus. This pattern of collateral spread (corresponding presumably to the synaptic connections made on the hilar neurons) would appear to reflect the gradient of granule cell development: cells in the infrapyramidal blade develop last and consequently their axon collaterals have a limited space in which to ramify.

Each mossy fibre was found to have approximately 150 *en passant* boutons (compare the estimation of 14 boutons in CA3 given in the same study), of which two types were distinguished: most of the synaptic boutons were filled with spherical synaptic vesicles and made asymmetric contacts onto the dendritic shafts of hilar neurons (Ribak and Seress 1983), while the smaller varicosities were generally located at the distal ends of the collaterals and are believed to synapse on the spines of mossy cells (Blackstad and Kjaerheim 1961; Amaral 1978; Ribak *et al.* 1985).

### 1.3. THE HILUS

#### 1.3.1. Cell types in the hilus

Amaral (1978) identified at least 21 cell types in a Golgi study of the hilar region, of which two functional types have been studied in detail on account of their interconnections with the granule cells. Several different morphologies of aspiny hilar neurons are found to share characteristics in their immunoreactivity to GAD (Seress and Ribak 1983), electrophysiology (Scharfman and Schwartzkroin 1988, 1991) and dendritic morphology (Amaral 1978) and are therefore grouped together as one functional type, which will be referred below as "basket cells".

#### *The basket cell*

The first of these is the basket cell, which lies typically just beneath the granule cell layer and gives off ascending dendrites, which traverse the granular layer to attain the distal reaches of the molecular layer, where they receive asymmetric synapses onto

the dendritic shaft from fibres of the perforant path and from axons of hilar cells (see below). Descending dendrites receive an excitatory input from the granule cells, and inhibitory inputs from subcortical regions. The number of basket cells is believed to be far less than that of the granule cells, with estimates of 500-1000 cells (about one- to two-hundredth the number of granule cells), but the ramification of the descending dendrites and the possibility of multiple contacts by granule cells onto basket cells (Amaral 1978), suggests that each basket cell is the recipient of connections from a large number of granule cells.

Basket cell axons are found to cover 30 percent or more of the longitudinal and transverse extent of the dentate gyrus: GAD-positive axon terminals form pericellular plexuses around granule cell somata and make symmetric synapses on the somata and proximal dendrites (Seress and Ribak 1983). It is estimated (McNaughton 1989) that each basket cell may contact about 1000 granule cells, and that each granule cell is the recipient of 10 inhibitory inputs from GABAergic basket cells.

### *The mossy cell*

The most numerous cells in the hilus are the large, spiny multipolar cells with numerous thorny excrescences on their somata and proximal dendrites (hence the term "mossy cell") which are located deeper in the hilus (Amaral 1978; Ribak *et al.* 1985). Their dendrites are rectilinear and show infrequent branching, and are organized in such a way as to maximise the transverse and, to a lesser degree, the longitudinal extent of the dendritic tree. In addition, at least one dendritic branch penetrates the granule cell layer and extends as far as the distal end of the molecular layer. Studies differ as to the morphology of this dendritic extension; Amaral (1978) noted that it was

devoid of spines as far as the molecular layer, whereupon it became spiny, while Scharfman (1991) observed the opposite: the dendrite was seen to be spiny before it reached the molecular layer, where it became aspiny. This disagreement is significant in the light of the incoming inputs to the dendrite, since an input onto a dendritic spine is believed (Koch and Poggio 1982; Miller *et al.* 1985) to cause a five- to tenfold attenuation of the synaptic signal as observed at the cell body.

The axon of the mossy cell divides into fine collaterals, some of which run along the septotemporal axis of the dentate gyrus in the inner third of the molecular layer, where asymmetric contacts are made on the dendrites of granule and basket cells (Swanson *et al.* 1978; Scharfman *et al.* 1989), with the ipsilateral projection to the granule cells displaying a septotemporal divergence as great as 6.6mm (Amaral and Witter 1989). Interestingly, the granule cells at the same septotemporal level as the mossy cell body are very weakly innervated or not innervated at all.

Other collaterals traverse the stratum oriens of proximal CA3 to reach the alveus, from where they join the commissural system en route to the contralateral dentate gyrus, where they are considered to contact basket cells, thus providing feedforward inhibition to the contralateral granule cells (Buszaki and Eidelberg 1981; Frotscher *et al.* 1984; Seress and Ribak 1984). The number of mossy cells is estimated at  $2 \times 10^4$ , and each granule cell is deemed to receive about  $2 \times 10^3$  mossy cell inputs, so that every mossy cell contacts 1 in 10 granule cells.

While the excitatory nature of the mossy cell synapse onto the granule cells is accepted (Deadwyler *et al.* 1974), the identity of the neurotransmitter(s) involved has yet to be clarified. Storm-Mathisen *et al.* (1983) observed an immunoreactivity to glutamate, while the results from other experiments show that the mossy cells failed to display immunoreactivity to glutamate or a variety of neuropeptides (Ribak *et al.* 1985).

### 1.3.2. Connectivity within the hilus

The interconnections between the three cell types discussed above leads to the image of a highly complex circuit, which acts on the input from the perforant path and sets an appropriate output from the granule cells to the pyramidal cells of CA3. Knowledge of the nature of the individual synapses within the circuit provides some indication of the temporal flow of activity through the circuit, which might in turn yield some information as to the nature of its function.

Perforant path fibres terminate in the molecular layer on the dendrites of all three cell types: since this input is to the dendritic spines of the granule cells and to the dendritic shafts of the basket and mossy cells, it might be assumed that the cell bodies of the latter two types receive a stronger and more rapidly conducted synaptic signal (Turner 1984,1988), overcompensating for the increased distance to the parent cell bodies. The "fast-spiking" basket cells (Scharfman *et al.* 1990) are able to transmit a strong inhibitory signal directly onto the cell bodies of numerous granule cells located over a large extent of the dentate gyrus with near instantaneous speed (transmission time is estimated at around 1ms). The mossy cells provide an excitatory input onto the dendrites of granule and basket cells (assumed to contact the dendritic spines and shafts respectively), with the latter basket cells supplying further inhibitory inputs. The effect on the granule cells may be assumed to lag further temporally. The granule cell output synapses on both types of hilar neuron before the contact with the CA3 pyramidal cells is effected.

The granule cells are therefore subject to direct and indirect inhibition, both of which act before the excitatory effect of the perforant path input, as has been shown in studies where commissural fibres (originating from mossy cells) and perforant path fibres were stimulated concurrently (Buszaki and Eidelberg 1981), resulting in

suppression of the perforant path-evoked population spike. A recent study (Scharfman 1991) has demonstrated that both types of hilar neuron have lower thresholds for perforant path stimulation than granule cells, suggesting that the hilar circuitry acts as a filter, such that weak signals excite the hilar neurons but not the high threshold granule cells. A transient, strong signal would have little excitatory effect on the granule cells, due to the two inhibitory pathways described above; a prolonged (or multiple) strong excitation would cause an initial depolarization of the sensitive hilar neurons, with the concomitant disinhibition of granule cells, which could be activated by the later stages of the perforant path excitation.

The substantial transverse expanse of the mossy cell dendritic tree contrasts with its axonal spread, which is observed to innervate granule cells located at septotemporal levels other than that of the mossy cell body. This organization prompts further conjecture as to the directive rôle of the mossy cell: excitatory inputs to the cells arise mainly from granule cells occupying the same lamella as the mossy cell, which then modulates upwards or downwards the activity of granule cells across a broad septotemporal sweep of the dentate gyrus. In the case of upward modulation, the mossy cells would act to generate widespread granule cell excitation, with a resultant afferent volley to a similarly large septotemporal extent of the CA3 field; in the case of downward modulation, they would serve to shut down activity in lamellae other than that from which the mossy cell received its initial input, thus creating a "window of activity" in the dentate gyrus, with a subsequent specific projection to CA3.

### *The long-spined multipolar cell*

Another, less investigated, hilar neuron is the long-spined multipolar neuron

(Amaral 1978). This cell is distinctive for the long spines with which its dendrites are uniformly covered, and for the unique longitudinal spread of the dendrites, which have been observed to extend over 500  $\mu$ m along the septotemporal plane. Since mossy fibre expansions have been observed to terminate on its dendritic spines, it is tempting to attribute to the long-spined multipolar cell a similar integrative rôle as has been postulated for the mossy cell, with incoming inputs from granule cells located over a substantial longitudinal extent of the dentate gyrus, rather than from cells in the same transverse plane. It is of further interest that its axon has been seen to extend into the molecular layer, where it may conceivably synapse on the dendrites of the three cell types discussed above. More information is needed, however, before this idiosyncratic cell can be incorporated into any model of hilar connectivity.

### *Extrinsic regulation*

Subcortical afferents to the hilar region include a noradrenergic input from the locus coeruleus (Swanson and Hartman 1975), a 5HTergic input from the raphe nuclei (Conrad *et al.* 1974; Moore and Halaris 1975; Kohler and Steinbusch 1982) and a projection from the medial septal complex (Swanson and Cowan 1979; Houser *et al.* 1983). It has been established (Bilkey and Goddard 1987) that a non-cholinergic (and probably GABAergic) component of the septohippocampal pathway terminates on the same population of interneurons (namely the basket cells) as the commissural pathway from mossy cells located in the contralateral hilus, and that they exert antagonistic control on this cell group, since stimulation of the medial septal complex caused inhibition of the interneurons and concomitant facilitation of the granule cell population spike.

An increase in the granule cell population spike was observed after

administration of fenfluramine, a 5HT releasing drug (Richter-Levin and Segal 1988). This is believed to be a result of a reduction in the feedforward inhibition (and not the feedback inhibition) which is active in the hilar region, which would suggest that the raphe-hippocampal system, which has a dense 5HTergic plexus in the hilus (Moore and Halaris 1975; Kohler 1982), terminates on mossy cells, where its inhibitory action is mediated by 5HT<sub>1</sub> receptors (Segal 1980; Assaf *et al.* 1981; Bech *et al.* 1985).

The ability of subcortical systems to modulate the activity within the hilar circuit is interesting in view of the belief that the flow of information through the hippocampus is state dependent and sensitive to alterations in the monoaminergic systems (Winson and Abzug 1977, 1978; Dahl *et al.* 1983).

## 1.4. FIELD CA3

### 1.4.1. Structure

The CA3 field extends from the hilus to the transition zone CA2 which separates CA3 and CA1. Lorente de No (1934) divided CA3 along this extent into subfields CA3<sub>a-c</sub>, on the basis of pyramidal cell morphology, such that nearly all cells in CA3<sub>c</sub> were believed to give off a Schaffer collateral (which projected to CA1), with almost none of these characteristically thick collaterals were found in CA3<sub>a</sub>. In addition, Lorente de No defined the border between CA3<sub>c</sub> and CA3<sub>b</sub> as the point where the infrapyramidal bundle of mossy fibres ended. Since regions of CA3 distal to the hilus are now known to project to CA1, albeit by way of thin collaterals (Ishizuka *et al.* 1990), and studies of the infrapyramidal bundle of mossy fibres show considerable variation across the septotemporal extent of the hippocampus (Gaarskjaer 1986), the subdivisions of Lorente de No would appear to have no functional relevance. In this dissertation, therefore, regions of CA3 and CA1 will be specified according to their location with respect to the dentate gyrus, such that the area of CA3 abutting the hilus (roughly equivalent to CA3<sub>c</sub> of Lorente de No) is described as "proximal CA3", and "distal CA3" being used to represent the CA3 region at the CA3/CA2 border. The region of CA3 equidistant from these two poles will simply be referred to as "middle CA3". The adoption of the dentate gyrus as a reference point corresponds with its usage by Ishizuka *et al.* (1990) in their description of the intrahippocampal projections from the CA3 field.

## *The structure of the pyramidal cell*

### *Dendritic fields*

The projection neurons of CA3, the pyramidal cells, are arranged in a cell layer several cells deep, with the basal dendrites comprising the stratum oriens deep to the pyramidal cell layer. The apical dendritic field is divided into the stratum radiatum and the more superficial stratum moleculare, while the region of this dendritic field most proximal to the cell body layer contains the mossy fibre input from the dentate gyrus and is termed the stratum lucidum and is peculiar to the CA3 field. There is a "radial" organization of the inputs onto the dendritic fields of CA3: the entorhinal input terminates in the stratum moleculare, while the CA3 associational projection synapses more proximally on the apical dendrites in the stratum radiatum and in the stratum oriens. As mentioned above, the mossy fibre projection terminates on the proximal extent of the apical dendrites. The excitatory inputs from these regions are all seen to terminate on the dendritic spines, while the inhibitory input from the basket cells of CA3 is directed onto the cell body.

### *Axonal projections*

In general, the principal axon arises from the base of the pyramidal cell body, and runs in the stratum oriens or the more superficial white matter of the alveus. Intracellular tracing experiments (Ishizuka *et al.* 1990) have shown that 3 to 8 primary collaterals of varying thickness are given off from the principal axon, all of which bifurcated further and displayed substantial local ramifications in the stratum radiatum and /or the stratum oriens. The extent of these ramifications differed according to the location of the parent cell body within CA3, such that proximal cells (near the hilus) exhibited limited ramifications near the cell body, while distal CA3 cells had axonal

plexuses extending throughout CA3. In addition, a greater number of the axonal collaterals of these latter cells were found to run in the stratum oriens. Many of the axonal collaterals constitute the extensive longitudinal association pathway of Lorente de No (1934) which runs parallel to the septotemporal axis of the hippocampus.

The Schaffer collateral, which is distinguishable by virtue of its thickness (which is nearly as great as that of the principal axon), is observed in cells located more proximally in CA3, while none were found in distal CA3 (Lorente de No 1934; Ishizuka *et al.* 1990). It branches off the principal axon in the stratum oriens and is seen to penetrate the pyramidal cell layer to reach the stratum radiatum, in which it runs before terminating in CA1. Ishizuka *et al.* (1990) specify a "projection zone" corresponding to the superficial quarter of the stratum radiatum, in which the Schaffer collaterals course, and an "associational zone" encompassing the deeper three-quarters of the apical dendritic field, in which collaterals comprising the association pathway run and make synaptic connections with other CA3 cells. The thinner collaterals given off by distal CA3 cells which terminate in CA1 either run in the stratum radiatum or penetrate the pyramidal cell layer to run in the stratum oriens.

Axon collaterals attain the contralateral hippocampus by way of the dorsal hippocampal commissure; others join the fornix-fimbria system to innervate subcortical structures; others still run caudally to terminate in the entorhinal cortex. Multiple retrograde labelling studies conducted by Swanson *et al.* (1980, 1981) have shown that the same neurons in CA3 can give rise to collaterals that contribute to the associational, commissural and septal projections.

A large body of data exists which indicates that the neurotransmitter utilized in the axonal projections of CA3 pyramidal cells is an excitatory amino acid (Nadler *et al.* 1976; Storm-Mathisen and Iversen 1979; Collingridge *et al.* 1983; Ottersen and Storm-Mathisen 1985).

### 1.4.2. Heterogeneity of the CA3 field

It has already been noted (see Section 1.2.1.) that there is considerable disparity in the ratio of granule cells to CA3 pyramidal cells across the septotemporal axis of the hippocampus, ranging from 10:1 at the septal end to 2:3 at the temporal pole. Since the granule cells project to the CA3 pyramidal cells occupying the same transverse region (by way of the lamellar mossy fibre system), one might conclude that this discrepancy is reflected in the convergence of mossy fibre inputs onto CA3 cells, such that septally-located CA3 cells receive inputs from fifteen times the number of granule cells that project to CA3 cells at the temporal pole (assuming a uniformity in the distribution of mossy fibres to CA3 cells along the transverse length of the projection).

Differences in the electrophysiological characteristics have been observed in pyramidal cells located in different transverse regions of CA3 (Masukawa *et al.* 1982; Bilkey and Schwartzkroin 1990), with cells located close to the CA2 border and cells deep in the pyramidal layer having a greater tendency to display burst-type activity, indicating a degree of heterogeneity in the firing patterns of CA3 cells. It is postulated that the propensity for burst-type firing is a result of a greater length in the proximal part of the apical dendrite, which possesses a high density of calcium channels believed to modulate burst-type firing (Traub and Llinas 1979). If this is so, then there is added significance to the convergence of the mossy fibres onto this part of the CA3 dendritic field

### 1.4.3. The projection from CA3 to CA1

Pyramidal cells in all regions of CA3 provide an input to the stratum radiatum and stratum oriens of CA1 pyramidal cells, as well as to GABAergic interneurons

within CA1 (Frotscher *et al.* 1984).

Lorente de No (1934) believed that the intra-ammonic projections of CA3 were orthogonal: the CA3 association pathway ran longitudinally (parallel to the septotemporal axis), while the CA3-CA1 pathway was oriented transverse to this axis. Later studies have shown that this is not the case: using a variety of techniques, Hjorth-Simonsen (1973), Swanson *et al.* (1978), Laurberg (1979), Ishizuka *et al.* (1990) have demonstrated a considerable septotemporal divergence in the CA3-CA1 projection, in stark contrast to the strictly delimited projection from the dentate gyrus to CA3.

### *Topographical organization within the projection*

A detailed study by Ishizuka *et al.* (1990) using the PHA-L anterograde tracer has highlighted gradients of topographic organization in the septotemporal, transverse and radial axes of Ammon's horn, with the latter axis representing the proximodistal extent of the dendritic fields of CA1.

The authors report that distal CA3 cells project further and more heavily in a septal direction while cells in proximal CA3 are found to project further and more heavily in a temporal direction. Additionally, for any given position of projecting cells within CA3, the corresponding labelling across the septotemporal extent is observed to follow a "long diagonal" trend (in a cuboidal model of the projection, with the x,y,z axes corresponding respectively to the longitudinal, transverse and radial axes), such that the input to progressively more septal regions of CA1 terminates progressively closer to the CA2 border and is found deeper in the stratum radiatum (and in the stratum oriens), while in the temporal direction the projection terminates progressively more distally in CA1, and more superficially in the stratum radiatum. Further organization was noted in the transverse plane. Proximally located CA3 cells near the

hilus projected to the superficial portion of the stratum radiatum of proximal CA1 bordering the subiculum, and axons from distal CA3 terminates in deep stratum radiatum (and stratum oriens) of distal CA1 cells.

The existence of this topographic organization has a significant bearing on the understanding of the transfer of information from CA3 to CA1. For example, any given region within the CA1 field is observed to receive a projection from a delimited area of CA3 which (according to the above gradients) is always oriented "diagonally" across the CA3 field such that the cells in septal CA3 are located close to the CA2 border, with a progressive shift towards the proximal end of CA3 as the group of projection neurons is followed into progressively more temporal regions. By the same token, CA3 cells arranged in an opposite fashion (ie stretching from the hilar end of CA3 at its septal pole to the region adjacent to CA2 at its temporal end) provide a minimal convergence of inputs, projecting instead to a large number of cells distributed across much of the CA1 field.

### *The CA3-CA1 synaptic relationship*

Anatomical data provides an estimate of the pattern of *potential* synaptic connectivity: an evaluation of the influence of the CA3 input on the generation of activity in CA1 cells is a more rigorous undertaking. Several of the parameters involved in this relationship were examined in a study by Sayer *et al.* (1990), in which unitary EPSPs were evoked in CA1 pyramidal cells following stimulation of single CA3 pyramidal cells.

It was found that the amplitude of the CA3-CA1 unitary EPSP (100 $\mu$ V) is approximately a tenth of the amplitude of the CA3-CA3 unitary EPSP elicited by activation of the CA3 association pathway (Miles and Wong 1986). A comparison of the

amplitudes and time courses of EPSPs evoked by stimulation of the proximal and distal regions of the apical dendritic field suggests that the spread of synaptic current to the CA1 pyramidal cell body has characteristics similar to those predicted by the passive cable model of CA1 cells (Turner 1984, 1988), despite the fact that CA1 pyramidal cell dendrites are known to possess voltage-dependent conductances (Kandel and Spencer 1961; Wong and Prince 1979; Miyakawa and Kato 1986). Since these do not appear to be activated by the CA3-CA1 synaptic contact, the time course of the EPSP might be used as a marker of the proximodistal position of the synapse on the dendritic tree.

In cases where a convergent input of two CA3 cells onto a single CA1 cell was noted, marked differences were seen in the amplitudes and time courses of the EPSPs. Since the converging CA3 cells were located very close to each other (less than 100 $\mu$ m apart) in each situation studied, there would appear to be a conspicuous heterogeneity in the dendritic termination and effect of single CA3 inputs on a CA1 cell, despite the relative proximity of the two projections. In the (more frequent) situations where a CA3 cell was found to provide a divergent input to several CA1 cells (located close together in the pyramidal layer), the amplitudes and time courses of EPSPs evoked in different CA1 cells again showed marked variation.

The implication of these findings is that individual CA3 cells making synaptic contact on CA1 cells may have widely differing effects on the generation of activity within the recipient CA1 cells, and that this is likely to be a result of differences in the position (and possibly morphology) of the termination sites on the dendritic tree. Since this variation is independent of the position of the projecting cells within the CA3 field, some heterogeneity in individual CA3 cells might be assumed.

#### 1.4.4. The CA3 association projection

An associational projection arises from all regions of CA3 (Ishizuka *et al.* 1990). Proximal CA3 cells project to the same transverse section of CA3, and not to middle or distal CA3 regions, with both the stratum radiatum and the stratum oriens being recipients of this input. In comparison, pyramidal cells located in these latter regions provide an input spanning the transverse extent of CA3, with a slightly less dense input to proximal CA3. The middle CA3 cells give rise to the densest association projections, whereas that from proximal CA3 is relatively weak.

##### *Topographic organization*

The radial gradient for these components of the association pathway is more marked than for the proximal component and appears similar to that noted for the CA3-CA1 projection: middle CA3 inputs terminate preferentially in the stratum radiatum, while distal CA3 fibres run in the stratum oriens. Again in accordance with the CA3-CA1 input, in regions progressively more septal to the cells of origin the axons terminate deeper within the stratum radiatum (and the stratum oriens), with the tendency shifting towards superficial stratum radiatum in progressively more temporal areas.

In the longitudinal plane, proximal CA3 cells project preferentially in septal directions while distal CA3 regions tend to project temporally (cells in middle CA3 display impartiality). A "diagonal" pattern is observed in the distribution of projection cells across the longitudinal and transverse extents of CA3: septally, the recipient CA3 cells are located closer to the CA2 border while the shift in the temporal direction is towards cells in distal CA3.

### *Implications of CA3-CA3 connectivity*

The association projection onto CA3 cells is excitatory in nature (Lebovitz *et al.* 1971; Miles and Wong 1986) and makes synaptic contact on distal regions of the dendritic trees. In the above section the distribution of cells projecting to any given region in CA3 was noted: the orientation of the projection bears a rough resemblance to that seen for CA3 cells providing an input to any specified region in CA1 (see Section 1.4.2.). This coincidence implies that there is a raised probability that cells providing mutual excitation by way of the association pathway project to the same area within the CA1 field, with an especially high probability for cells in the centre of the CA3 field, where the overlap of the two distribution patterns is most pronounced. In theory therefore any given region of CA1 is the recipient of a mono- and polysynaptic input derived in the main from a discrete band of interconnected CA3 cells.

It is likely, however, that only a fraction of this band of cells is functionally active as a result of the excitatory association pathway. Additional CA3 axon collaterals synapse onto inhibitory interneurons (Andersen *et al.* 1964; Knowles and Schwartzkroin 1981; Miles and Wong 1984), and experiments (Miles and Wong 1987) indicate that this feedforward inhibition controls the spread of activity in CA3 via the polysynaptic feedforward excitatory pathway outlined above. Removal of inhibition leads to synchronous firing of pyramidal cells throughout the CA3 field, as a result of the ability of burst firing in one cell to trigger firing in cells coupled monosynaptically.

#### **1.4.5. Field CA2**

Lorente de No (1934) defined the CA2 field as a separate region on account of its differences in connectivity (unlike CA3, it was not observed to receive a mossy fibre input) and morphology (the pyramidal cells of CA2 were notably larger than those found in CA1). Since the CA2 pyramidal cells were seen to contribute axon collaterals to the longitudinal association pathway as well as to the projection to CA1, there has been a tendency to regard CA2 as functionally indistinct from the adjacent distal CA3. Recent studies, however, indicate that this may prove to be inaccurate: the projections from this region possess several characteristics that lend weight to the consideration of CA2 as separate from CA3 (Ishizuka *et al.* 1990).

Axon collaterals projecting to CA1 are noticeably thinner than those stemming from distal CA3 cells: in addition, they were seen to travel obliquely through the stratum radiatum and the stratum oriens (some fibres ran at right angles to the pyramidal layer), whereas collaterals from CA3 course parallel to the cell layer. Within CA1, the distribution of fibres is less marked and more diffuse than is characteristic of the CA3 projection. The contrast between CA2 and CA1 is highlighted by the observation that CA2 does not provide an input to the subicular complex. More work needs to be done before a functional correlate of this anatomical distinction can be provided.

#### **1.4.6. Field CA4**

The discussion about the inclusion of the hilar region within the bounds of the dentate gyrus rather than within field CA3 has been mentioned previously; however, this region does contain some cells similar in morphology to the proximal CA3 cells,

which are best considered as "displaced pyramidal cells of CA3". Examination of the connections of these cells reveals that they contribute axon collaterals to the CA3 association pathway, as well as to the Schaffer collateral outflow to CA1. Furthermore, the projections from these cells is notably extensive in both the transverse and longitudinal directions (Swanson *et al.* 1978). Final confirmation of the status of these displaced pyramidal cells would follow the incorporation of the pattern of their projections within the extant model of the CA3 outflow.

## 1.5. FIELD CA1

### 1.5.1. Structure

The CA1 field extends from CA2 towards the midline; in more caudal regions it is bounded medially by the subiculum (Lorente de No specifies a discrete region, the prosubiculum, upon which the CA1 field abuts). The pyramidal cell layer of CA1 is markedly different from that of CA3, in that there appear to be two types of pyramidal cells, with the superficial cells organized in one or two dense rows and the deep cells "scattered" below the superficial pyramids for several rows.

In accordance with the consideration of the CA3 field, Lorente de No (1934) divided CA1 into subfields CA1<sub>a-c</sub> on the basis of differences in cell morphology and in the thick Schaffer collateral projection from CA3. It has previously been mentioned (see Section 1.4.1.) that, contrary to the belief of Lorente de No, cells from all parts of CA3 project to CA1, and so the functional segregation of CA1 into the aforementioned subfields appears unjustified. In this dissertation, regions of CA1 will be specified on the basis of their proximity to the dentate gyrus: hence, the part of CA1 adjacent to CA2 (occupying the CA1<sub>c</sub> region of Lorente de No) is hereby referred to as "distal CA1", while the area located by the "prosubiculum" is termed "proximal CA1", and corresponds roughly with subfield CA1<sub>a</sub>.

#### *The structure of the pyramidal cell*

#### *Dendritic fields*

The CA1 pyramidal cells are arranged such that their apices are deep to the their basal surfaces, so that the apical dendritic field lies in juxtaposition to that of the

CA3 field. The CA1 apical field is divided into the stratum radiatum and the deeper stratum moleculare, and differs from CA3 in the absence of an equivalent to the stratum lucidum (since the mossy fibres do not innervate CA1). The basal dendritic field, the stratum oriens, is bounded by the pyramidal layer deep to it and the white matter of the alveus, which comprises the outflow of the CA1 field. Axons from CA3 terminate in the stratum radiatum and stratum oriens (Ishizuka *et al.* 1990), while perforant path fibres make synaptic contact in the stratum moleculare (Steward 1976). Both these excitatory inputs are believed to terminate on dendritic spines.

#### *Axonal projections*

The principal axon of the CA1 pyramidal cell is considerably thinner than its CA3 counterpart. Collaterals run both in the stratum radiatum and in the stratum oriens, while the main axon runs in the alveus, the outflow of which is directed towards the retrohippocampal region and the lateral septal complex. No collaterals have been demonstrated to project to the CA3 field or to the dentate gyrus and the existence of an association and/or commissural projection within the CA1 field is a subject for conjecture. While some authors (Raisman *et al.* 1965) specified a commissural connection to the contralateral CA1, its presence was disputed in later studies (Gottlieb and Cowan 1973; Segal and Landis 1974; Hjorth-Simonsen and Laurberg 1977; Laurberg 1979). However, some electrophysiological studies (Christian and Dudek 1988; Thomson and Radpour 1991) have demonstrated the existence of excitatory connections between CA1 pyramidal cells, and a recent anatomical study using the sensitive PHA-L anterograde tracing technique (Van Groen and Wyss 1990) has demonstrated a contralateral CA1-CA1 projection. In these studies, however, it is noted that the size of this association/commissural projection is substantially less than that of the projection from CA3.

Less data exists on the identity of the neurotransmitter of the CA1 outflow than on that of CA3, but it also appears to be an excitatory amino acid (Ottersen and Storm-Mathisen 1985).

### 1.5.2. The projection to the retrohippocampal region

#### *The subicular complex*

CA1 pyramidal neurons give rise to a projection to the ipsilateral subiculum which terminates in the pyramidal layer and in the stratum radiatum (Hjorth-Simonsen 1973; Swanson *et al.* 1978; Tamamaki *et al.* 1987; Van Groen and Wyss 1990). Fibres run caudally within the alveus to all regions of the subiculum from all parts of the CA1 field, with a topographic organization such that septal regions of CA1 provide an input to dorsal areas of the subiculum, while cells in temporal CA1 project to ventral levels of the subiculum.

In addition to this septotemporal organization, Tamamaki *et al.* (1987) showed that axons of CA1 cells terminated in a "columnar" fashion in the subiculum, with extensive coverage of the latter in the septotemporal plane but with a restricted field of termination along the transverse extent of the field. The projection was also found to be topographically organized in the transverse plane, such that CA1 cells adjacent to CA2 provided inputs to distal parts of the subiculum (adjacent to the presubiculum), whereas proximally-located CA1 cells projected to proximal subiculum (adjacent to the CA1 field). This pattern of projection was found to be invariant across the septotemporal length of the hippocampus (Tamamaki and Nojyo 1990; Amaral *et al.* 1991).

Different septotemporal levels of the CA1 field appear to innervate differing

fields (Van Groen and Wyss 1990). For example, fibres originating from the septal region of CA1 are observed to cross the midline in the dorsal hippocampal commissure to terminate in the contralateral subiculum and postsubiculum (with a further limited projection to contralateral CA1 and lateral septum), in addition to the ipsilateral inputs. In comparison, cells in the midportion of CA1 do not appear to give rise to a contralateral projection, but innervate instead the ipsilateral subiculum and postsubiculum. Temporally-located CA1 cells project to the ipsilateral subiculum and layers II and III of the parasubiculum, with no indication of a commissural component.

### *The entorhinal cortex*

Lorente de No (1934) observed some "long recurrent collaterals" which coursed through the alveus and the subiculum towards the entorhinal cortex. Further work has confirmed that the entorhinal cortex receives a topographically-organized projection from the CA1 field (Beckstead 1978; Swanson *et al.* 1978), which overlaps with the small projection from CA3 (Hjorth-Simonsen 1973). It is suggested (Van Groen and Wyss 1990) that the collaterals constituting the CA1 projection are given off from the fibres which innervate the subiculum and lateral septum.

### *The lateral septal nucleus*

Afferents from the CA1 field terminate ipsilaterally in the lateral septal nucleus by way of the posterior septal nuclei. Swanson and Cowan (1979) have indicated that there exists a clear separation of the inputs from the hippocampus to the lateral septum, with the fibres from CA1 (and the subiculum) projecting preferentially to rostral parts of the lateral septal nucleus while the CA3 afferents terminate bilaterally

in the caudal two-thirds of the nucleus. As with the reciprocal connections from the medial septal complex (which, with the projection from the lateral nucleus to the medial parts of the septal complex, form a loop of septohippocampal connectivity), the input from CA1 is topographically organized, such that cells in septal CA1 project to dorsal parts of the lateral septal nucleus, whereas fibres originating from temporal CA1 terminate in ventral parts of the nucleus.

### 1.5.3. The CA1 association projection

As mentioned above, some electrophysiological evidence exists for an association pathway within CA1. Excitation of neurons in the CA1 pyramidal cell layer was observed to increase the frequency of spontaneous EPSPs in CA1 pyramidal cells (Christian and Dudek 1988), while Thomson and Radpour (1991) demonstrated that the excitatory connection between CA1 pyramidal neurons is partially NMDA-mediated. The number of CA1-CA1 connections (1 in 130 pairs of neurons) is almost a tenth that of CA3-CA1 connections (1 in 16; from Sayer *et al.* 1990), although the validity of this ratio is offset by usage of the slice preparation, which is highly unlikely to contain all the synaptic connections of the projection cells tested. In one case, two inputs were seen to converge on a single CA1 neuron, but little is known about the relative amplitudes and time courses of the convergent EPSPs, or the relative location of the projecting CA1 neurons in the pyramidal cell layer. The greater incidence of evoked polysynaptic IPSPs supports the notion that the circuitry within CA1 is controlled by inhibitory inputs onto CA1 pyramidal cells from interneurons (Knowles and Schwartzkroin 1981; Lacaille *et al.* 1987), in common with the inhibitory control observed in CA3 (Miles and Wong 1987).

These electrophysiological findings are backed up by those of recent anatomical

studies (Tamamaki and Nojyo 1990; Amaral *et al.* 1991) which confirm the existence of a sparse association projection which terminates in the stratum radiatum (and possibly also the stratum oriens) of CA1. The present paucity of anatomical and electrophysiological data, however, prevents an understanding of the pattern or influence of the association projection upon the information processing and outflow of the CA1 field.

## 1.6. INTERNEURONS IN AMMON'S HORN

### 1.6.1. Heterogeneity of interneurons

#### *Morphological heterogeneity*

Morphologically heterogeneous varieties of local circuit neuron have been described in all layers of Ammon's horn (Ramon y Cajal 1911; Lorente de No 1934). Among these are the pyramidal basket cells which are located in the stratum pyramidale and share similarities with the pyramidal cells in the shape of the cell body and in dendritic arrangement (in field CA3 they differ from the pyramidal cells in the lack of a mossy fibre input and the concomitant absence of spines). The axon of these cells gives off a number of horizontal branches which form a dense network in the stratum pyramidale, with pericellular plexuses arranged around pyramidal cell somata in a manner similar to the basket cell-granule cell relationship in the dentate gyrus.

Several types of cells with "short axon cylinder" are found in the stratum oriens, including horizontal cells (which have also been observed in the alveus) and basket cells whose axon collaterals ramify in the characteristic "basket" fashion in around the pyramidal cells. Lorente de No (1934) subdivided these latter cells into two groups:

polygonal basket cells possessed dendrites that ramified solely in the stratum oriens, while the axon ascended to the apical dendritic field before giving off collaterals which descended into the pyramidal cell layer; in comparison, the horizontal basket cells were characterised by one or two dendrites in the apical dendritic field. The horizontally-directed axon of these cells was found to project to the basal surface of the pyramidal cell somata by way of collaterals running in the stratum oriens. Other local circuit neurons are noted in all parts of the apical dendritic field, the axons of which ramify mainly within the dendritic field, with some axon collaterals found in the pyramidal cell layer.

#### *Neurochemical heterogeneity*

Most of these interneurons contain the inhibitory neurotransmitter GABA (Kunkel *et al.* 1986, Sloviter and Nilaver 1987), and in addition interneurons have also been found to be immunoreactive for vasoactive intestinal peptide (Loren *et al.* 1979; Sloviter and Nilaver 1987), corticotrophin releasing factor (Swanson 1983), cholecystokinin (Innis *et al.* 1979; Greenwood *et al.* 1982; Stengaard-Pedersen *et al.* 1983), somatostatin (Morrison *et al.* 1982), neuropeptide Y (Kohler *et al.* 1986), substance P (Davies and Kohler 1985) and the opioid peptides dynorphin and Leu-enkephalin (Gall *et al.* 1981, 1984).

#### **1.6.2. The role of interneurons in Ammon's horn**

Electrophysiological studies on the intrinsic circuitry of Ammon's horn (Miles and Wong 1986, 1987; Lacaille *et al.* 1987; Sayer *et al.* 1990; Thomson and Radpour 1991) demonstrate a potent control exercised by inhibitory interneurons over the activity of

the pyramidal cells. At present, the majority of studies on hippocampal interneurons have focused on the basket cells which lie adjacent to the pyramidal cells in the stratum oriens of CA1 (Ramon y Cajal 1911; Schwartzkroin and Mathers 1978; Schwartzkroin and Kunkel 1985). It has been shown that these GABAergic cells receive an excitatory input from the pyramidal cells, and that they mediate a feedback inhibition by way of symmetrical synapses onto the pyramidal cell bodies (Knowles and Schwartzkroin 1981). Some evidence also exists which suggests that basket cells receive direct excitatory inputs from afferents which traverse the stratum radiatum and stratum oriens (Frotscher *et al.* 1984), indicating that they may exercise an additional means of control in the form of feedforward inhibition.

Lacaille *et al.* (1987) have concentrated instead on the function of a group of interneurons located at the border of the stratum oriens with the alveus whose axons ramify throughout the dendritic fields of CA1 (Ramon y Cajal 1911; Lorente de No 1934). It is postulated that these cells utilize GABA and/or somatostatin release inhibiting factor (SRIF) in their interaction with CA1 pyramidal cells (Kohler and Chan-Palay 1982; Somogyi *et al.* 1984; Bakst *et al.* 1985). These bipolar and multipolar cells receive excitatory synapses from axon collaterals of pyramidal cells, as well as from afferent fibres running in the dendritic fields of CA1, and their inhibitory output is directed in turn at the CA1 pyramidal cells. Given that the excitatory synapses onto these oriens/alvear cells, and onto the basket cells, is rapid and powerful, it is likely that these interneurons are activated before the pyramidal cells, and that the resultant feedforward inhibition may affect the propensity of the CA1 projection cells to be activated in response to an afferent volley.

These studies provide some indication of the interactions between the various populations of interneurons and the projection cells of the hippocampus. Not only does the work of Lacaille *et al.* (1987) show that there exist *at least* two inhibitory systems

within CA1, but also the difference in the dendritic distributions of the two types of interneuron raise the possibility that the two systems are governed by different sets of afferent fibres. As a final consideration, the presence of undefined connections between the two groups of interneurons hints at a capacity for interaction between the two inhibitory systems.

## 2. THE SUBICULAR COMPLEX

The subicular complex is divided into a number of cytoarchitectonically-defined fields: these are the subiculum (first described by Ramon y Cajal 1901), presubiculum (Ramon y Cajal 1901), and the parasubiculum (Brodmann 1909). An additional region medial to the subiculum and dorsal to the presubiculum has been defined as the postsubiculum (Brodmann 1909; Rose and Woolsey 1948), but the similarity of the latter to the presubiculum has led some later reports (Blackstad 1956; Sorensen and Shipley 1979) to consider this region as the dorsal portion of the presubiculum. However, recent anatomical (Swanson and Cowan 1977; Vogt and Miller 1983; Van Groen and Wyss 1988) and electrophysiological (Taube *et al.* 1990a,b) data argues for the consideration of the postsubiculum as an entity separate from the presubiculum.

In his description of the subiculum and presubiculum, Ramon y Cajal (1901) failed to distinguish a region on the lateral edge of the subiculum, separating the latter from the medial extreme of the CA1 field, which was later defined as the prosubiculum (Vogt and Vogt 1919). This region was described further by Lorente de No (1934), but was incorporated by Blackstad (1956) into his definition of the subiculum. While there exists some evidence for differences in connectivity (Raisman *et al.* 1966) most contemporary authors choose to consider the prosubiculum as a subset of the subiculum in studies of this region.

## 2.1. THE SUBICULUM

### 2.1.1. Structure

The subiculum is composed of three major layers: a molecular layer which is continuous with that of CA1 and the presubiculum on either side; an intermediate layer containing relatively few cells (and corresponds roughly with the stratum radiatum of CA1), and a broad layer of pyramidal cells, which has been subdivided by some authors (for example, in the 1934 classification of Lorente de No, this layer is split into three laminae, with cells of differing morphology predominating in the different layers). The molecular layer is notable for the quantity of axons arising from various fields of the hippocampal formation which course through the layer, of which the perforating fibres of the entorhinal cortex are the most prominent. It is clear from the above description that the laminar organization of the subiculum differs markedly from the "simple cortex" of the neighbouring CA1 field (and the rest of the hippocampus proper), and in this respect the subiculum is sometimes regarded as the first region of a transitional zone, which continues through the pre- and parasubiculum, which links the 3-layered archicortex of the hippocampus proper with the 6-layered isocortex. The 6-layered (pro)isocortical entorhinal area possesses morphological, and hodological, characteristics which differ from those commonly identified in the isocortex and is thus often regarded as the final stage in this intermediate zone.

### 2.1.2. Projections

As mentioned in Section 1.5.2., the subiculum is the recipient of a dense, topographically organized input from the CA1 field. In accordance with the concept of

the hippocampal formation as a predominantly unidirectional excitatory loop, the output of the subiculum is principally directed at the entorhinal cortex and other fields of the subicular complex.

### *The entorhinal cortex*

Caudally-directed fibres leave the subiculum to reach the angular bundle, where they separate before innervating different parts of the entorhinal cortex (Swanson and Cowan 1977; Beckstead 1978; Finch *et al.* 1983; Kohler 1985). The primary terminal field of these fibres is situated in layer IV, with fibres additionally observed in layers V and VI, but in the rat these appear destined for layer IV and are not believed to constitute a terminal field in the deep layers, although this has been suggested for the projection in the guinea pig (Sorensen and Shipley 1979). Restricted bands of subicular cells project to layer IV across the entire dorsoventral axis of the medial and lateral entorhinal areas (with the majority of the fibres terminating in the MEA), indicating a substantial degree of divergence of the subicular output, which contrasts with the highly lamellar input to this field from CA1. In addition, the superficial layers of the caudal portion of the MEA receives fibres from the subiculum (Witter *et al.* 1989). The projection to the entorhinal cortex is ipsilateral in the rat (Swanson and Cowan 1977; Kohler 1985), while a contralateral component has been noted in the cat and in the monkey (Amaral *et al.* 1984; Van Groen *et al.* 1986).

### *The pre- and parasubiculum*

In the rat, subicular fibres terminate preferentially in layer I of the pre- and parasubiculum, with the deep layers containing axons *en route* to the plexiform layer

(Swanson and Cowan 1977; Kohler 1985b). This again contrasts with the reported projection in the guinea pig which is predominantly directed at the deep layers, with some additional termination within the superficial layers (Sorensen and Shipley 1979), although this disparity across species might be explained by a lack of specificity in the technique used in the latter study (which has been shown to label axons *en passage*).

The projection is topographically organized, such that dorsal regions of the subiculum provide an input to dorsal and caudal regions of the pre- and parasubiculum, while ventral subiculum projects to ventral and rostral parts of the pre- and parasubiculum (Swanson and Cowan 1977; Van Groen and Lopes da Silva 1986).

Kohler (1985) additionally observed a projection from the subiculum to all layers of CA1 and to the stratum moleculare of CA3, as well as a prominent ventral association pathway within the subiculum. These inputs, as well as the prominent projections outlined above, appear to be ipsilateral in nature. Little is known about the neurotransmitter content of the reportedly excitatory (Finch *et al.* 1986) subicular projections.

### **2.1.3. Hodological heterogeneity within the subiculum**

Different subpopulations of subicular cells possess different afferents and efferents, which indicates the existence of a hodological heterogeneity independent of any differences in the cytoarchitectonics of the subiculum. It has been suggested (Witter and Groenewegen 1990) that the subiculum may be divided into functional subunits, with an overall structure which may resemble the columnar organization of the neocortex (Mountcastle 1957), or the compartmentation of the neostriatum (Graybiel 1983). If this proves to be the case, then the subiculum, considered to govern the outflow of the hippocampus, would appear to be organized upon radically different

lines to the hippocampus proper, the fields of which are seemingly homogeneous both cytoarchitectonically and hodologically.

## **2.2. THE PRE- AND PARASUBICULUM**

### **2.2.1. Structure**

The presubiculum lies adjacent to the subiculum; the parasubiculum is located between the presubiculum and the entorhinal cortex. As noted above, Brodmann (1909) specified the postsubiculum (area 48) as distinct from the presubiculum (area 27), but it is considered below as the dorsal region of the presubiculum, since it is not differentiated in reports of the connections of the presubiculum. The parasubiculum is often divided into two regions (areas 49a and 49b), with a third region (area 29e) considered by some to be distinct from the retrosplenial area (area 29) and hence a subset (area 49c) of the parasubiculum. As is the case for the presubiculum, a detailed comparison of the connectivity of these separate regions is lacking at present.

The pre- and parasubiculum are regarded as periallocortical in structure, with six layers arranged as external and internal principal laminae, separated by the lamina dissecans. The external lamina consists of the molecular layer and layers II and III; the three deep layers (which are roughly continuous with the two cellular layers of the subiculum) constitute the internal lamina. The neuronal constituents and the structure of the six layers is similar to that found in the (pro)isocortex of the entorhinal cortex, with the main difference being an increase in size of layer IV in the latter. The border between layers II and III is also less well demarcated in the pre- and parasubiculum.

### 2.2.2. Projections of the pre- and parasubiculum

#### *The presubiculum*

Layers II and III of the presubiculum contribute most of the fibres to the entorhinal cortex, where they terminate in the superficial layers (most notably in layer III) of the MEA (Beckstead 1978; Kohler 1985b). Some axosomatic contacts on cells in layer II were observed by Kohler (1985b). There is an additional projection to the contralateral MEA by way of the dorsal hippocampal commissure which is similar in termination pattern to the ipsilateral input. The projection is topographically organized, with dorsal presubiculum projecting to lateral parts of the MEA, while the ventral portion of the presubiculum provides an input to medial MEA (Swanson and Cowan 1977; Amaral *et al.* 1984; Kohler 1985b; Room and Groenewegen 1986). Intrinsic connections are distributed within layers I and II of the presubiculum, and all layers of the presubiculum (especially the superficial layers) contribute a modest projection to the parasubiculum.

Weak projections are noted from the presubiculum to the subiculum and the hippocampus proper: in the dentate gyrus, projections from the presubiculum (and the parasubiculum) terminate in the middle third of the molecular layer in a topographically organized fashion, such that dorsal regions project to dorsal regions of the dentate gyrus, and ventral parts of the pre- and parasubiculum project to the ventral regions of the dentate gyrus (Kohler 1985b; Witter *et al.* 1988). It is worthy of note that the region of the dendritic field in which these fibres terminate is the region towards which the axons of the MEA are directed, since the MEA is the major recipient of the output of the pre- and parasubiculum. The presubiculum additionally sends a crossed projection to areas homotopic to the fields to which an ipsilateral input is

directed (Kohler 1985b).

### *The parasubiculum*

In common with the presubiculum, layers II and III of the parasubiculum project to the entorhinal cortex, with layer II of the MEA (and to a lesser extent the LEA) receiving the greatest input (Kohler 1985b). Within this layer, the termination pattern has a mosaic aspect, with areas of dense termination interspersed with regions of less dense innervation. A smaller crossed component to this projection has been demonstrated, although this appears to be directed instead at the deep part of layer I of the MEA. As mentioned above, the parasubiculum sends a small, rostrally-directed projection to the subiculum and the hippocampus proper.

Kohler (1985b) observed a massive intrinsic innervation of the ventral parasubiculum and area 29e, with a small input crossing in the ventral hippocampal commissure to the contralateral parasubiculum in the rat (Swanson and Cowan 1977), although this crossed projection appears to be absent in the cat and in the monkey (Amaral *et al.* 1984; Room and Groenewegen 1986). A reciprocal connection from the parasubiculum to the presubiculum has not been noted.

### 3. THE ENTORHINAL CORTEX

#### 3.1. STRUCTURE AND NEURONAL TYPES

Ramon y Cajal (1911) and Lorente de No (1933) employed the Golgi technique to study the structure and neuronal distribution in the entorhinal cortex, the details of which were used to divide the entorhinal cortex into discrete layers. It is commonly subdivided into lateral and medial components on the basis of cytological differences (Kohler 1985a, 1986a; Witter *et al.* 1986; Van Hoesen and Pandya 1975), although some authors have presented evidence for further subdivision (Rose 1927; Haug 1976; Amaral *et al.* 1987; Krettek and Price 1977).

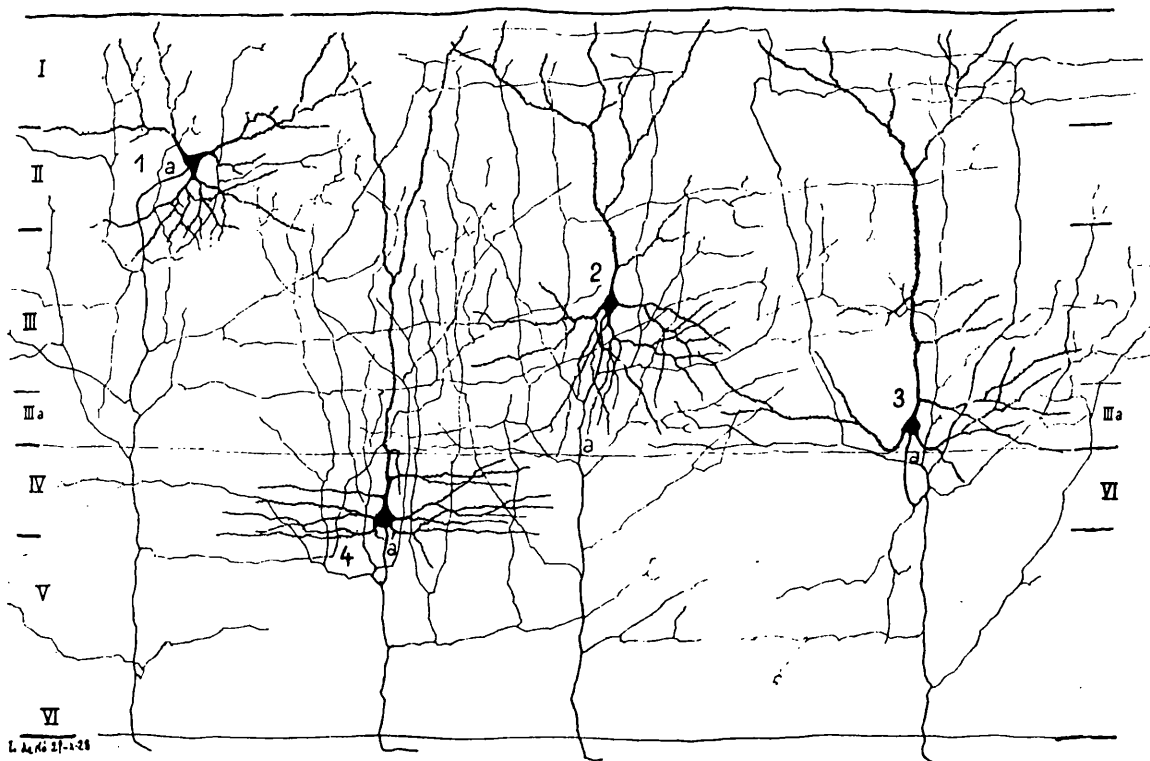


Fig.2 Four cells with complete axonal arborizations and dendritic processes are shown in the above section through the entorhinal cortex. 1 stellate cell; 2,3 layer III pyramidal cells; 4 deep pyramidal cell. *a* denotes the primary axon. Drawing taken from Lorente de No (1933).

The classification of the entorhinal cortex into six layers follows the description of Lorente de No (1933). Additional differences between the lateral and medial entorhinal areas are highlighted below. The figures quoted for the diameters of the various neuronal types represent the mean sizes as reported by Lingenhohl and Finch (1991).

### *Layer I*

The plexiform layer is the recipient of collaterals of afferents terminating deeper in the entorhinal cortex, as well as collaterals of the projection and local circuit neurons of the entorhinal area itself. Thick fibres originating in the pre- and parasubiculum run through this layer. Some horizontal "short axon" local circuit neurons are also present in this layer.

### **Layer II**

Medium size (20  $\mu$ m diameter) cells with a body of polygonal or star form and spiny dendrites are found in great abundance, with comparatively few pyramidal cells and horizontal short axon cells in this layer. In all species examined, layer II of the lateral entorhinal area (LEA) was well defined, with densely-packed cells arranged in islands. In the medial entorhinal area (MEA), the cells were larger and less packed, with little evidence of clustering.

### **Layer III**

The pyramidal cells of this layer are similar in size to the pyramidal cells found elsewhere in the neocortex. This broad layer (narrower in the LEA) contains several strata of spiny pyramidal cells differing slightly in size (large pyramids of 20  $\mu$ m diameter; small pyramids of 12  $\mu$ m diameter) but displaying similar axonal and

dendritic arrangements. Various short axon cells were noted in this layer.

#### **Layer IV**

The cell-sparse lamina dissecans (less well defined in the LEA than in the MEA) runs from the rhinal sulcus laterally to the parasubiculum medially and separates layer III from layer IV, in which the deep pyramids (diameter 20 m) are the most numerous. These cells, and the multipolar cells, lie in a thin layer between the lamina dissecans and layer V (Haug 1976). Layer IV of the LEA is broader than for MEA, due both to a greater number of cells as well as a lower cell density. Amaral *et al.* (1987) incorporated layer IV with layer V in the monkey.

#### **Layer V**

The "layer of the small pyramids with recurrent axis cylinder" has a stratified appearance and contains a high number of pyramids (diameter 15 m) arranged in dense groups. Short axon globular and spindle cells are distributed throughout the layer.

#### **Layer VI**

Lorente de No subdivided this layer into the superficial layer VIa, containing most of the globular cells (diameter 14 m), and the deep layer VIb, containing the polygonal cells. This polymorph layer contains relatively few cells and displays a similar expansion in the LEA as layer IV.

## 3.2. INTRINSIC CONNECTIONS OF THE ENTORHINAL CORTEX

### 3.2.1. Dendritic spreads

The dendritic spreads of entorhinal neurons have been characterized in a study using intracellular labelling with HRP (Lingenhohl and Finch 1991). An analysis of these spreads provides some indication as to the intrinsic sources of input to the projection cells of the different layers, which in turn depicts the pattern of information processing within the entorhinal cortex. Cells in layers II-IV possessed dendritic branching which was restricted to the same layer as the parent cell body, or to the immediately adjacent regions of neighbouring layers. In comparison the dendrites of cells of the deep layers were seen to ramify in layers I and II in addition to the deep layers, suggesting (in contrast to the cells of layers II-IV) that the deep projection cells are influenced by inputs from every lamina of the entorhinal cortex.

An interesting feature is the magnitude of the dendritic spreads and dendritic lengths (average 10mm), with those of cells in layer II being among the most notable. This attribute, coupled with the high density of spines characteristic of these neurons, suggests that entorhinal cells have the facility to integrate a large number of inputs originating from a substantial longitudinal extent of the entorhinal cortex.

### 3.2.2. Axonal domains

Anterograde studies in the rat (Kohler 1986, 1988) have described differences in the intra-entorhinal connections of the MEA and LEA which, in view of the cytoarchitectonic differences outlined above, further highlight the functional disparity in the entorhinal cortex. Additional work on the intrinsic and extrinsic connectivity of

the various cytoarchitecturally-defined subregions (see above) of the entorhinal area needs to be conducted before further parcellation of the MEA and LEA into functional subdivisions can be justified. Supplementary data on the axonal domains of entorhinal neurons is taken from the work of Lingenhohl and Finch (1991); however, it must be noted that in this latter study no distinction is made between neurons of the MEA and those of the LEA.

### *Layer II*

#### MEA

Most of the axons were found to form a dense, horizontal plexus within layer II, with heavy innervation of ventral levels of the LEA. Fibres also run in the deeper layers of the MEA, but these appear to be destined for the angular bundle, with no significant termination within the deep layers.

#### LEA

Both sides of the LEA receive an innervation, with axosomatic contacts being made on stellate cells. Other fibres run in layer I where they ran medially (passing the MEA) to reach the presubiculum, while others course laterally en route to layer I of the piriform cortex. Collaterals from the latter fibres (but not the former) descend to innervate layer II neurons. Innervation of layers II-VI of the MEA is negligible.

A comparison of layer II axonal domains (Lingenhohl and Finch 1991) suggests that the cells of this layer might subserve a dual function: one of these functions is the transmission of information to the hippocampus proper, with the relevant cells characterized by a direct projection to this region with little branching within the

entorhinal cortex; the other function is that of association within the entorhinal cortex (especially layer II), and is typified by an extensive intrinsic axonal network, although are seen to project to the hippocampus (as well as to the subicular cortex and to olfactory cortical regions).

### **Layer III**

#### **MEA**

Ascending fibres innervate the longitudinal extent of layer II in the MEA, and massive termination within layer I is also noted. Fibres in layer I are found to run ventrolaterally towards the LEA and the piriform cortex. The deep layers receive a sparse innervation.

#### **LEA**

Layers I-III of the LEA on both sides contain dense terminal plexuses. Varicose axons in layer I run medially through the MEA to terminate in the subicular complex and, as for layer II of the LEA, few fibres are found in layers II-VI of the MEA. Laterally-directed fibres in layer I terminate in the piriform cortex. The deep layers of the LEA are not believed to receive substantial innervation.

### **Layer IV**

#### **MEA**

A prominent innervation, which becomes denser at more ventral levels, is noted in the superficial layers, with dense terminal fields present in layer II and III. Layer I contains fibres running parallel to the long axis of the MEA. Fibres running in layers

V and VI are destined for layers II and III of the LEA, and all layers of the perirhinal cortex.

LEA

Layers I-IV of the LEA are heavily innervated by layer IV. Loosely-arranged plexuses are also found in layers V and VI. While layers II and III of the MEA receive little input, layer IV is noted to receive a heavy projection throughout its longitudinal extent.

Layer V

MEA

All layers of the MEA contain fibres originating in layer V, with the densest innervation within layers II and III.

LEA

Layers I-IV receive an innervation, with a prominent termination zone in the deep part of layer III. The projection from layer V appears orientated in such a way that most fibres are directed laterally from their cells of origin and are seen to run as far as the rhinal fissure. A smaller component of this projection is observed in layer V and VI, with the fibres eventually terminating in the perirhinal and piriform cortices. Very few fibres reach the MEA.

## Layer VI

### MEA

In conjunction with layer V, all layers of the MEA contain fibres from layer VI. In addition, fibres course ventrolaterally to form terminal plexuses in layers I-III of the LEA.

### LEA

All six layers of the LEA receive an innervation, with a dense terminal field in layer V across its longitudinal extent. Fibres are seen to run horizontally within layer VI. Layers IV-VI of the MEA also receive an input from this layer.

Some similarity can be observed in the pattern of intrinsic connections of the MEA and LEA: the projection from each layer is mainly directed to the more superficial layers. Axons directed towards the deep layers are generally found to have extra-entorhinal terminations. In general, fibres from layers IV-VI of the MEA and LEA are observed to have a greater dorsoventral and laminar divergence than those emanating from the superficial layers, in accordance with the principle of intracortical connectivity of Rockland and Pandya (1979).

The extensive projection from the MEA to the LEA contrasts sharply with the weak LEA-MEA projection which, when collated with the connections between the subicular complex and the MEA, indicates a largely unidirectional flow of information from the subicular complex to the MEA and thence to the LEA.

### 3.3. EXTRINSIC AFFERENTS OF THE ENTORHINAL CORTEX

#### 3.3.1. Cortical afferents to the entorhinal cortex

A strong olfactory input from the olfactory bulb and from most of the cortical regions which receive a projection from the olfactory bulb is received by both the LEA and MEA, although the input to the LEA is of greater density (Krettek and Price 1977). A similar bias has been described (Deacon *et al.* 1983; Cechetto and Saper 1987) for the inputs from temporal cortex (auditory, visual and polymodal association areas), medial prefrontal cortex (frontal eye field and supplementary motor areas) and insular cortex (autonomic and limbic association areas).

These cortical inputs show laminar segregation: the olfactory projection arises mainly from layer II of olfactory cortex and terminates in layers I and II of the entorhinal cortex, which is also the destination for the fibres from layer VI of the medial prefrontal cortex, whereas the insular inputs originate from layer III and end in the deeper layers.

The results of studies on corticocortical patterns of projection in the monkey (Jones and Powell 1970; Pandya and Seltzer 1982; Pandya and Yeterian 1984) and the rat (Saper 1982) has led to the notion of a stepwise connection of cortical regions for the sensory modalities, with the complexity of the information increasing with every step: primary sensory areas project via secondary and tertiary sensory cortex to multimodal association areas in frontal and temporal cortex. The information reaching the entorhinal cortex from these latter regions is therefore believed to be of a highly processed "supramodal" form. The cortical afferents show a specificity of termination in the LEA and MEA, but the degree to which this segregation is reflected in the function of these regions is at present unclear. The existence of prominent intrinsic

connections in the LEA and MEA which spread both across layers and in a longitudinal direction (Kohler 1986; Kohler 1988) suggests that projection neurons in a given locality may have similar access to a diversity of information, although the information content may differ for different localities, depending on the extent of the intrinsic connectivity. In this light, it is of further interest that the intra-entorhinal projections of the LEA and MEA remain largely within the borders of their respective areas.

### 3.3.2. Hippocampal afferents to the entorhinal cortex

The dentate gyrus is not known to provide an input to the entorhinal cortex, while there exists only a restricted projection from the temporal part of the CA3 field (Hjorth-Simonsen 1973). The CA1 field of the hippocampus has been found to innervate every layer of the entorhinal cortex in the rat (Beckstead 1978; Swanson *et al.* 1978), with layer IV receiving the strongest input; additionally, the LEA has a heavier innervation than the MEA.

The pyramidal cell layer of the subiculum gives rise to an ipsilateral input which terminates in layer IV of the entorhinal cortex (Kosel *et al.* 1982; Kohler 1985). This projection displayed a high degree of divergence, such that a restricted segment of subicular cells innervates an extensive dorsoventral extent of the entorhinal area.

The superficial layers of the MEA receive a massive, bilateral input from the pre- and parasubiculum (Shipley 1975; Swanson and Cowan 1977; Kohler *et al.* 1978). The LEA does not appear to be innervated by these regions. Layer III of the MEA receives the densest innervation from the presubiculum, while the parasubiculum provides an input to layer II of the MEA ipsilaterally and the deep part of layer I contralaterally (Kohler 1985). The projection is topographically organized: septal parts of the pre- and parasubiculum innervate septal parts of the MEA, and progressively

more temporal regions receive an input from progressively more temporal regions of the pre- and parasubiculum. Since the dendrites of the projection neurons in layers II and III of the entorhinal cortex ramify in the first three layers, while those of the projection neurons in Layers IV-VI are distributed throughout all six layers, the laminar specificity of the projections to the entorhinal cortex from the various regions of the subicular complex suggests that the input from the pre- and parasubiculum may influence bilaterally all the efferent systems of the MEA, while the ipsilateral subicular input controls the projections from the entire entorhinal area to the frontal cortex and subcortical regions.

#### 3.4. THE PROJECTION FROM THE ENTORHINAL CORTEX TO THE HIPPOCAMPUS

The perforant path, first described by Ramon y Cajal in 1911, is the major route by which the entorhinal cortex sends afferents to the hippocampal formation. Axons of the projection neurons enter the white matter underlying the cortex to join the angular bundle. The fibres then run dorsally before perforating the subiculum along its long axis to reach the hippocampal fissure and thence the molecular layer of the dentate gyrus, the stratum moleculare of the CA3 field and the molecular layer of the subiculum. Some fibres, however, run along the stratum moleculare before traversing the fissure. The stratum oriens of CA3 does not appear to receive any fibres. The termination pattern of the perforant path fibres is still unclear at present: it appears that the axons that innervate the dentate gyrus do not constitute a separate group to those that provide an input to CA3, but that some, or all, of the fibres project to both fields.

The temporo-alvear pathway (Lorente de No 1934) is another route from the

entorhinal cortex to the hippocampus. Fibres travel through the alveus before terminating in the pyramidal layer of the subiculum and the stratum oriens of CA1 (Raisman et al. 1965; Steward 1976; Swanson and Kohler 1986).

#### 3.4.1. Projection neurons of the perforant path

The projection neurons were identified by Ramon y Cajal (1911) and Lorente de No (1933) as the spiny stellate and pyramidal cells of layers II and III. An investigation of their ultrastructure revealed that these two populations of cells had similarities in the distribution of symmetric and asymmetric synapses on the cell body and the dendritic shafts and spines. Both groups were also found to make local asymmetric connections (Germroth *et al.* 1991) on other excitatory neurons and onto aspiny local circuit neurons. The respective excitation and disinhibition may be indicative of some capacity of the projection neurons to cause amplification of the excitatory signal within a region of the entorhinal cortex.

Asymmetric contacts, using glutamate (and possibly also aspartate) as the excitatory neurotransmitter, are made on the dendritic spines of the dentate granule cells and the pyramidal cells of the hippocampus. Studies on the input from medial perforant path fibres onto granule cells (McNaughton *et al.* 1981) showed that 2-3% of the perforant path synapses generated an activation which was greater by a factor of 10 to 20 than that caused by other synapses. It is suggested that these "strong" synapses represent a termination of the perforant path fibers onto the dendritic shaft, which are not subject to the five- to tenfold attenuation that is believed (Koch and Poggio 1982; Miller *et al.* 1985) to affect the synaptic signals coming in from inputs onto spines.

Collaterals of the perforant path fibres also make asymmetric contacts on the dendritic shafts of hilar basket and mossy cells (Zipp *et al.* 1989; Scharfman 1991),

indicating that the perforant path has the capacity to cause excitation and feedforward inhibition of the granule cells through activation of the hilar circuitry (see Section 3.3.2.).

In addition to the spinous cells, some aspiny GABAergic neurons are also believed to provide a relatively weak direct inhibitory input to the hippocampal formation (Germroth *et al.* 1989), which appears to make contact with inhibitory cells, thus augmenting by disinhibition the excitation caused by the spinous cell input.

#### **3.4.2. Activation of Ammon's horn by the entorhinal cortex**

Although the original work of Andersen *et al.* (1971) was notable for the lack of activation in the CA3 and CA1 fields following direct excitation of the entorhinal cortex, a later electrophysiological study of the entorhinal input to the hippocampus *in vivo* (Yeckel and Berger 1990) has demonstrated that stimulation of the perforant path results in near-simultaneous monosynaptic excitation of the dentate gyrus, CA3 and CA1. Furthermore, the evoked responses from CA3 cells was often observed to precede those from the dentate granule cells, which has been interpreted as being representative of the establishment of *en passant* synapses of perforant path fibres on CA3 cells prior to their termination on granule cell dendrites. Responses evoked from CA1 were coincident with those from the dentate gyrus, suggesting that (unlike CA3) different fibres convey an input to CA1.

These electrophysiological findings complement the anatomical data in demonstrating the existence of three distinct entorhinal projections to the three hippocampal regions; in addition, the fact that disynaptic and trisynaptic activation of CA3 and CA1 respectively through the classical trisynaptic circuit were found to be subthreshold for spike generation strongly suggests that excitation through the

monosynaptic pathways may be more critical for spike generation in CA3 and CA1 than the feedforward excitation conveyed through the trisynaptic circuit. Since the latter excitation is insufficient to generate action potentials alone, it may instead represent some co-operativity in the afferents to the Ammon's horn, allowing synaptic potentiation of the stronger monosynaptic input.

### 3.4.3. Laminae of origin and bilateral connectivity

The entorhinal projection to the dentate gyrus and CA3 in the rat was found to originate from layer II, whereas the projection to CA1 arises from layer III (Steward and Scoville 1976). A later study (Kohler 1985) showed that projection neurons in layers IV and VI also contributed to the perforant path. A similar organization of the layer II and III inputs was discovered in the monkey (Witter and Amaral 1991), with the additional discovery that some neurons in layers VI and V contributed respectively to the dentate gyrus/CA3 and CA1 inputs. Since the hippocampus projects to the deep layers (Hjorth-Simonsen 1971; Swanson and Cowan 1977), this reciprocal connection may represent a feedback system between the entorhinal cortex and the hippocampus.

The existence of a crossed projection from the entorhinal cortex has been reported in a number of species (Hjorth-Simonsen and Zimmer 1975; Steward 1976; Amaral *et al.* 1984; Witter and Groenewegen 1984), which is mostly directed towards the dentate gyrus and CA1. Wyss (1981) has noted a very weak contralateral projection to a small part of CA3 in the rat. Steward and Scoville (1976) have portrayed the bilateral projection to CA1, originating in layer III, as being similar in density on both sides. The size of the crossed projection to the dentate gyrus, as compared to the ipsilateral pathway, is variously described as slight (Steward 1976) and substantial (Hjorth-Simonsen and Zimmer 1975; Wyss 1981; Witter and Groenewegen 1984). In the

latter studies, a variation was noted such that dense labelling in dorsal ipsilateral dentate gyrus was accompanied by similarly dense contralateral filling, while strong ventral labelling was coupled with a weak crossed projection. In addition, the commissural pathway to the dentate gyrus was described as originating only from lateral and caudal parts of the LEA and MEA, whereas the crossed pathway to the Ammon's Horn arose almost entirely from the MEA.

The perforant path appears to utilize glutamate (and possibly aspartate) as its excitatory neurotransmitter (Storm-Mathisen 1977), with an additional finding that the input from the LEA also utilizes Leu-enkephalin (Chavkin *et al.* 1985).

#### **3.4.4. The organization of the termination of entorhinal fibres within the hippocampus**

Anterograde studies in the rat have revealed that different areas of the entorhinal cortex distribute their fibres in a laminar pattern to the dendritic fields of the dentate gyrus and CA3 (Hjorth-Simonsen and Jeune 1972; Steward 1976; Wyss 1981). Fibres from the LEA terminate in the outer third of the molecular layer of the dentate gyrus and the outer half of the stratum moleculare of CA3, whereas those from the MEA terminate in the middle third and inner half respectively, giving rise to the belief that the perforant path has discrete lateral and medial components. Electrophysiological work by McNaughton (1980) supports this segregation. Additionally, there is a gradient of contact along the proximodistal extent of the dendrites: axons originating in the far lateral region of the LEA synapse on the most distal portions of the dendritic fields of the dentate gyrus and CA3, while progressively more medial regions of the LEA and MEA terminate on progressively more proximal to the projection cell layers.

The projection to CA1 displays a differing organization (Steward 1976). Neurons

of far lateral LEA project to CA1 cells on the subicular border, while progressively more medial LEA and then MEA project to regions of CA1 progressively closer to the CA1/CA2 boundary. Instead of the laminar organization reported for the dentate gyrus/CA3 pathway, both the LEA and MEA inputs terminate in the outer two-thirds of the stratum moleculare (Witter *et al.* 1989).

Further organization in the perforant path was revealed in several studies (Hjorth-Simonsen and Jeune 1972; Ruth *et al.* 1982, 1988; Witter and Groenewegen 1984), demonstrating a topographical relationship such that cells in rostralateral LEA and MEA project to septal hippocampus, while progressively more caudomedial parts of the LEA and MEA projected to progressively more temporal parts of the hippocampus. The discovery that the LEA and MEA display separate progressions adds weight to the dual-component concept of the entorhino-hippocampal pathway.

In view of such organization, it is of interest that this projection does not appear to show "point-to-point" specificity; instead a localized region of entorhinal cortex provides a divergent input onto the hippocampus (Steward 1976; Wyss 1981; Witter and Groenewegen 1984). A double-labelling study using retrograde fluorescent tracers (Witter *et al.* 1989) has shown that the divergence is due to collateralization of the perforant path axons, such that individual entorhinal neurons innervate the hippocampus at different levels along its septotemporal axis. This would result in considerable overlap of the termination zones of entorhinal neurons, so that any given group of hippocampal cells is the recipient of information from a substantial portion of the entorhinal cortex.

The differences in the origins, terminations and bilateral representation of the projection to the dentate gyrus and CA3 and that to CA1 strongly suggests that the two must be considered as separate entorhinal projections. Given the segregation of the information coming in to the entorhinal cortex, it may be presumed that the nature of

the information received by the CA1 field differs to that received by CA3 (and the dentate gyrus), which in turn may highlight a difference in the processing of information by these two fields of Ammon's Horn.

## 4. SUBCORTICAL AFFERENTS TO THE HIPPOCAMPAL FORMATION

### 4.1. THE SEPTAL COMPLEX

Caudally-directed fibres from the medial septal complex (the medial septal nucleus and the nucleus of the diagonal band) take several routes to the hippocampal formation: the majority run through the fimbria and dorsal fornix (Daitz and Powell 1954; Cragg and Hamlyn 1957; Raisman 1966), with additional projections from the nucleus of the diagonal band that run near the cingulum bundle en route to temporal subiculum and presubiculum (Swanson and Cowan 1979; Milner *et al.* 1983), or through the amygdala to innervate temporal regions of the hippocampal formation (Milner and Amaral 1984; Gage *et al.* 1984).

All fields of the hippocampal formation receive an input (Mellgren and Srebro 1973; Swanson and Cowan 1976; Alonso and Kohler 1984), with the densest termination in the hilar region (Rose *et al.* 1976). Fibres also terminate in both apical and basal dendritic fields of CA3, in the stratum oriens of CA1, and in all layers of the subicular complex, with layer II receiving the heaviest innervation. The medial septal complex sends a substantial projection to the entorhinal cortex in the rat, with a further weak projection from the nucleus basalis of Meynert in the monkey (Mellgren and Srebro 1977; Meibach and Siegel 1977; Alonso and Kohler 1984; Milner and Amaral 1984; Insausti *et al.* 1987). The MEA is the major recipient of this input, which terminates in the lamina dissecans and in layer II, while the lateral extreme of the entorhinal cortex in the rat receives a specific input from neurons in the horizontal limb of the nucleus of the diagonal band (Milner and Amaral 1984).

#### 4.1.1. Topographic organization

The projection is topographically organized such that cells near the midline of the medial septal complex project to medial parts of the entorhinal cortex and to septal regions of the remainder of the hippocampal formation, while more laterally-situated cells project to lateral parts of the entorhinal cortex and to temporal parts of the hippocampal formation (Meibach and Siegel 1977; Monmaur and Thomson 1983; Saper 1984). There is also a rostrocaudal-to-septotemporal gradient in the septohippocampal projection, with additional evidence that the septal input becomes progressively heavier for more temporal hippocampal regions (Milner *et al.* 1983).

#### 4.1.2. Neurotransmitters

The medial septal projection is widely held to utilize acetylcholine as a neurotransmitter (Lewis and Shute 1967; Alonso and Kohler 1984; Amaral and Kurz 1985), although immunostaining tests have shown that at least 30% of the cells projecting to the hippocampal formation are GABAergic (Kohler *et al.* 1984) and constitute a largely separate group to the cholinergic neurons (Brashear *et al.* 1986). Other studies have noted that some cholinergic medial septal cells also contain galanin (Melander *et al.* 1985).

## 4.2. THE AMYGDALAR DEEP NUCLEI

*(The projections from the corticomедial nuclei are considered, by virtue of their substantial direct input from the olfactory bulb, as a component of the input from the olfactory cortical regions)*

The lateral nucleus projects to layer III of the LEA, and caudolateral parts of the basolateral nucleus provide an input to layers III and IV of the LEA, and to the ventral subiculum and the adjacent CA1 region in the rat (Krettek and Price 1977; Beckstead 1978). The cortical areas that project to the basolateral complex are believed to convey data involving the five sensory modalities (Van Hoesen 1981) and it is of interest that these regions also provide an input to the entorhinal cortex and to the subicular complex.

There is an additional input from the endopiriform nucleus which terminates in layers I and III of the LEA, and in layer I of the ventral subiculum (Krettek and Price 1978); this projection is thought to be excitatory in nature (Wilhite 1986).

## 4.3. THE THALAMUS

The nucleus reuniens sends a substantial, topographically organized input to layers I and III of the entorhinal cortex, the molecular layer of the parasubiculum, and to the ventral subiculum and ventral two-thirds of CA1 (Herkenham 1978). The parataenial and paraventricular nuclei innervate the dentate gyrus (with a dense termination in the hilus) and CA3. Thalamic inputs to the entorhinal cortex vary in the site of termination: the paraventricular nucleus projects mainly to the most medial part of the MEA, the nucleus centralis medialis projects to lateral LEA, whereas fibres from

the nucleus reuniens cover the entire extent of the entorhinal cortex (Yanagihara *et al.* 1987).

The anterior thalamic group of nuclei projects to layers I and III of the presubiculum and may provide feedforward information from the mammillary bodies

#### 4.4. THE HYPOTHALAMUS

Cells in the lateral preoptic area, the magnocellular preoptic area and the substantia innominata provide a cholinergic projection to the hippocampal formation (Wyss *et al.* 1979). A cell group distributed across the lateral hypothalamic area, the anterior dorsomedial nucleus and zona incerta (Pasquier and Reinoso-Suarez 1976) provides an additional diffuse innervation throughout the hippocampal formation.

Other hypothalamic inputs arise from cells around the supramammillary nucleus, which project to the dentate gyrus, CA3 and the retrohippocampal region (Segal 1979; Stanfield and Cowan 1984; Haglund *et al.* 1984), and from cells situated around the tuberomammillary nucleus and around the posterior hypothalamic area (Wyss *et al.* 1979).

#### 4.5. THE BRAINSTEM

##### 4.5.1. Midbrain - 5HT from the raphe nuclei (B6, B9)

The projection arises from the midbrain raphe, neurons in the tegmental reticular nucleus (Kohler and Steinbusch 1982) and the apical interpeduncular nucleus (Groenewegen and Steinbusch 1984). Both median and dorsal raphe nuclei innervate the entire hippocampal formation, while the tegmental reticular nucleus projects to the

entorhinal cortex only. All fibres except for 5-15% of those from the raphe nuclei are 5HTergic. All regions of the hippocampal formation receive an input, with the strongest innervation in the hilar region, and a less dense projection to the stratum moleculare of Ammon's horn. The retrohippocampal region has a grid-like innervation throughout every layer which is strongest in the molecular layers. Kohler (1982) highlights the existence of a dense terminal plexus in layer III of the LEA as indicative of a direct control over the lateral perforant path.

Fibres pass initially through the medial forebrain bundle. Two ascending fibre bundles, the median and dorsal raphe-forebrain tracts, split to run in three main fibre groups to the hippocampal formation (Azmitia 1978).

#### **4.5.2. Midbrain - dopamine from the ventral tegmental area (A8-10)**

Fibres from the ventral tegmental area terminate in all layers of the LEA, with a clustering pattern found in layers I, II and III (Hokfelt *et al.* 1974), and additional concentration in far lateral LEA. A relatively weak projection (the level of dopamine in the hippocampal formation is estimated to be one tenth that of noradrenaline) also reaches the ventral subiculum, the hilus, Ammon's horn and the pre- and parasubiculum (Scatton *et al.* 1980).

#### **4.5.3. Pons - noradrenaline from the locus coeruleus (A6)**

The diffuse noradrenergic input to the entire hippocampal formation (Fuxe 1965; Blackstad *et al.* 1967) is densest in the hilar region and ramifies in all layers of the retrohippocampal regions, thereby showing great similarity to the 5HT input. Within Ammon's horn, there is a dense innervation of the stratum lucidum of CA3 (the

termination zone of the dentate mossy fibres). In conjunction with the 5HTergic projection, the fibres run in the medial forebrain bundle before separating into the three fibre groups described above (Loy *et al.* 1980). The dorsal pathways innervate preferentially the septal parts of the hippocampal formation, while the ventral pathway provides an input to the temporal regions and the entorhinal cortex.

## 5. EXTRINSIC EFFERENTS OF THE HIPPOCAMPAL FORMATION

Extrinsic efferents are classed into two groups: one group innervates the neocortex while the other, known as the fornix-fimbria system, comprises the subcortical outflow of the hippocampal formation. Descending fibres from the hippocampal formation run in the fimbria and dorsal fornix to reach the ventral hippocampal commissure, in which run fibres destined for the contralateral hemisphere, while the remaining axons split to form two fibre bundles, the pre- and postcommissural fornix at the level of the septofimbrial nucleus. The precommissural fornix contains fibres directed towards the septal complex, the nucleus accumbens septi and the medial prefrontal cortex. The postcommissural fornix continues past the anterior commissure, at which point two fibre bundles split off. One of these, the medial cortico-hypothalamic tract, projects to the hypothalamic region, while the subiculo-thalamic tract projects to nuclei of the thalamus. The remnant of the postcommissural fornix, often described as the "column of the fornix", terminates in the mammillary body.

### 5.1. PROJECTIONS TO THE NEOCORTEX

#### 5.1.1. Efferents from the entorhinal cortex

The entorhinal cortex projects to several cortical olfactory areas, including the anterior olfactory nucleus, the olfactory tubercle and the piriform cortex (Krettek and Price 1977; Wyss 1981; Sorensen and Witter 1983). In the guinea pig, there are further projections to the cingulate gyrus and medial prefrontal cortex, and to regions of the insular and perirhinal cortex (Sorensen 1985). In the monkey, layer IV provides an

input to adjacent regions in the temporal cortex including areas 35, TA, TE, TF, TG and TH (Van Hoesen and Pandya 1975; Kosel *et al.* 1982).

In the rat, Swanson and Kohler (1986) reported that the entire cortical mantle ipsilaterally appeared to receive fibres from the LEA, while the projection to the contralateral side was less pronounced but still extensive. Most heavily innervated regions were the infralimbic, prelimbic and anterior limbic regions. It is of interest that this projection stemmed from a small population of layer IV pyramidal neurons located around the ventral bank of the rhinal sulcus, which incorporates the border with the perirhinal cortex.

In addition, layers II-IV of the LEA (and less so the MEA) were reported by Kosel *et al.* (1982) to send inputs to the perirhinal, ectorhinal and temporal areas.

#### **5.1.2. Efferents from the hippocampus and subicular complex**

The cortical projection from the hippocampus proper is limited: no projection is believed to arise from the dentate gyrus while in CA3, the projection is restricted to septally-located cells which provide an input to the retrosplenial cortex. Pyramidal cells in the septal region of CA1 have been found to project to the perirhinal cortex (Swanson and Cowan 1977), while an input to the infralimbic and prelimbic cortex arises from temporal CA1 (Swanson 1981).

Cells in the dorsal subiculum and in layers V and VI of the dorsal presubiculum (the postsubicular region) and parasubiculum send fibres which terminate in the superficial layers of the retrosplenial cortex (Meibach and Seigel 1977a; Swanson and Cowan 1977; Vogt and Miller 1983), with a further projection from the dorsal subiculum to the deep layers of the perirhinal cortex (Swanson and Cowan 1977; Deacon *et al.* 1983). Ventral parts of the subiculum and cells in the superficial layers of

the pre- and parasubiculum project to the medial prefrontal cortex in the rat (Swanson 1981; Swanson and Kohler 1986). Some evidence exists for an input to the inferior temporal region from superficially-located cells in the subiculum (Swanson and Kohler 1986).

## 5.2. THE PRECOMMISSURAL FORNIX

### 5.2.1. The septal complex

#### *Efferents from the entorhinal cortex*

The return connection with the septal region is provided mainly by the pyramidal neurons of layer IV of the LEA and MEA, with an additional contribution from layer II neurons located in the medial zones of both areas (Alonso and Kohler 1984; Witter and Groenewegen 1986). The fibres terminate in the lateral septal nucleus in a topographical fashion, such that lateral parts of the LEA and MEA innervate its dorsomedial region, while the medial parts of the two areas provide a dense projection to its ventrolateral extent. Some fibres are additionally distributed to the medial septal nucleus and to the horizontal limb of the nucleus of the diagonal band (Witter and Groenewegen 1986).

#### *Efferents from the CA3 field*

Fibres from the hippocampus and subiculum distribute to the lateral septal nucleus and to the triangular and septofimbrial nuclei (Raisman *et al.* 1966). The projection from the CA3 field is dense, and collaterals of CA3 axons are found to terminate across most of the expanse of the lateral septal nucleus, with the exception

of the rostral third of the nucleus. Additional collaterals cross in the ventral hippocampal commissure to provide a symmetrical (but slightly less dense) projection to the contralateral nucleus. Axon collaterals from the pyramidal cells of the CA2 field are also believed to project bilaterally to the lateral septal nucleus (Swanson and Cowan 1977). There is the possibility that a non-pyramidal projection exists: Alonso and Kohler (1982) have suggested that non-pyramidal cells provide a weak input to the medial septal complex, and several reports have indicated a contribution to the precommissural fornix of fibres originating in cells located in the stratum radiatum and the stratum oriens (Chronister and DeFrance 1979; Swanson *et al.* 1981; Alonso and Kohler 1982; Schwerdtfeger and Buhl 1986).

The projection from CA3 to the lateral septal nucleus (LSN) is topographically organized in two planes: septal regions of CA3 innervate dorsal regions of the LSN, while progressively more temporal parts of CA3 project to progressively more ventral areas of the LSN. In addition, there is a mediolateral gradient in the transverse plane, such that cells in medial (proximal) CA3 abutting the hilus provide an input to medial regions of the LSN, while lateral (distal) parts of CA3 near the CA2 border project to lateral parts of the LSN (Swanson and Cowan 1977).

The neurotransmitter utilized in the excitatory projection from CA3 pyramidal cells is believed to be glutamate (DeFrance *et al.* 1973; Storm-Mathisen and Opsahl 1978; Walaas and Fonnum 1980). The identity and action of the neurotransmitter(s) found in the non-pyramidal projection has yet to be elucidated.

#### *Efferents from the CA1 field*

The unilateral projection to the LSN from CA1 possesses a topographic organization in the longitudinal plane, with a septotemporal-dorsoventral gradient

similar to that observed in the CA3 pathway. Unlike the latter, CA1 fibres distribute to the rostral extreme of the LSN, with some fibres running further rostrally to terminate in the nucleus accumbens septi and the taenia tecta (Swanson and Cowan 1977; Swanson *et al.* 1981). As with the CA3 projection, the neurotransmitter in this pathway is assumed to be an excitatory amino acid.

#### *Efferents from the subiculum*

The subicular input is believed to be arranged in a similar fashion to the CA1 input, with additional collaterals from cells in ventral subiculum distributing to the bed nuclei of the stria terminalis (Swanson and Cowan 1977) and the nucleus accumbens (Yang and Mogensen 1984).

The subicular output is excitatory, and probably involves glutamate (Walaas and Fonnum 1980; Yang and Mogensen 1984), although the existence of neurotensin in this pathway has also been reported (Totterdell and Smith 1986).

#### **5.2.2. The nucleus accumbens septi**

A unilateral projection to the medial and anterolateral regions of the nucleus accumbens arises from cells in ventral CA1 and from the subiculum (Phillipson and Griffiths 1985). Asymmetric contacts are made on medium-sized spiny neurons (the output cells of the nucleus accumbens), suggesting that the projection to the nucleus accumbens represents a pathway through which the motor systems might be influenced (DeFrance and Yoshihara 1975; Yang and Mogensen 1984).

The pathway is believed to utilize glutamate as the neurotransmitter (Kelley and Domesick 1982), although additional data suggests the presence of another hitherto unidentified excitatory neurotransmitter (Yang and Mogensen 1985).

### 5.3. THE POSTCOMMISSURAL FORNIX

#### 5.3.1. The hypothalamus

The fibres of the medial cortico-hypothalamic tract run caudally through the anterior hypothalamic area to terminate in the shell of the ventromedial nucleus, the arcuate nucleus and basomedial parts of the lateral hypothalamic area (Nauta 1956). Cells in the ventral subiculum provide the majority of the fibres of this tract (Swanson and Cowan 1977; Krettek and Price 1978), with a limited number of CA3 cells located near to the ventral subiculum observed to project to the medial preoptic nucleus.

#### 5.3.2. The thalamus

Cells in the ventral subiculum project to several of the midline group of nuclei, notably the nucleus reuniens, the paraventricular nucleus and the parataenial nucleus by way of the subiculo-thalamic tract (Nauta 1956; Raisman *et al.* 1966; Krettek and Price 1978).

The projection to the anterior thalamic group is bilateral, and originates in the subicular complex. Cells in the deep regions of the pre- and parasubiculum project mainly to the anteroventral nucleus (Swanson and Cowan 1975, 1977), while the input to the anteromedial nucleus arises principally from the deep half of the subiculum (Meibach and Siegel 1977b). The subicular complex projects additionally to the anterodorsal, lateral dorsal and lateral posterior nuclei (Swanson and Cowan 1975, 1977). Donovan and Wyss (1983) have shown a degree of hodological heterogeneity in the subicular complex, in that the cells projecting to the thalamus constitute a separate population to those projecting to the entorhinal cortex.

### 5.3.3. The mammillary body

The final remnant of the postcommissural fornix terminates in the medial and lateral mammillary nuclei. A bilateral, topographically organized projection to the medial mammillary nucleus originates in the subiculum (Swanson and Cowan 1975), with dorsal subiculum projecting to dorsal parts of the nucleus, and ventral subiculum providing an input to ventral parts of the nucleus (Meibach and Siegel 1975). The pre- and parasubiculum project bilaterally to the medial and lateral mammillary nuclei (Swanson and Cowan 1975, 1977, Meibach and Siegel 1977a).

The hodological heterogeneity within the subicular complex suggested by Donovan and Wyss (1983) is also evident in the subiculo-mammillary projection: many cells in the subiculum projecting to the entorhinal cortex also give rise to an input to the medial mammillary nucleus (and constitute a population distinct from those projecting to the thalamus), whereas separate groups of neurons in the pre- and parasubiculum project to the entorhinal cortex and the mammillary body. The functional segregation within the subiculum is curious in view of the fact that the mammillary body provides a dense input to the anterior thalamic nuclei.

## SECTION 2

## MATERIALS AND METHODS

### Surgery

Forty-four adult male 250-500g Lister Hooded rats (supplied by Olac) were used in these studies. Animals were anaesthetized with a mixture of halothane and N<sub>2</sub>O/O<sub>2</sub>, and placed in a stereotaxic frame (Baltimore Instruments). Atropine sulphate was delivered subcutaneously to inhibit mucous secretions. Hollow trephine drill bits were used to create holes in the skull and incisions of the underlying dura mater were made using the tips of 25G syringe needles.

After sonication for a minimum of 30 minutes, 2.5-5% aqueous Fast Blue (Dr. Illing, Germany) and 25-50% aqueous rhodamine microspheres (Lumafluor Inc., New York USA) were injected through glass micropipettes (inside tip diameter 16-30µm for Fast Blue, 10-16µm for rhodamine microspheres). Co-ordinates for injections into the CA1 field, the CA3 field, and the lateral septal nucleus were calculated using the atlas of Paxinos and Watson (1986), although for the last thirty-three subjects the dorsoventral position of injections into the hippocampus was determined instead using an electrode adjacent to the pipette tip. Dye expulsion was achieved using a high pressure valve (Lee Instruments) connected to an air reservoir, allowing pressurised air of up to 40 psi (pounds per square inch) to reach the pipette. The period for which the valve remained open was regulated by an electronic timer with a bandwidth of 10-200ms. Injections of 10-50nl were delivered in increments over a ten minute period, after which the pipette was withdrawn and the skin sutured. 0.15ml Temgesic (buprenorphine) was administered intramuscularly to provide post-operative analgesia.

## **Perfusion and Histology**

Preliminary studies (see Appendix I) have shown that optimal labelling with Fast Blue occurs after a survival time of 4-6 days, while the optimal labelling of the rhodamine microspheres is attained after 2 days, with no diminution in the quality of labelling over longer survival periods (Katz 1984). This persistence of the rhodamine microspheres obviated the need to inject the two dyes at separate times.

After a survival time of 4-6 days, 0.3-0.4ml of Lethobarb (pentobarbitone) was given intraperitoneally. This range of lethal dose resulted in a gradual depression of respiration and concomitant rise in blood CO<sub>2</sub> levels, which led in turn to cerebral vasodilatation, allowing a better passage of perfusate through the brain.

After a rapid (2 minute) exsanguination with isotonic saline, the animal was perfused transcardially with 500ml of 4% formaldehyde in 0.1M phosphate buffer at pH 7.4, followed by a 15% sucrose solution in 500ml of the above. Total perfusion time was 30 minutes. The brain was then removed and bisected along the midline. Both halves were then postfixed for 1-3 days in 20% sucrose cryoprotectant in 0.1M phosphate-buffered 4% formaldehyde.

Serial coronal sections were cut on a Leitz freezing microtome at 35µm and mounted from distilled water onto ungelatinised slides. After overnight drying in air the slides were coverslipped using D.P.X. mountant.

### **Hippocampal extension**

For the last eighteen subjects, the brain was halved and the hemibrain containing the injection sites was postfixed and cut coronally as described above. The contralateral hippocampus was dissected from the remaining half and extended along

its septotemporal axis by compression between four microscope slides, in accordance with the technique described by Gaarskjaer (1978a,b). The extended hippocampus and the rest of the hemibrain were then postfixed as above. Further extension of the hippocampus was achieved by manipulation of the tissue on the microtome chuck as it was frozen gradually from the temporal pole up, although a degree of curvature at this end could not be removed entirely. Serial sections of 35 $\mu$ m thickness were cut transverse to the septotemporal axis and mounted as above.

### **Acute electrophysiological recording**

During the initial stages of this study, the rat atlas of Paxinos and Watson (1986) was used to obtain co-ordinates for injections across the extent of the hippocampus. Given the variations in brain dimensions for different strains, and across individual rats, such an atlas could not be relied upon for accurate dye placement in the hippocampal dendritic fields. Instead, an acute electrophysiological recording setup was incorporated alongside the injection apparatus to monitor the complex spike activity of the hippocampal pyramidal cells in order to determine the dorsoventral injection placement. For these experiments, the anteroposterior and mediolateral co-ordinates were calculated from the rat atlas and previous results.

A single length of 17 $\mu$ m diameter Teflon-coated platinum-iridium wire (California Fine Wire Company) was glued with epoxy resin to the barrel of a glass micropipette such that the electrode tip was positioned from 300 $\mu$ m behind to 300 $\mu$ m in front of the pipette tip. The electrode tip was plated with platinum black (Merrill and Ainsworth 1972) before assembly in order to reduce the impedance to the range 100-250 k $\Omega$  at 1 kHz. The other end of the wire was flamed clean of Teflon and affixed to 30G metal tubing mounted with epoxy resin onto the pipette barrel at least 2cm from

the tip. The metal tubing was connected by a crocodile clip to a field effect transistor head stage and the output fed into an AC preamplifier (Neurolog System, Digitimer Ltd., UK). After filtering (bandpass 800Hz-8kHz) and further amplification, the trace was displayed on a Gould oscilloscope. Peak-to-peak spike amplitude was in the order of  $200\mu\text{V}$ . The signal to noise ratio was around the order of 5:1.

As the electrode/pipette was lowered into the brain, single spike activity was recorded from pyramidal cells in the deeper cortical layers (about  $1400\text{-}1800\mu\text{m}$  deep to the brain surface), which ceased upon passage through the corpus callosum. Upon reaching the alveus and stratum oriens of CA1, small complex spikes were recorded which grew in amplitude as the electrode neared the cell layers. As the electrode/pipette punctured the pyramidal cell layer there was a sustained complex spike discharge which persisted for  $150\text{-}250\mu\text{m}$ . Recording of spike activity ceased as soon as the electrode exited the cell layer. For injections within CA3, passage through the stratum moleculare of CA1/CA3 preceded the small complex spikes recorded in the proximal stratum radiatum of CA3, followed by a second pyramidal cell discharge lasting for  $250\text{-}300\mu\text{m}$  through the thicker CA3 layer. Dye injections in proximal CA3 (adjacent to the hilus) required that the electrode/pipette pass through the dentate gyrus: in these cases, granule cell discharge in the form of a short burst of single spike firing (peak-to-peak amplitude  $80\mu\text{V}$ ) preceded the complex spike activity in CA3 by approximately  $250\mu\text{m}$ .

With this apparatus, the pipette tip could be located with confidence at any level in the dendritic fields of CA1 and CA3 to provide specific injections. Since the electrode diameter was smaller than the outside diameter of the pipette tip, extra tissue damage due to the inclusion of an electrode next to the pipette was relatively minor.

50 $\mu$ V  
20ms

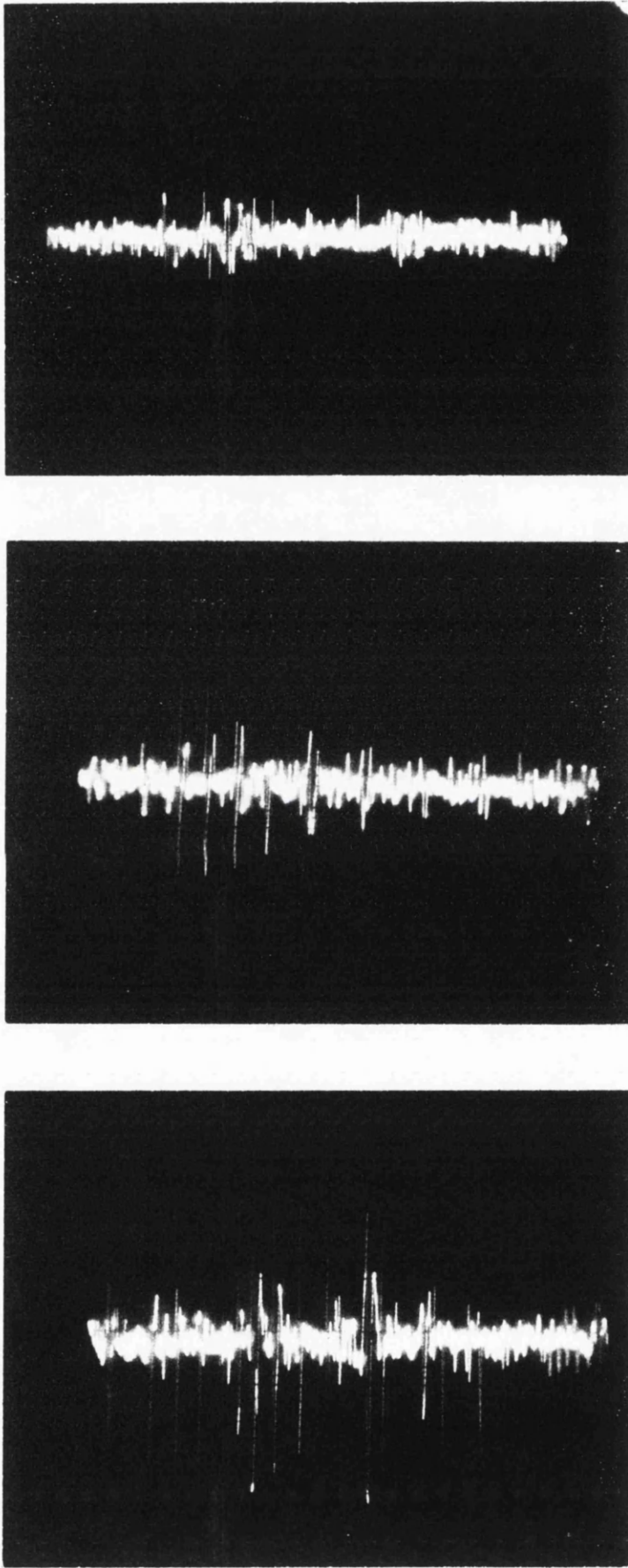


Fig.3a Traces of complex spike hippocampal activity recorded by the microelectrode as the pipette is lowered into the hippocampus. In all cases a 100ms time sweep is shown. *Top* alveus, 250 $\mu$ m above CA1 cell layer (peak-to-peak spike amplitude 60 $\mu$ V) *Middle* entry into CA1 (peak-to-peak 130 $\mu$ V) *Bottom* middle of the CA1 cell layer (peak-to-peak 200 $\mu$ V).

Fig.3b (Overleaf) A typical complex spike firing pattern in CA1 (20ms time sweep; peak-to-peak 150 $\mu$ V)

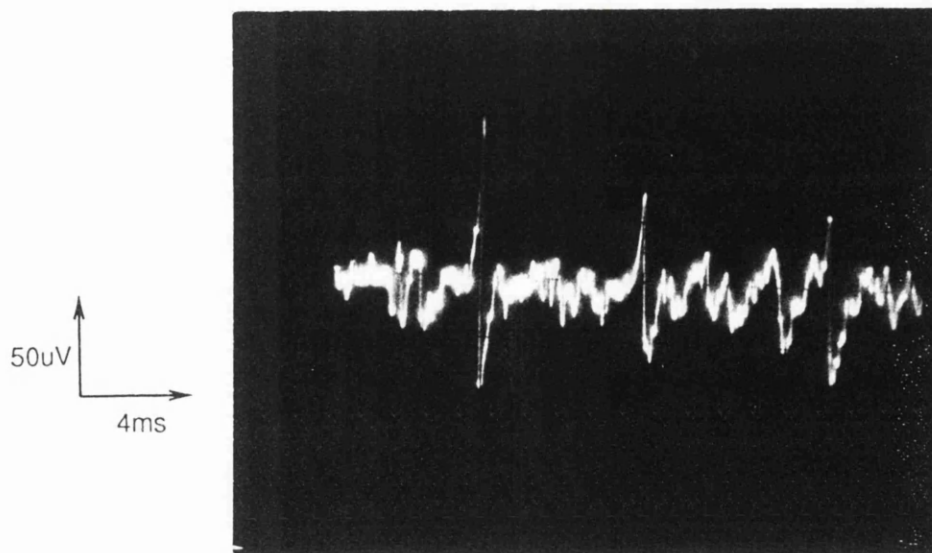


Fig.3b

### Data analysis

Fluorescent and transmitted light microscopy was carried out using a Nikon Labophot-2 microscope equipped with a dual epifluorescent filter block (excitation wavelength 365nm for Fast Blue, 546nm for rhodamine). Alternate coronal sections from one brain were mounted onto gelatinised slides and counterstained with Cresyl Fast Violet to provide Nissl-stained templates of the hippocampus and of the entorhinal cortex. A similar template of the extended hippocampus was taken from sections transverse to the septotemporal axis. Twenty-five representative sections (equivalent to every fifth section from the coronal hippocampus and entorhinal cortex templates, and every eighth section from the template of the extended hippocampus) were drawn by camera lucida and digitized onto a Summagraphics Bitpad. The injection sites, and the resultant labelling, were plotted onto the corresponding parts of the templates and digitized to provide a pattern of labelling across the extent of the hippocampus (and, where appropriate, the entorhinal cortex). Data was transferred from the Bitpad onto an Opus PCIII and was plotted using an Apple Laserwriter IINT.

## RESULTS

### **Preliminary studies**

Prior to the experiments detailed below, preliminary double-labelling studies were conducted using the fluorescent tracers Fast Blue and Diamidino Yellow. Poor transport of the Diamidino Yellow tracer, allied to dissatisfaction over the yellow artefact characteristic of Fast Blue which served to obscure the Diamidino Yellow labelling, led to the substitution of rhodamine microspheres for Diamidino Yellow.

### **Representation of results**

Results are displayed in the following manner: 12 of the 25 sections taken from each hippocampus are shown, with sections 1 and 23 representing respectively in coronal view the rostral and caudal poles of the CA3 field or, in the case of transverse sections cut from extended hippocampi, the septal and temporal poles of CA3. The position of the injection site within CA1 is shown as a blue (Fast Blue) or red (rhodamine) circle. The injection site represents the estimated region of CA1 pyramidal cells whose dendrites are encompassed by the uptake zone of the injection. In bilateral studies, Fast Blue was routinely injected into the right CA1 field, and rhodamine microspheres into the homotopic area in the left CA1 field, whereas in unilateral experiments both dyes were injected into the left side. Injection site diameters were measured using a calibrated eyepiece graticule fitted onto the microscope.

Retrograde labelling is displayed in the form of circles (for Fast Blue labelling) or crosses (for rhodamine labelling). For the sake of clarity, the backfilling for each dye is represented separately; note that this does *not* indicate that the two groups of labelled cells are distinct and that individual cells were preferentially labelled with one or other dye (the proportion of double-labelled cells will be discussed presently). Individual cells are shown as single circles (or crosses), while areas of the cell layer in which the number of backfilled cells was estimated to be in excess of 90% of the total number of cells within those areas are represented by a solid line of circles (or crosses).

## CONTROL INJECTIONS

### A. A test of the labelling due to disruption of extrahippocampal fibres of passage

*En route* to the hippocampus, the injection pipette penetrates the fibre bundles of the corpus callosum, the dorsal hippocampal commissure and the alveus. Since Fast Blue is believed to be taken up by damaged axons, with preliminary reports suggesting a similar property of the rhodamine microspheres, control injections were delivered. The injection site spanned the corpus callosum and dorsal hippocampal commissure (the small size, and proximity to the basal dendritic field of CA1, rendered infeasible a control injection into the alveus). In this fashion the consequences of damage to extrahippocampal fibres of passage can be evaluated; in comparison, the problem of damage to *intra*hippocampal fibres of passage is addressed on pages 111-112.

In subject T144, the two dyes were delivered unilaterally, and the survival time and histological technique were similar to that described in *Materials and Methods*.

#### *Fast Blue injection*

10nl of Fast Blue were delivered at a location in the caudal half of the hippocampus. The site covered a part of the corpus callosum (underlying the occipital cortex) and dorsal hippocampal commissure with no discernible leakage of dye into the stratum oriens of CA1. A rostrocaudal analysis of the backfilling demonstrated sparse labelling of cells located in all layers of frontal cortex, and a virtual absence of labelled cells within the parietal region. More caudally, dense labelling was observed in the postsubiculum and dorsal presubiculum (but not the parasubiculum). Dense cortical labelling was noted in occipital cortex and sparse labelling within the temporal area, with the backfilled cells located mainly in the deep cortical layers (although some cells

were also seen in layers II and III). No labelling was observed within the hippocampus proper, subiculum, ventral pre- and parasubiculum, or in the entorhinal and perirhinal areas.

### *Rhodamine injection*

15nl of rhodamine microspheres were injected near the rostral pole of the hippocampus. The injection site remained located within the corpus callosum (underlying the frontal cortex). No leakage into the stratum oriens of CA3 was noted. Rostrally, few labelled cells were found within the frontal cortex, while the parietal cortex exhibited substantial backfilling in all layers. In caudal regions, the labelling within the occipital cortex and temporal cortex was found to be very sparse and was confined to the deep layers. Labelled cells in the dorsal subiculum were also seen, although the density of labelled cells was markedly less than that observed following the injection of Fast Blue described above. No labelling was noted in the hippocampus proper, the subiculum, ventral presubiculum, parasubiculum, or the entorhinal and perirhinal regions.

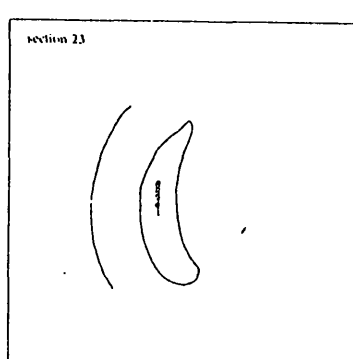
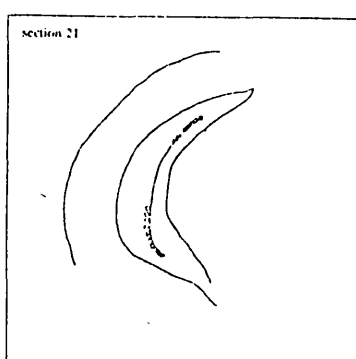
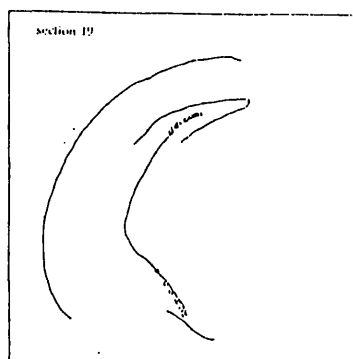
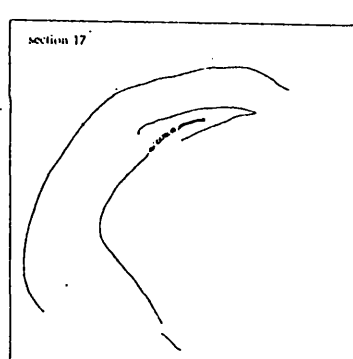
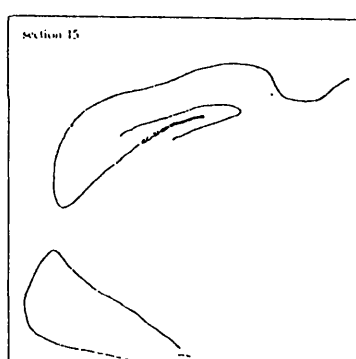
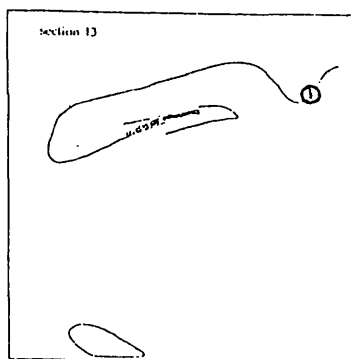
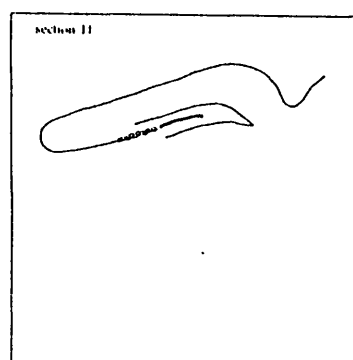
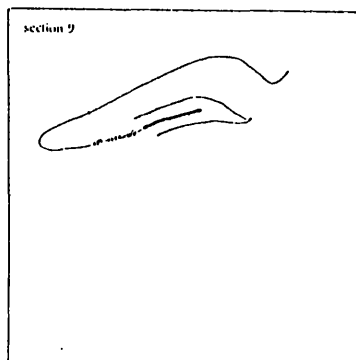
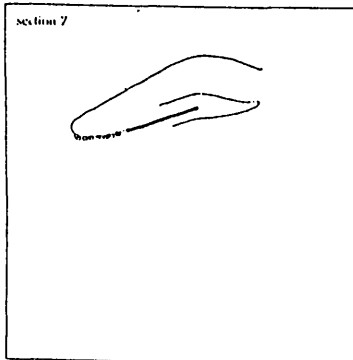
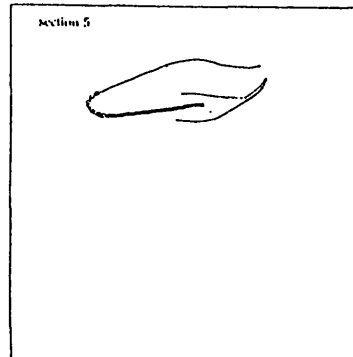
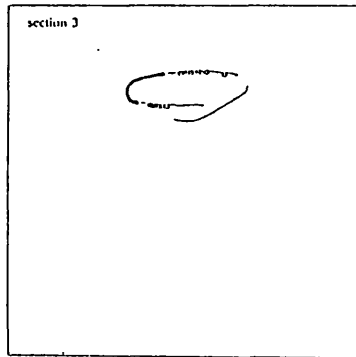
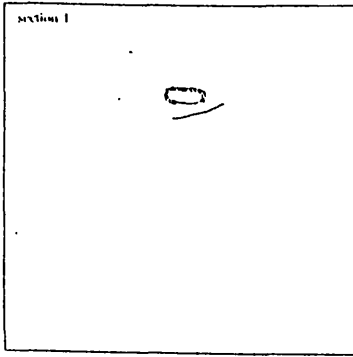
The conclusion from this experiment is that the damage to fibres in the corpus callosum and the dorsal hippocampal commissure caused by the passage of the injection pipette results in labelling of cells in the area of neocortex in the neighbourhood of the injection site, which presumably send an axon to the contralateral hemisphere through the damaged callosal region. The backfilling in the presubiculum is presumed to stem from injury to the axons coursing through the dorsal hippocampal commissure *en route* to the contralateral entorhinal area. In view of these findings, damage to extrahippocampal fibres of passage was not believed to influence the patterns of labelling following intrahippocampal injections.

## B. Co-injection of dyes: a test of relative dye characteristics

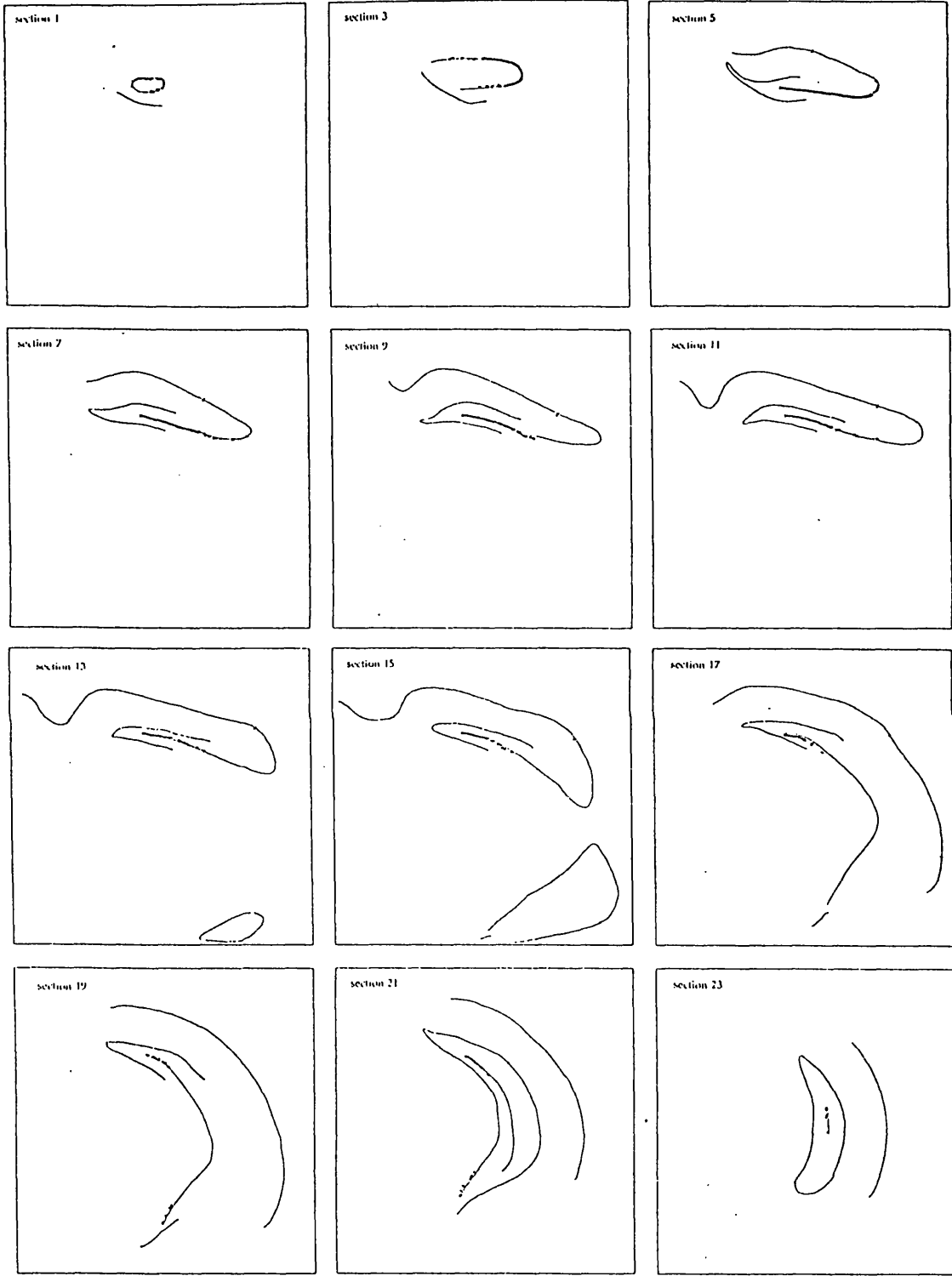
In one subject (T73), a comparison of the labelling characteristics of the two fluorescent tracers was undertaken. Equal quantities of the two dyes were mixed and sonicated for an hour and 20nl of the mixture were injected into one site in CA1. The extent of the resultant backfilling could therefore be used to compare the characteristics of the two dyes: if these were equivalent, then one would expect every backfilled cell to be double-labelled, whereas differences in dye transport or sensitivity, size of uptake region at the injection site, or in the degree of labelling as a result of damage to fibres of passage would cause a disparity in the extent of backfilling of each dye. Further studies could then be undertaken to determine the cause of the disparity.

The Fast Blue labelling in the ipsilateral hippocampus, and the rhodamine labelling in the contralateral hippocampus are shown in the following pages. Both dyes produced labelling in both CA3 fields and the bilateral labelling for each dye was found to be symmetrical in nature (see Experiment I for a discussion of this phenomenon). Although the diffusion of Fast Blue at the injection site appears to suggest an uptake area far greater than that of the rhodamine microspheres (which do not diffuse from the site of injection), the comparable labelling achieved with the two co-injected dyes suggests that the region of uptake of Fast Blue is equivalent to the central necrotic zone at the injection site (which corresponds approximately in extent with the rhodamine injection site), in agreement with the conclusion reached by Condé (1987).

An analysis of the backfilling in CA3 revealed that over 95% of backfilled cells were double-labelled, indicating a near-total correspondence of the two dyes. In view of this, the dyes were deemed suitable for use in the following experiments.



T73(RHO) - contralateral



### C. A comparative study of an injection of 2nl of rhodamine microspheres

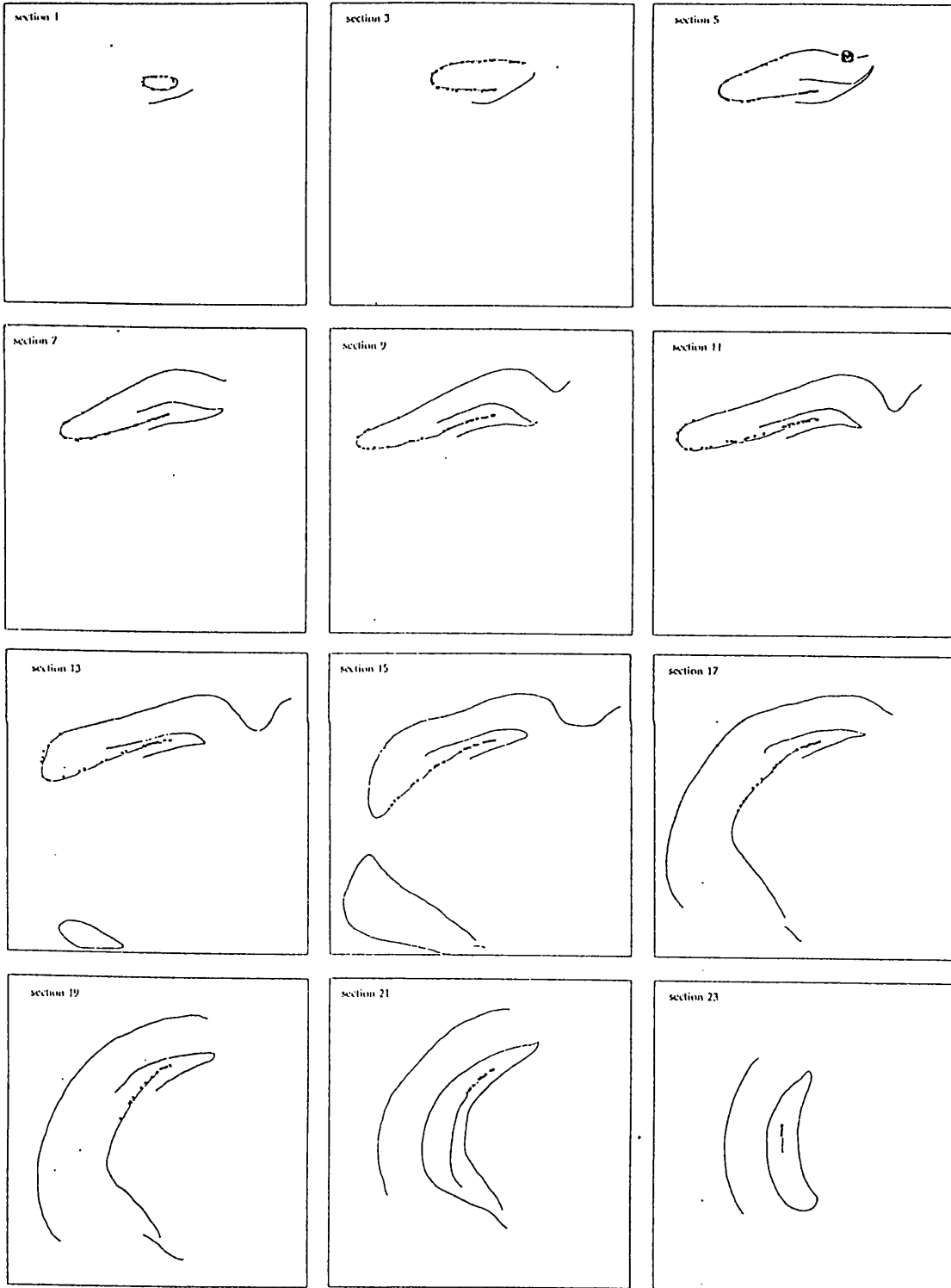
Results from the previous experiments indicate that an injection of 20nl of dye, resulting in a region of uptake approximately 500 $\mu$ m in diameter, produces backfilling which spreads across a large fraction of the septotemporal and transverse extents of the CA3 field. Although the uptake site covers an area of the stratum pyramidale of CA1 which is less than 1% of the total area of the CA1 pyramidal cell layer (a diameter of 500 $\mu$ m gives a site area of 0.2mm<sup>2</sup>, in comparison with the total area of CA1, which is estimated at around 21mm<sup>2</sup>), such an injection is calculated to encompass approximately 2x10<sup>3</sup> CA1 cells, given that there are approximately 2x10<sup>5</sup> pyramidal cells in a (unilateral) CA1 field (figure quoted from Amaral *et al.* 1990), and assuming that there is a homogeneity in cell density across the CA1 field.

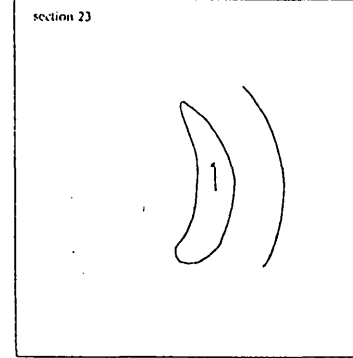
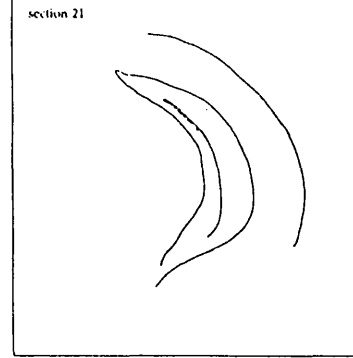
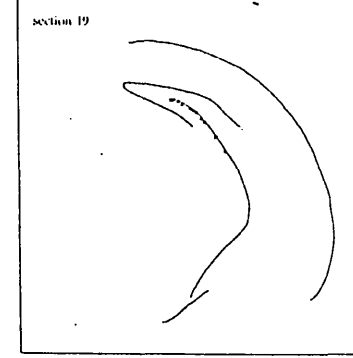
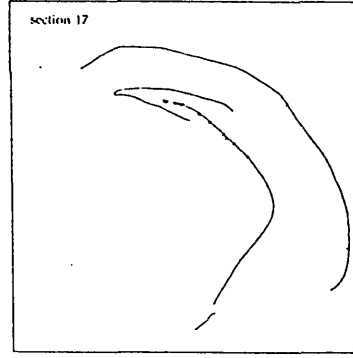
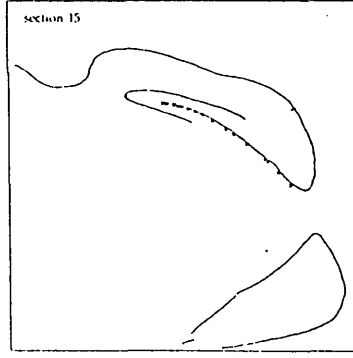
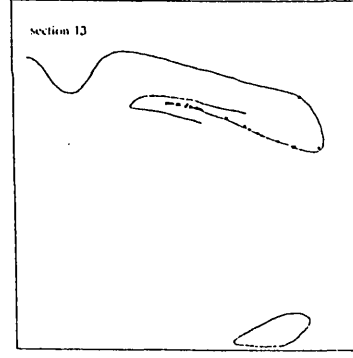
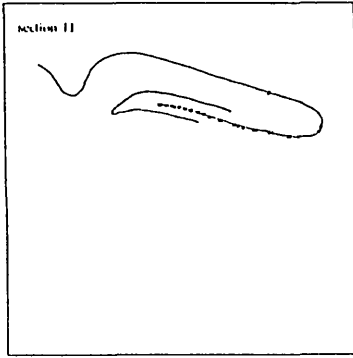
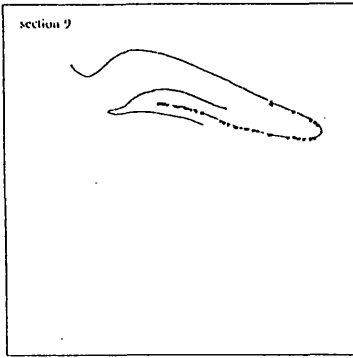
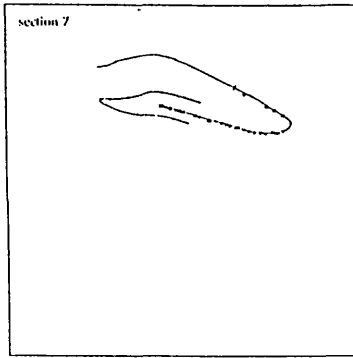
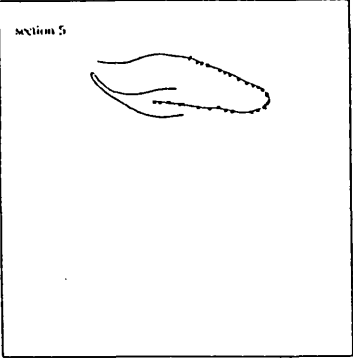
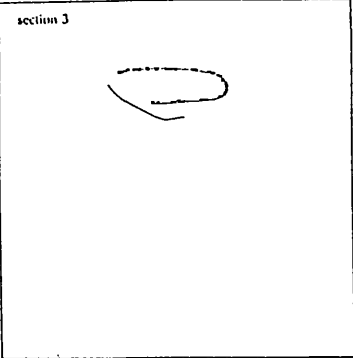
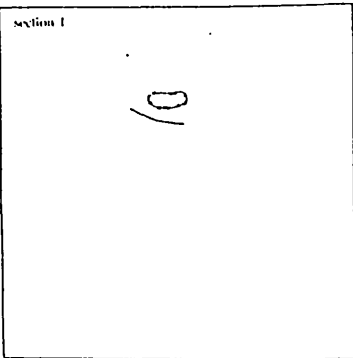
The degree of convergence of inputs from CA3 to CA1 cannot therefore be calculated using injections of this magnitude: at one end of the spectrum of possible explanations, CA3 cells send out numerous collaterals, so that each CA1 cell is the recipient of a collateral from *every* cell backfilled in CA3. At the other extreme, one might assume that the outflow from every CA3 cell is restricted to a single collateral, such that an individual CA1 cell only receives a limited group of inputs, the number of which can be obtained by dividing the number of labelled cells in CA3 by the number of CA1 cells constituting the uptake area.

A clearer understanding of the convergent properties of the projection was attempted by the application of a very small quantity (2nl) of rhodamine microspheres into CA1, in the hope of creating a much reduced area of uptake. The results from this experiment (T74) are shown overleaf.

Although a quantitative comparison of this sort is best made following an injection of different size into the same location, some conclusions can be drawn by

T74(RHO) - ipsilateral





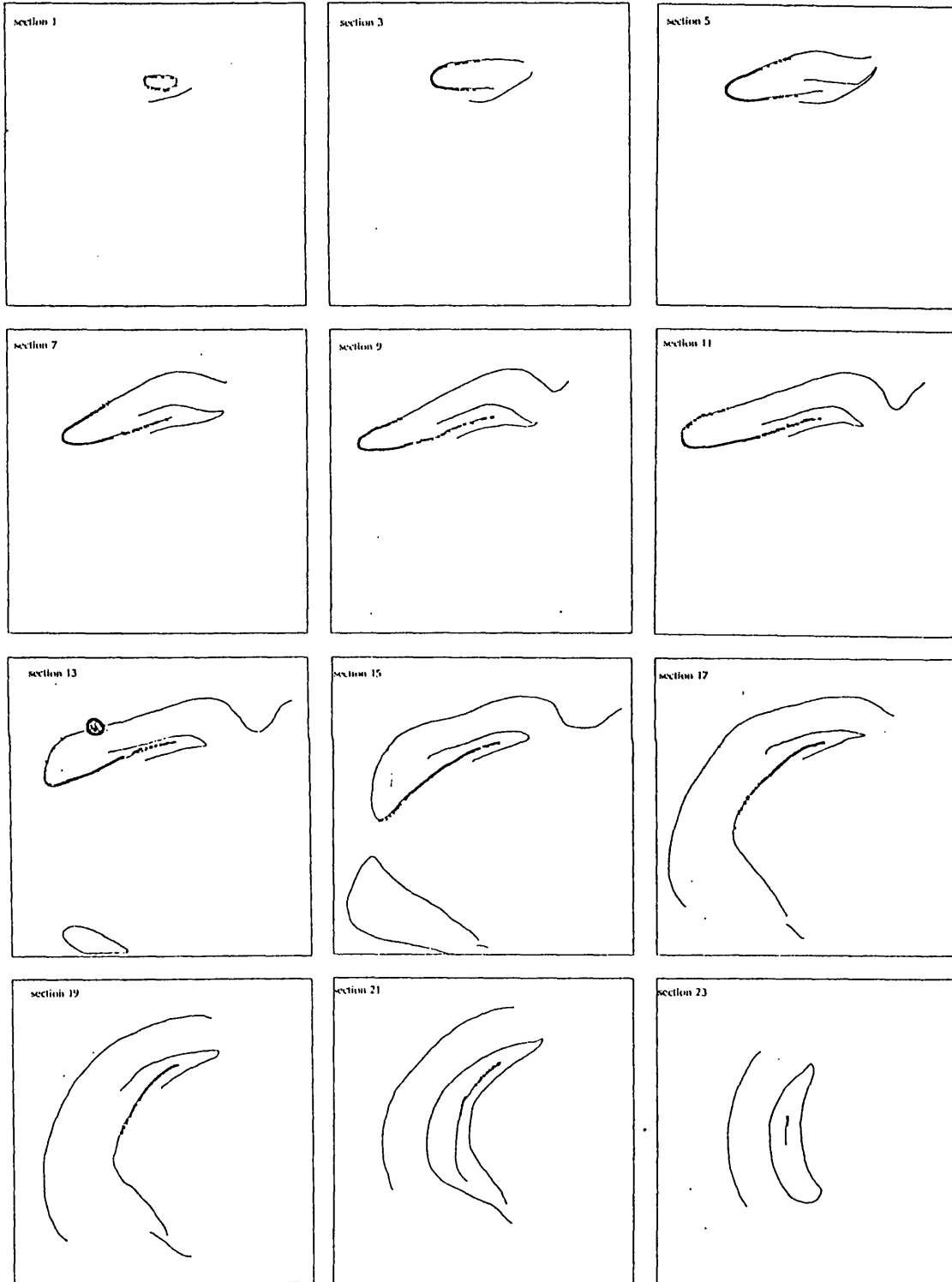
contrasting the results from this injection with those from injections placed into other parts of CA1 which are an order of magnitude greater in quantity and in extent (such as the injections T64 and T65, the results of which are displayed on pages 106-113). The extent of the CA3 field covered by the labelled cells following injection T74 is seen to be of a similar magnitude to that observed for injections ten times greater in quantity. Within this expanse, however, the density of labelling is much sparser, both in terms of the fraction of cells labelled, and in the intensity of backfilling in each cell (with a much reduced number of microspheres per labelled cell in this instance). Injection T74 also demonstrates several features of the CA3-CA1 projection common to the larger injections. Firstly, the labelling was mostly confined to a specific region in CA3, with a negligible number of individually-filled cells present outside its boundaries. Secondly, the position of labelled cells varied according to rostrocaudal level, with a shift in position towards the hilar end of CA3 noted in the caudal direction. Finally, the labelling in the contralateral CA3 field was found to be comparable both in terms of extent and of the number of cells labelled, in accordance with the bilateral symmetry of the projection shown in Experiment I.

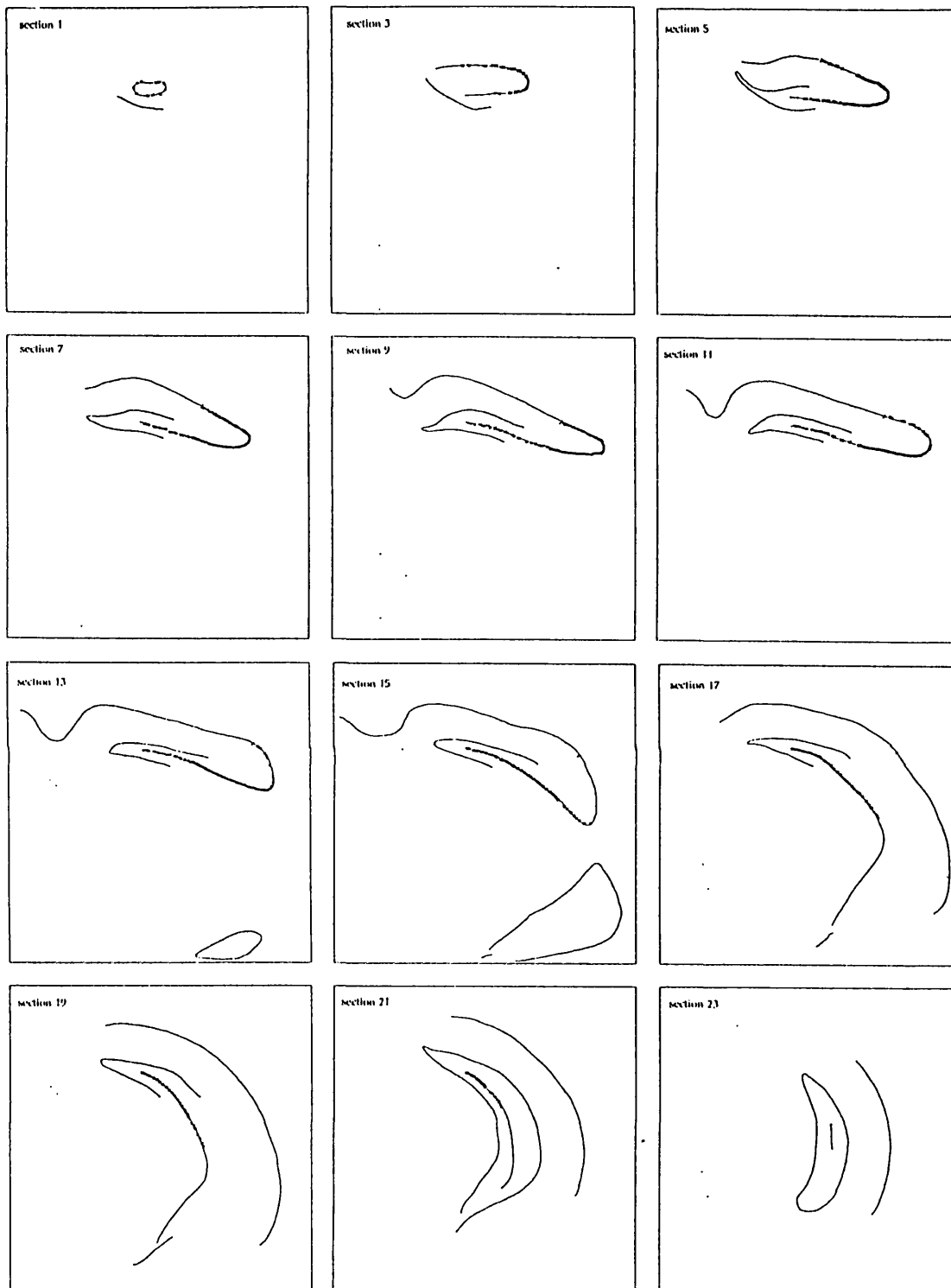
The conclusion to be drawn from this experiment is that there appears to be a rough correlation between the number of projecting CA3 cells and the number of CA1 cells receiving the projections. Furthermore, the cells projecting to a small area of CA1 are scattered over a large extent of CA3 similar in magnitude to that occupied by CA3 cells projecting to a much larger number of cells located in the same part of the CA1 field. It would seem therefore that the CA3-CA1 projection does not follow any "point-to-point" topography, with the implication that a group of cells located in a restricted part of the CA1 field are the recipients of inputs from cells situated over a large part of the septotemporal extent of CA3.

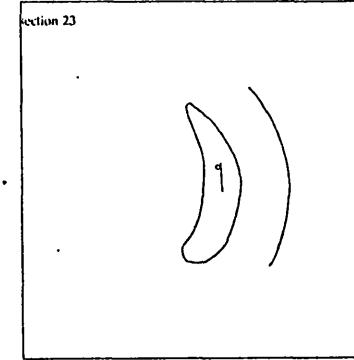
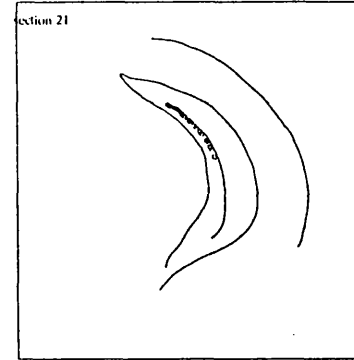
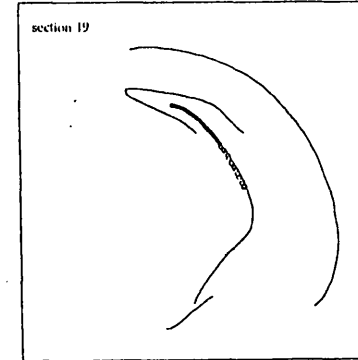
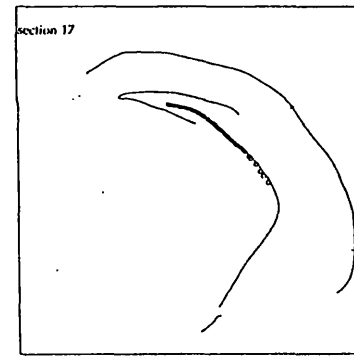
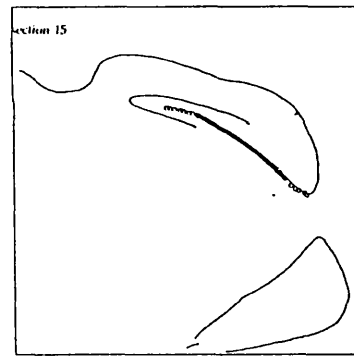
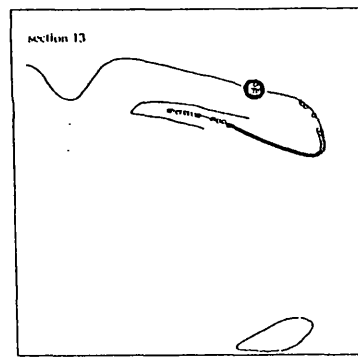
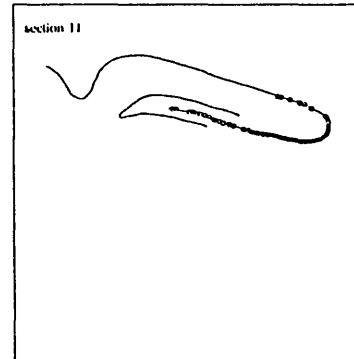
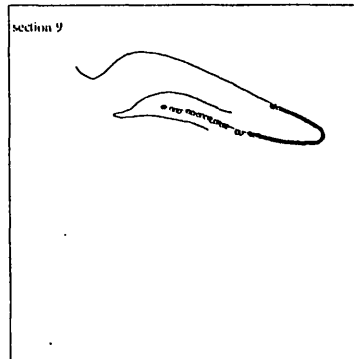
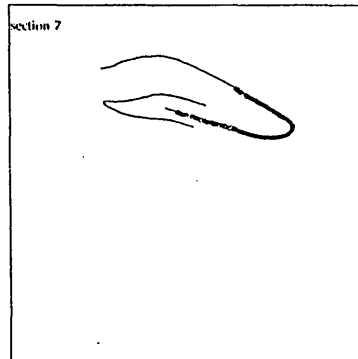
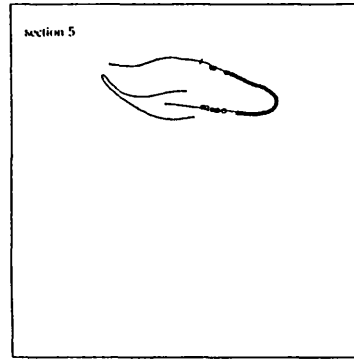
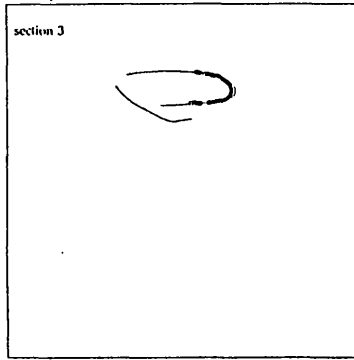
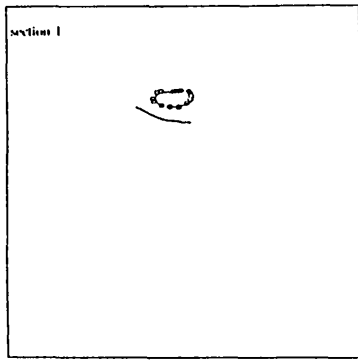
## **EXPERIMENT I: A double-labelling study of the bilateral organization of the CA3-CA1 projection**

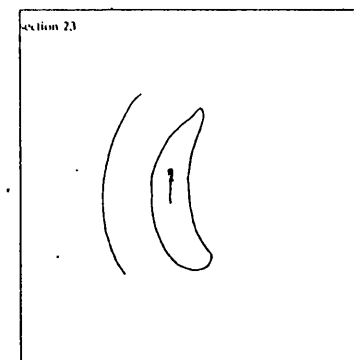
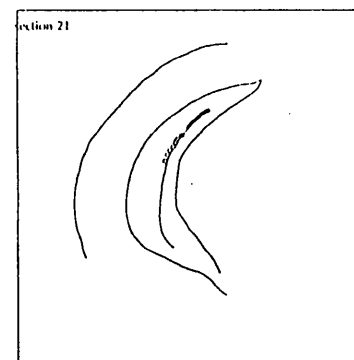
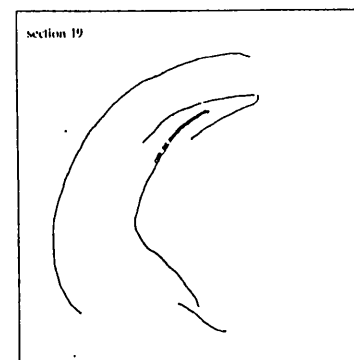
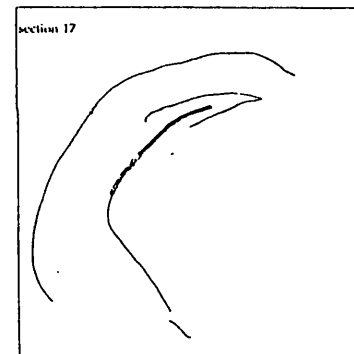
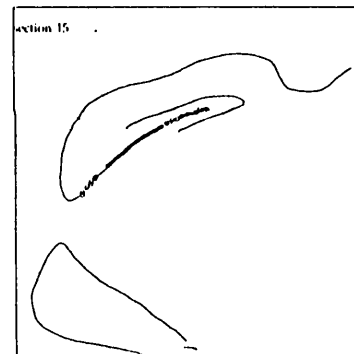
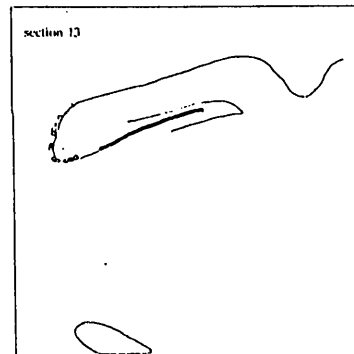
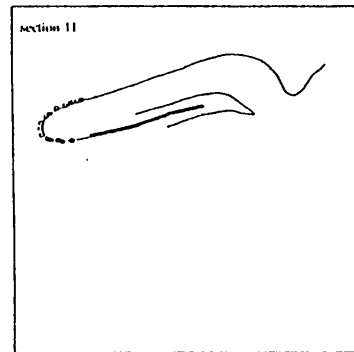
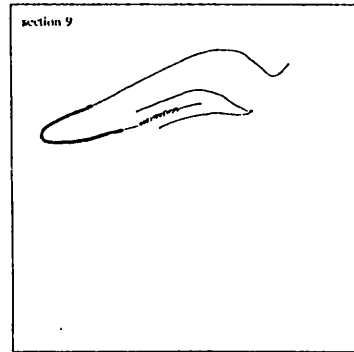
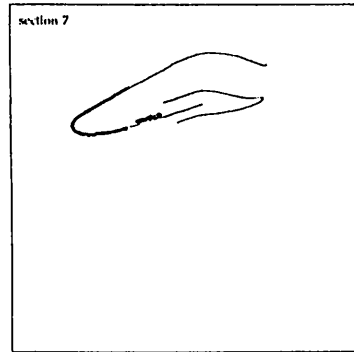
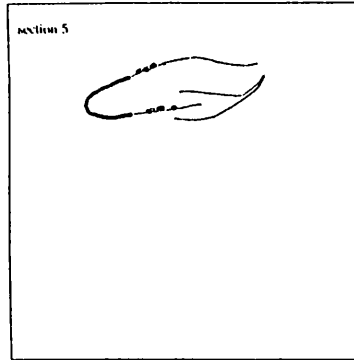
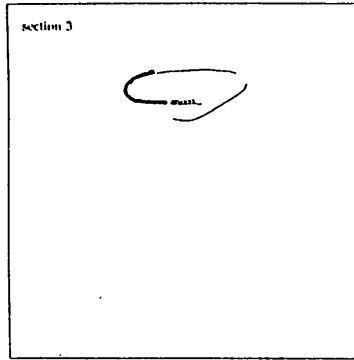
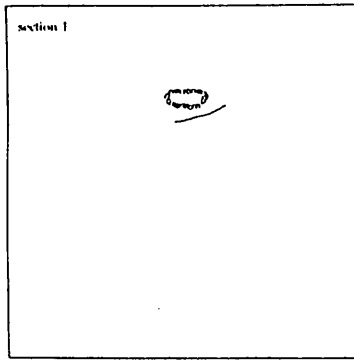
This study aimed to evaluate the bilateral organization of the CA3-CA1 projection by comparing the distribution of labelling in the CA3 field bilaterally following injections of the retrograde fluorescent dyes Fast Blue and rhodamine microspheres into homologous sites in the two CA1 fields. Data were taken from six brains (out of a total of ten subjects), in which the injections were deemed to be similar enough in size and placement within the CA1 fields for an adequate comparison of the bilateral projection to be made.

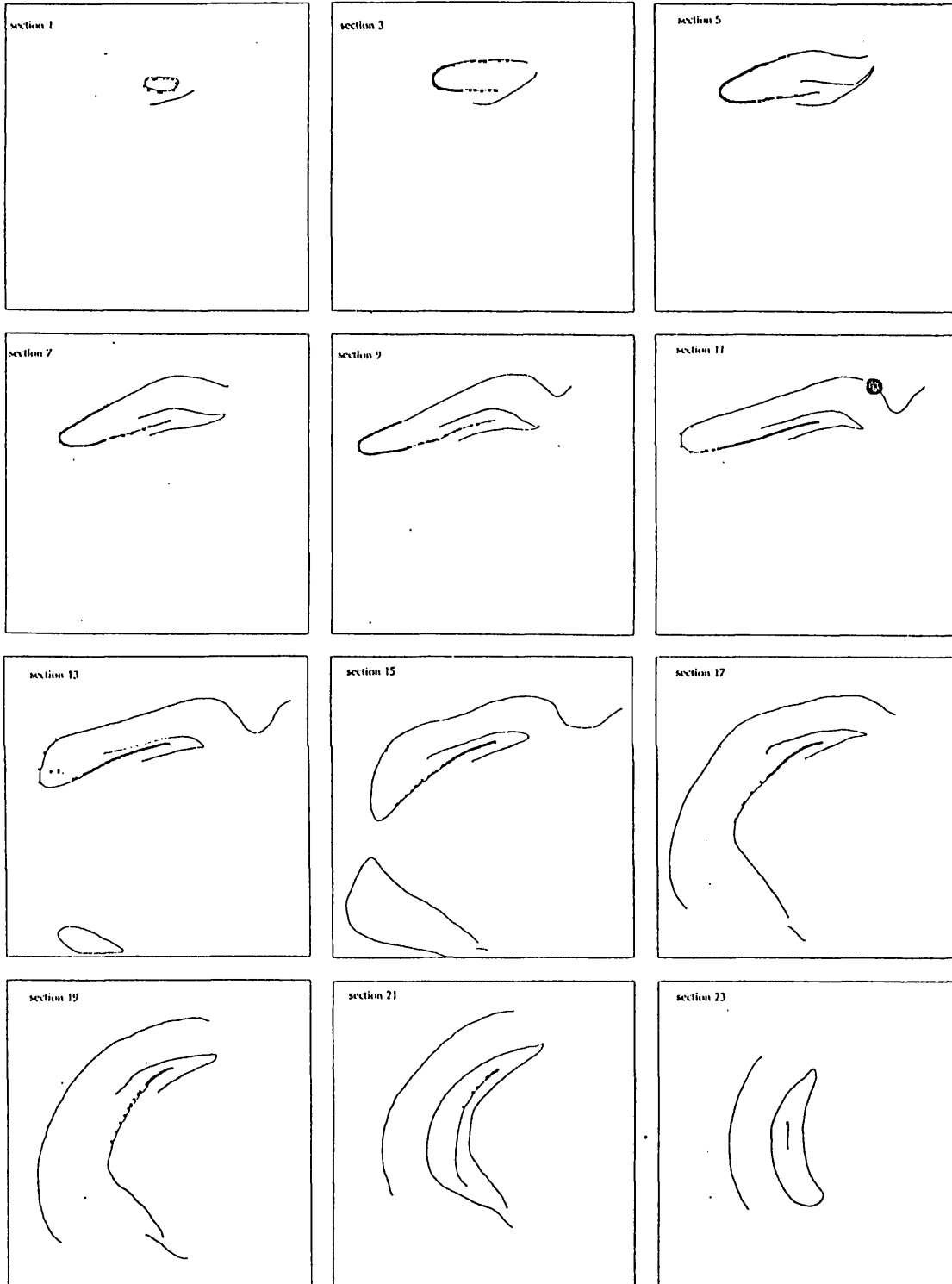
In the two examples displayed overleaf, injections were placed around the middle of the rostrocaudal extent of the hippocampus, with one placement in proximal CA1 (T64 - pages 106-109) and one in distal CA1 (T65 - pages 110-113). All injection sites were located within the stratum radiatum. In each case the bilateral labelling from each dye is shown separately.

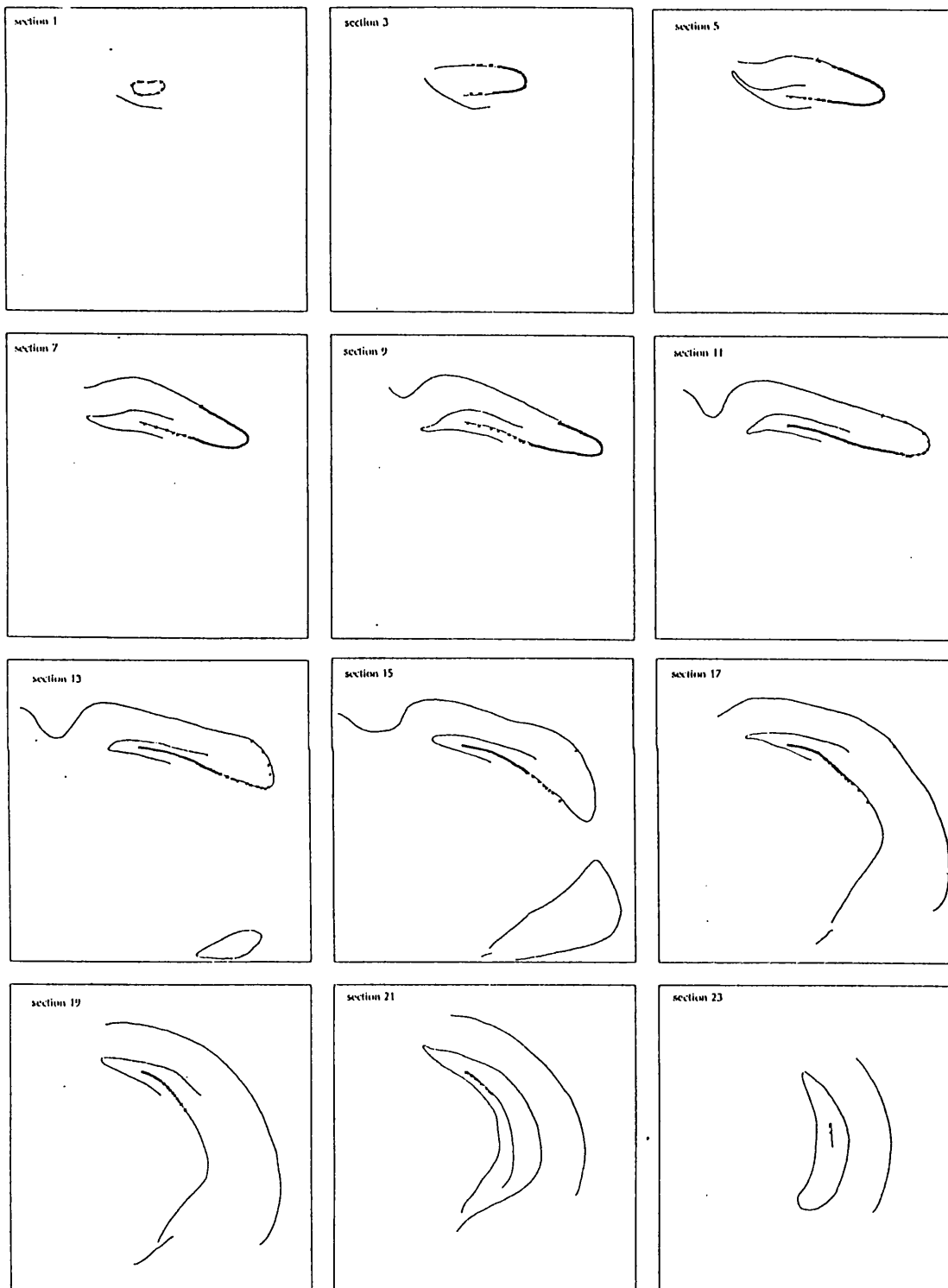


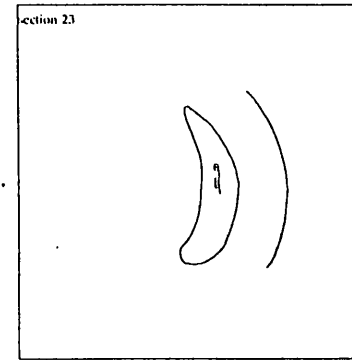
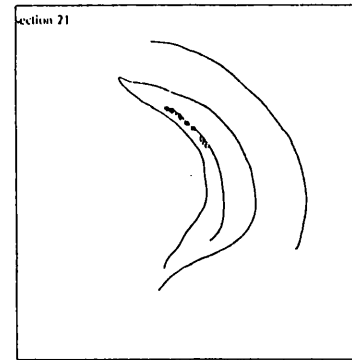
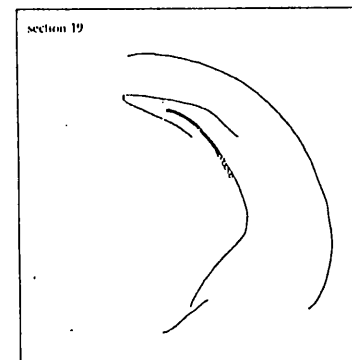
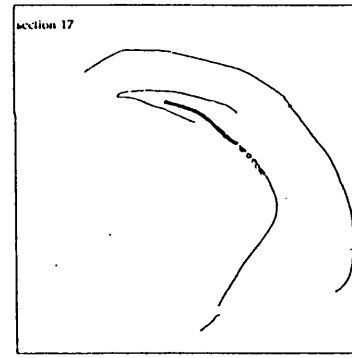
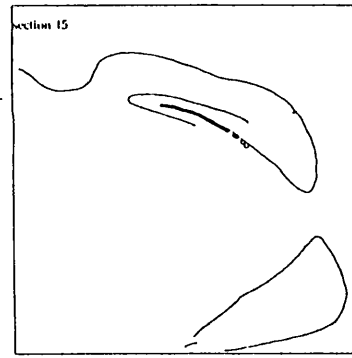
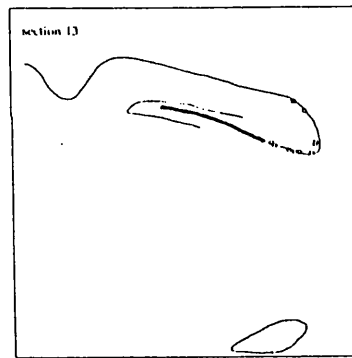
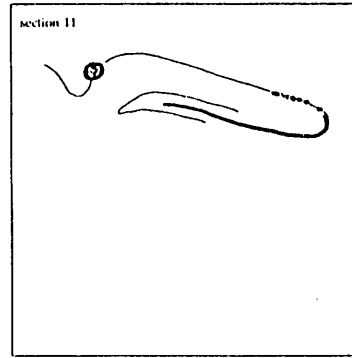
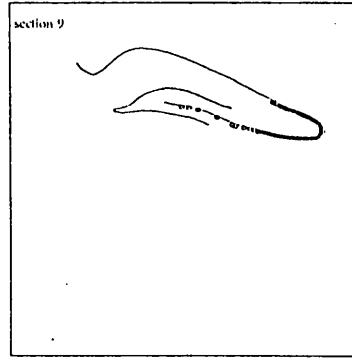
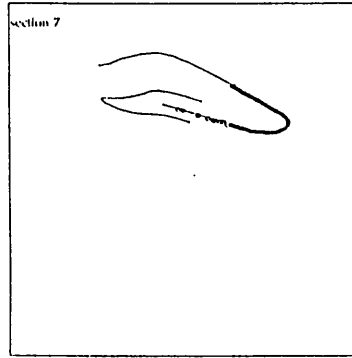
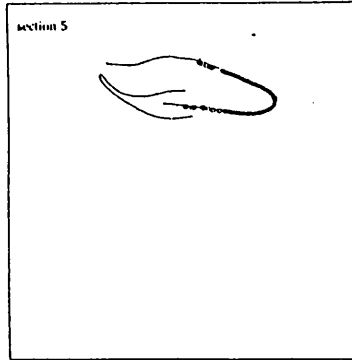
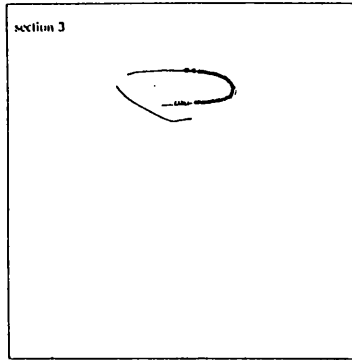
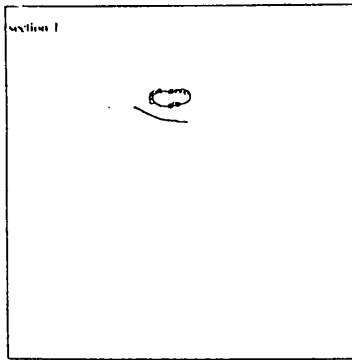


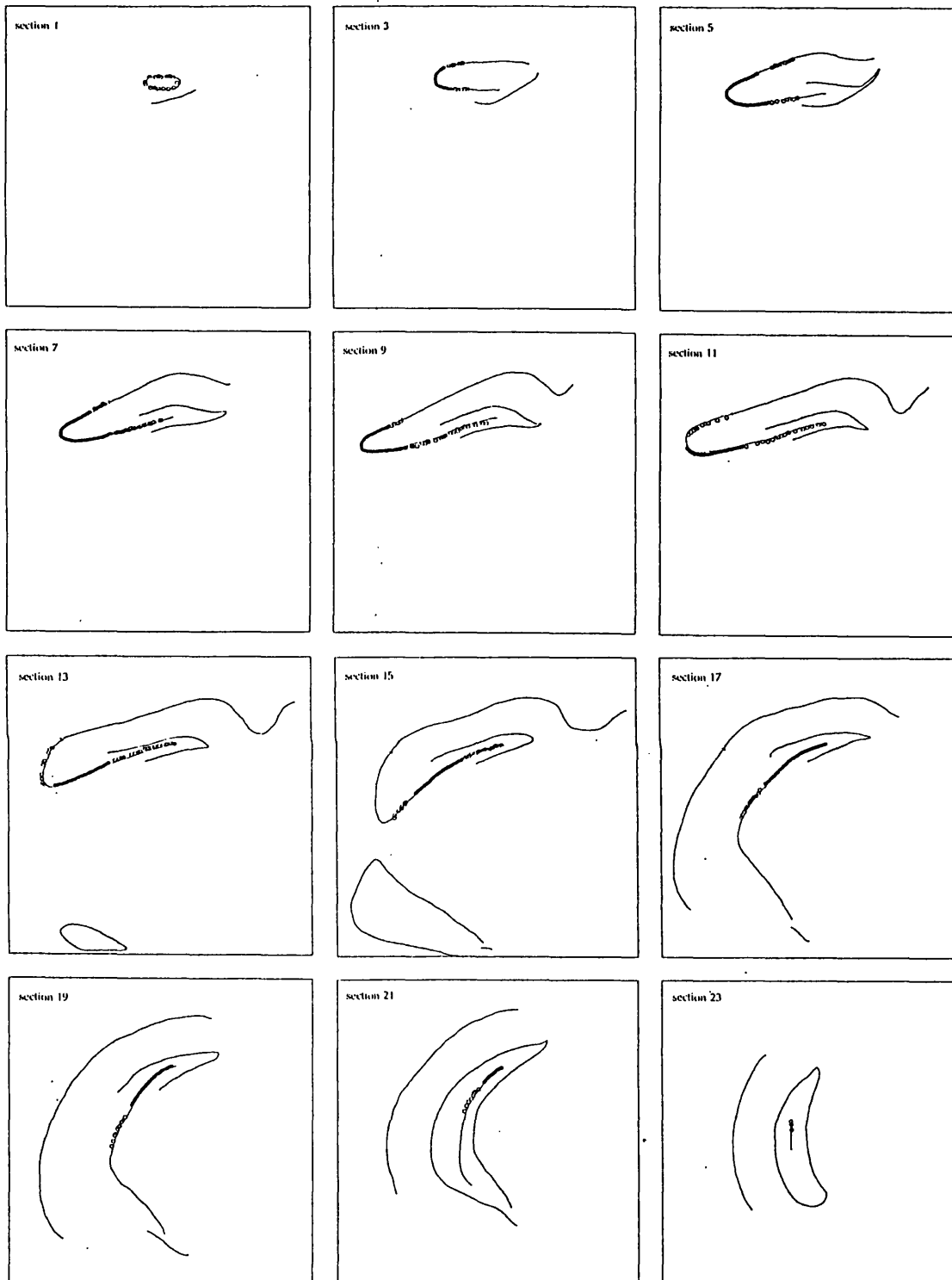












## I.1 The pattern of labelling

*[An analysis of the topography of the projections from CA3 to CA1 is conducted in Experiment II]*

The pattern of backfilling in the two CA3 fields shows that the distribution of cells in the contralateral CA3 field projecting to a specific region within CA1 is almost identical in extent and density to that of cells in ipsilateral CA3. This finding corresponds with the observation made by Gottlieb and Cowan (1972) on the strength of autoradiographic data, which states that neurons which give rise to a contralateral projection exhibit an ipsilateral pathway which terminates in the same region of the hippocampus (and on identical parts of the dendrites). The results of this experiment, however, suggest that the commissural pathway is identical in size to the ipsilateral pathway (a discovery which is *not* necessitated by the above observation).

Further analysis revealed that, in areas of the CA3 field where the backfilling encompassed nearly all the cells (shown by the solid lines), almost 100% of cells were double-labelled, although the proportion of double-labelling in the scattered individually-filled cells was markedly lower (about 50%). Since these latter cells constituted only a small fraction of the total number of backfilled cells, it was estimated that over 95% of filled cells were double-labelled, indicating that the same population of neurons projects bilaterally to homotopic regions in CA1.

Taken together, the fact that the ipsilateral and commissural CA3-CA1 pathways appear identical, and that homotopic regions in the two CA1 fields receive equivalent inputs, strongly suggests that the CA1 field functions as a single structure.

## I.2 The "fibres of passage" problem

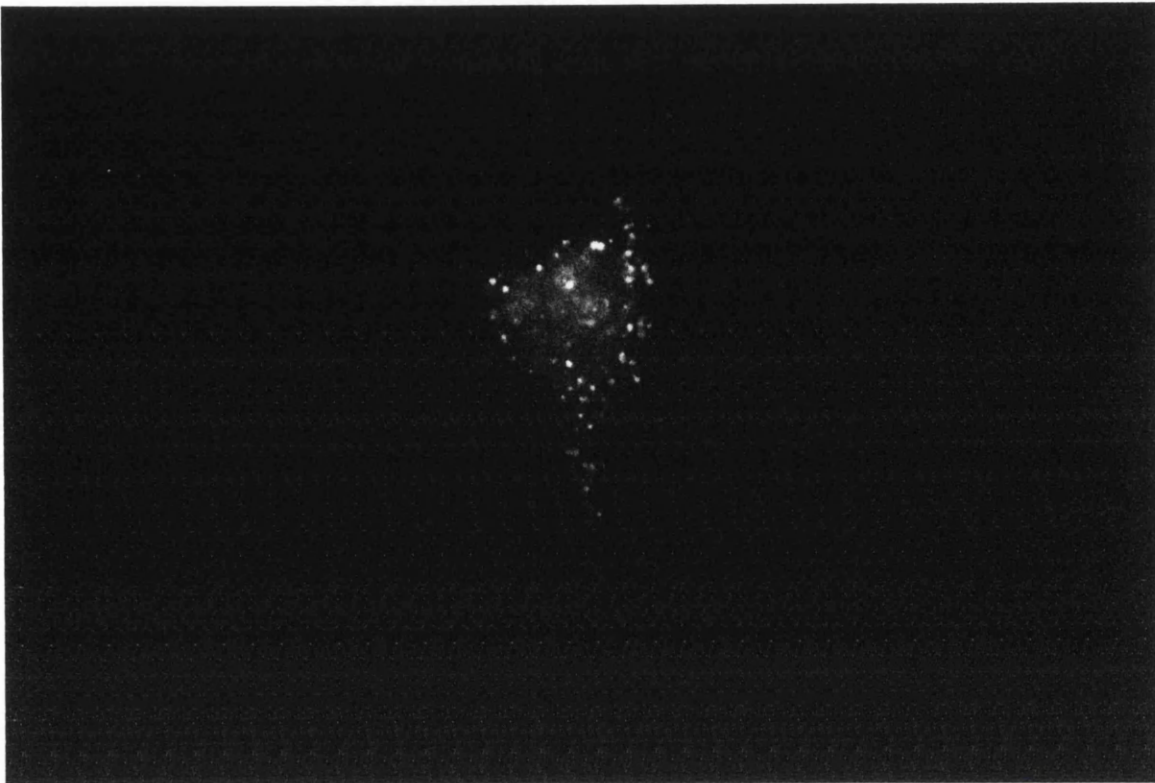
The nature of the labelling in the contralateral CA3 field is significant in the evaluation of the validity of the results of the fluorescent dye injections carried out throughout this dissertation. Since labelling due to damaged fibres of passage is a notorious problem associated with retrograde tracers, it might be argued that the backfilling seen in CA3 need not necessarily be restricted to those cells projecting to the region of CA1 contained within the uptake zone of the injection, but comprises additionally cells in CA3 whose axons pass through the injection zone *en route* to more distal regions of CA1. The *true* population of cells projecting to the targetted area in CA1 would in this case be a subset (of unknown size) of the labelled population.

The observation that the contralateral labelling is equivalent in spread and density to the labelling found in the ipsilateral field appears to suggest that the situation is not as depicted above. If the ipsilateral labelling did indeed include a group of cells whose fibres were disrupted by the injection then the equivalence of the contralateral pattern would imply that a similar group of cells in the contralateral field were labelled as a result of damage to their axons. The commissural fibres from CA3 are known to cross in the dorsal hippocampal commissure, but their trajectory within the contralateral hippocampus has not been documented. It is unlikely, however, to mirror the trajectory of the ipsilateral Schaffer collateral fibres. The latter are given off close to the cell body and penetrate the CA3 cell layer before running in the stratum radiatum of CA3 and then CA1 (Ishizuka *et al.* 1990); upon exiting the commissure, the contralateral fibres must necessarily run in the stratum oriens of CA1 before any perforation of the pyramidal cell layer in order to attain the stratum radiatum. This difference in bilateral fibre trajectory renders unlikely the notion that the commissural fibres damaged by the injection originate from an identical group of cells in the

contralateral field to those ipsilateral cells whose fibres were also disrupted.

The most convincing point against the "fibres of passage" argument is highlighted by investigating the direction of the damaged fibres: ipsilaterally, the disrupted fibres would be running medially away from CA3 to terminate in more proximal parts of CA1; in comparison, commissural fibres course laterally from the dorsal hippocampal commissure towards the contralateral CA3 and would therefore terminate in regions of CA1 closer to the CA2 border than the injection site (as well as in CA3). It is therefore extremely implausible, given the proximodistal disparity in the postulated termination sites in CA1 of the disrupted fibres of the two CA3 fields, that the "fibres of passage" problem has any significance in retrograde intrahippocampal studies of the types described in this dissertation. As a final point, however, it must be noted that some labelling might indeed be due to damaged fibres: conceivably, the contralateral projection from CA3 to CA1 might arise from collaterals of the commissural projection to the CA3 field, which might be given off in the stratum radiatum of CA3 to course medially towards the stratum radiatum of CA1 in an identical fashion to the ipsilateral Schaffer collaterals. While this seems unlikely, the possibility cannot be discounted, and further information is needed on the trajectory of the contralateral CA3-CA1 fibres before this argument can be satisfactorily resolved.

The observations that the ipsilateral and commissural pathways appear equivalent, and that the labelling in CA3 is a valid representation of the CA3-CA1 projection, in spite of any damage to fibres of passage, are used as guidelines for the interpretation of results in subsequent experiments.



*Above* (T64) A double-labelled hilar pyramidal cell

*Below* (T74) A rhodamine-labelled CA3 cell and proximal dendrite



## **EXPERIMENT II: A study of the topographical organization of the CA3-CA1 projection**

In this experiment the organization of the projection from CA3 to CA1 was examined using injections of the dyes Fast Blue and rhodamine microspheres into two different sites unilaterally within CA1 in the same subject. In addition to providing data on the patterns of projection in CA3 to different regions of CA1, the distribution of double-labelling can be used to demonstrate the collateralization of the CA3 pyramidal cell axons.

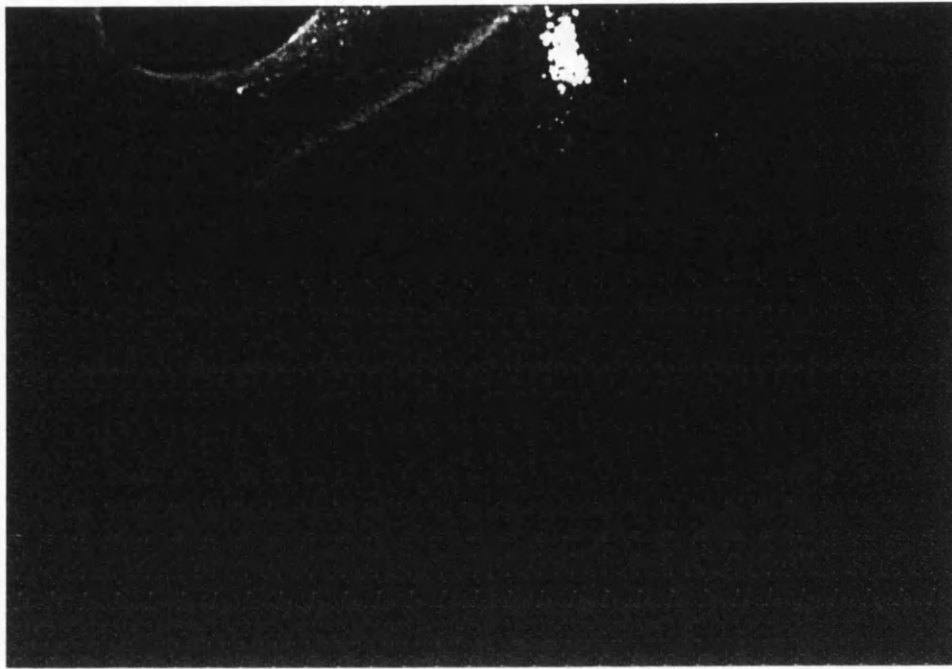
Two factors influenced the decision to cut the ipsilateral hemibrain (containing the injection site) in coronal section for the first part of this experiment. Firstly, additional data was collected concerning the backfilling in the entorhinal cortex following injections into the hippocampus. It was found that the dissection procedure used for extension of the hippocampus involved unavoidable damage to the entorhinal cortex, and in view of this the technique was not adopted on the ipsilateral side. As a consequence of this, extension was only applied to the contralateral hippocampus. The second decisive factor arose as a result of the findings of Experiment I which demonstrate that the ipsilateral and contralateral projections from CA3 to CA1 are identical. It follows from this the pattern of labelling in the ipsilateral unextended hippocampus is equivalent to that in the extended contralateral hippocampus so that a comparison of the labelling in both hippocampi across a number of brains could be used to generate a topological transform between unextended and extended representations of the hippocampus. Such a transform would be of use in chronic electrophysiological studies since it could be employed to calculate the equivalent coordinates in the unextended hippocampus of desired electrode placements in the extended hippocampus.

In the second phase of this experiment, the hippocampi on both sides were extended following injections into the CA1 field. In addition to providing confirmation of the bilateral symmetry of the CA3-CA1 projection, these injections were used to calibrate the first set of results.

Results from several injections placed at different levels across the CA1 field are represented on pages 134-138. In each case the labelling in the ipsilateral hippocampus, which includes the injection site, is displayed in addition to the labelling in the extended contralateral hippocampus.

The photographs on the following pages depict injections placed into CA1 in the unextended and extended hippocampi. In the former (T93), an injection of rhodamine microspheres is used to show the localization of the injection site within the stratum radiatum of CA1 and demonstrates additionally the lack of diffusion from the site of injection. The top photograph illustrates the ability to observe the rhodamine injection site under the ultraviolet excitation normally employed for Fast Blue and the usefulness of this feature in determining the position of the injection within the hippocampus and in relation to the Fast Blue injection.

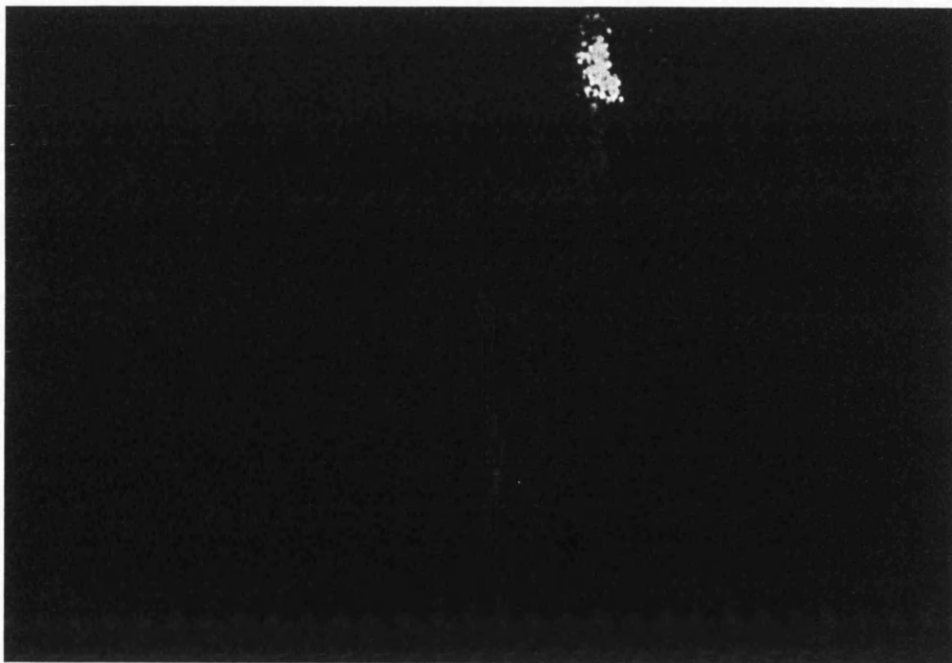
In the case of the Fast Blue injection into the extended hippocampus (T171), a blue-white diffusion area is clearly visible around the perimeter of the central site of uptake. It has been shown that this penumbral region does not contribute to the zone of uptake of the dye (Condé 1987).

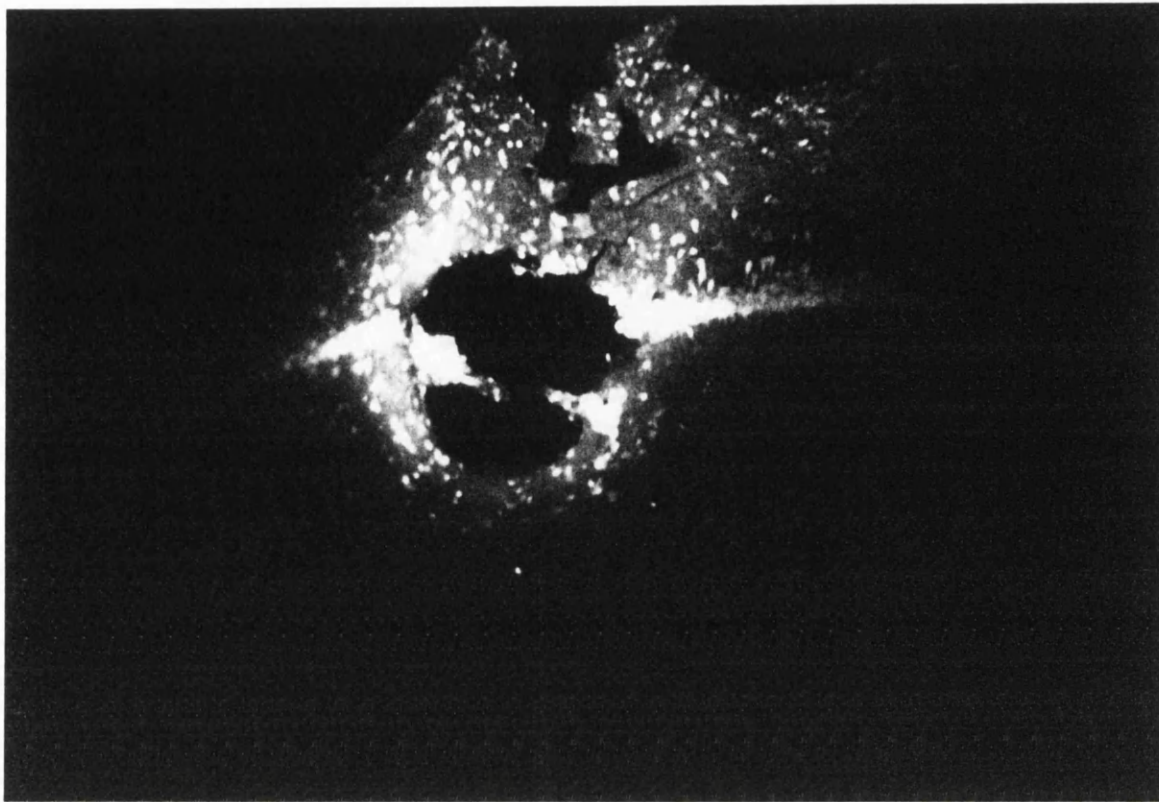


(T93) A rhodamine injection site in CA1 as viewed under

*Above* UV excitation

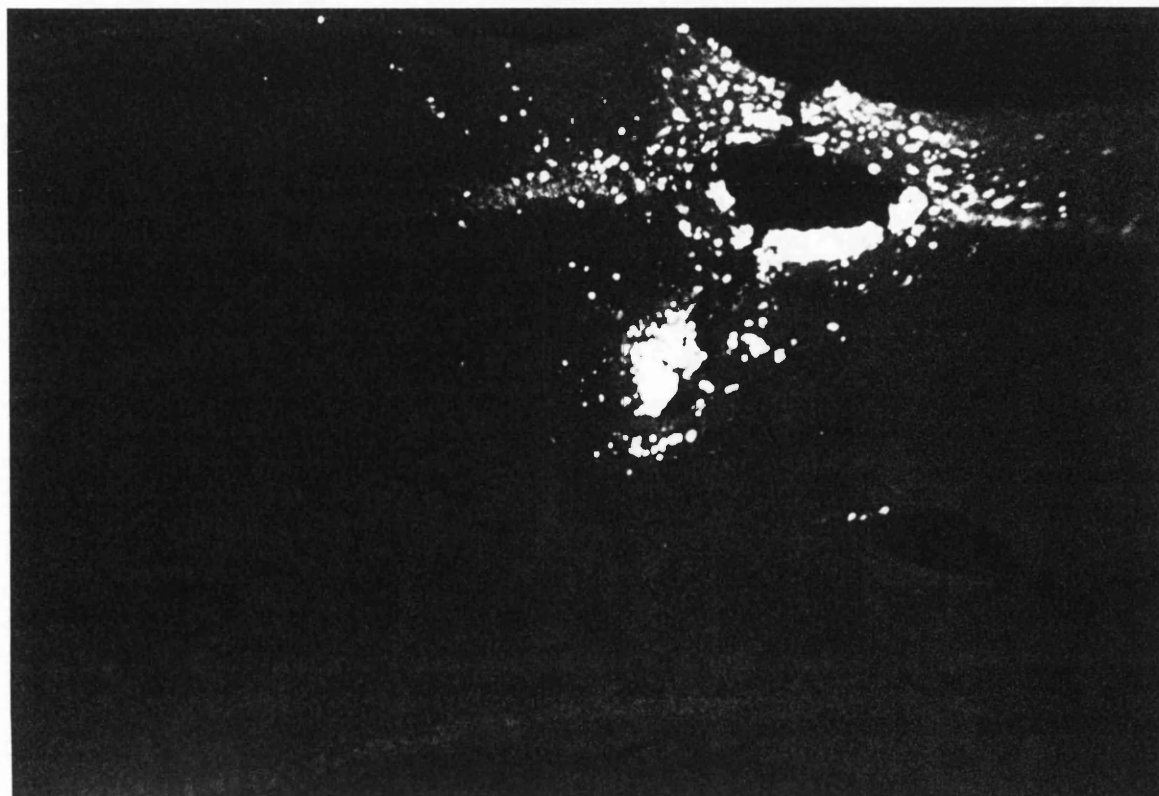
*Below* green excitation

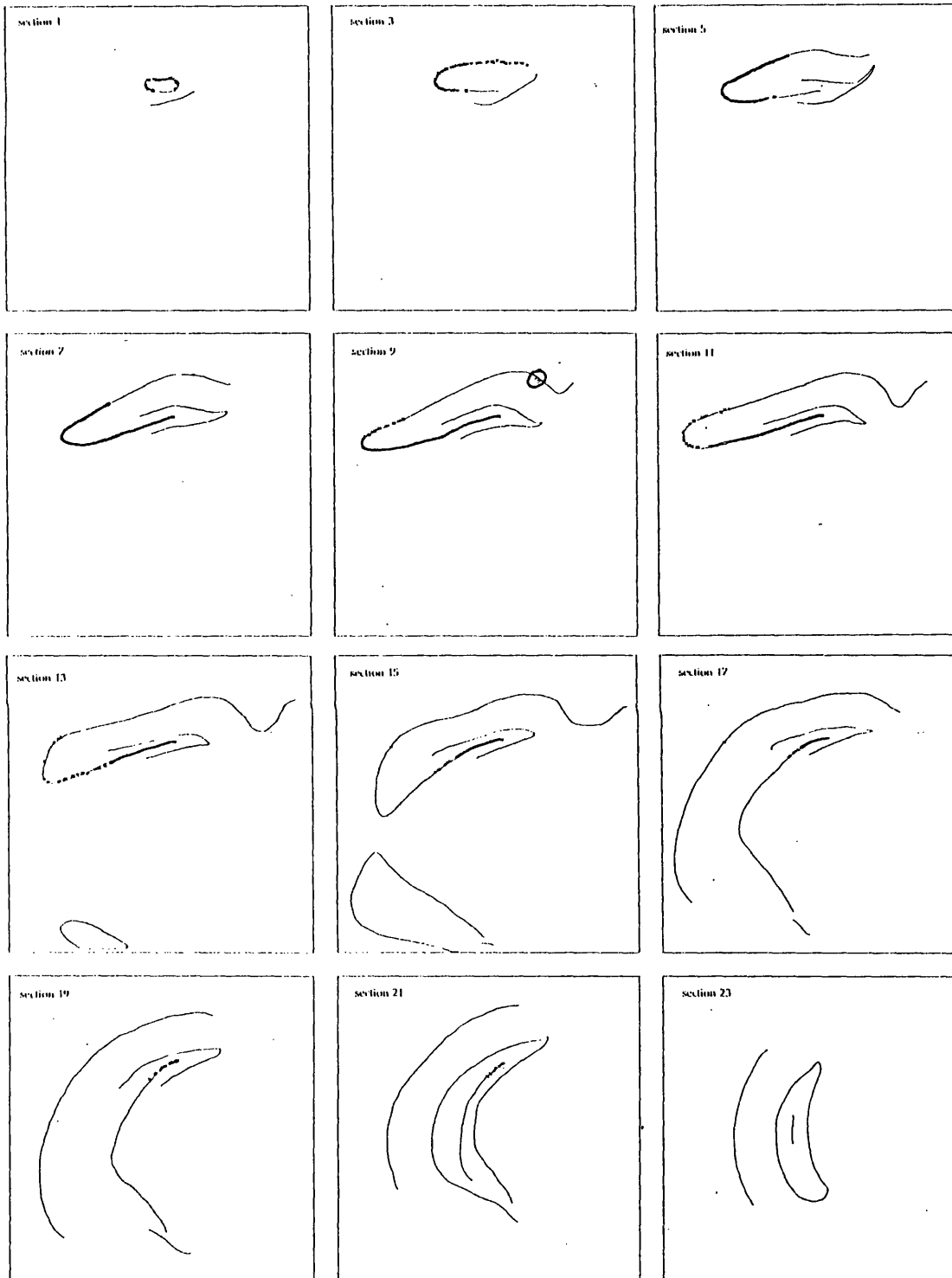


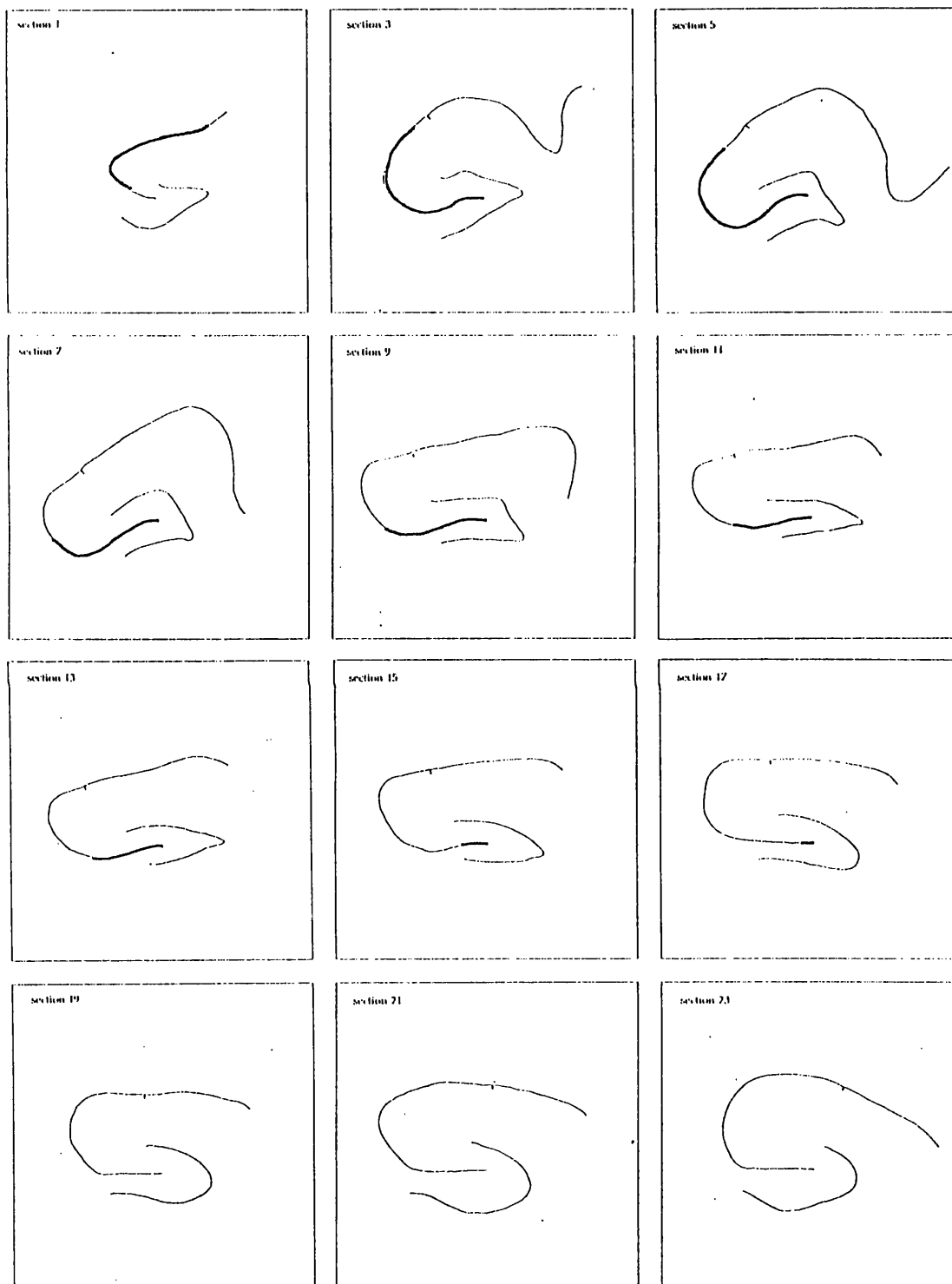


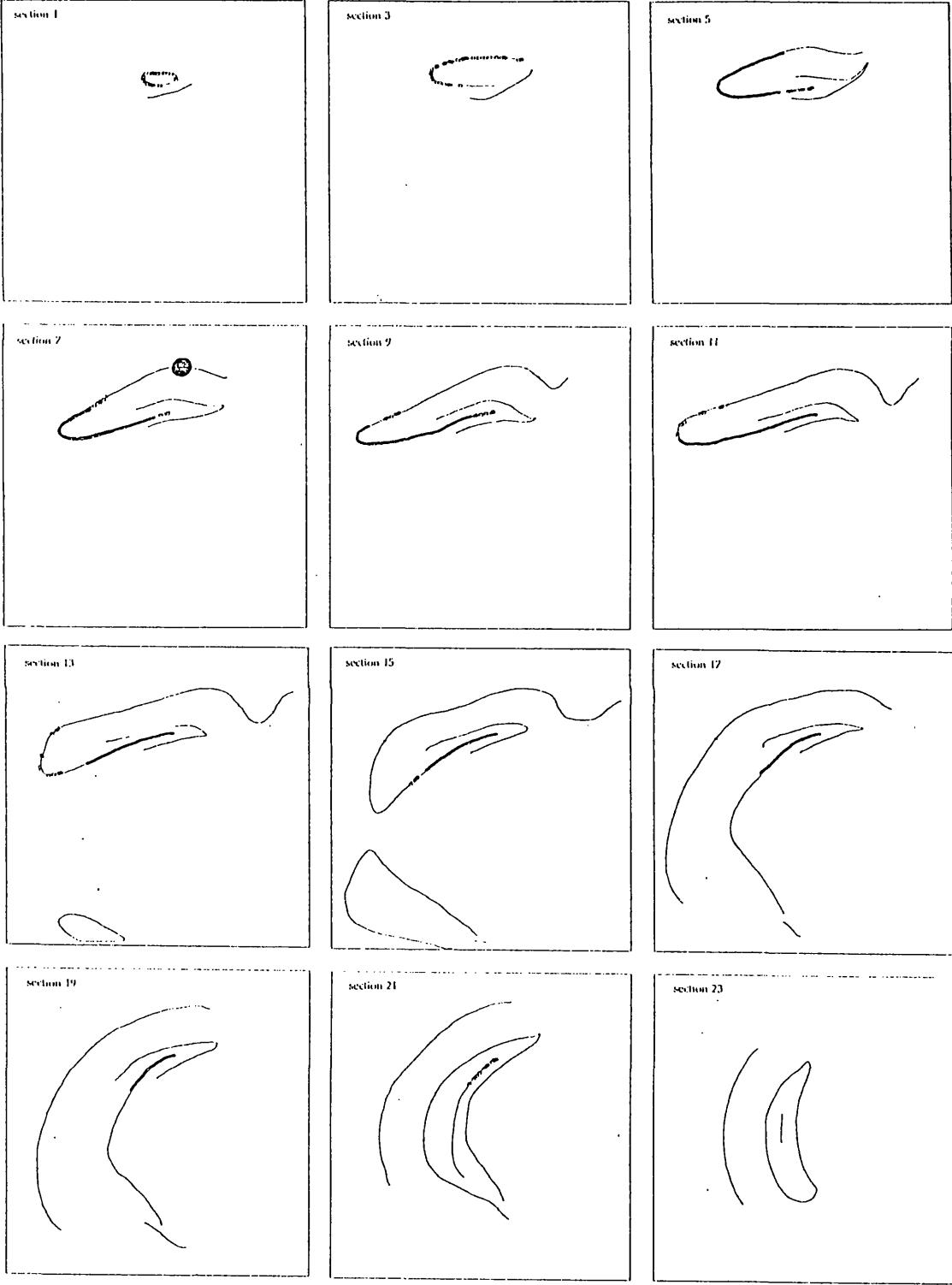
(T171) Injections into CA1 in the extended hippocampus

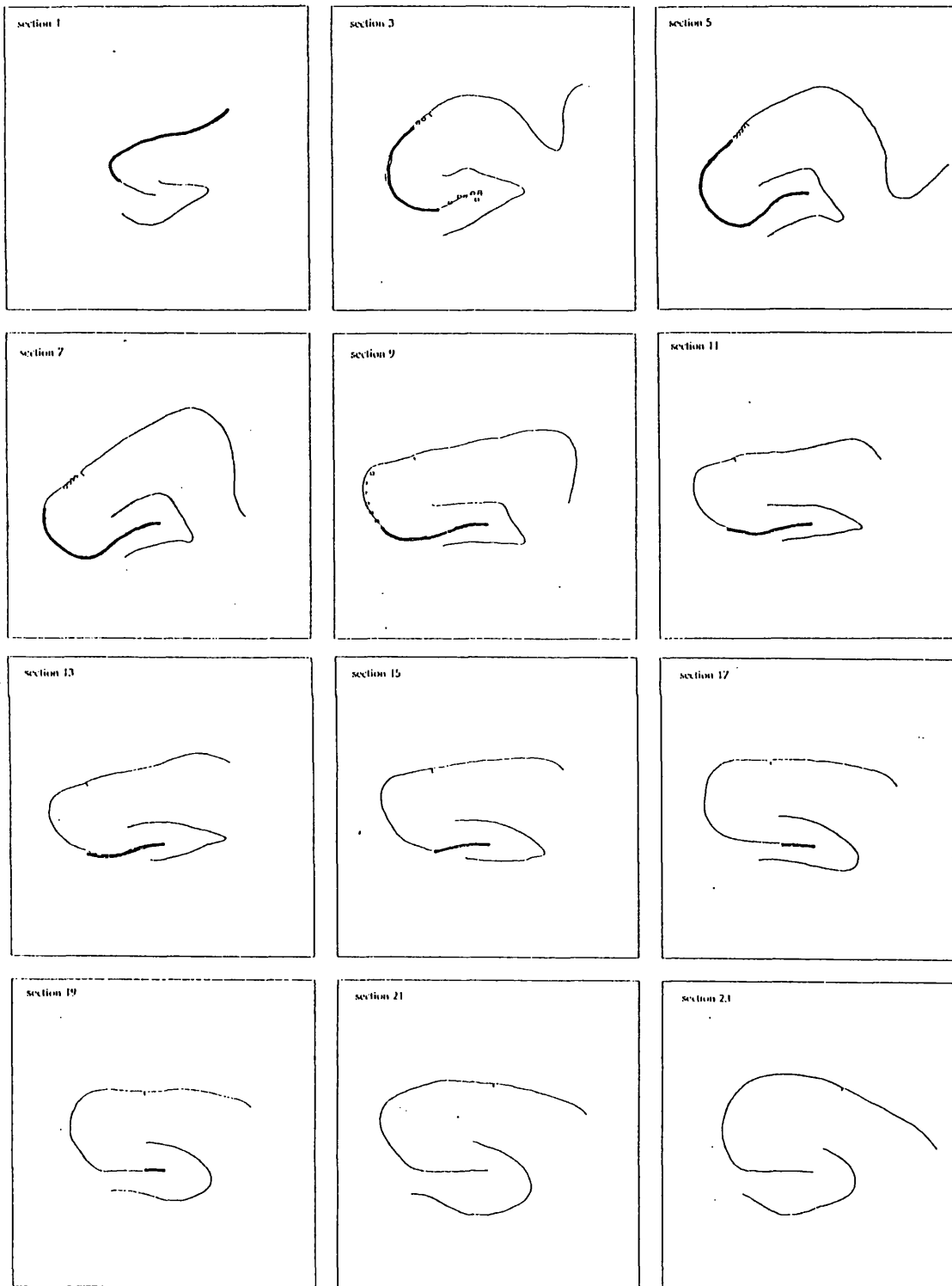
*Above* Fast Blue      *Below* Rhodamine

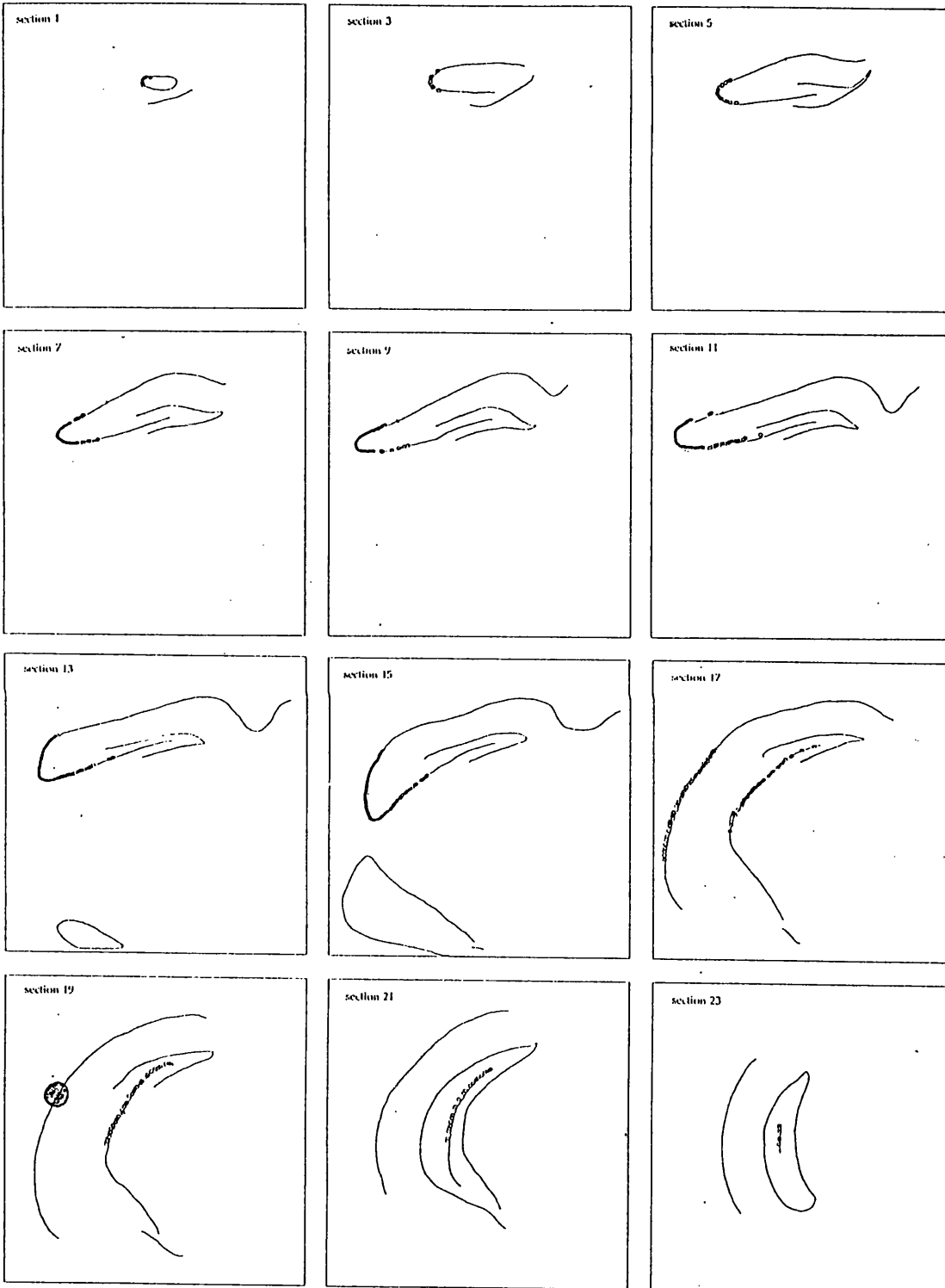


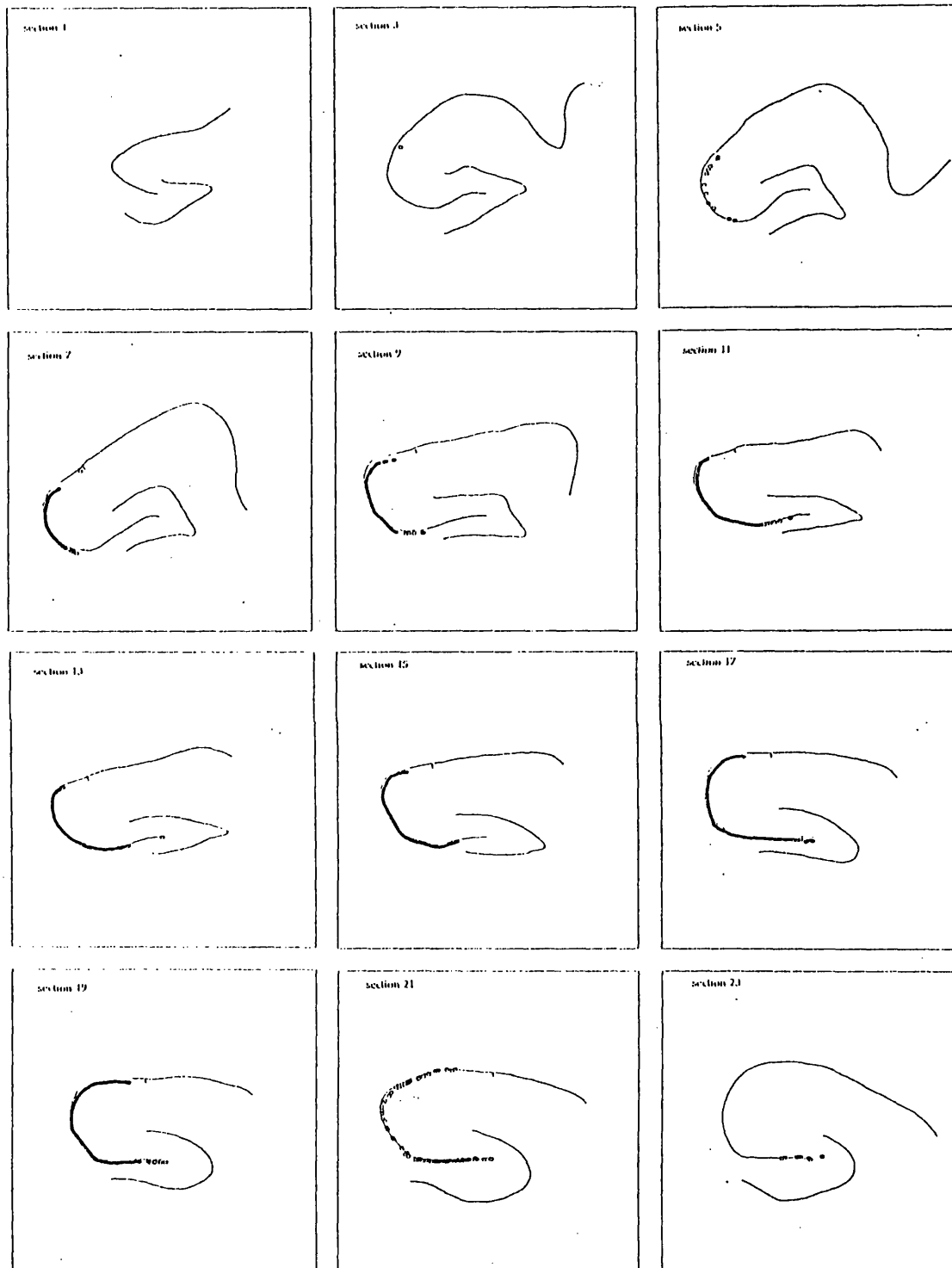












## II.1 The generation of the rostrocaudal-septotemporal topological transform

As mentioned in the introduction to this experiment, the topological transform between unextended and extended views of the hippocampus can be evaluated by comparing directly the various boundary points at the edges of the pattern of labelling in the unextended ipsilateral CA3 field and equivalent boundary points in the pattern of labelling in the extended contralateral field. From these data a topological transform can be generated which would map all the unextended points onto the corresponding extended points in CA3. Examples of the manner in which boundary points are first evaluated and then mapped are shown in four brains on pages 129-134.

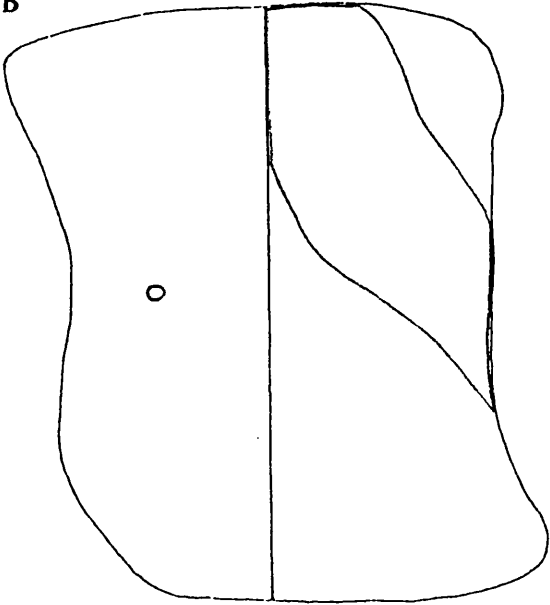
In the unfolded representation, the CA1 pyramidal cell layer can be regarded topologically as an extension of the CA3 cell layer, and as such will undergo a transformation similar to that of CA3. As a result of hippocampal folding around the bend of CA3, the CA1 field is superimposed on the CA3 field, such that the pattern of the CA1 transform can be obtained by reflecting the pattern of the CA3 transform onto the CA1 field through a plane running parallel to the septotemporal length of the hippocampus and which intersects it through the middle of the bend in the CA3 field.

The "unextended" injection sites are mapped onto equivalent points in the extended representation, which can then be compared with the extended pattern of labelling in CA3 to provide an understanding of the topographical organization of the projection.

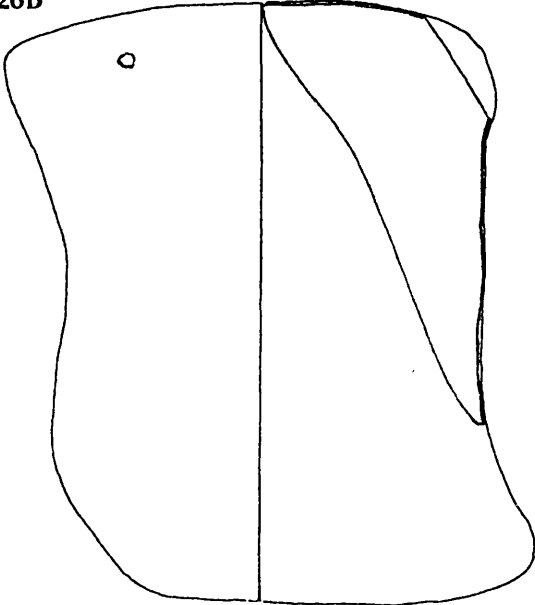
The accuracy of this transform was tested in two ways. In the first test, dyes were injected bilaterally into eight homotopic sites within CA1 (in two subjects, such that four sites were targeted in each subject). As for previous operations, one hippocampus was cut coronally, while the other was dissected and extended in order

CA1 INJECTIONS

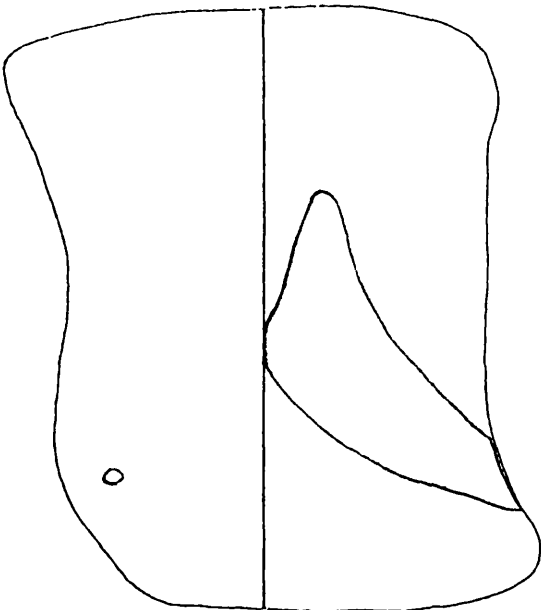
T93B



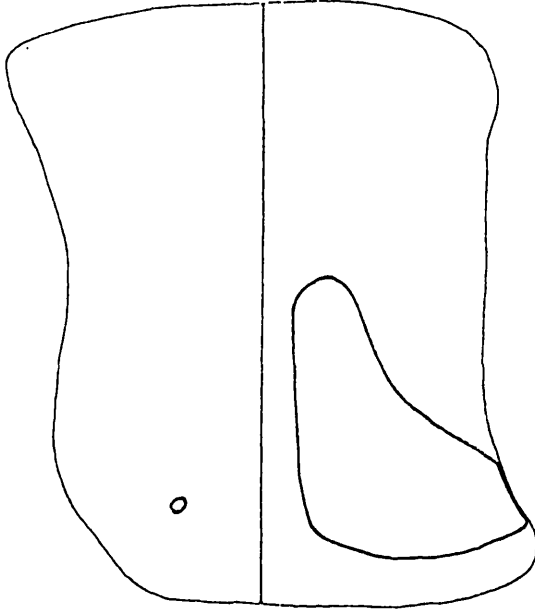
T126B

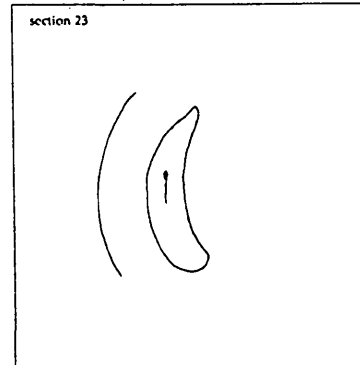
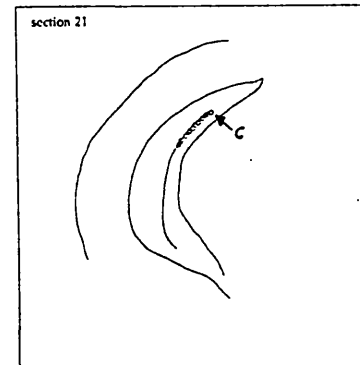
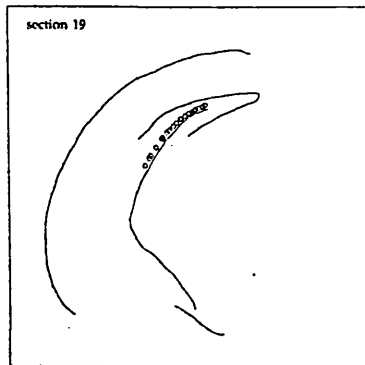
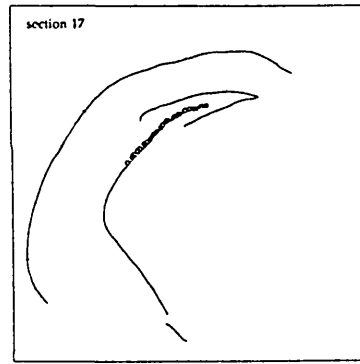
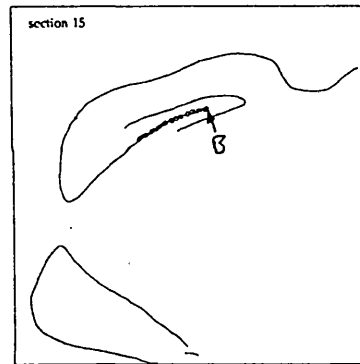
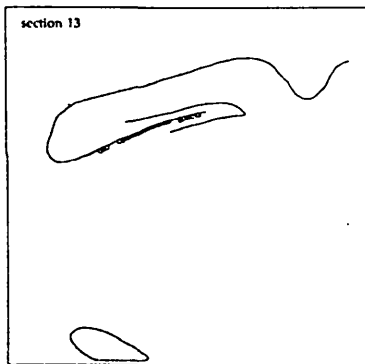
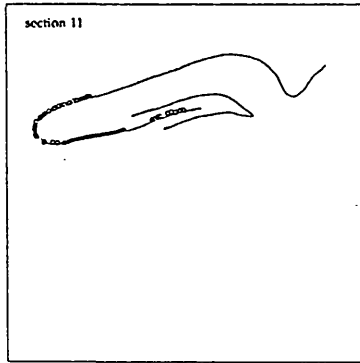
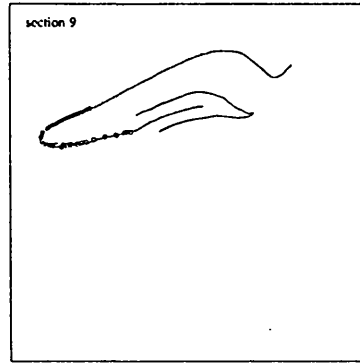
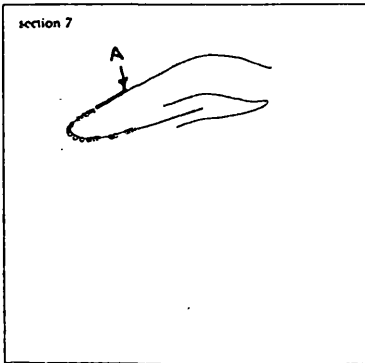
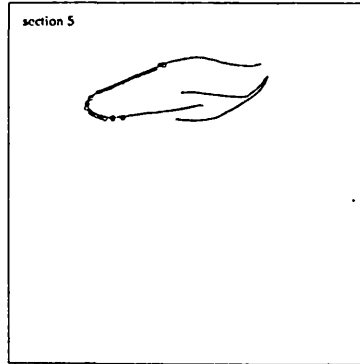
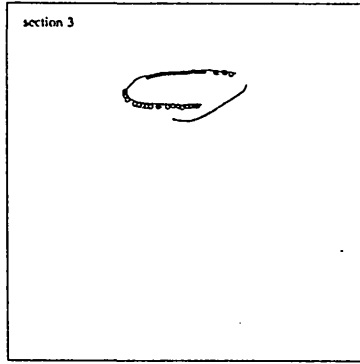
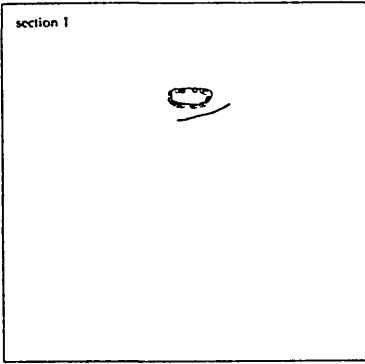


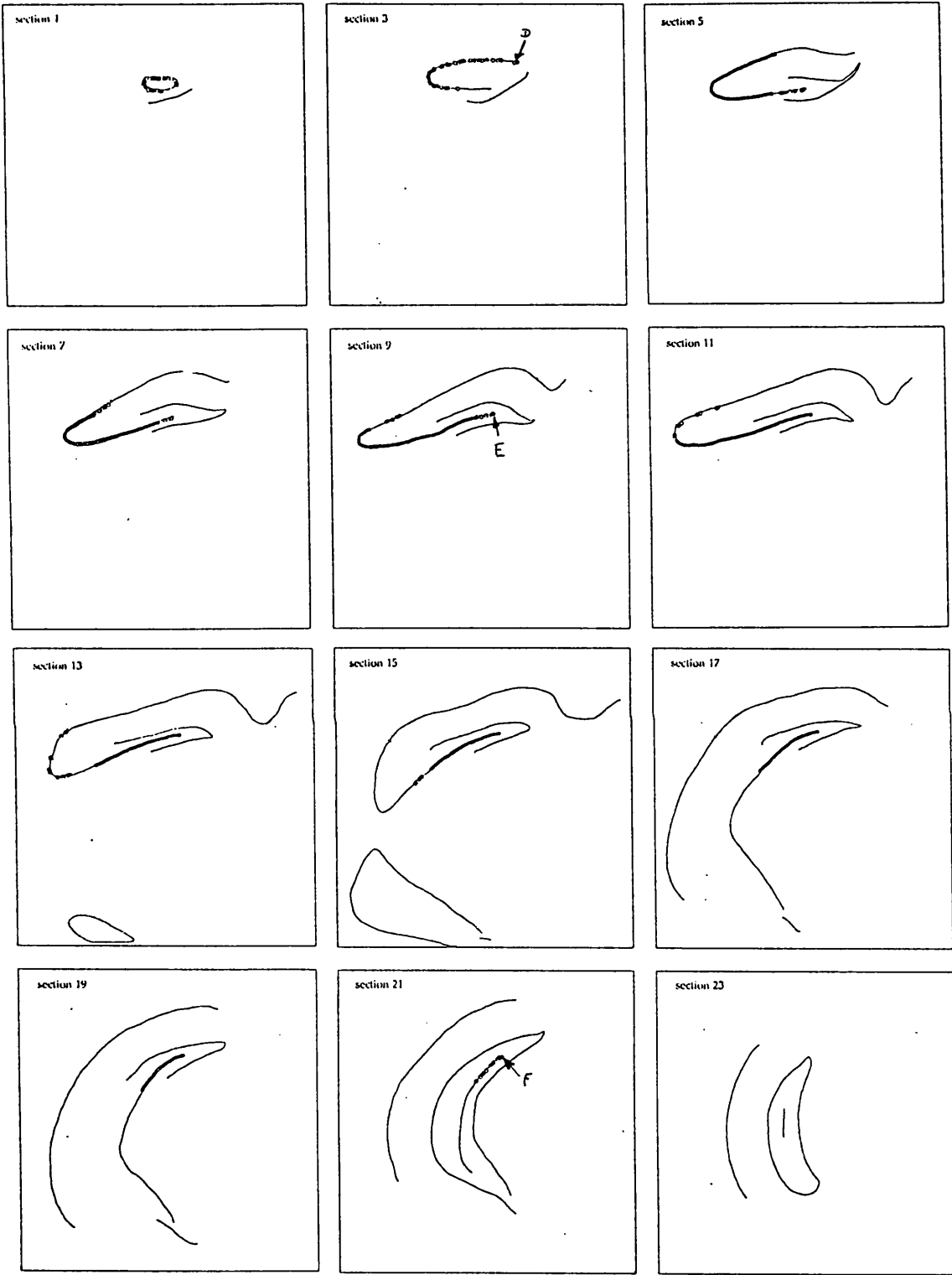
T153B

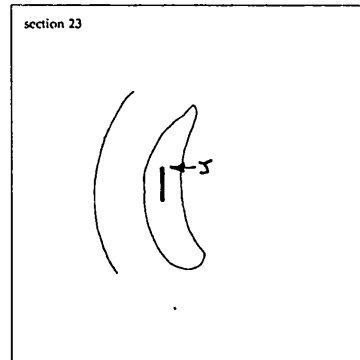
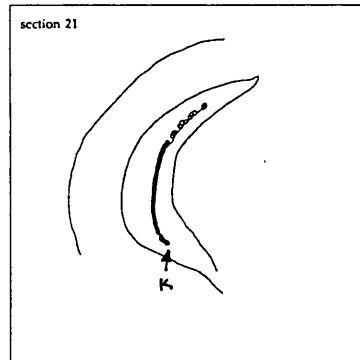
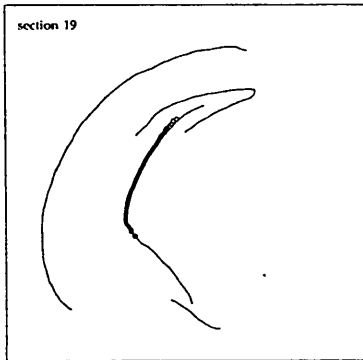
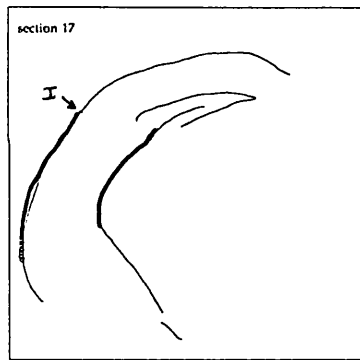
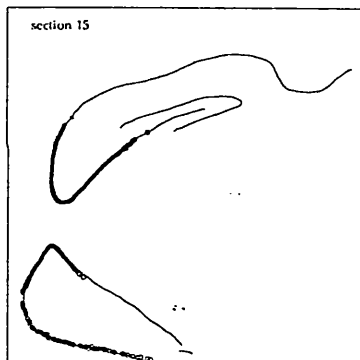
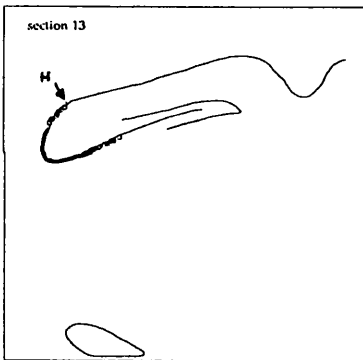
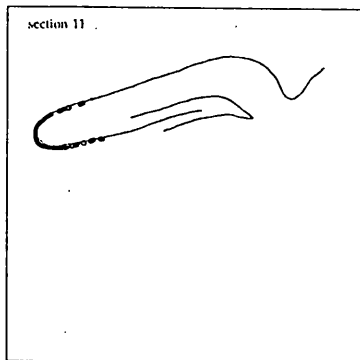
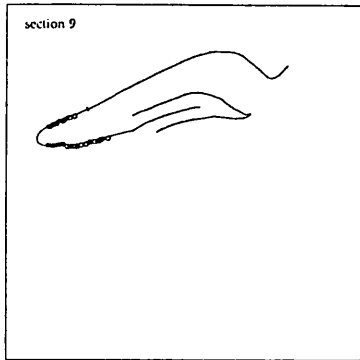
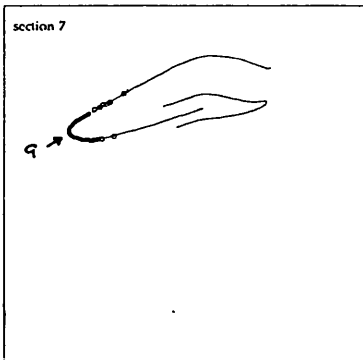
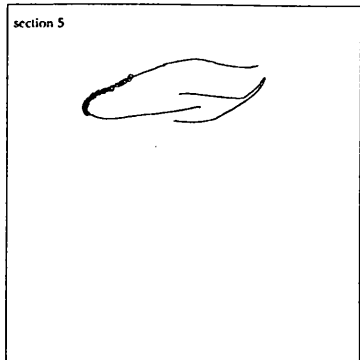
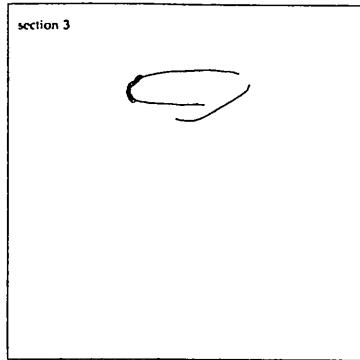
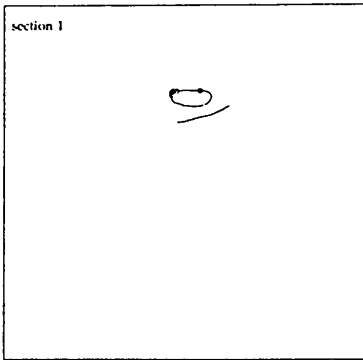


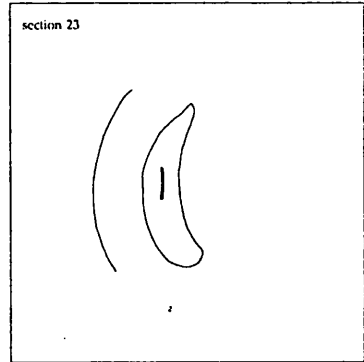
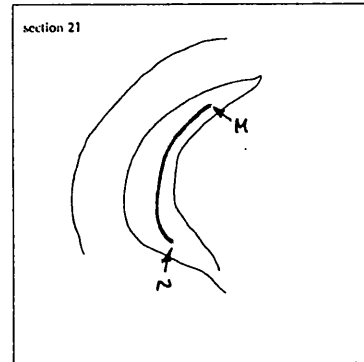
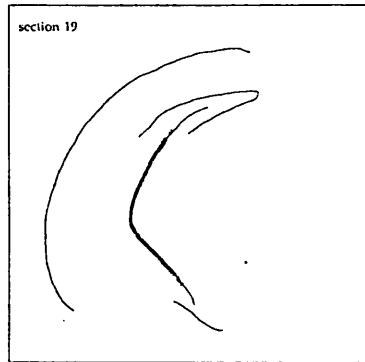
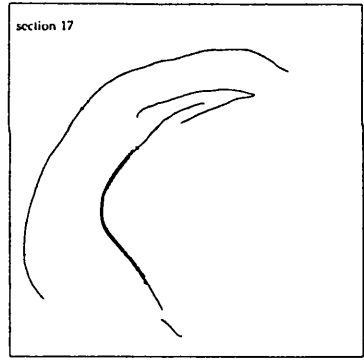
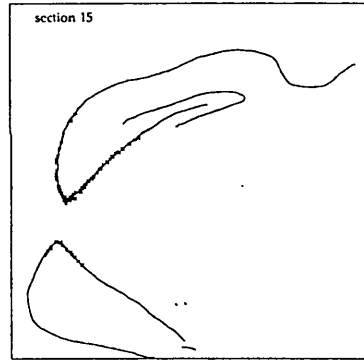
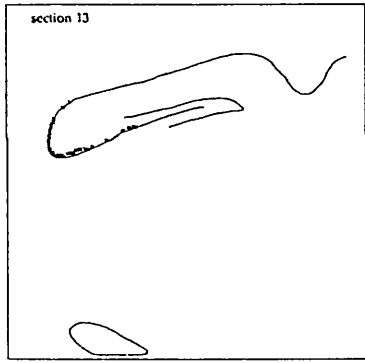
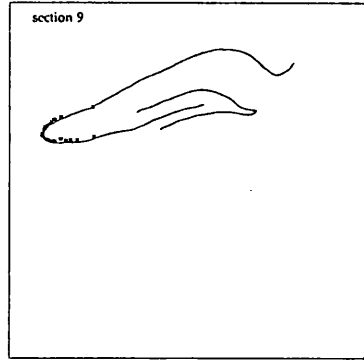
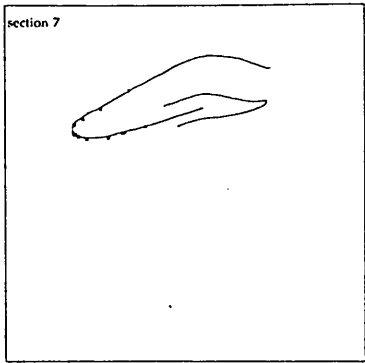
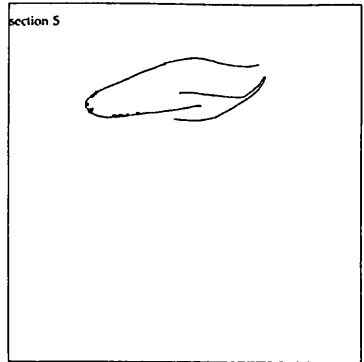
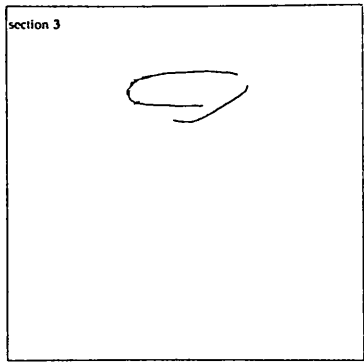
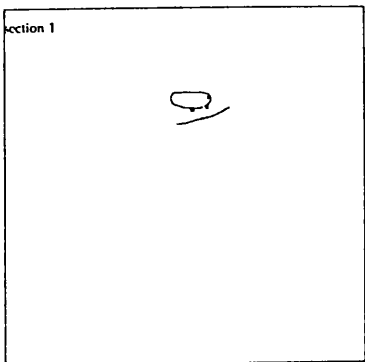
T160R











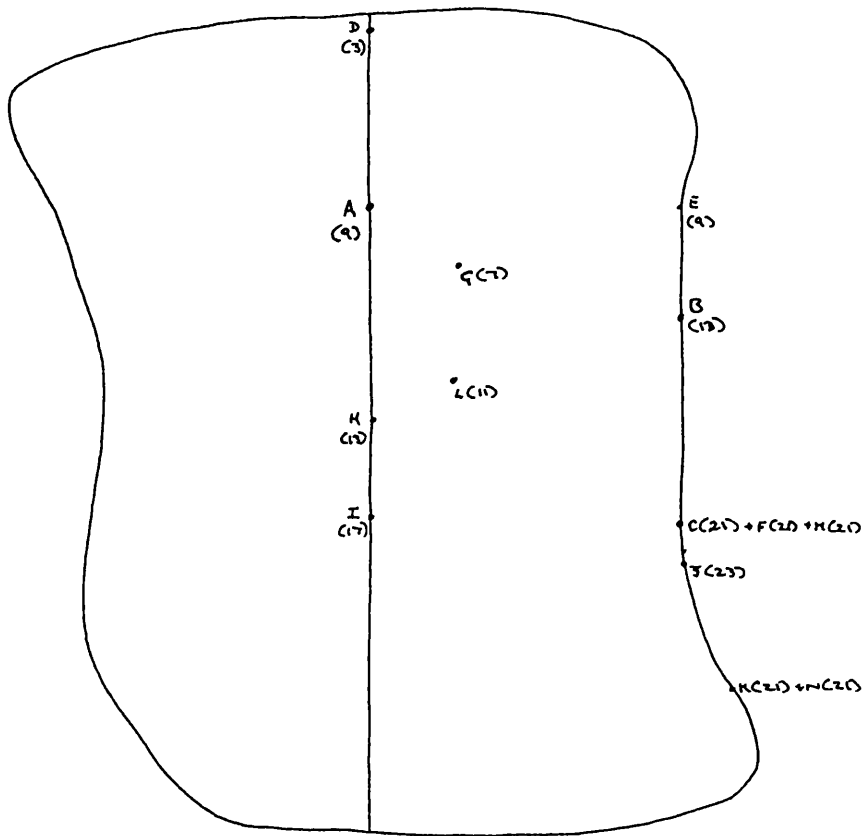


Fig.4a The various boundary points from the four example brains as mapped onto an unfolded representation of the hippocampus. Numbers in brackets refers to the sections in the unfolded hippocampus along which the boundary points are located.

The previous pages contain several brains in which boundary points were used in order to generate part of the topological transform. For example, the point at which the pattern of labelling first reaches the proximal end of the CA3 field is invariant across the two representations of the hippocampus, and hence this feature can be mapped in each of the four brains (points B, E, J, M). In this fashion an idea of the location of the various "unextended" sections within the extended representation of the hippocampus is created which, when expanded to include the mapped points from all the brains used in this study, yields the topological transform as shown in Figure 4b.

CA3

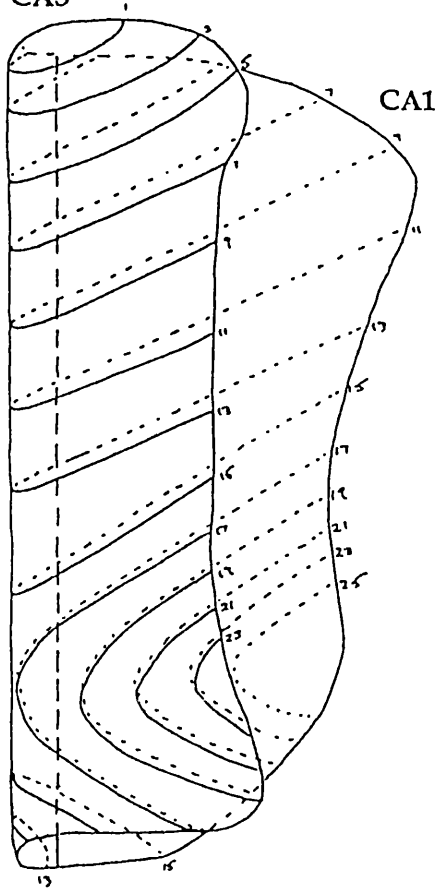
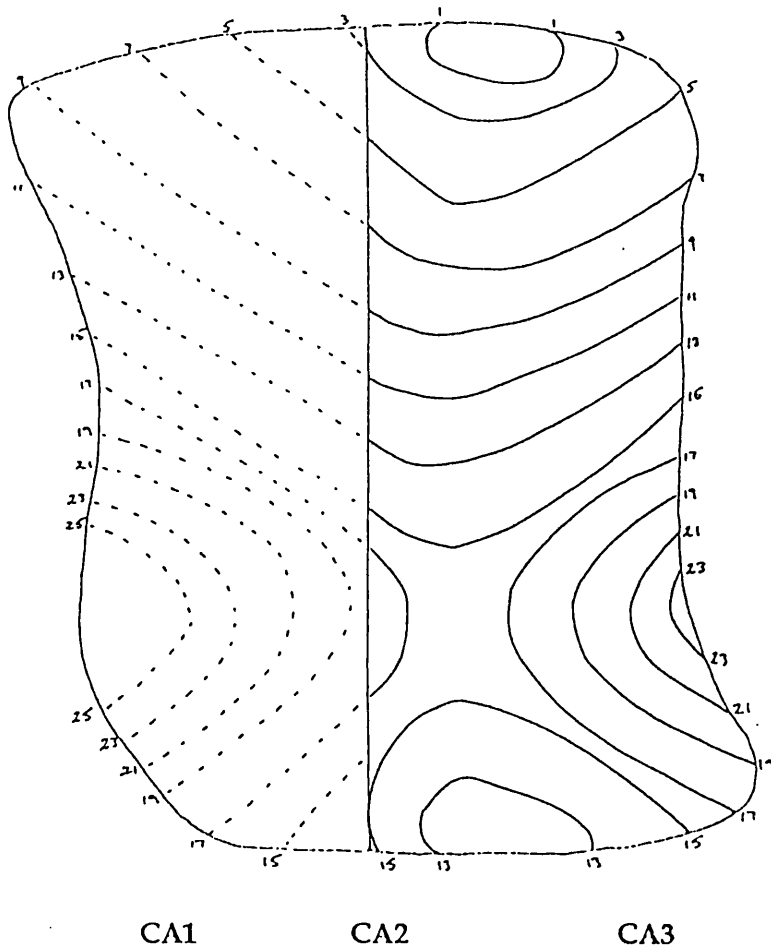


Fig.4b The septotemporal positions (shown in solid lines) of sections 1-23 cut coronally through the CA3 field are evaluated by direct comparison of the ipsi- and contralateral patterns of labelling (see main text). The equivalent septotemporal positions for CA1 (dotted lines) are generated by mapping the CA3 transform onto the CA1 field in a folded representation of the hippocampus (diagram on left). This transform is extended to cover the entire CA1 field. The CA2 field is represented by a dashed line.

The topological transform in the unfolded hippocampus is displayed below. (Magnification approx. 15x)

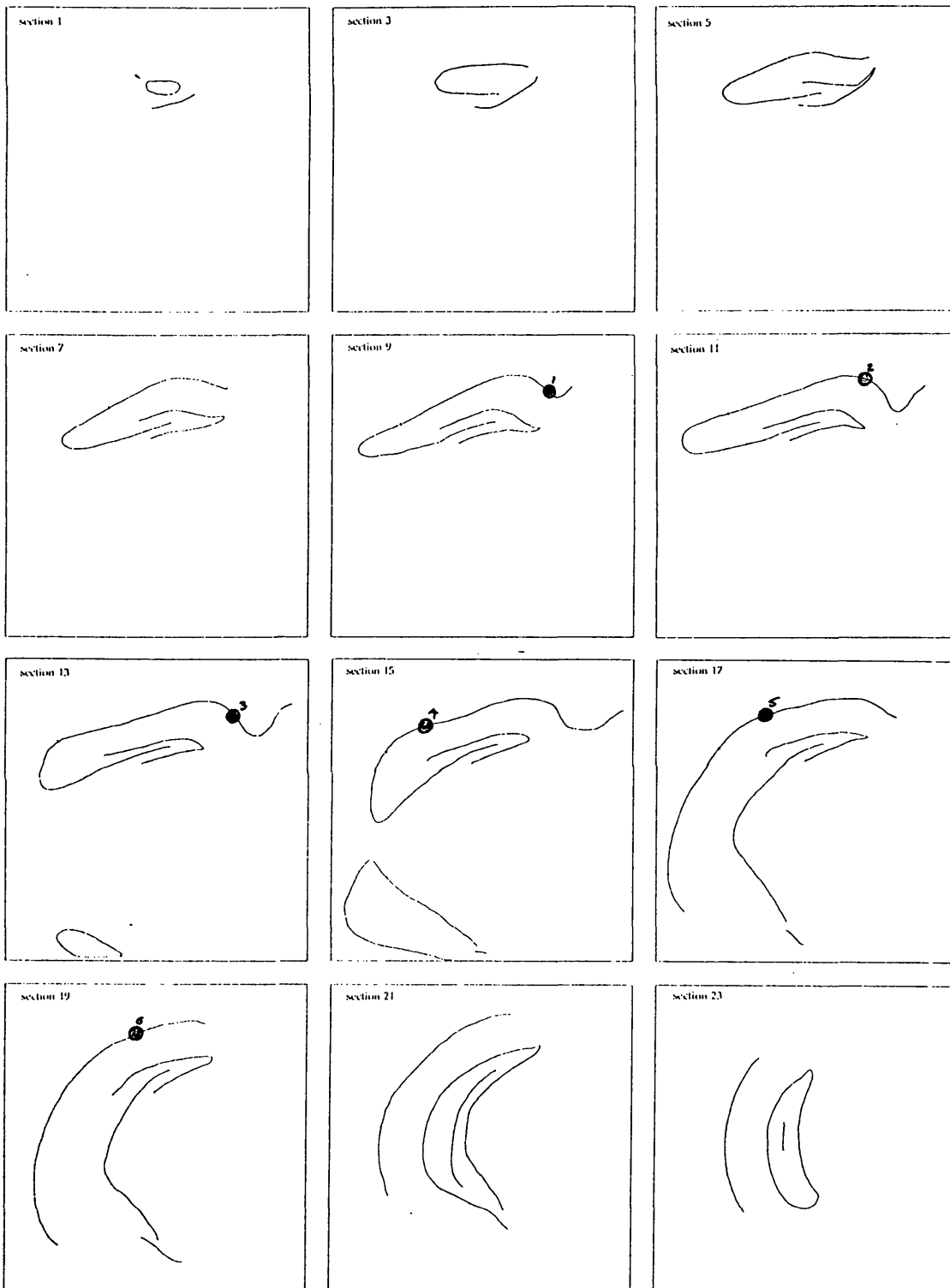


*(continued from page 128)* to provide transverse sections.

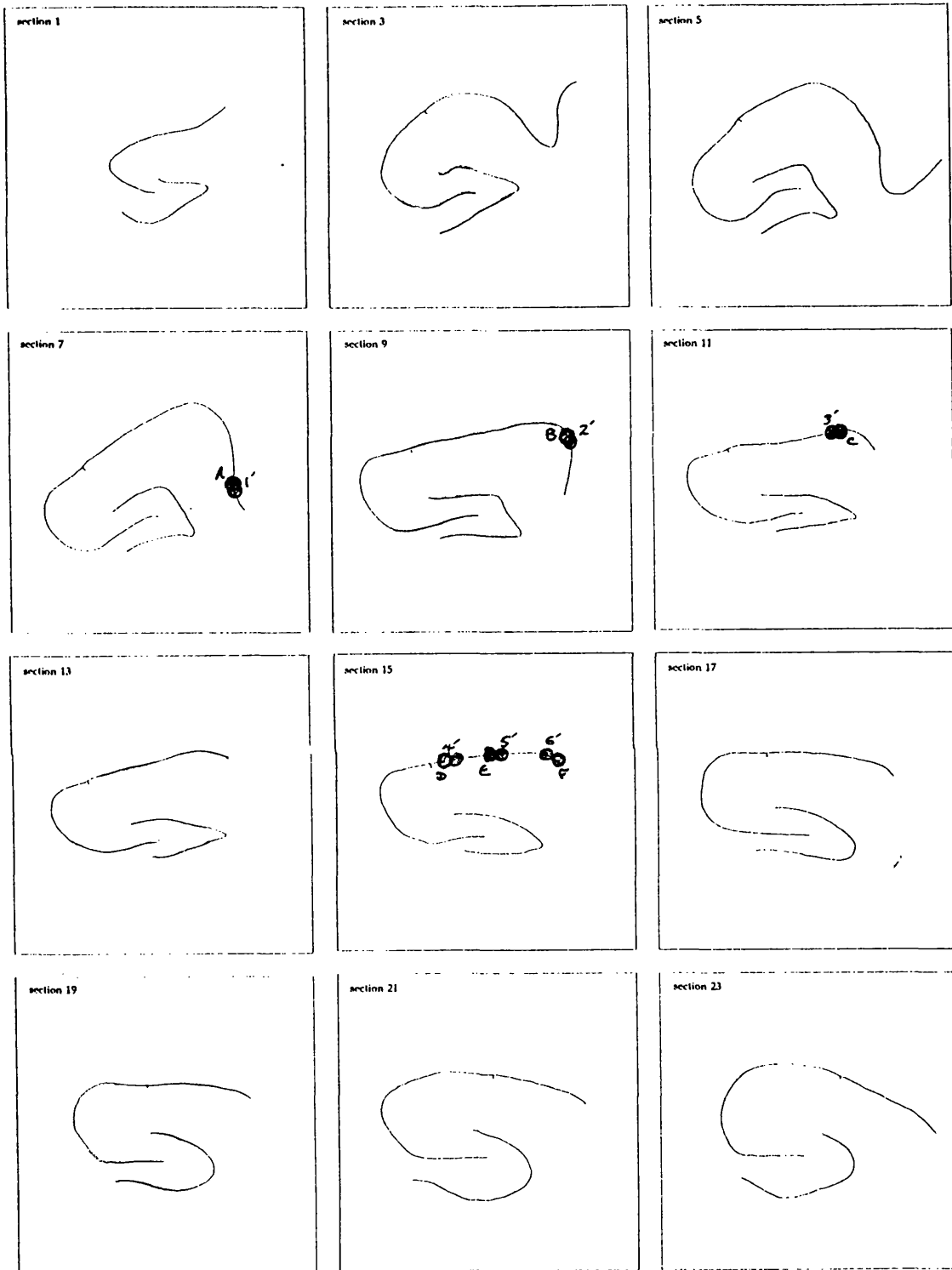
The topological transform was then used to calculate the equivalent positions in the extended CA1 field of the injection sites placed in the unextended hippocampus, and the results were compared with the locations of the homologous injections placed in the extended contralateral CA1 field (see overleaf). Of the six injections which were successfully located in CA1, all showed a good correspondence between "real" and "calculated" septotemporal positions, which testifies to the accuracy of the topological transform for CA1.

The accuracy of the transform was further tested in the second phase of the experiment, in which both hippocampi were extended following the unilateral injection of dyes into the CA1 field. As well as providing verification of the bilateral symmetry of the CA3-CA1 projection, the pattern of the projection from CA3 can be compared directly with the position of the injection site in CA1 in the extended plane, so that the projection organization as seen in these results can be used to calibrate the results of the injections in the initial part of the experiment.

The directly-calculated topographical organization noted in these latter operations (T168-T171) correlated strongly with the indirectly-calculated organization demonstrated in the earlier operations (T93-T161), and as such provide further vindication for the use of the topological transform in mapping experiments.



The equivalent septotemporal positions of the above injections 1-6 as calculated by the topological transform are found to correlate well with the injections into homologous sites in the extended contralateral field (see next page).



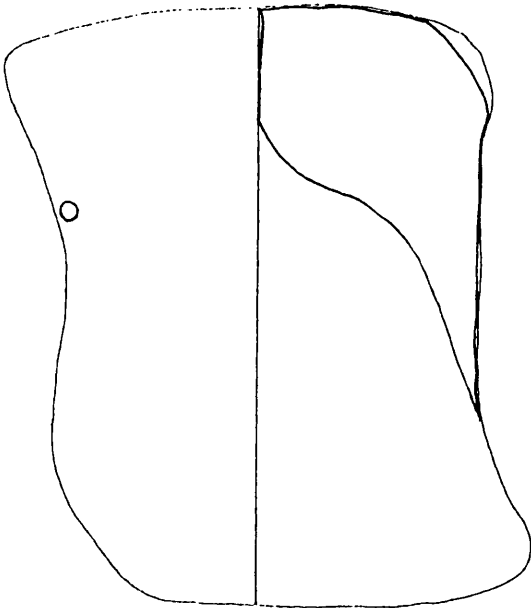
Sites 1'-6' represent the equivalent positions in the extended CA1 field of the injections 1-6 in the unextended hippocampus. A-F represent the homologous injection sites in the contralateral extended hippocampus.

## The pattern of labelling

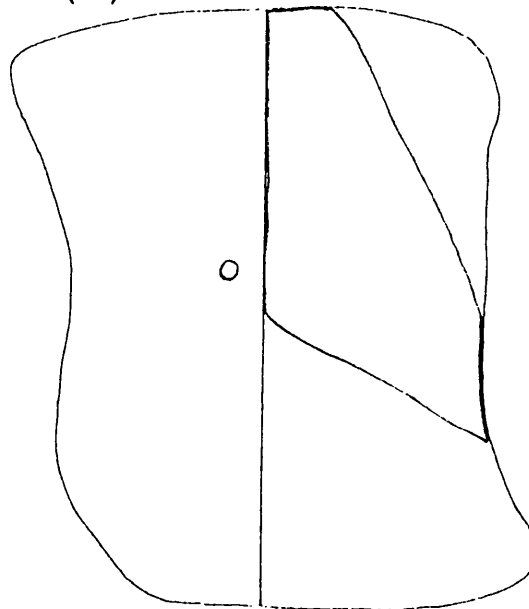
The following pages summarise the results from 18 injections using unfolded representations of the hippocampus. In all cases the band in CA3 represents the pattern of labelling in the extended hippocampus contralateral to the injection. The first 6 examples (T168-T171) are taken from operations in which both hippocampi were extended, so that the injection sites displayed in the unfolded CA1 field are as located in the extended ipsilateral hippocampus. In the remaining 12 cases (T93-T161), the positions of the injection sites in the unfolded CA1 field were calculated using the topological transform from their positions in the unextended ipsilateral hippocampus.

The surface area of the unfolded hippocampus (as used below) was calculated by incorporating the lengths of the transverse extent of the CA3 pyramidal cell layer at 12 regularly-spaced levels spanning the septotemporal breadth of the hippocampus with the width of the separation between each level. Transverse lengths were measured by camera lucida from a Nissl-stained extended hippocampus; the separation width was determined by the number of 35 $\mu$ m sections between each level. On the left of the midline divide (representing the CA2 region) is the CA1 field; on the right is the CA3 field.

T168 (RHO)

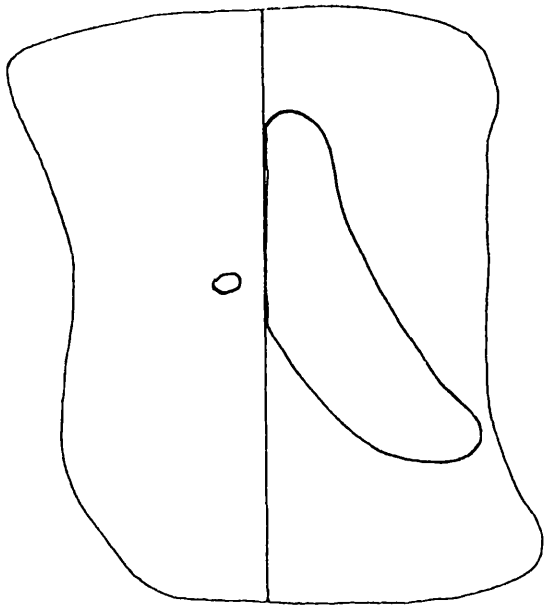


T169 (FB)

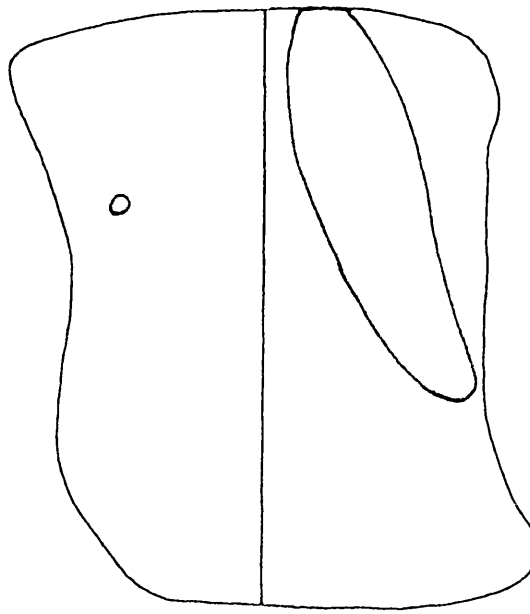


CA1 INJECTIONS

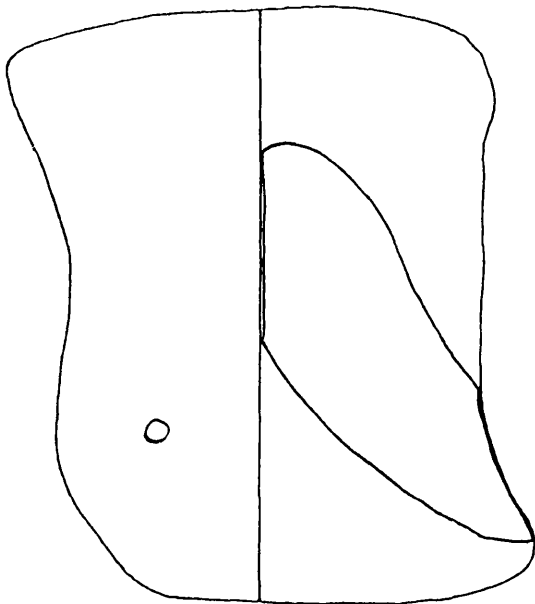
T170 (RHO)



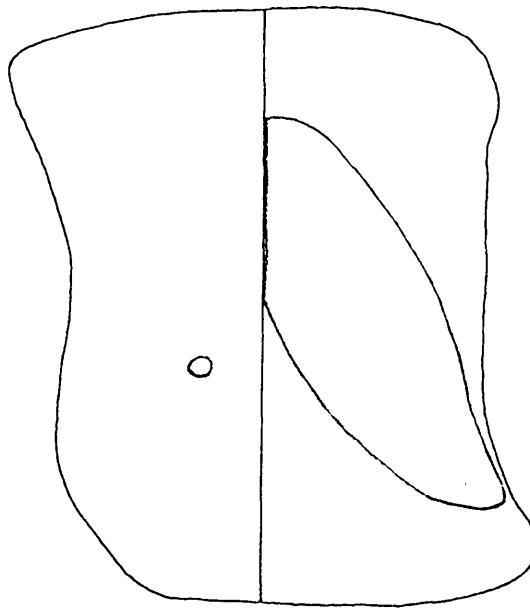
T170 (FB)



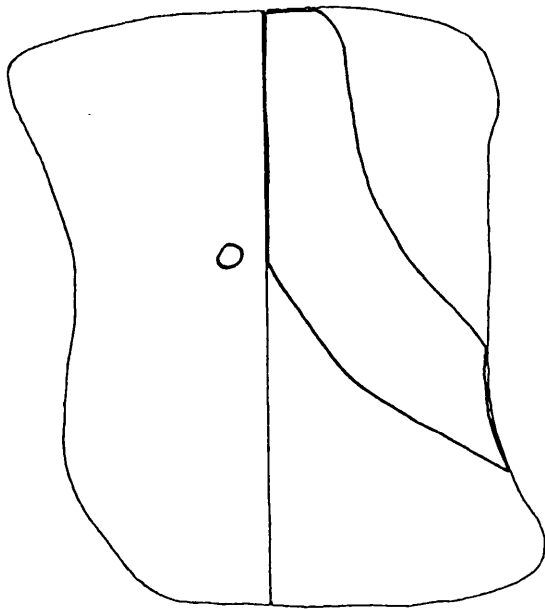
T171 (RHO)



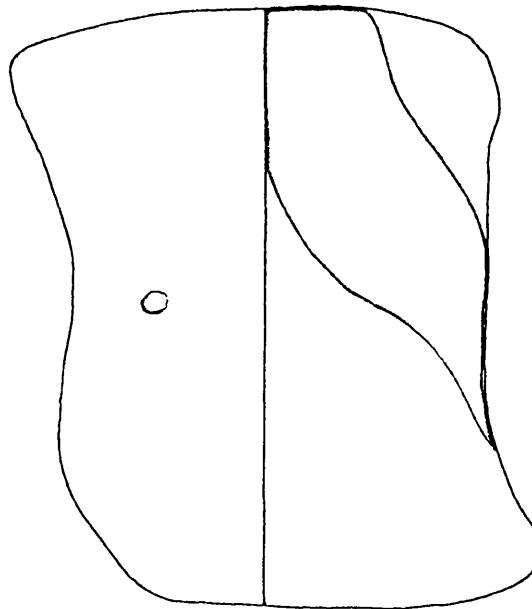
T171 (FB)



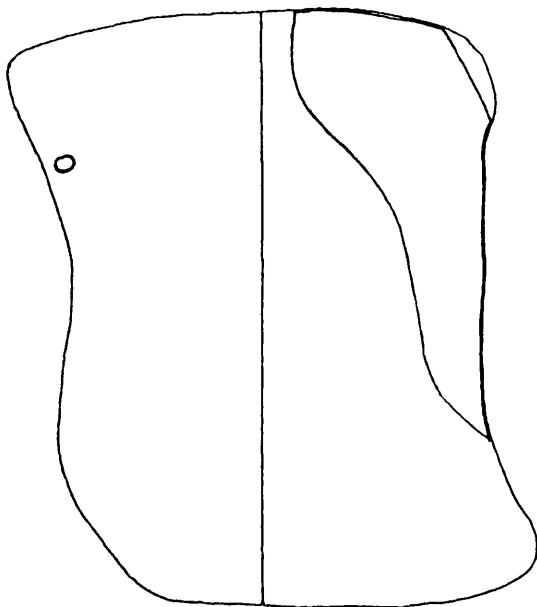
T93 (RHO)



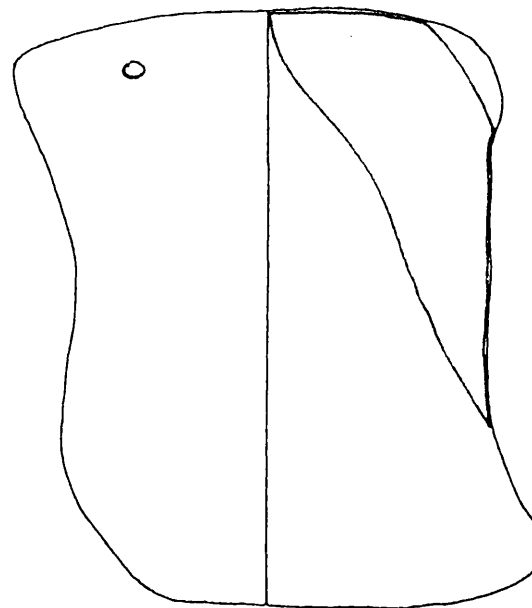
T93 (FB)



T126 (RHO)

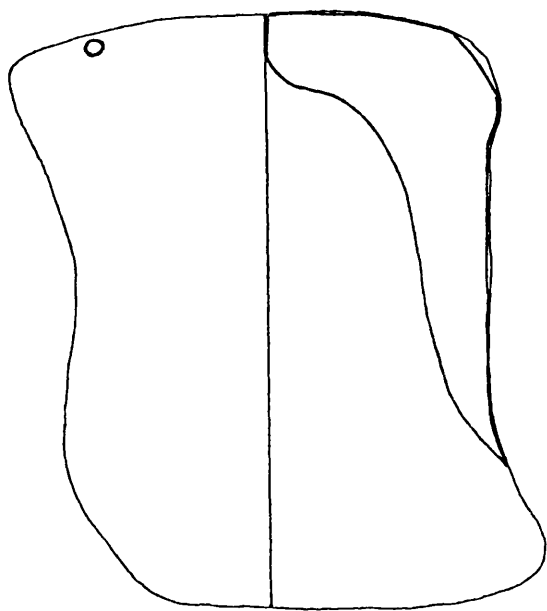


T126 (FB)

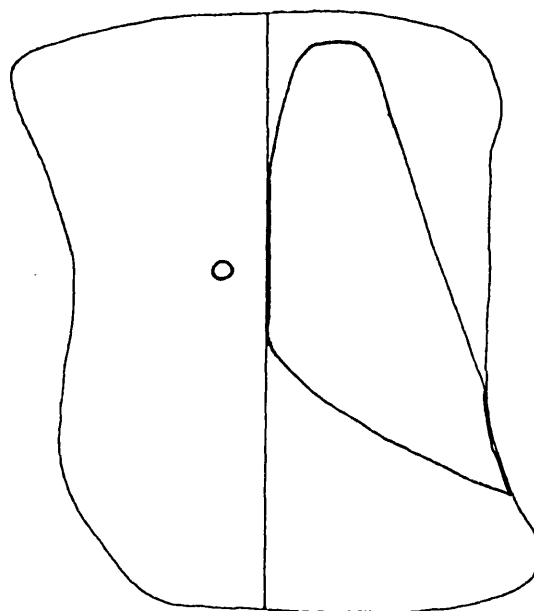


CA1 INJECTIONS

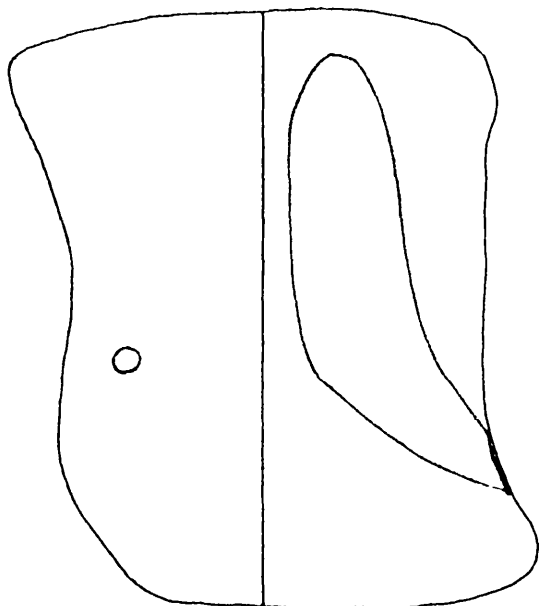
T129 (RHO)



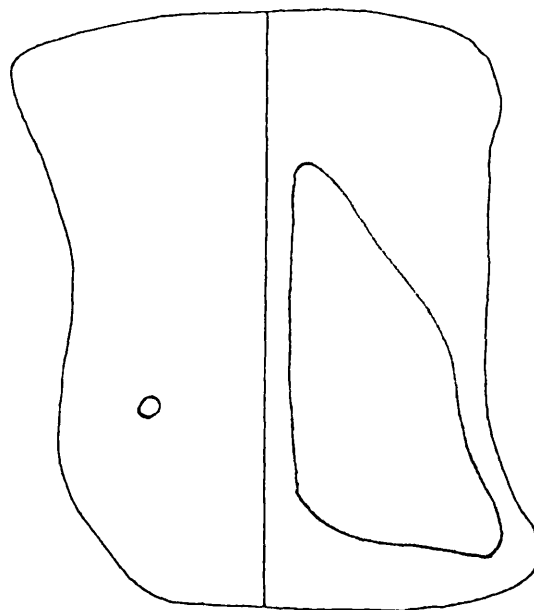
T133 (RHO)



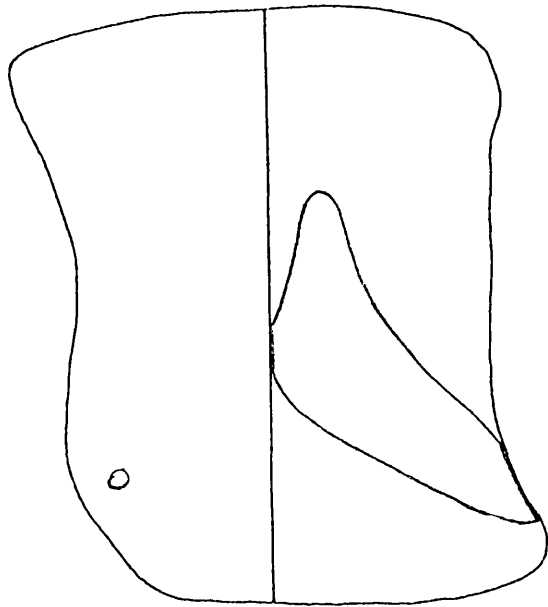
T148 (FB)



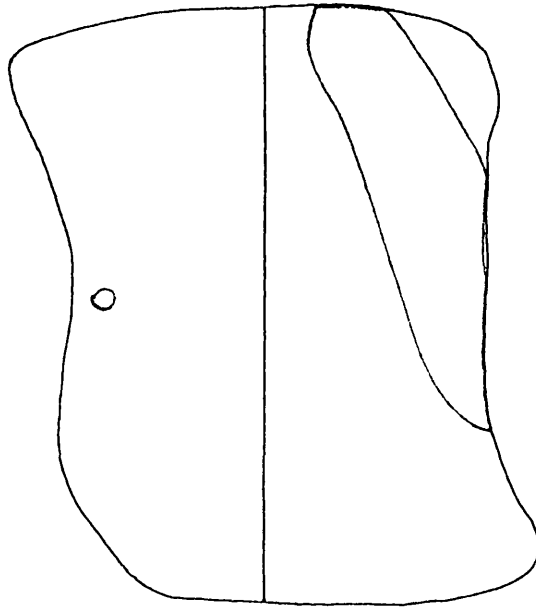
T150 (FB)



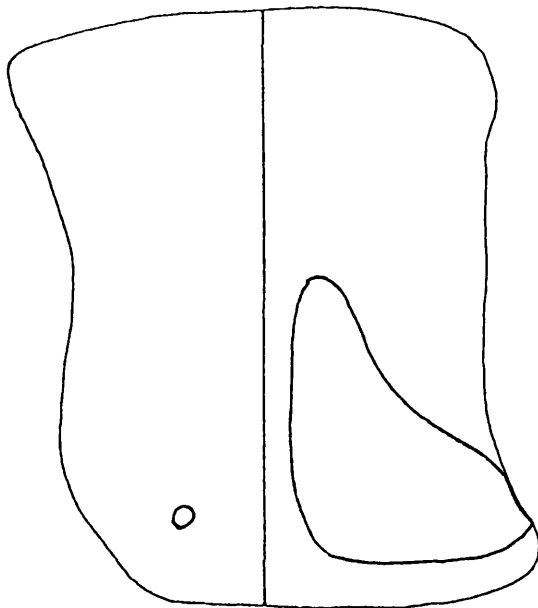
T153 (FB)



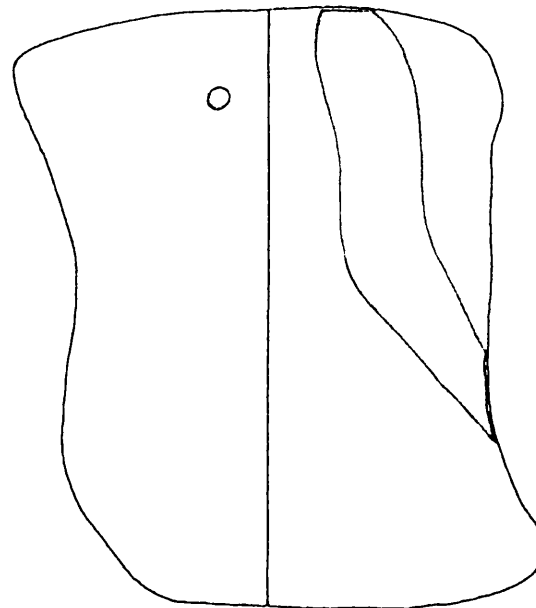
T158 (FB)



T160 (RHO)



T161 (FB)



## **The distribution of labelling**

In all cases the labelling took the form of a continuous band of cells extending over a substantial portion of the septotemporal extent of CA3, such that the labelling at any transverse level was manifested in the shape of a strip occupying a fraction of the proximodistal spread of the CA3 field. With the exception of a few individually-labelled cells located around the periphery of the band, labelling was not noted outside this band. Regardless of the positions of the injection sites within CA1, the resultant bands were oriented in a diagonal fashion across the CA3 field, such that the labelling was located progressively closer to the hilus for more temporal parts of CA3.

## **Topography in the septotemporal plane**

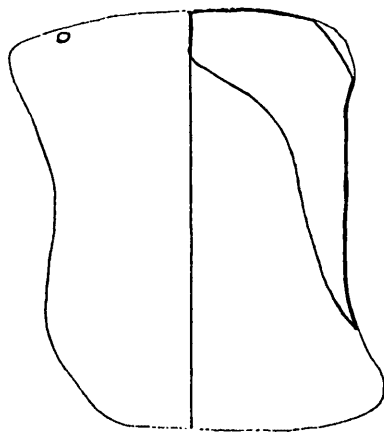
### *The position of labelling*

Although the widespread nature of the labelling necessarily discounts the possibility of any point-to-point specificity in the projection, two gradients were nevertheless detected in its organization. Firstly, the septotemporal position of each band was found to be related to the septotemporal position of the injection such that injections in septal CA1 gave rise to labelling concentrated in the septal part of CA3, whereas more temporal injections resulted in bands located more temporally in CA3.

### *The spread of labelling*

The spread of labelling along the septotemporal extent of CA3 was also related to the injection placement, with injections in septal CA1 producing bands which extended from the septal pole across most of the CA3 field, while injections in temporal CA1 gave rise to bands which were more restricted in their septotemporal spread and

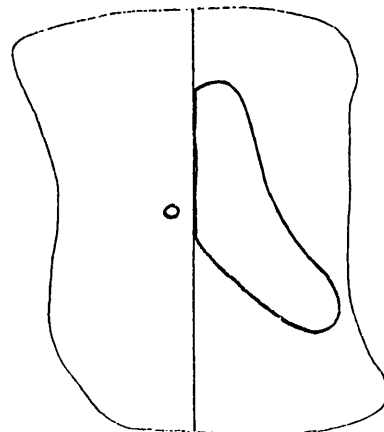
T129R



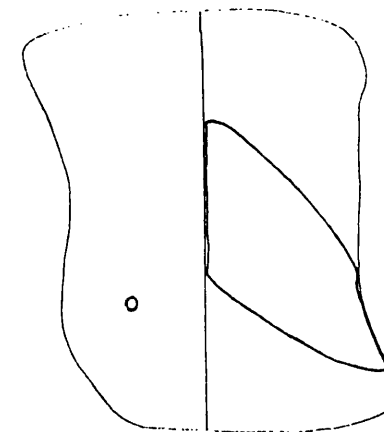
Left Fig.5 Examples of injections placed at different points along the CA1 field, giving rise to patterns of labelling which show a topographical organization in the septotemporal plane

were largely confined to the temporal half of the CA3 field. For example, in the case of the septally-located injection T129R (top left), labelling is seen as far as the most temporal quarter of the CA3 field (a septotemporal spread of approximately 6mm), whereas in the case of the temporal injection T160R (bottom left), labelling is entirely absent from the septal half of CA3 and possesses a septotemporal spread of only 3.5mm. Furthermore, injections into temporal CA3 produced bands which were found to have a more widespread transverse coverage of CA3, so that they appeared "compressed" in comparison with bands arising from the septal injections, while the amount of surface area covered remained of similar magnitude. This feature can be assessed quantitatively by comparing the ratio of the spread of labelling in the septotemporal plane with that in the transverse plane: in the case of injections T129R (septal) and T160R (temporal) the ratios are approximately 2:1 and 1:1. The difference is compounded by the fact that, in the

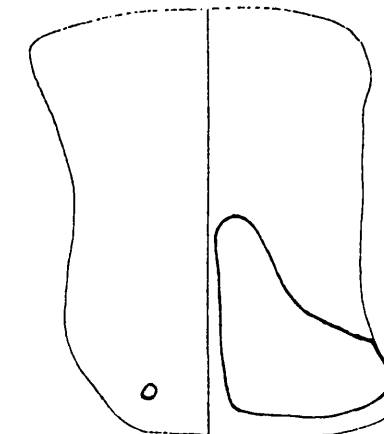
T170R



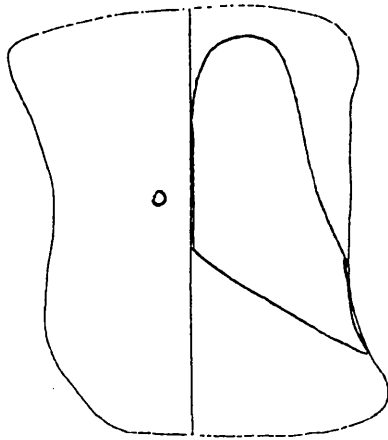
T171R



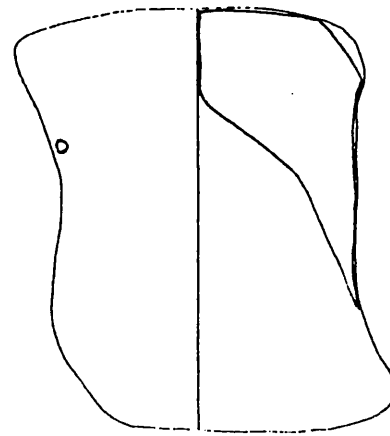
T160R



T133R



T168R



*Above* Fig.6 Two injections placed at approximately the same septotemporal level in CA1. Note the similarity between the bands of labelling in terms of septotemporal spread, and in the direction of spread. Note also the transverse gradient in the region of labelling at the same septotemporal level as the injection.

former case, the majority of labelling is confined to the proximal half of the CA3 field, with distal labelling occurring only at the septal pole, whilst in injection T160R, all but a small fraction of cells (located proximally and septally) are confined within a narrow septotemporal range, approximately 1.5mm in width, but which extends across the transverse plane.

#### *The direction of spread*

The direction of spread also appeared to be a function of the injection placement: injections in the septal half of CA1 resulted in labelling which extended for a greater distance in the temporal than in the septal direction, whereas the converse was true for labelling arising from injections in the temporal half of CA1. Injections in the middle of the CA1 field, such as T170R, produced labelling which extended for approximately equal distances septal and temporal to the injection. As with the total extent of coverage in the septotemporal plane, the direction of spread was invariant

across the transverse plane, with injections into proximal and distal parts of CA1 at the same septotemporal level giving rise to bands with a similar direction of spread.

### **Topography in the transverse plane**

A second, less well defined, gradient was observed in the transverse plane. In some cases (see examples T158 and T170) the relationship was clearly noted, with injections in proximal and distal CA1 producing bands located for the main part in distal and proximal CA3 respectively, while in others the gradient was less marked. For example, in injections T129 (distal CA1) and T168 (proximal CA1) the overall emphasis of the band is seen to correlate with this gradient but, at the level of the injections, labelling was noted across most of the proximodistal extent of CA3. In most cases, though, this gradient is best summarised by stating that *a region in CA1 located at a certain distance from the CA2 border preferentially receives fibres from cells located in CA3 at the same distance from the CA2 border at the same level.*

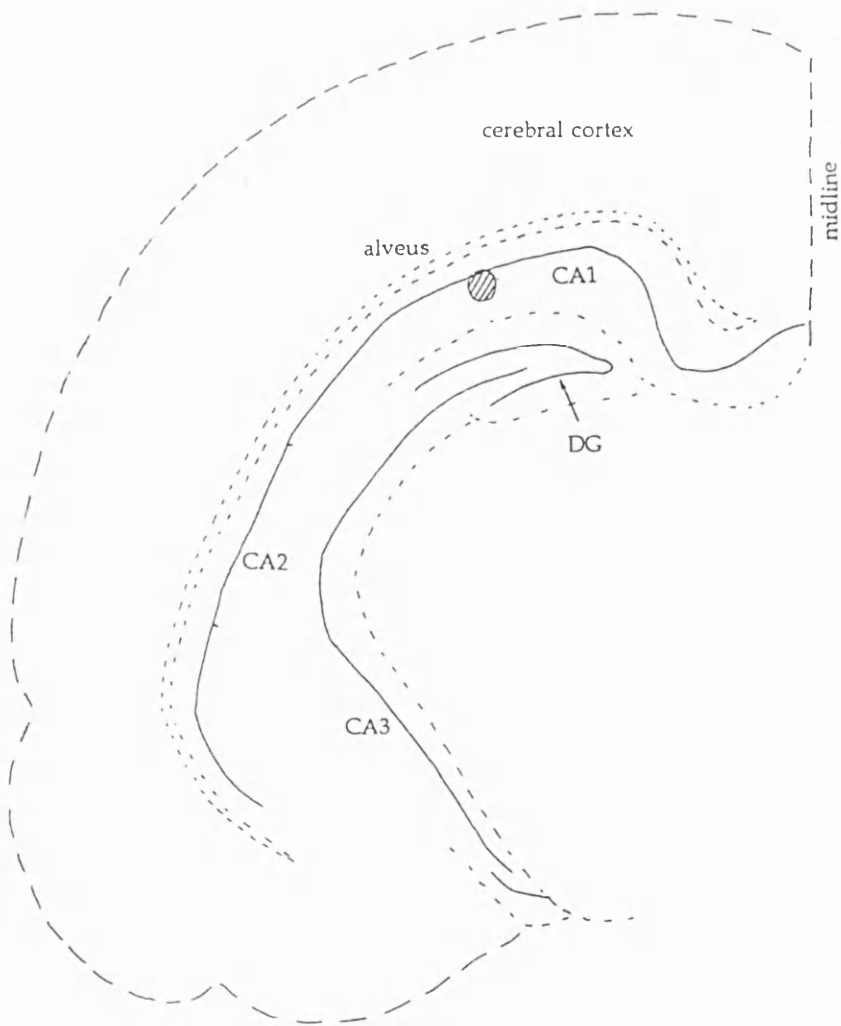
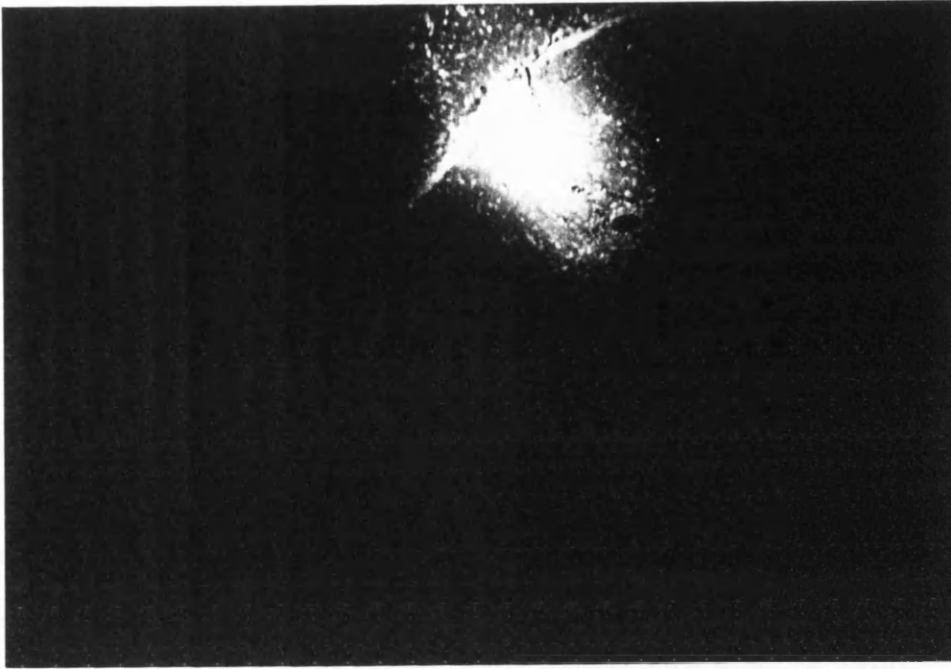
### **The extent of labelling**

Since all of the displayed injections had uptake sites spanning the stratum radiatum (and, in the case of the larger injections, parts of the stratum oriens and/or stratum moleculare), the relative uniformity of the resultant bands in CA3 suggests that most of the fibres projecting to these regions are encompassed by the sites of uptake, in accordance with the belief that the stratum radiatum of CA1 constitutes a major terminal field for the Schaffer collateral input, and that the number of fibres projecting to any given region in CA1 is independent of the location of that region in the CA1 field.

Two examples of the distribution of labelling in the unextended and extended CA3 fields are shown in photographic form on the following pages. Since the two injection sites are found to be in relative proximity on the extended model of the CA1 field (see page 135) it is worth noting the considerable difference in the patterns of labelling. Pages 149-150 display photographs of the two injections, along with diagrams which show the position of each injection site within the hippocampus.

# Injection T158B

200um

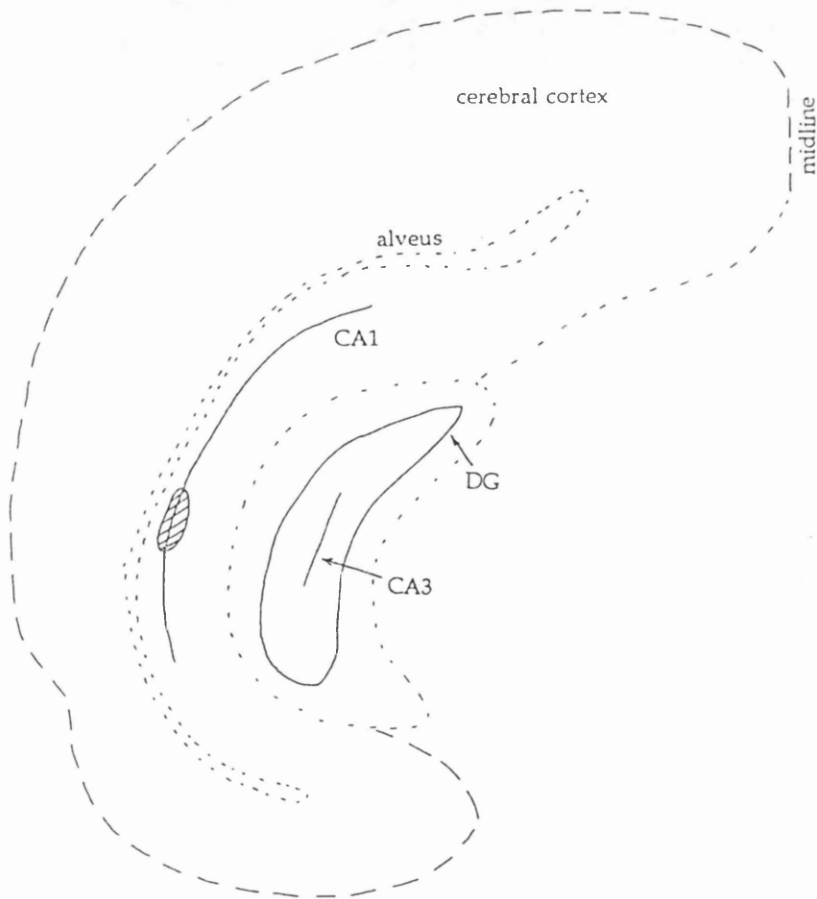
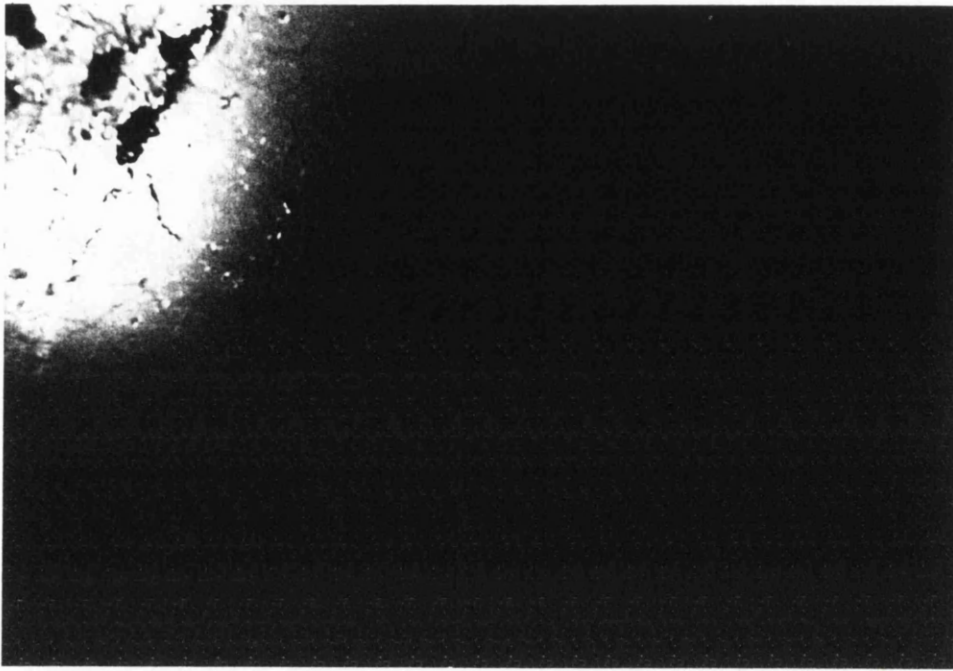


149

⊘ injection site

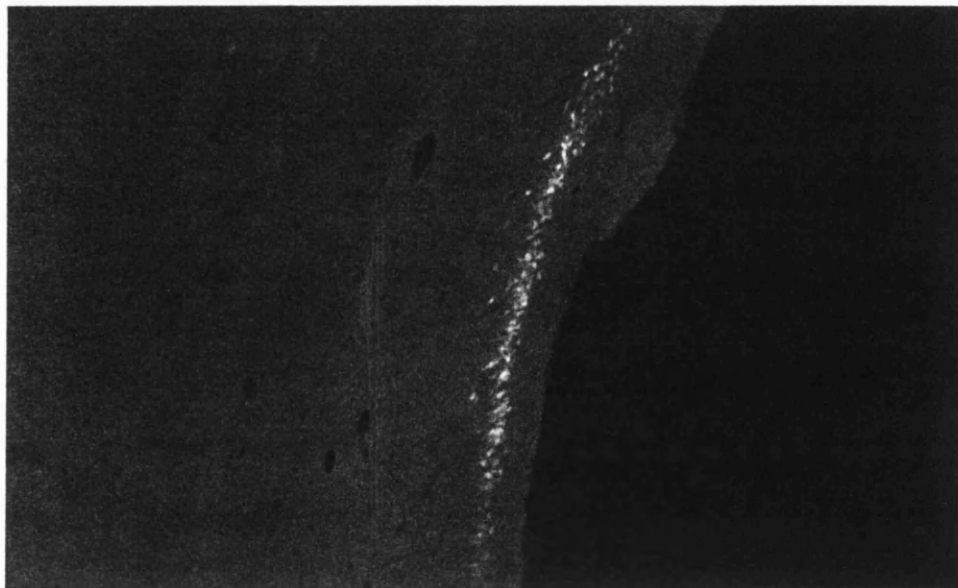
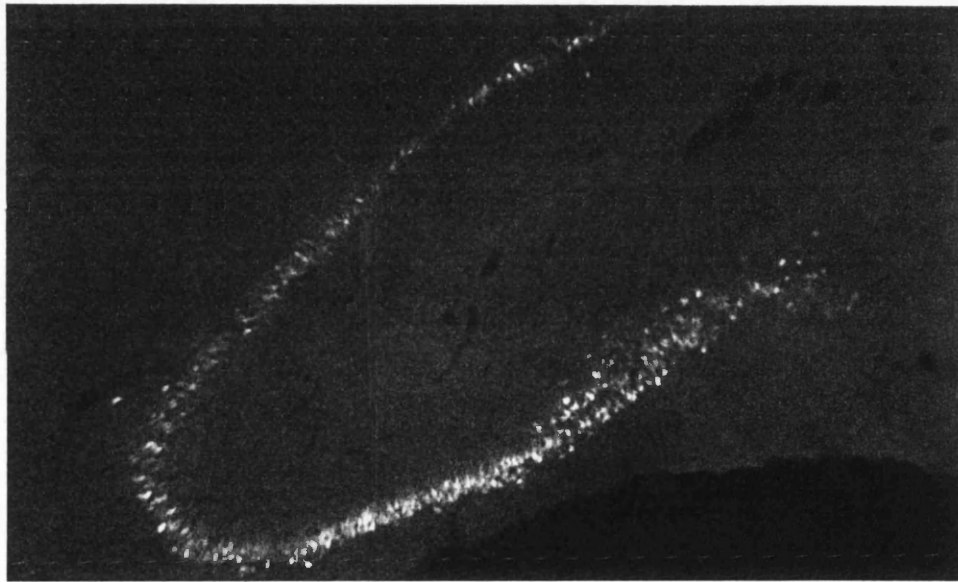
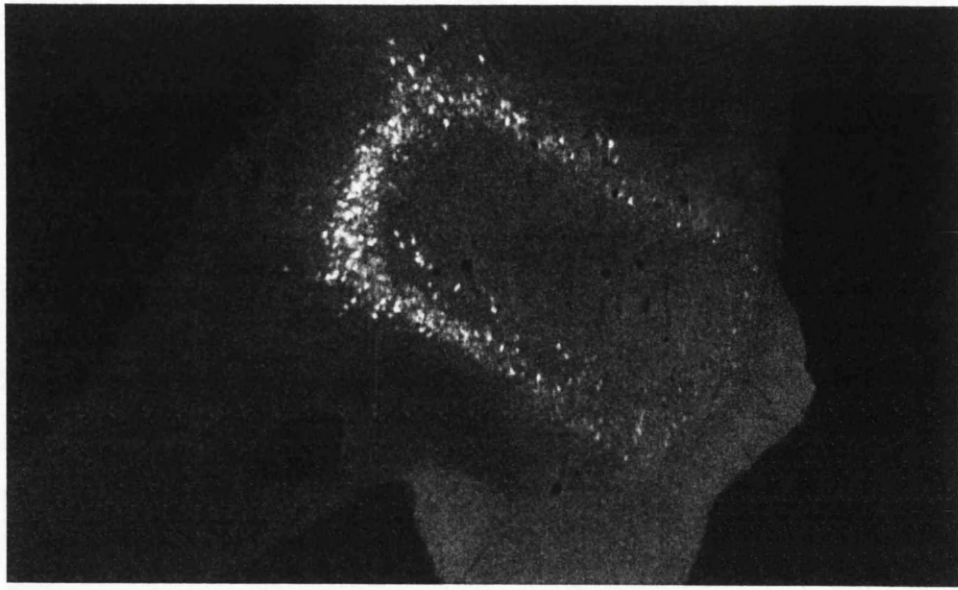
# Injection T153B

200um



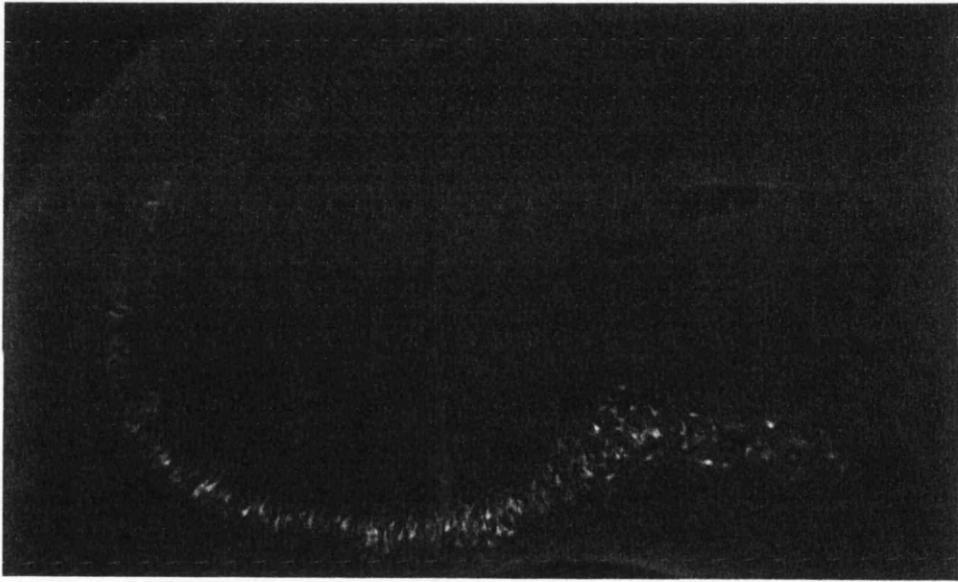
⊗ injection site

200um

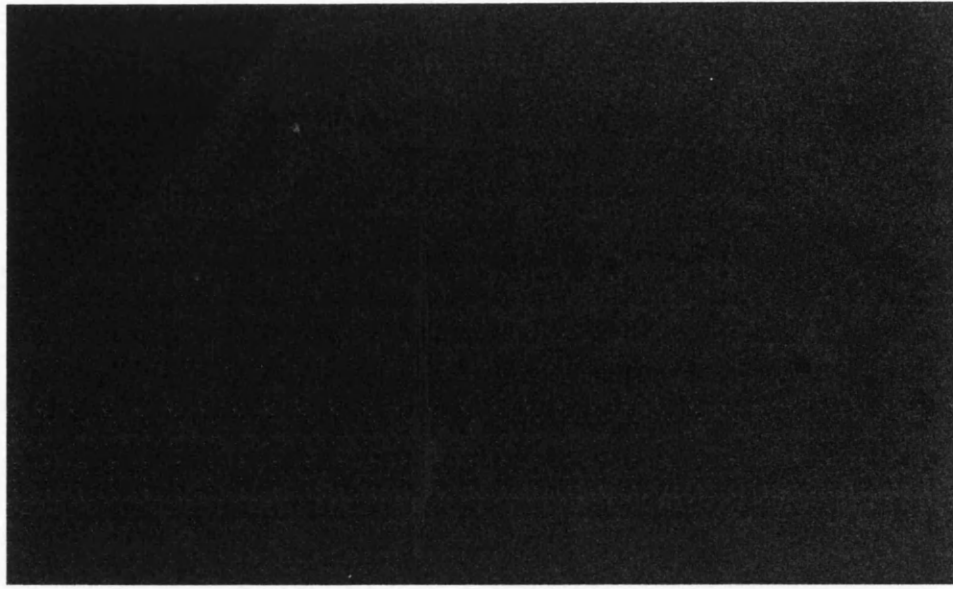
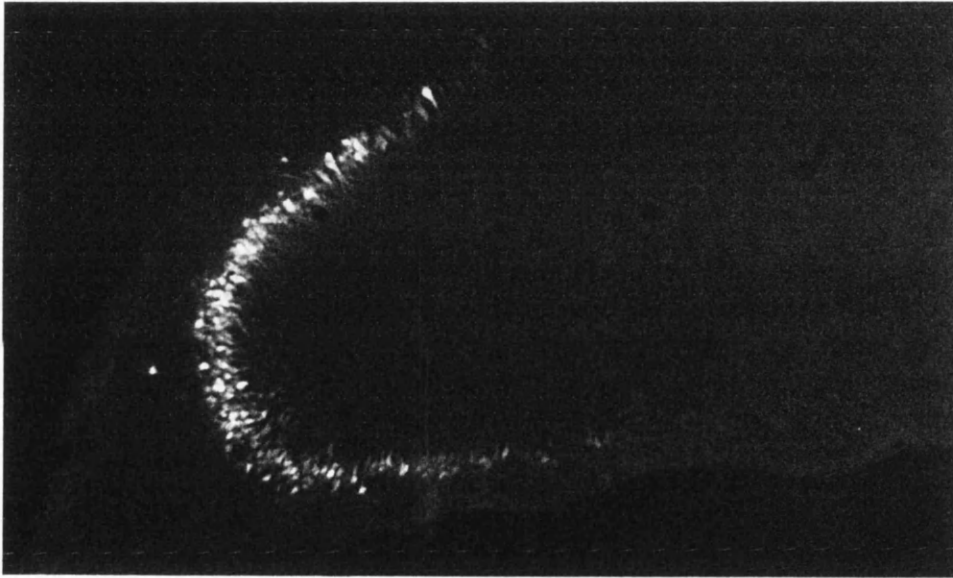
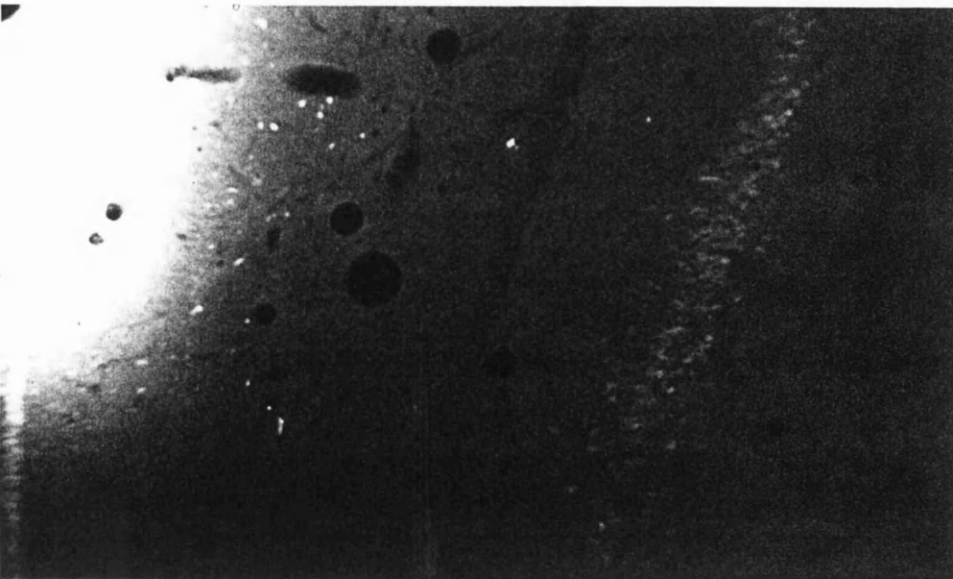


(T158) Fast Blue labelling in coronal sections through the unextended ipsilateral hippocampus at three levels.

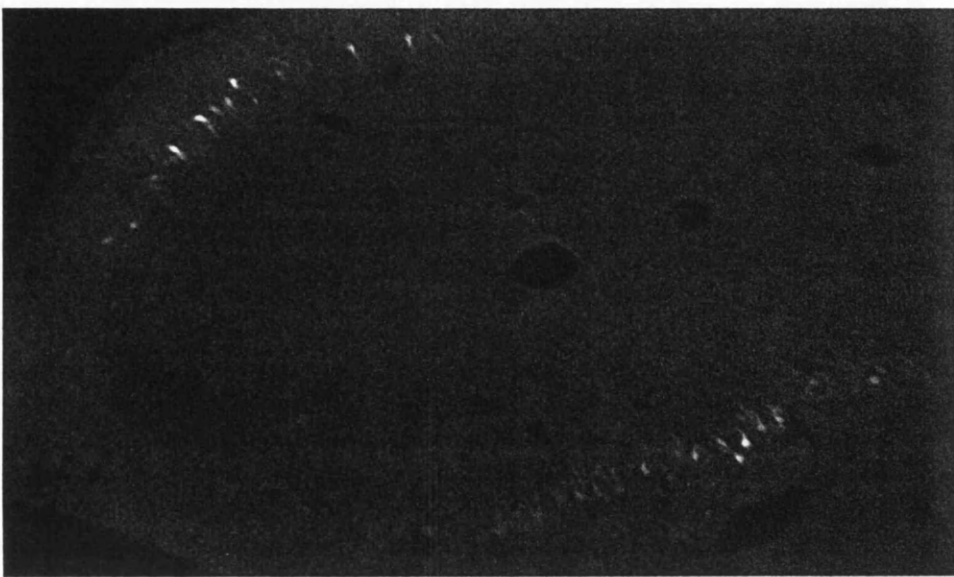
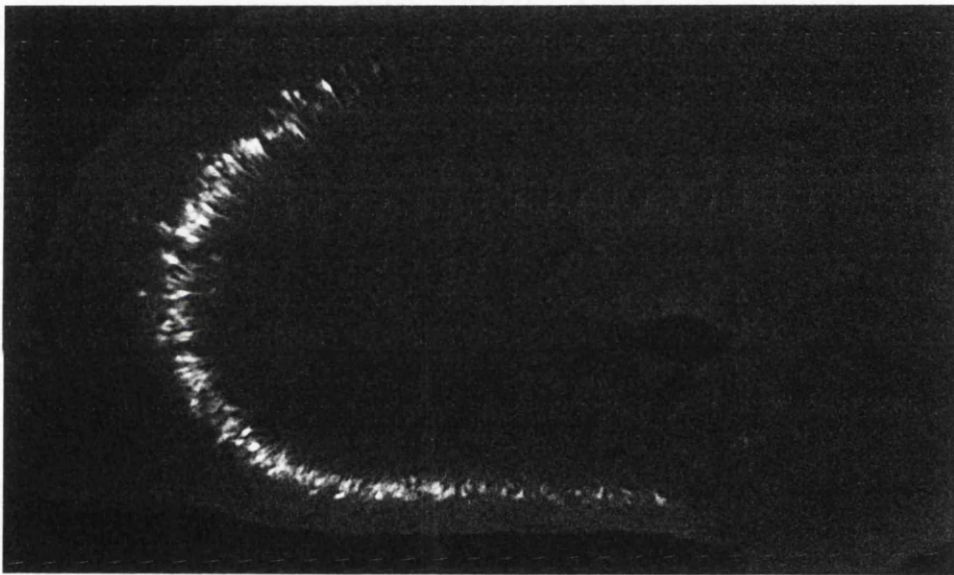
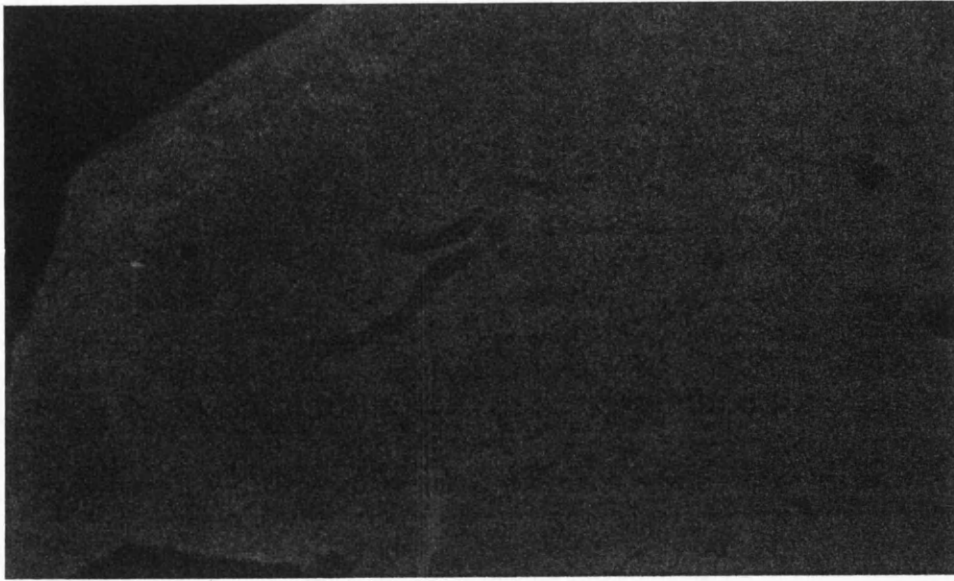
*Top* rostral CA3    *Middle* mid-rostrocaudal CA3    *Bottom* caudal CA3



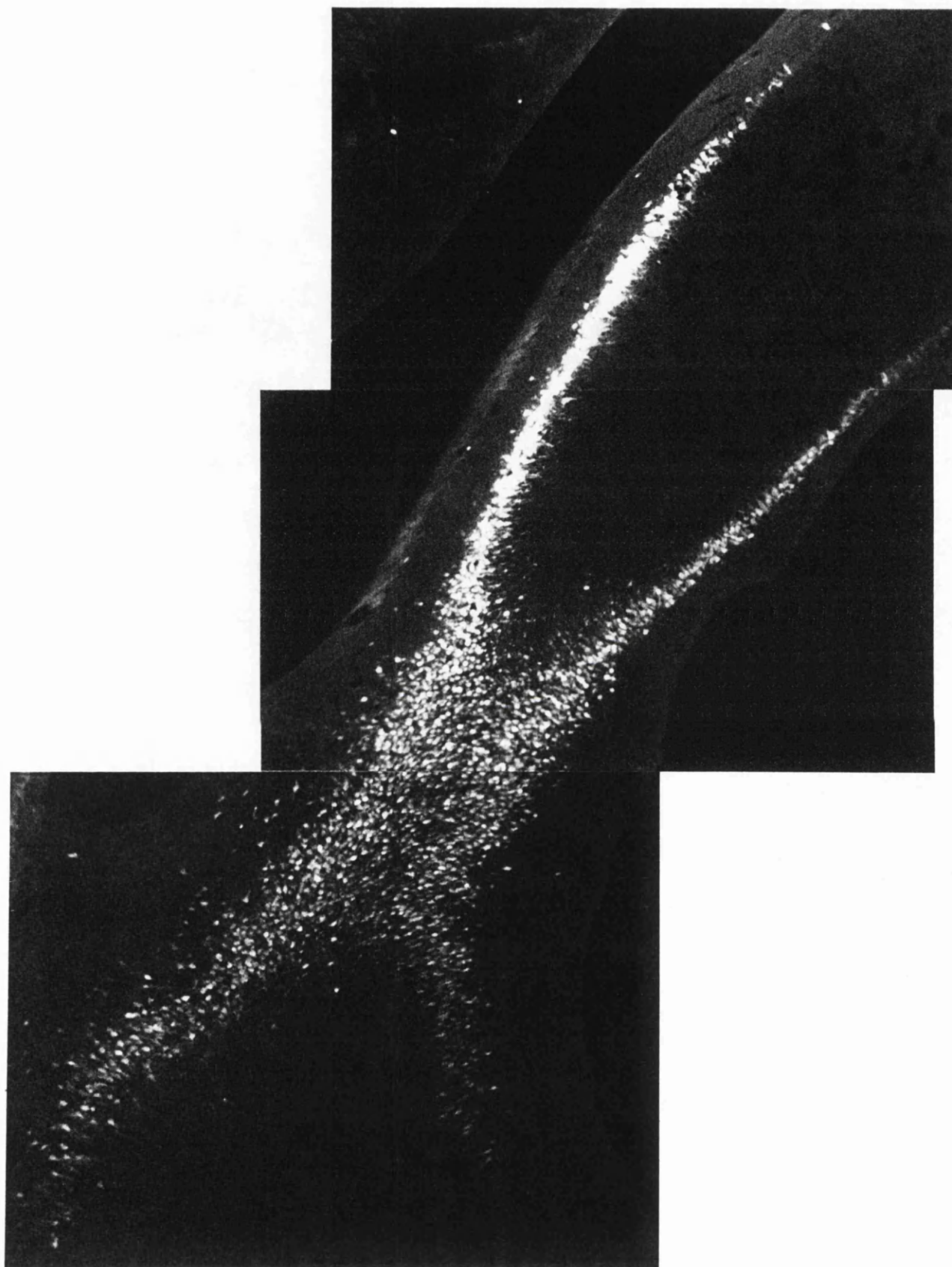
(T158) Fast Blue labelling in transverse sections through the extended contralateral hippocampus at three levels.  
*Top* septal CA3    *Middle* mid-septotemporal CA3    *Bottom* temporal CA3



(T153) Fast Blue labelling in coronal sections through the unextended ipsilateral hippocampus at three levels.  
*Top* rostral CA3    *Middle* mid-rostrocaudal CA3    *Bottom* caudal CA3



(T153) Fast Blue labelling in transverse sections through the extended contralateral hippocampus at three levels.  
*Top* septal CA3    *Middle* mid-septotemporal CA3    *Bottom* temporal CA3

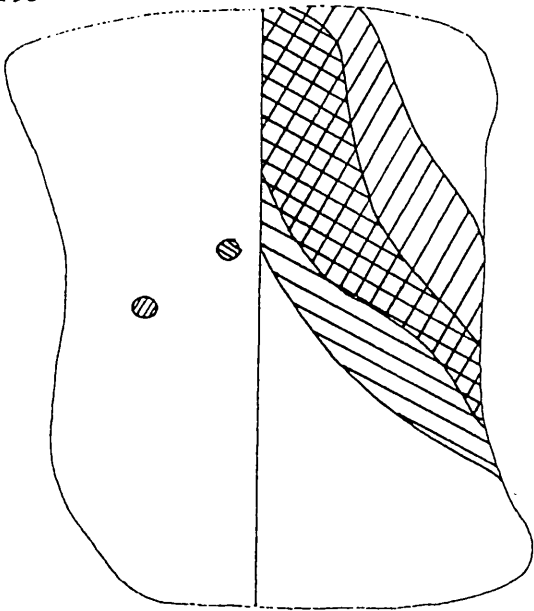


(T153) A montage showing the labelling in the unextended ipsilateral CA3 field. This coronal section cuts through the middle of the hippocampus as it bends back upon itself within the brain.

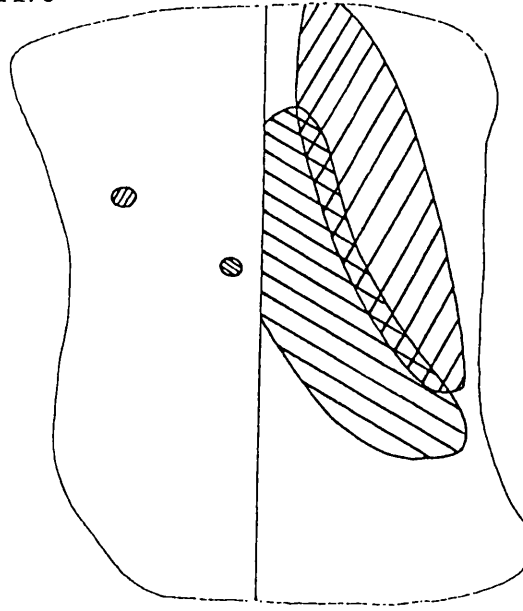
## The distribution of double-labelling within CA3

All operations involving a double injection of fluorescent dyes into CA1 were found to give rise to double-labelling within CA3. Two individually-labelled bands were observed in the CA3 field, with an area of double-labelling which corresponded with the overlap of the two bands. Within this overlap, the proportion of double-labelled cells was approximately 100%. In accordance with the topographical organization of the CA3-CA1 projection, the location and extent of the area of double-labelling in the CA3 field were found to be dependent on the positions of the injections in CA1. Two examples of the distribution of double-labelling (cross-hatched areas) are displayed below.

T93



T170



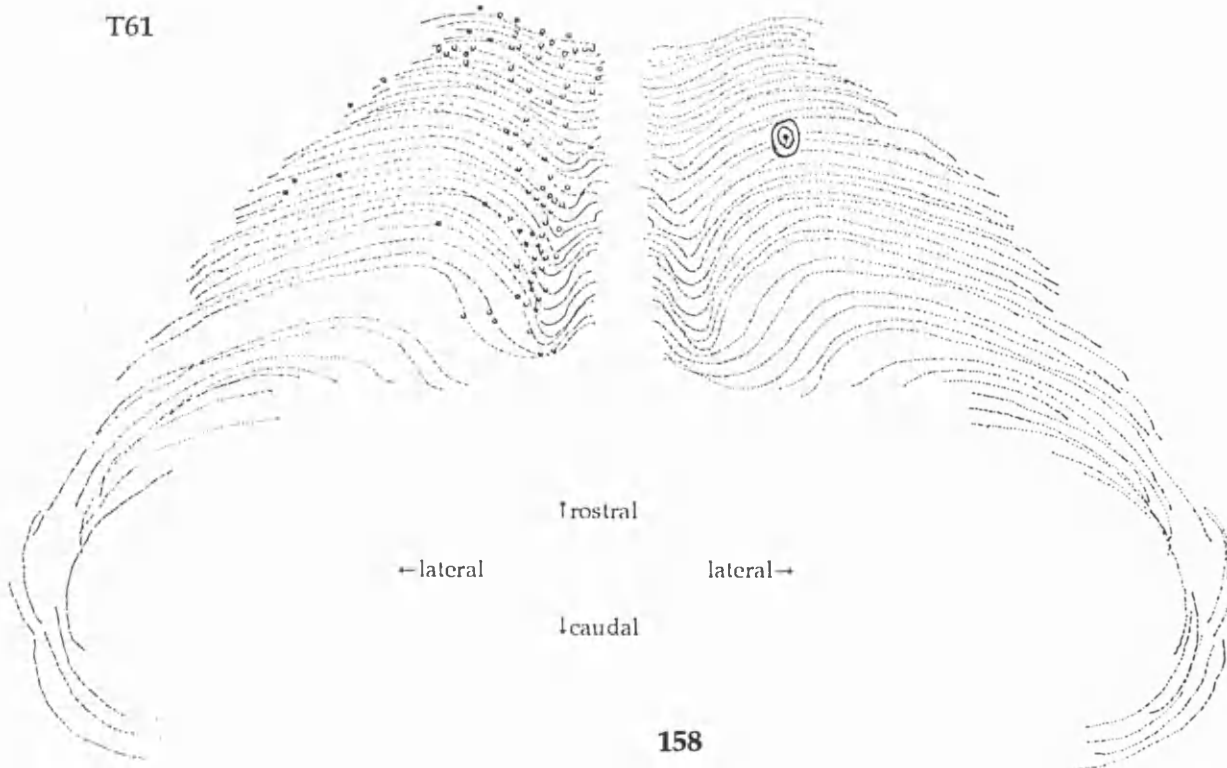
## Evidence for a CA1-CA1 commissural projection

A number of labelled cells was found bilaterally within CA1 following CA1 injections. While this would appear to suggest the presence of an association/commissural projection within CA1, for which some electrophysiological evidence exists (Christian and Dudek 1984; Thomson and Radpour 1991), a cautionary note must be inserted in the assessment of these findings. Since retrograde tracers are known to give rise to labelling as a result of damage to fibres of passage, it might be argued that the labelling of ipsilateral CA1 cells is due at least in part to backfilling from alvear fibres disrupted by the pipette *en route* to the stratum radiatum of CA1. Given that the number of cells labelled in the ipsilateral CA1 field far exceeds that of those labelled in the contralateral field, this argument would appear to have great significance in the rejection of the ipsilateral labelling as valid proof of an association pathway within CA1. However, the presence of labelling contralaterally cannot be explained by way of this reasoning, since efferent fibres from CA1 are not believed to run in the contralateral alveus. On these grounds, it is suggested that the labelling in contralateral CA1 provides evidence for a commissural pathway within CA1.

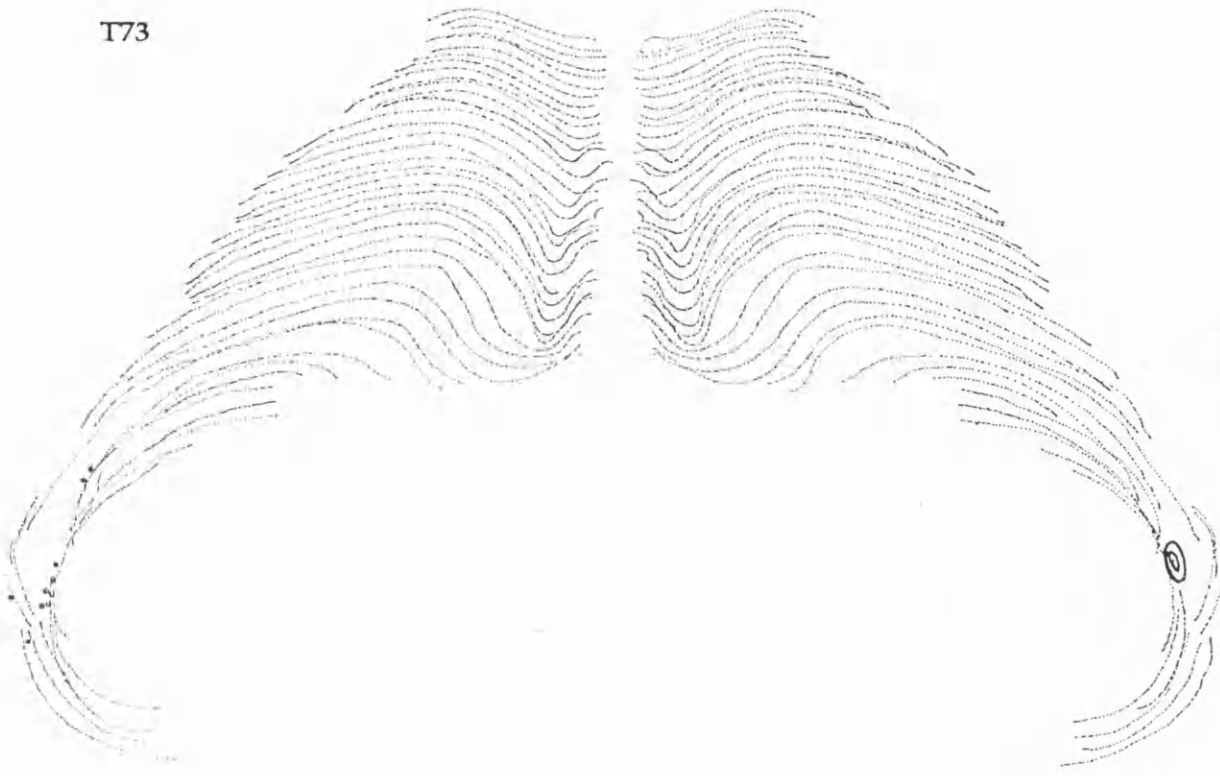
The number of contralateral CA1 cells labelled was never found to exceed 200 in a brain for any injection site, and the labelling was generally found to be in the form of individual cells scattered over a large part of the CA1 field (see T61 overleaf). In cases where the number of labelled cells was very small (for example T73 and T93), these cells were found to be clustered together within CA1. Furthermore, in these cases the cells were found to occupy a part of the CA1 field roughly homotopic to the location of the injection site in the opposite CA1 field. This pattern was not readily observed in other injections where a greater number of cells were labelled, since these tended to be distributed over a larger proportion of the field.

Although these data cannot be employed as evidence for an ipsilateral association pathway in CA1, it is worth recalling the comments of Gottlieb and Cowan (1973), to the effect that every hippocampal neuron giving rise to a contralateral projection also provides a projection which terminates in a similar region in the ipsilateral field.

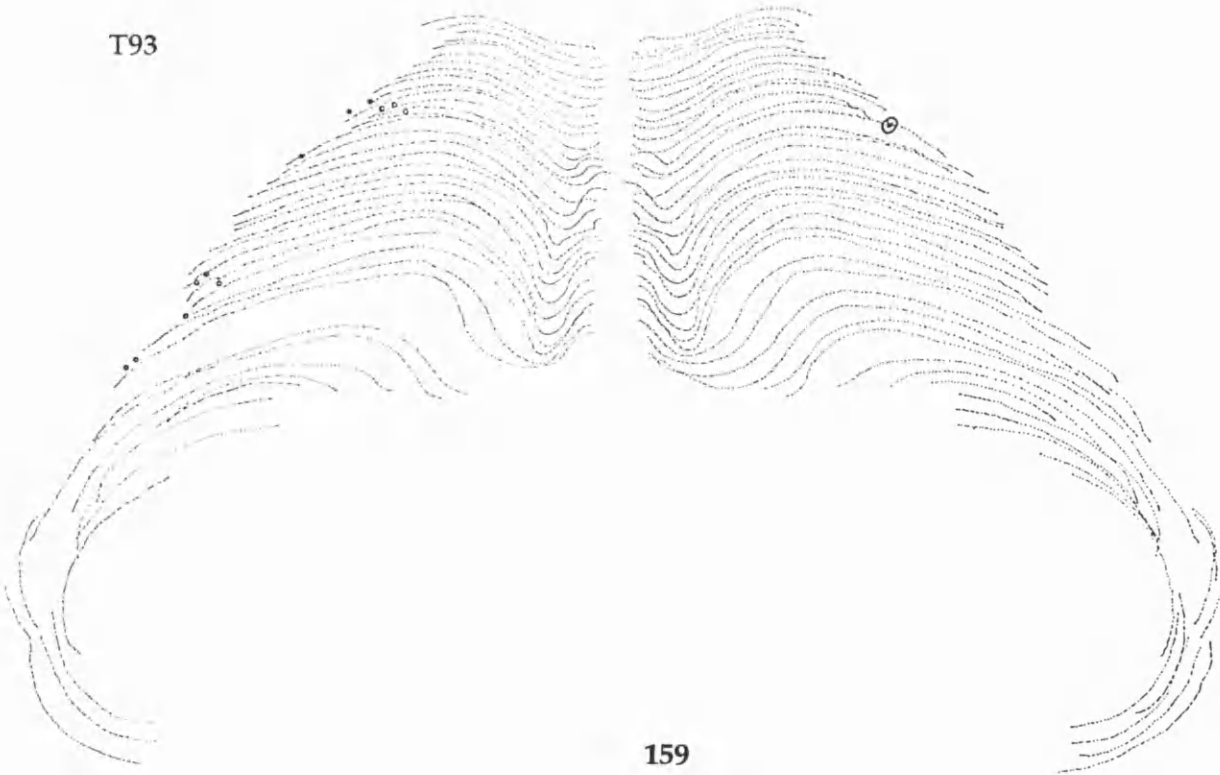
Three examples of contralateral filling in CA1 are shown below. In these diagrams a different representation of the CA1 field is employed in order to show the entire population of labelled cells. To this end, data was compiled from every section through the hippocampus, in contrast to the other experiments, in which data was collected from a fraction of the total number of sections. In the representation the outline of the CA1 cell layer bilaterally as seen in coronal section are drawn by camera lucida at 40 levels through the length of the unextended hippocampus. The lateral displacement from the midline of the brain of the CA1 layer at each level is also incorporated into the representation. Note that the CA3 field is *not* included in this representation.



T73



T93

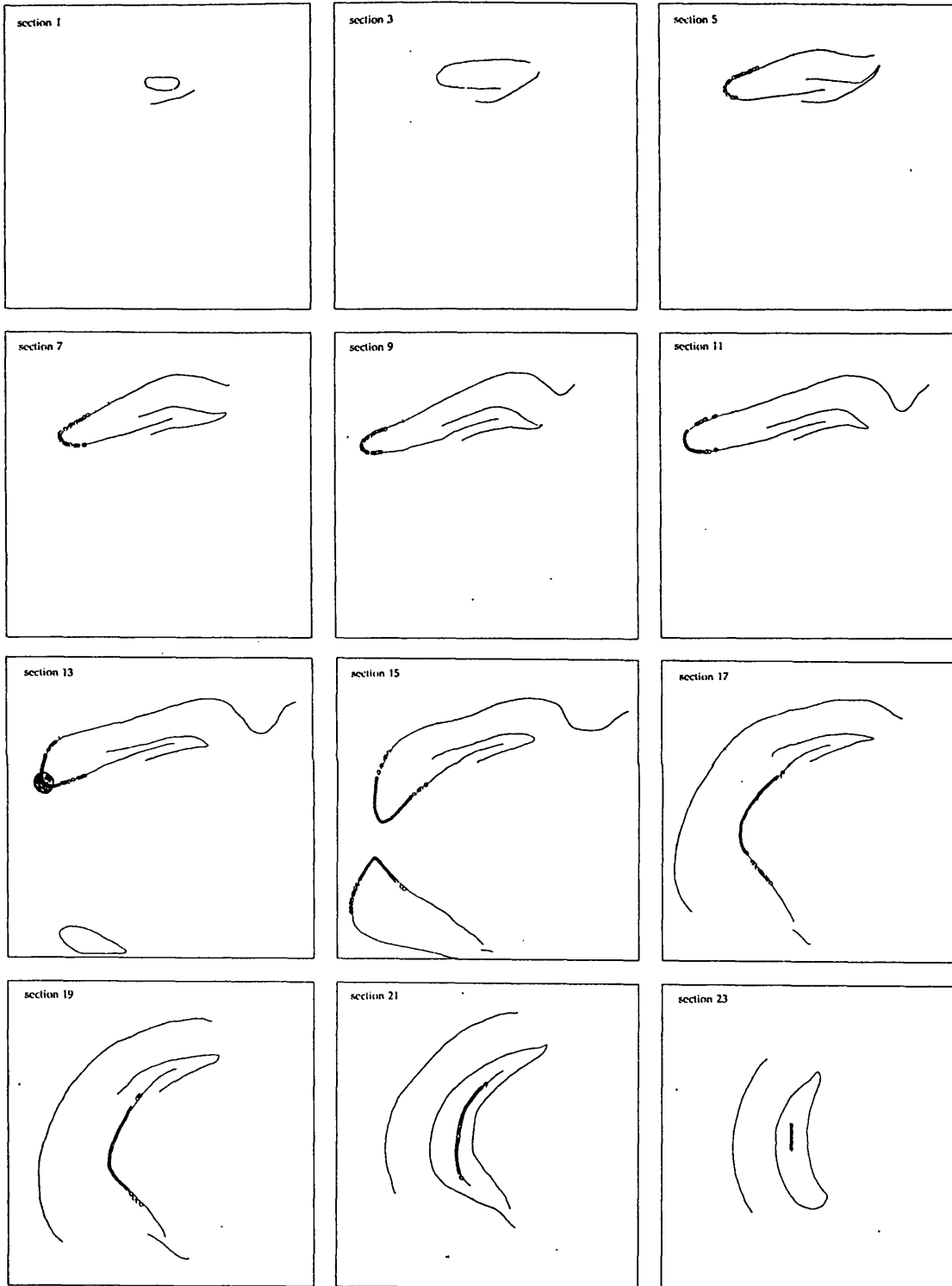


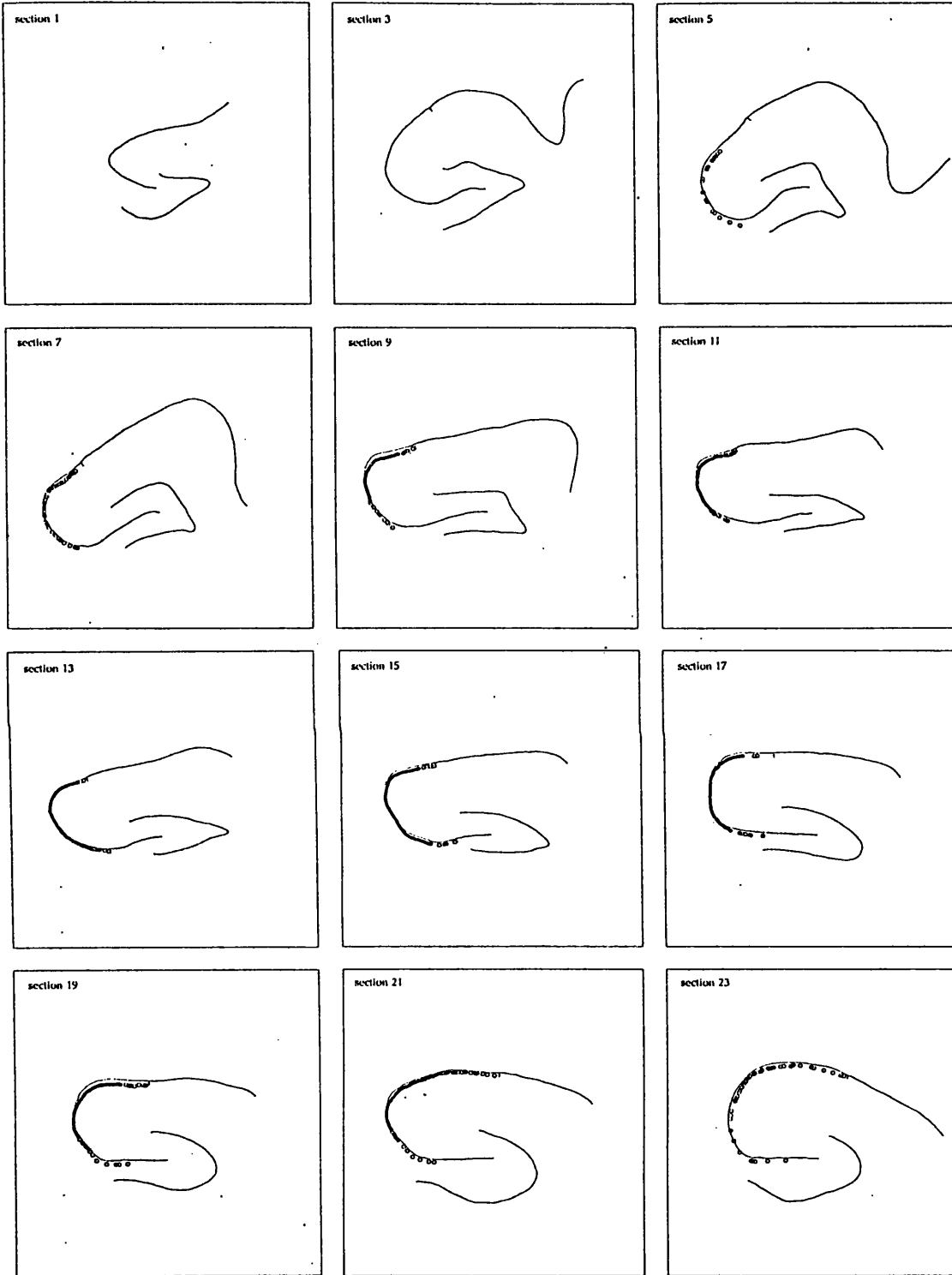
## **EXPERIMENT II(ii): A study of the topographical organization of the CA3-CA3 association pathway**

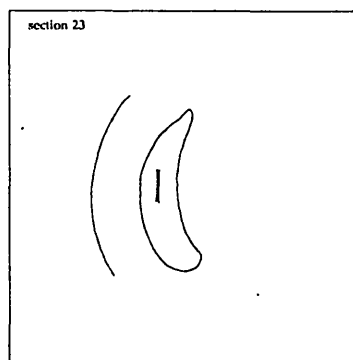
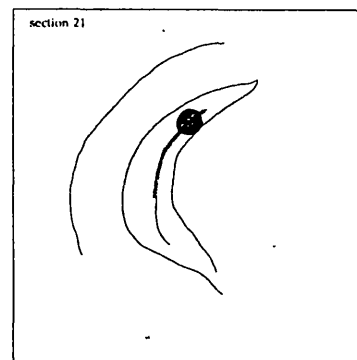
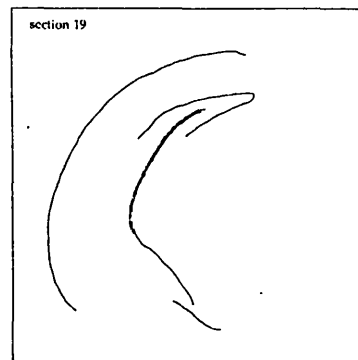
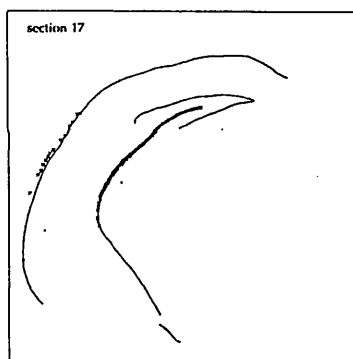
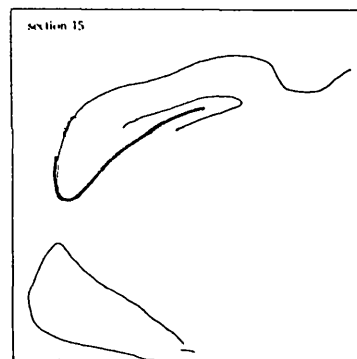
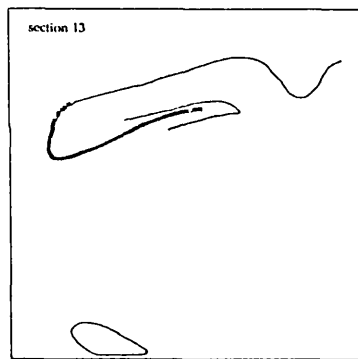
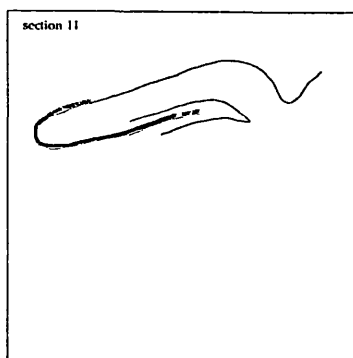
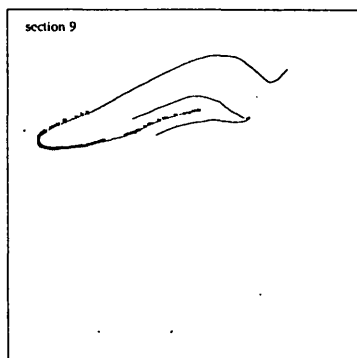
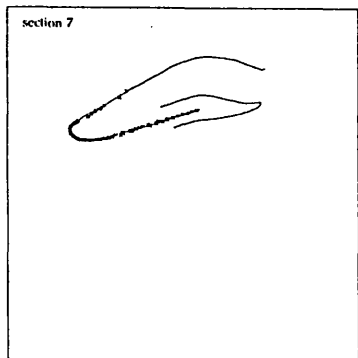
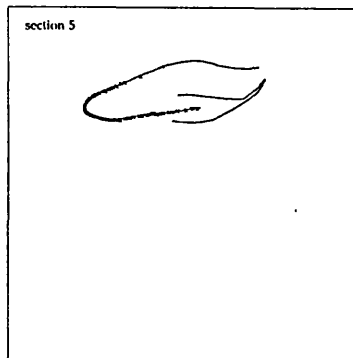
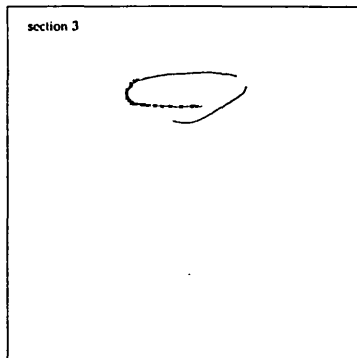
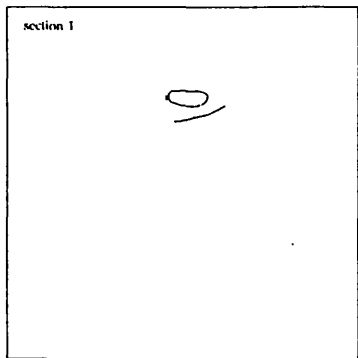
The association pathway of CA3 constitutes a further efferent system of the pyramidal cell axon collaterals. The injections which were placed into CA3 in Experiment III were therefore used in addition to compare the organization of the association pathway with that of the CA3-CA1 pathway.

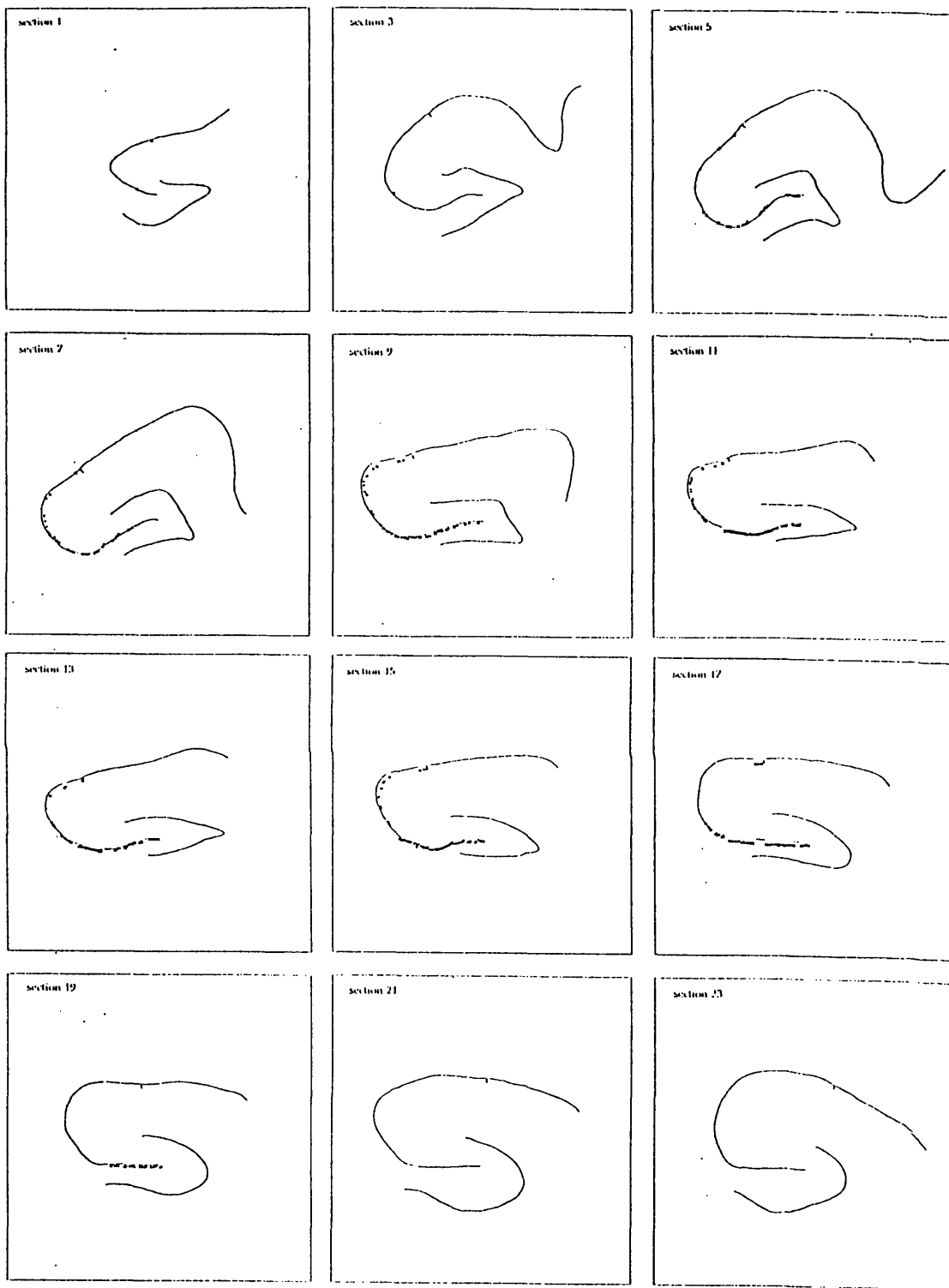
Data was collected from 12 injection sites spanning the extent of the CA3 field. Injections were placed in the stratum oriens or in the proximal part of the stratum radiatum of CA3, in order to minimise any backtracking of dye into the dendritic fields of CA1. Data from subjects in which uptake of dye from CA1 was deemed to have occurred were discarded. Similarly, efforts were made to avoid the inclusion of any part of CA1 within the uptake site of the injection, which prohibited the specific placement of dye into the region of CA3 abutting the CA2 border. Given the proximity of the granule cell layer to the pyramidal cell layer of distal CA3, injections into this part of the CA3 field necessarily encompassed part of the dentate gyrus and the hilar region within the uptake site. As in Experiment Iii, the septotemporal positions of the injection sites in CA3 were calculated using the topological transform. In order to ensure that this means of representation was sufficiently accurate for data analysis, the injection sites (and labelling) for the last 3 injections (T168-T172) were observed in the extended ipsilateral hippocampus.

Two examples of bilateral labelling are shown in full on the following pages. In addition, the results from all 12 injections are displayed on pages 165-167. The injection sites in examples T113-T161 are calculated using the topological transform; in all cases the band in CA3 represents the pattern of labelling found in the extended hippocampus contralateral to the injection.



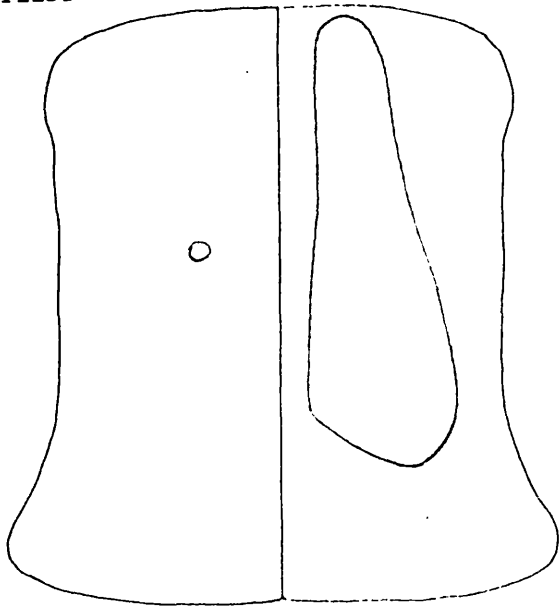




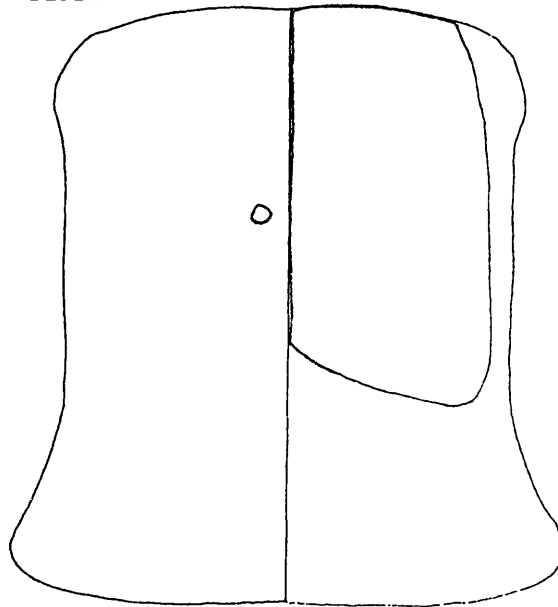


CA3 INJECTIONS

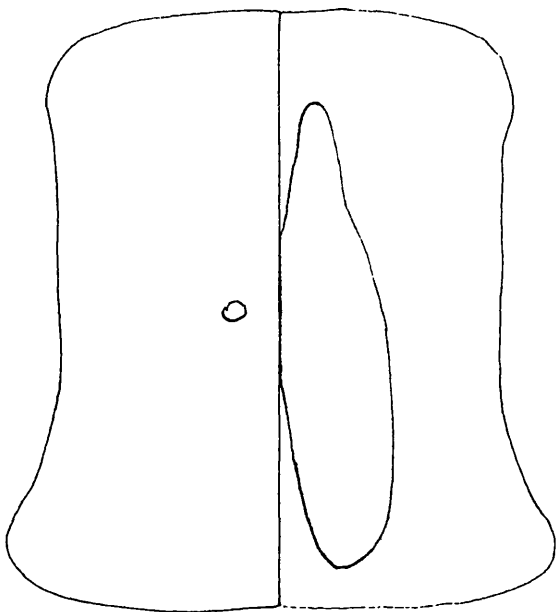
T113B



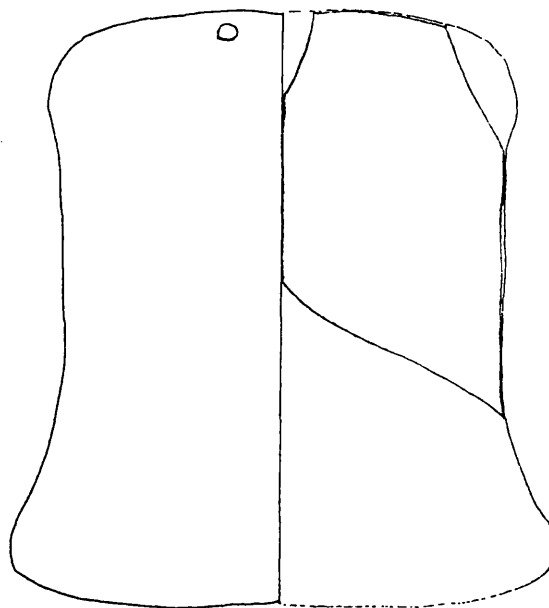
T131B



T133B

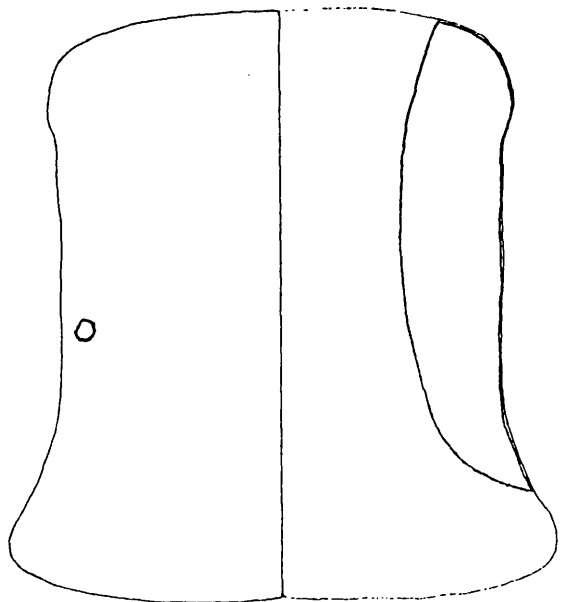


T136B

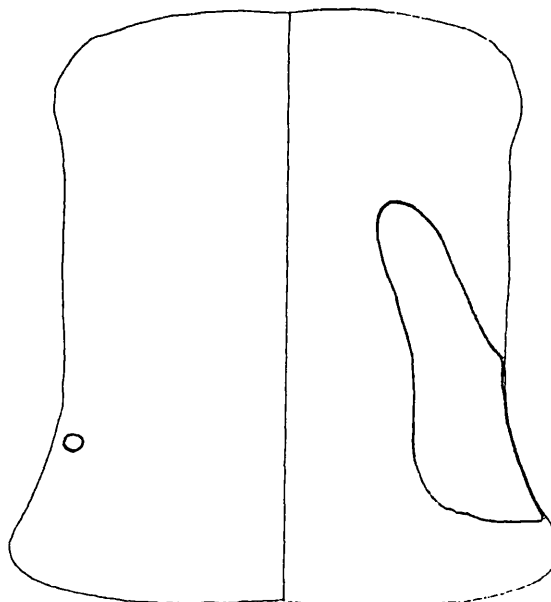


CA3 INJECTIONS

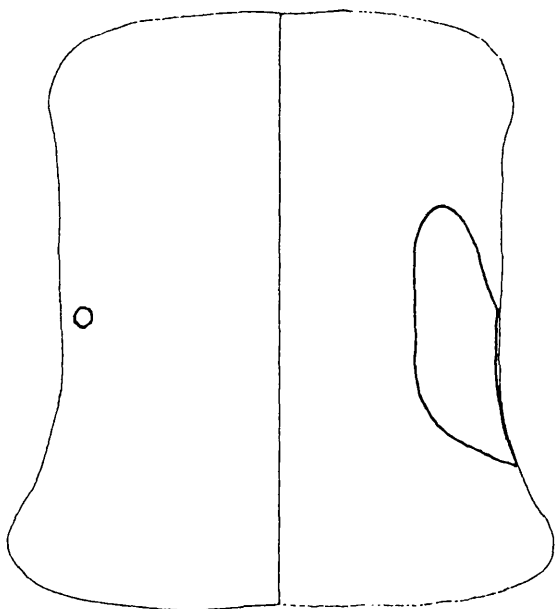
T148R



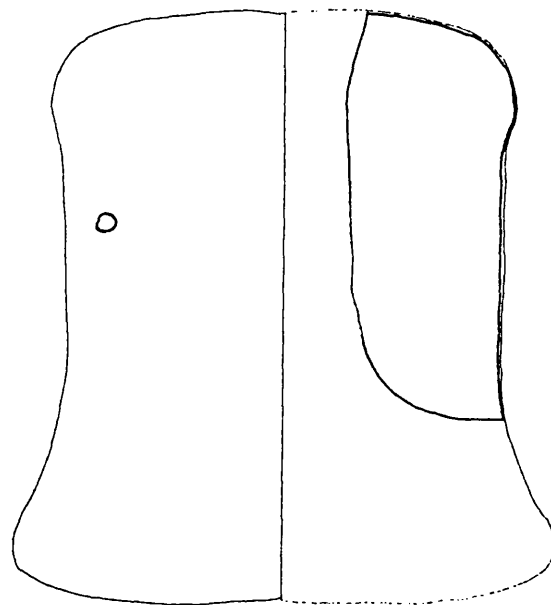
T153R



T157R

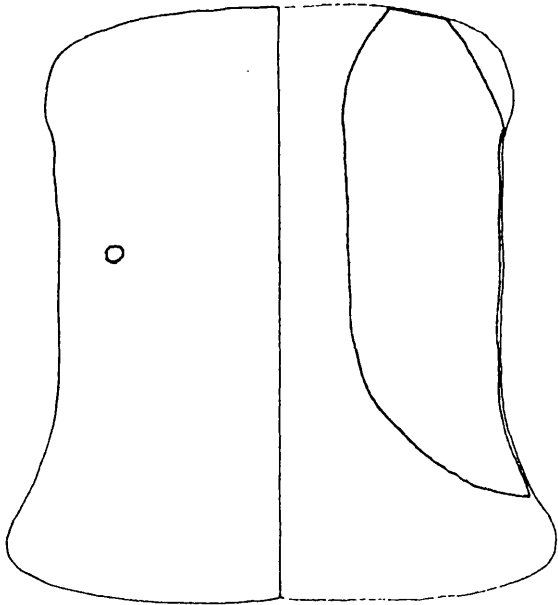


T159R

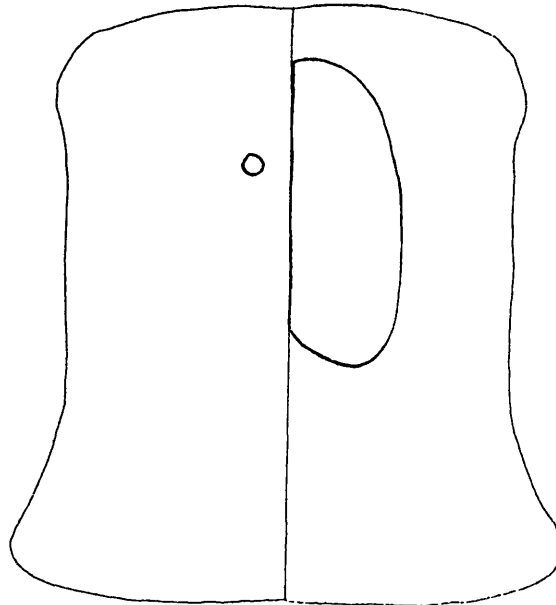


CA3 INJECTIONS

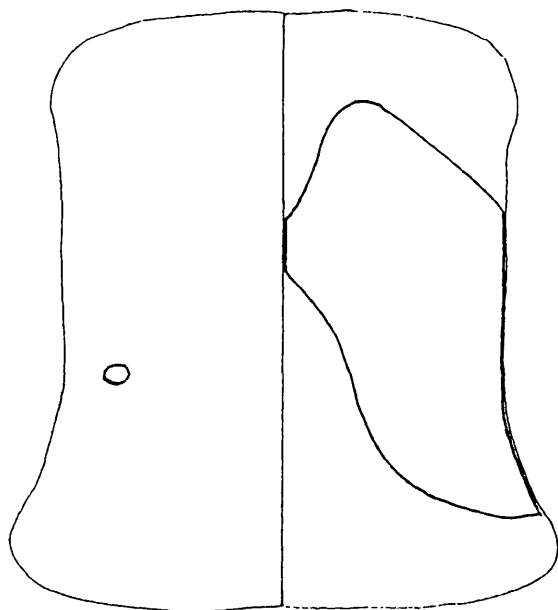
T161R



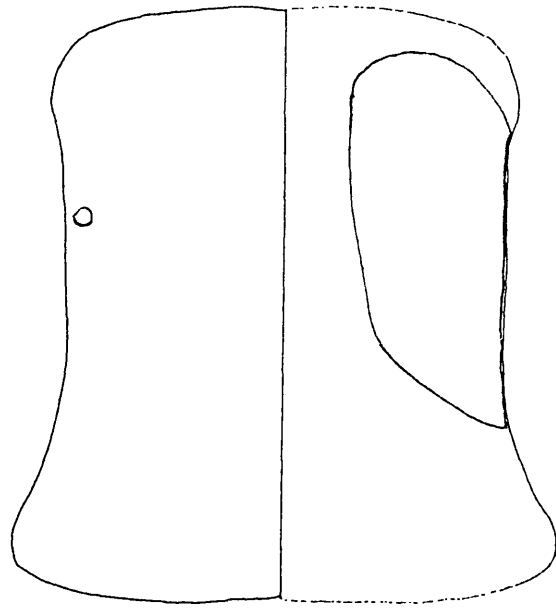
T168R



T172R



T172B



## **The topographical organization of the CA3-CA3 projection**

As with the CA3-CA1 pathway, the projections to any given site in CA3 arise from a group of cells covering a substantial portion of the septotemporal extent of CA3, with scant labelling outside this region. A comparison of the ipsilateral and contralateral patterns of backfilling suggests that the association and commissural CA3-CA3 projections are identical, in agreement with the bilateral symmetry noted in the CA3-CA1 projection.

Two gradients can be noted in the organization of this projection. Septal injections gave rise to labelling which was located in the septal part of CA3, whereas injections placed more temporally produce backfilling in more temporal regions of the CA3 field. This septotemporal gradient, however, was not strongly defined as a result of the extensive labelling along the septotemporal plane which appeared to be a feature of this projection. The majority of injections produced bands of labelling whose centres were found to be at approximately the same septotemporal level as the injections, demonstrating equal proportions of labelling septal and temporal to the injection. The two cases which did not exhibit this relationship arose from injections at the extremes of the field: the injection in septal CA3 (T136) gave rise to labelling which was largely located temporal to the injection site, whereas the temporal injection (T153) produced backfilling predominantly septal to the injection.

In addition to the organization in the septotemporal plane, there was a marked transverse gradient in the projection, with injections giving rise to patterns of labelling which were centred around the same proximodistal level. Furthermore, the location of the labelling in the transverse plane did not vary with septotemporal position, so that the pattern of labelling was organized parallel to the septotemporal axis of CA3.

## The extent of labelling in CA3

In contrast to the similarity in size of the bands of labelling observed in CA3 following injections into CA1, a marked variation was noted in the extent of labelling following CA3 injections. Furthermore, the size of the labelled area was not seen to be correlated with the spread along the septotemporal plane of the hippocampus - several injections gave rise to labelling that extended over a large fraction of this plane, but covered a relatively small area of the CA3 field, due to a restricted spread of labelling in the transverse plane.

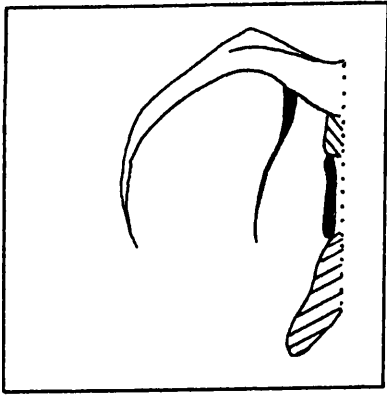
The trajectories of the various axon collaterals of CA3 have been elucidated in intracellular studies (Ishizuka *et al.* 1990; Tamamaki and Nojyo 1991). To recap briefly, the Schaffer collateral runs for the main part in the stratum radiatum of CA3 and then CA1, while the CA3 associational collaterals run both in the stratum radiatum and in the stratum oriens of CA1. It has already been mentioned that the CA1 injections conducted in this study, being centred on the stratum radiatum, can be assumed to encompass the majority of projecting fibres within the injection site; in comparison, any injection located either in the stratum radiatum or the stratum oriens of CA3 will include within the uptake site only a fraction of the CA3 fibres terminating in that region of CA3, leading to an underestimation of the size of the projecting area. Variations in the extent of labelling are therefore taken to be a reflection of the amount of the dendritic field of CA3 incorporated within the injection site, and thus the proportion of projecting fibres enclosed within that site.

## **EXPERIMENT II(iii): A preliminary study of the organization of the projection from CA3 to the lateral septal nucleus**

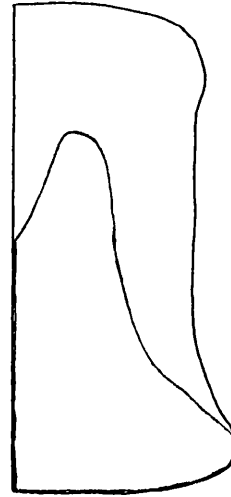
In addition to the projection to CA1 and the association pathway within CA3, the projection to the lateral septal nucleus constitutes a third major efferent pathway of CA3 cells. The organization of this projection was compared in a preliminary study in which several injections were placed into the lateral septal nucleus.

In 3 subjects, a quantity (40-60nl) of rhodamine microspheres was placed in the lateral septal nucleus, in addition to an injection of Fast Blue into the CA1 field. This procedure therefore provided further information on the collateralization of CA3 pyramidal cell axons. Due to a lack of discernible neuronal activity in the lateral septal nucleus under conditions of halothane anaesthesia, the dorsoventral placement for the septal injections was estimated using the atlas of Paxinos and Watson (1986). The CA1 injections were directed at the stratum radiatum in accordance with earlier experiments.

The location and extent of each injection is shown in diagrams of different coronal sections through the nucleus at the injection centres. The patterns of labelling following the septal injections are shown overleaf using unfolded representations of the CA3 field. The labelling is shown in full on pages 172-174.



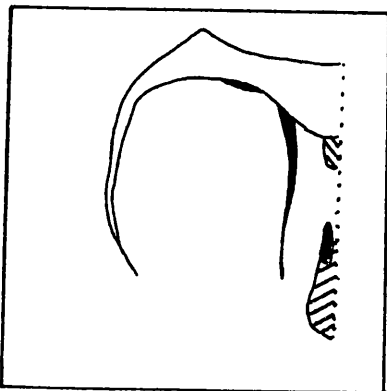
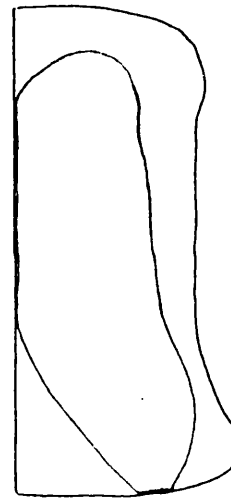
T150  
{AP 1.0; ML 0.6; DV 4.0}



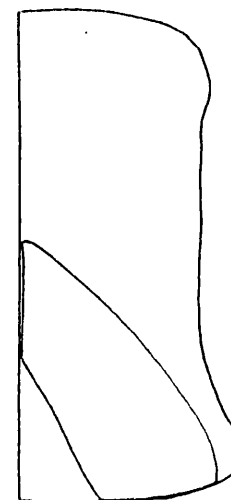
CA3

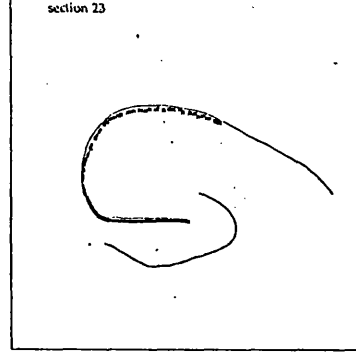
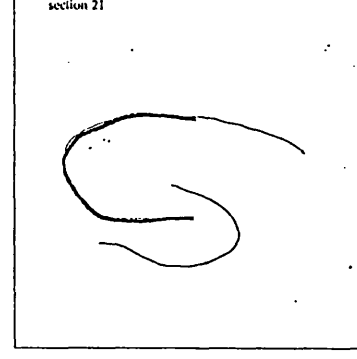
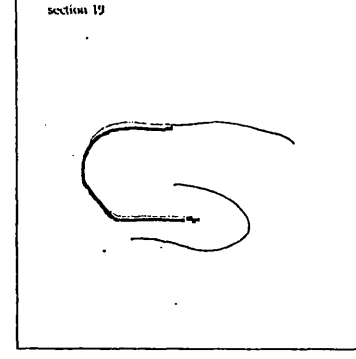
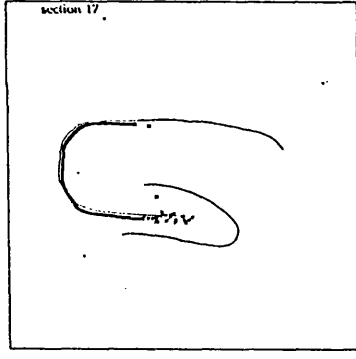
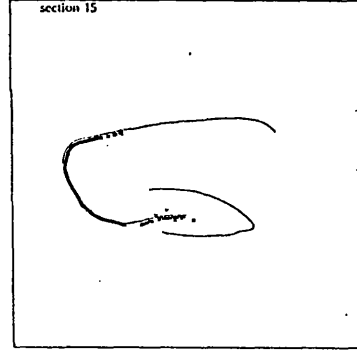
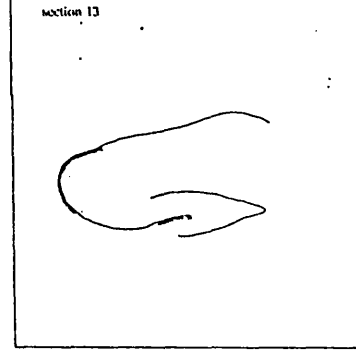
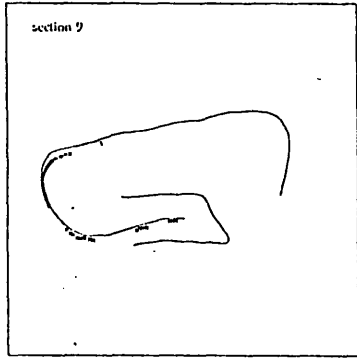
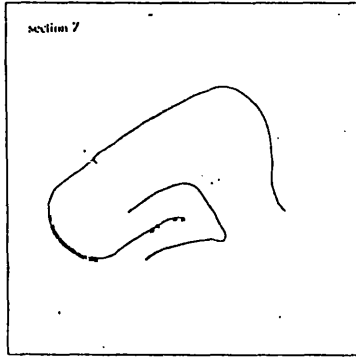
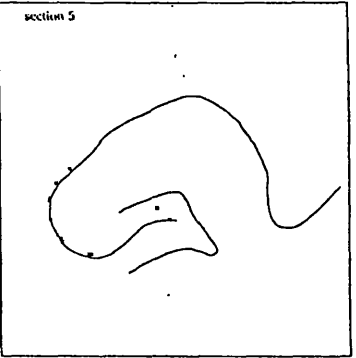
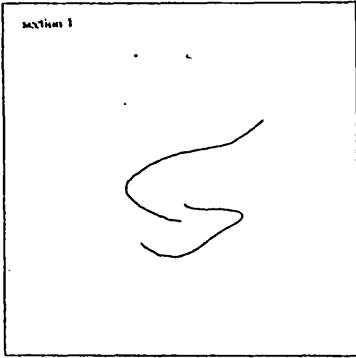


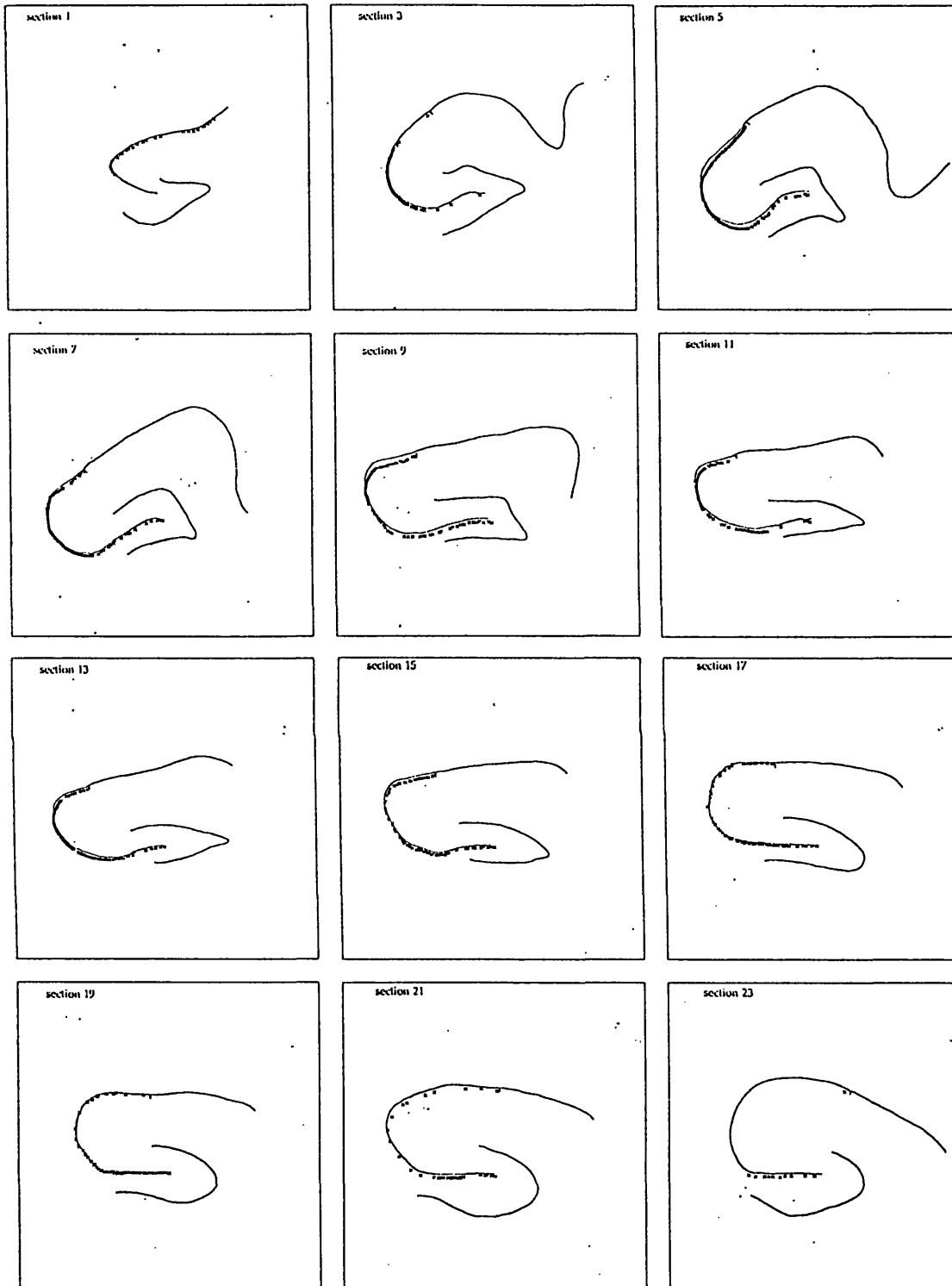
T154  
{AP -0.4; ML 0.6; DV 3.8}



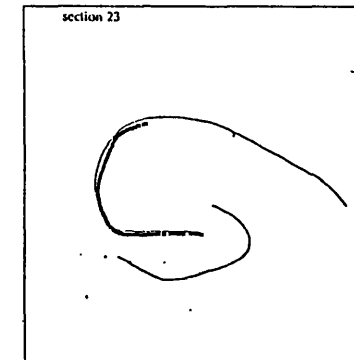
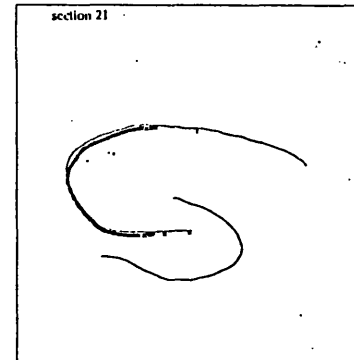
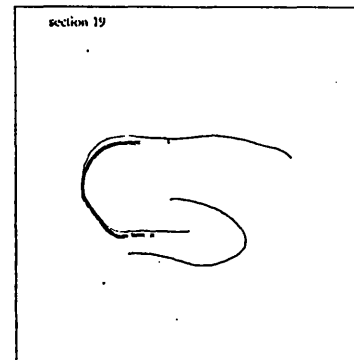
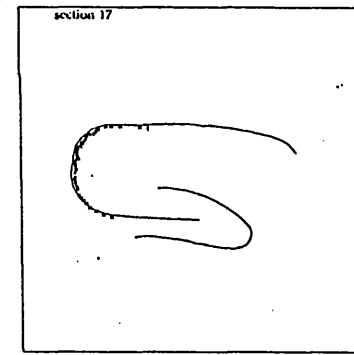
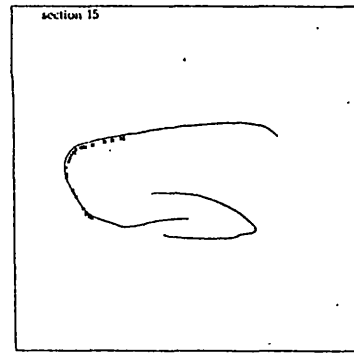
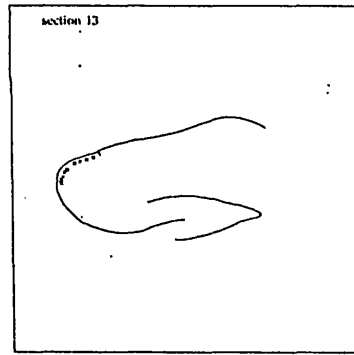
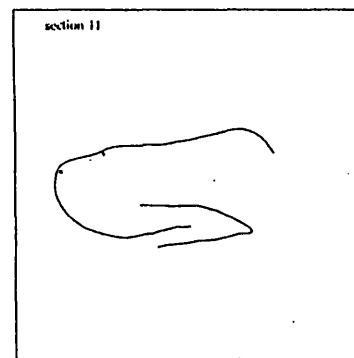
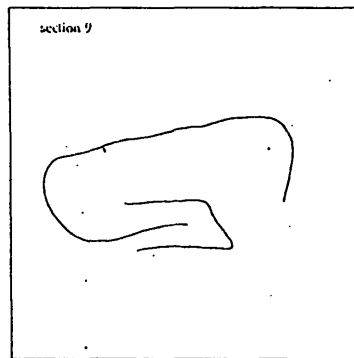
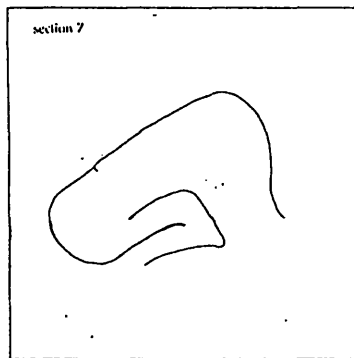
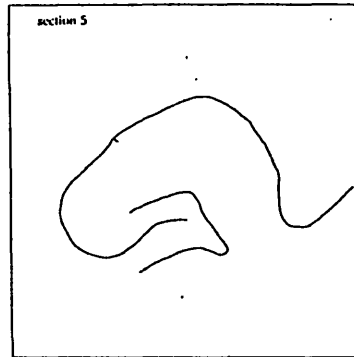
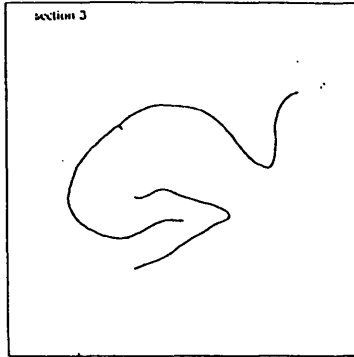
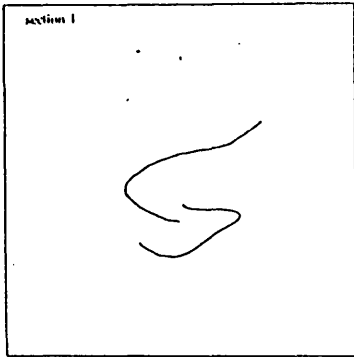
T156  
{AP 1.0; ML 0.6; DV 5.3}







T156(RHO) - ipsilateral



## The pattern of labelling

While some restraint is necessary in interpreting the data from the limited number of injections performed, some tentative conclusions on the pattern of the projection from CA3 to the lateral septal nucleus might be drawn.

In contrast to the band-like organization of the CA3-CA1 projection, the groups of CA3 cells providing inputs to different parts of the lateral septal nucleus show a greater degree of heterogeneity in appearance, although some features common to both projections were noted. For example, the labelled cells are observed to lie in a continuous band extending across a large fraction of the septotemporal extent of CA3, rather than in the form of discrete patches. At the temporal end, the band of labelling displayed a tendency towards the hilar border of CA3, although in only one case (T156) did the band of labelling display an orientation similar to that characteristic of the CA3-CA1 projections.

These results correlate with the topographical organization in the projection similar to that reported by Swanson and Cowan (1977): injections placed medially in the ventral part of the lateral septal nucleus gave rise to labelling located distally in the temporal half of CA3, whereas the injection positioned more laterally in a more dorsal part of the nucleus resulted in a band of labelled cells which is spread over more septal and proximal parts of the CA3 field.

Since the ipsilateral and contralateral hippocampi were cut differently in this experiment, a direct comparison of the patterns of projection from the CA3 field bilaterally could not be made. However, in an attempt to achieve an indirect comparison, the equivalent septotemporal pattern for the ipsilateral CA3 field was calculated using the topological transform, and the resultant similarities between the contralateral pattern and the "calculated" ipsilateral pattern suggests that the projection

from CA3 to the lateral septal nucleus is symmetrical bilaterally.

In these experiments the injection was coupled with an injection of Fast Blue into CA1. An inspection of the pattern of double-labelling in CA3 shows that, in the area of overlap of the two bands of labelling resulting from the injections, the degree of double-labelling approached 100%. This observation therefore correlates with the report of Swanson *et al.* (1981), with each cell giving rise to several collaterals which terminate in each of the known projection fields of CA3.

#### **Iliv A preliminary study of the projection from the dentate gyrus to CA3 using anterograde tracing techniques**

In several experiments a quantity of rhodamine microspheres was placed in the distal portion of CA3 lying between the blades of the dentate gyrus. A part of the granule cell layer was included within the uptake site of the injection as a result of the proximity of the CA3 dendritic fields at this point to the granule cell layer, and in three cases (T153, T157, T159) anterograde transport of the rhodamine microspheres along the mossy fibre system was noted. The appearance of the anterograde labelling, which manifested itself as a faint, uniformly diffuse cloud of microspheres located exclusively within the proximal part of the apical dendritic field of CA3, differed greatly from that of retrograde labelling, in which the microspheres were confined intracellularly within the pyramidal cells. The fact that anterograde labelling was observed in parts of the CA3 field from which retrograde labelling was absent provides some evidence to refute the belief that the diffuse labelling might simply represent a weak form of retrograde backfilling.

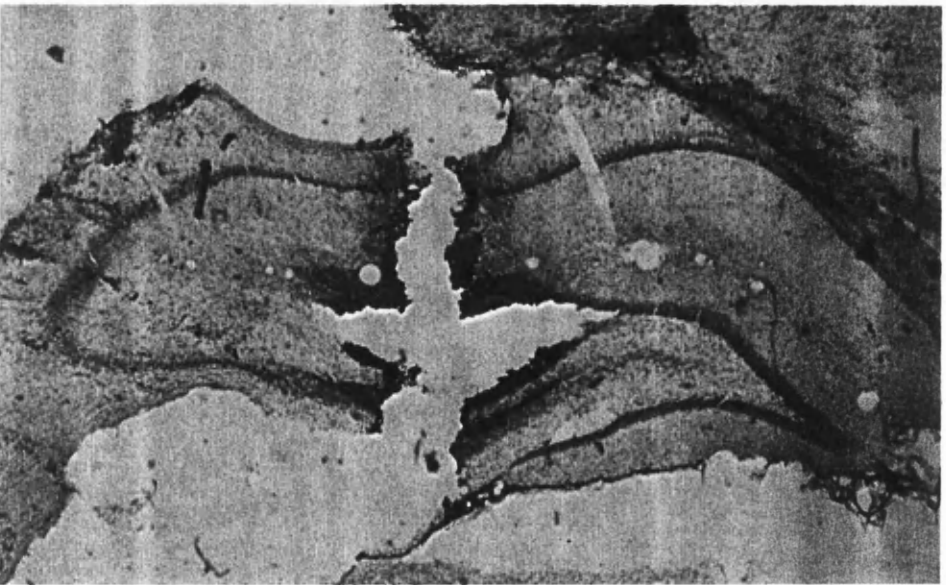
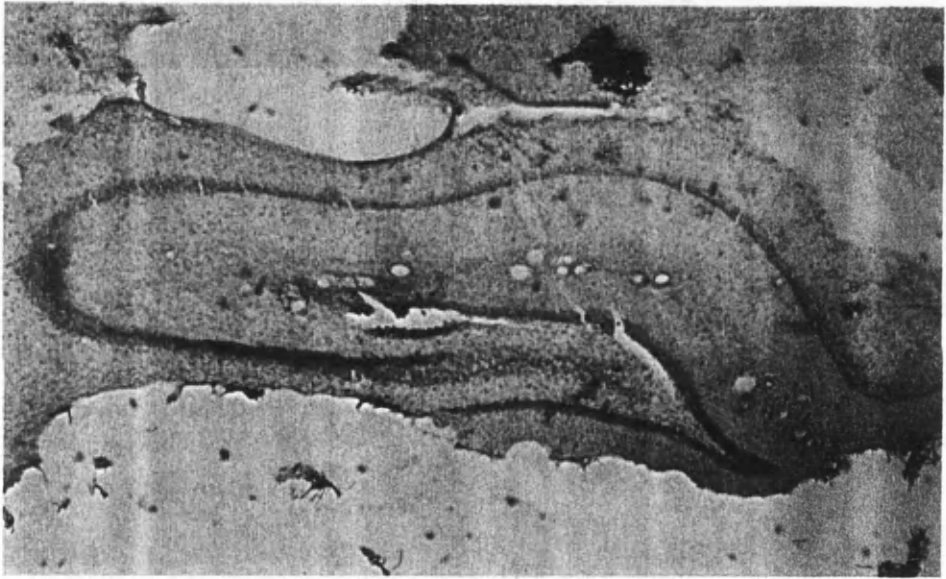
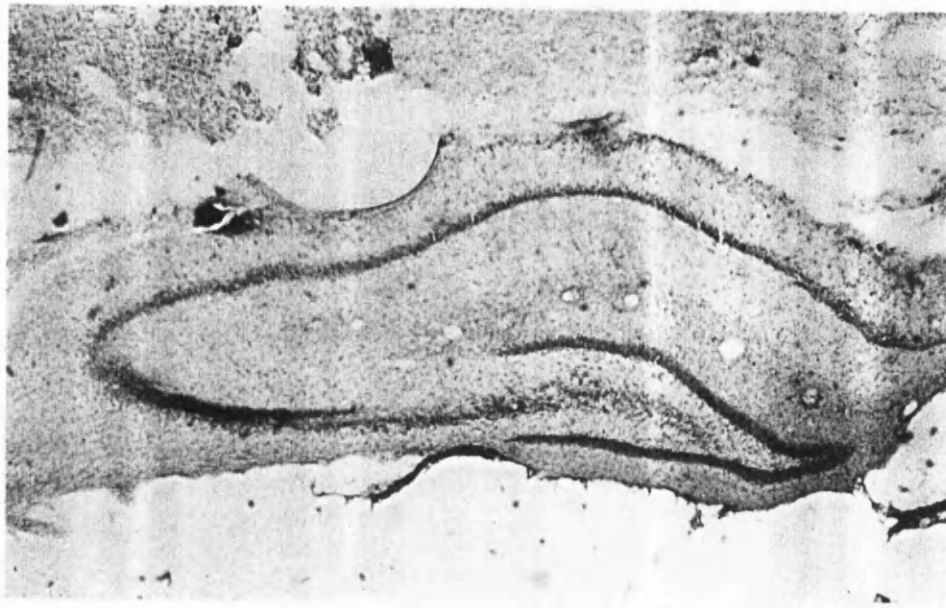
These anterograde findings complement those of an experiment (T117) in which 120nl of the naturally-occurring biotin-lysine conjugate, biocytin, was injected into the hippocampus under electrophysiological control. Several recent studies have shown that biocytin is taken up by neuronal somata and dendrites and transported in an anterograde fashion (King *et al.* 1989; Bolam and Smith 1990; Izzo 1991). Serial coronal sections (through both hippocampi) were prepared using the glucose oxidase-DAB-nickel enhancing technique (Shu *et al.* 1988). Light microscopic analysis revealed that, in spite of an injection which encompassed a considerable fraction of the suprapyramidal blade of the dentate gyrus and the underlying part of the CA3 field, labelling was only noted along the mossy fibre trajectory in CA3 in the ipsilateral

hippocampus. No labelling was found in the contralateral hippocampus. The implications of the confinement of labelling to the mossy fibre projection in this injection , as well as in the three rhodamine injections, are discussed in full in the *Discussion*.

The results of these four cases of anterograde labelling are shown on pages 181-184.

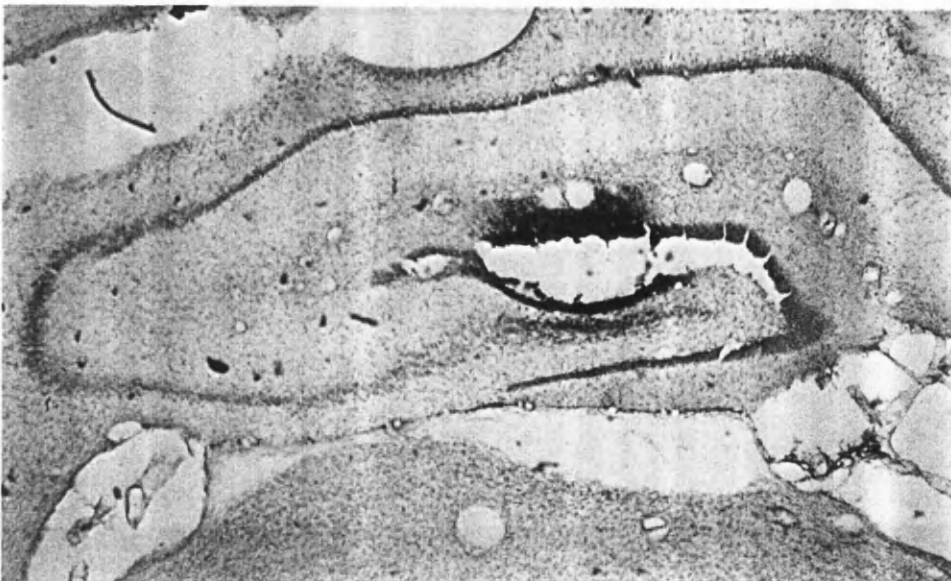
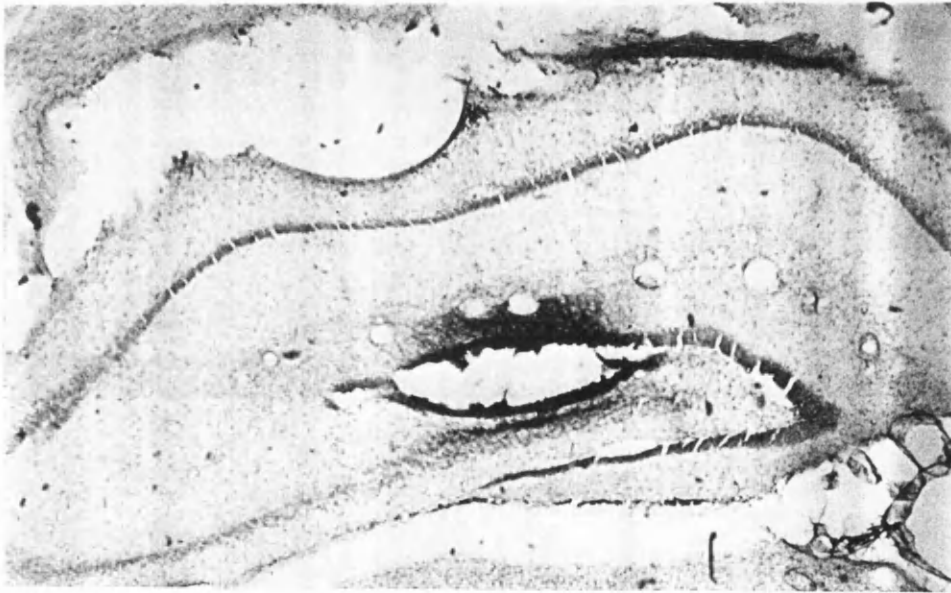
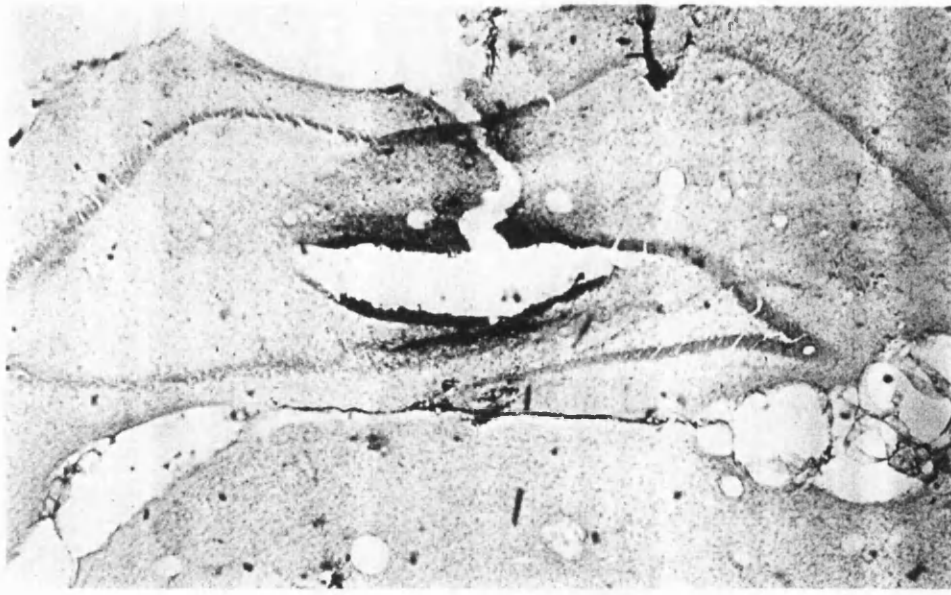
The photographs overleaf show the nature and pattern of labelling following the injection of the biocytin tracer. Note the substantial disruption to the dentate gyrus (and to the CA3 and CA1 fields) caused by the injection.

300µm



(T117) Biotin labelling in coronal sections at several levels through the unextended ipsilateral hippocampus. Note the faint labelling in the stratum lucidum of CA3 adjacent to the CA2 border.

Top 400µm rostral to the centre of the injection Middle 200µm rostral Right The centre of the injection

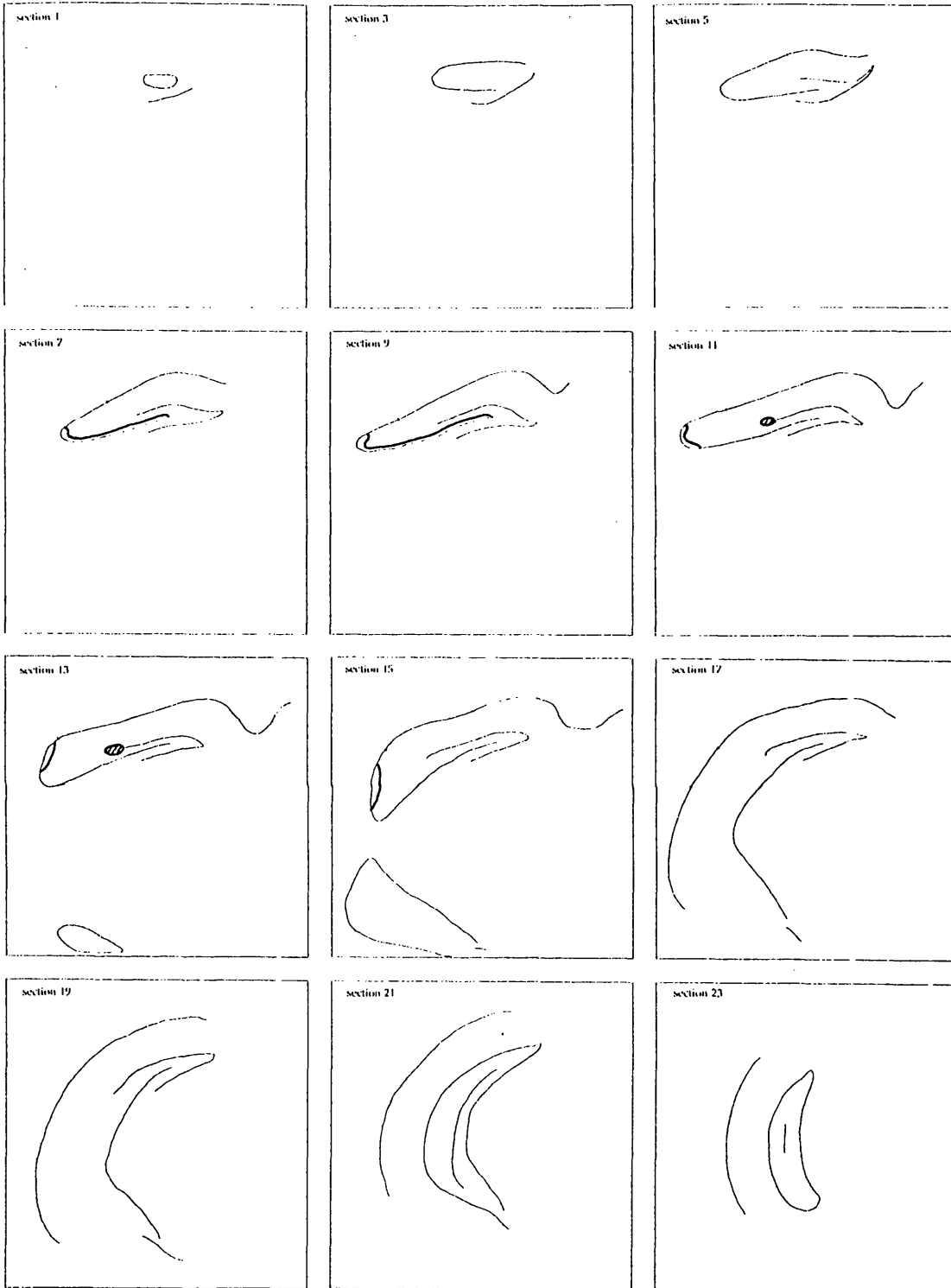


(T117) Biocytin labelling in coronal sections at several levels through the unextended ipsilateral hippocampus. Note the faint labelling in the stratum lucidum of CA3 adjacent to the CA2 border.  
Top 200 $\mu$ m caudal to the centre of the injection Middle 400 $\mu$ m caudal Right 500 $\mu$ m caudal

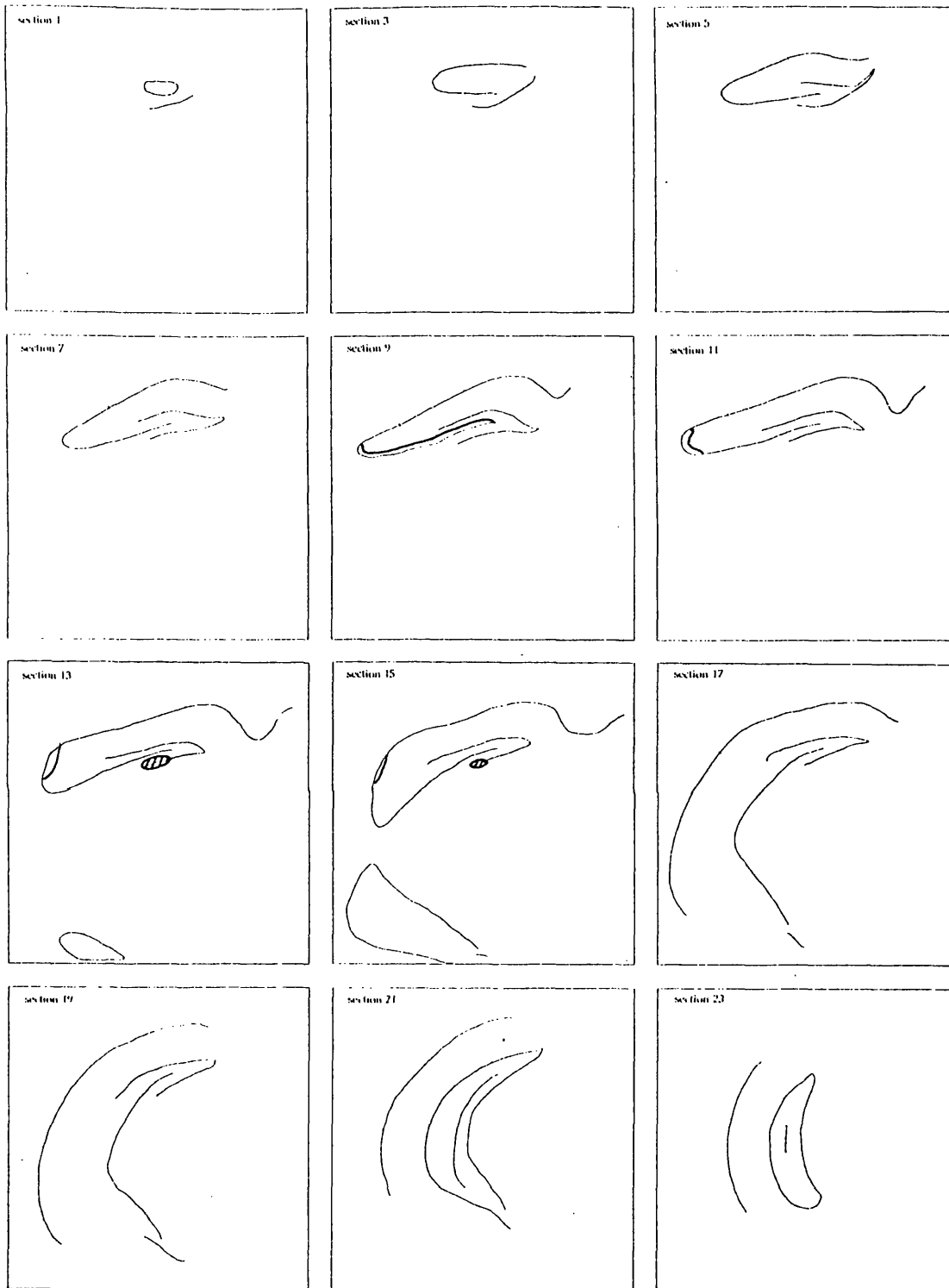
T117 - biocytin



T159 - anterograde RHO



T157 - anterograde RHO



T153 - anterograde RHO



T117

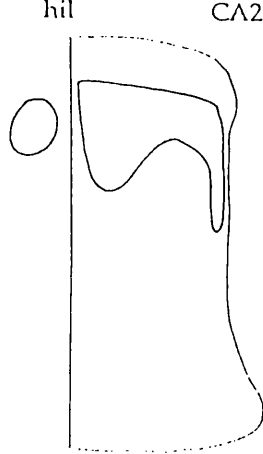
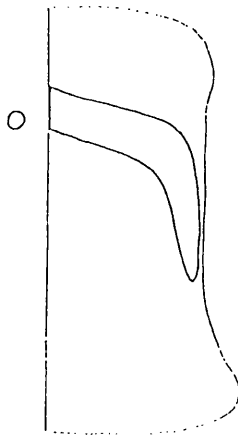


Fig.7 The figures on the left represent the pattern of labelling in the extended CA3 field (as calculated using the topological transform). The estimated position of the injection site in the extended dentate gyrus is placed alongside the CA3 field. Note that the orientation of the CA3 field is reversed in comparison with earlier diagrams, with the straight edge representing the hilar border in this instance.

T159

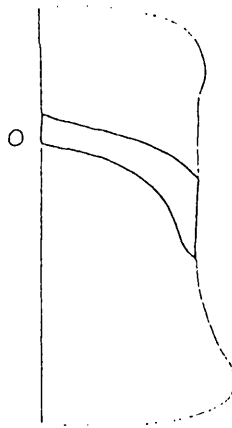


### The pattern of labelling

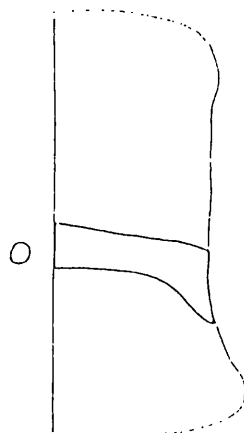
#### *Anterograde rhodamine labelling*

Two components to the pattern of labelling could be described for each of the injections. The first component, which extended from the hilar border across all but the most proximal quarter of the proximodistal length of CA3, was organized approximately transverse to the septotemporal axis of the hippocampus. This "transverse" component was restricted in the septotemporal direction, with a mean coverage of approximately  $800\mu\text{m}$ , or one-tenth of the septotemporal length of CA3. The projection was topographically organized along this length, with injections giving rise to transverse labelling which occupied the same septotemporal level, although in all three cases the transverse component of labelling extended additionally for a further  $300\mu\text{m}$  septal to the injection site at its hilar end.

T157



T153



In two of the three cases the transverse component showed a slight deviation in the temporal direction which appeared of uniform gradient throughout its length such that the labelling in proximal CA3 was shifted temporally in relation to that in distal CA3. In the third case (T153), the labelling remained at approximately the same transverse level throughout its length.

The pattern of labelling in these injections exhibited an abrupt shift of direction towards the temporal pole in proximal CA3. In all three cases this shift occurred at approximately 1200 $\mu$ m from the CA2 border and the labelling was organized approximately parallel to the septotemporal axis of CA3. Unlike the transversely-directed part of the projection, this second "longitudinal" component appeared to vary in extent with the septotemporal position of the injection site, with injection T159 (the most septal) giving rise to labelling that extended for approximately 3mm temporal to the injection site, whereas that from T153 (the most temporal) covered only 1.2mm of the CA3 field temporal to the injection.

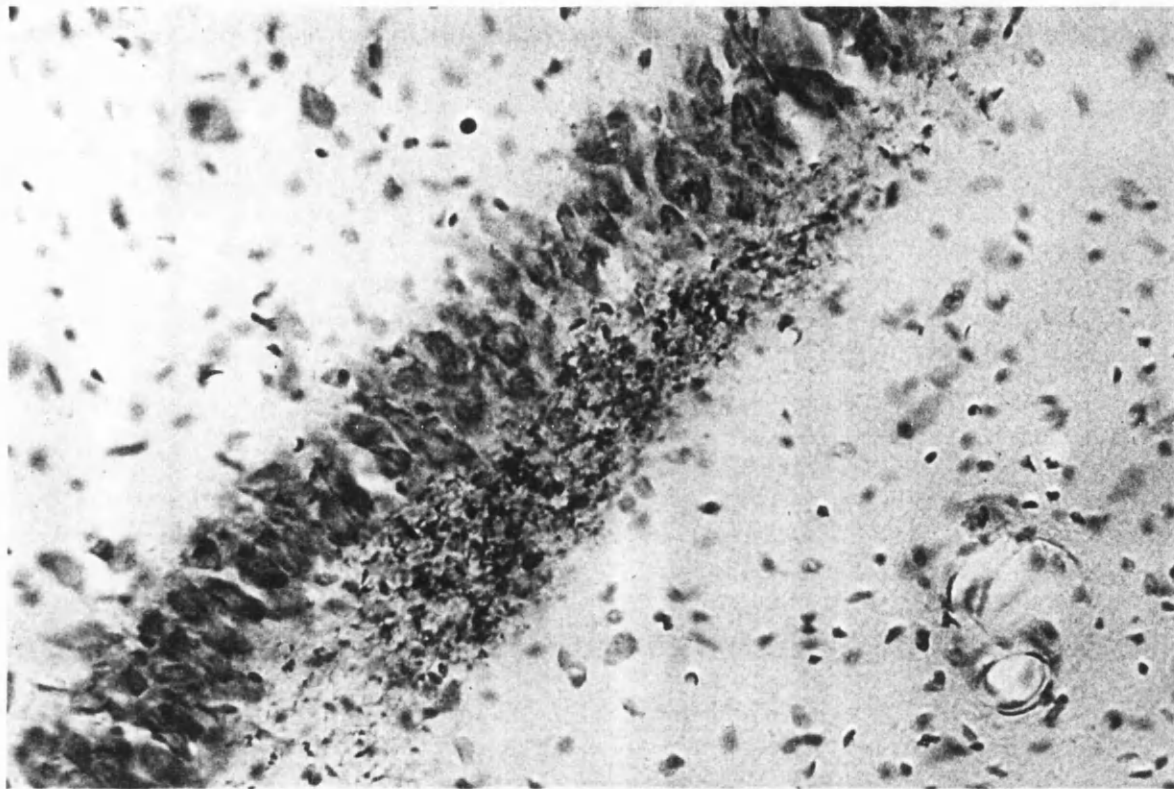
### *Biocytin labelling*

Although the size of the biocytin injection was several times greater than that of the rhodamine injections, the pattern of labelling exhibited several similarities. The projection contained a transverse component extending across most of the proximodistal length of CA3, the septotemporal level of which was the same as that of the injection site, as well as a longitudinal component in proximal CA3 which ran parallel to the septotemporal axis for approximately 2mm temporal to the centre of the injection site.

Some differences between the patterns of labelling were also noted. Firstly, labelling was not found to extend to the hilar border of CA3 at any point along the

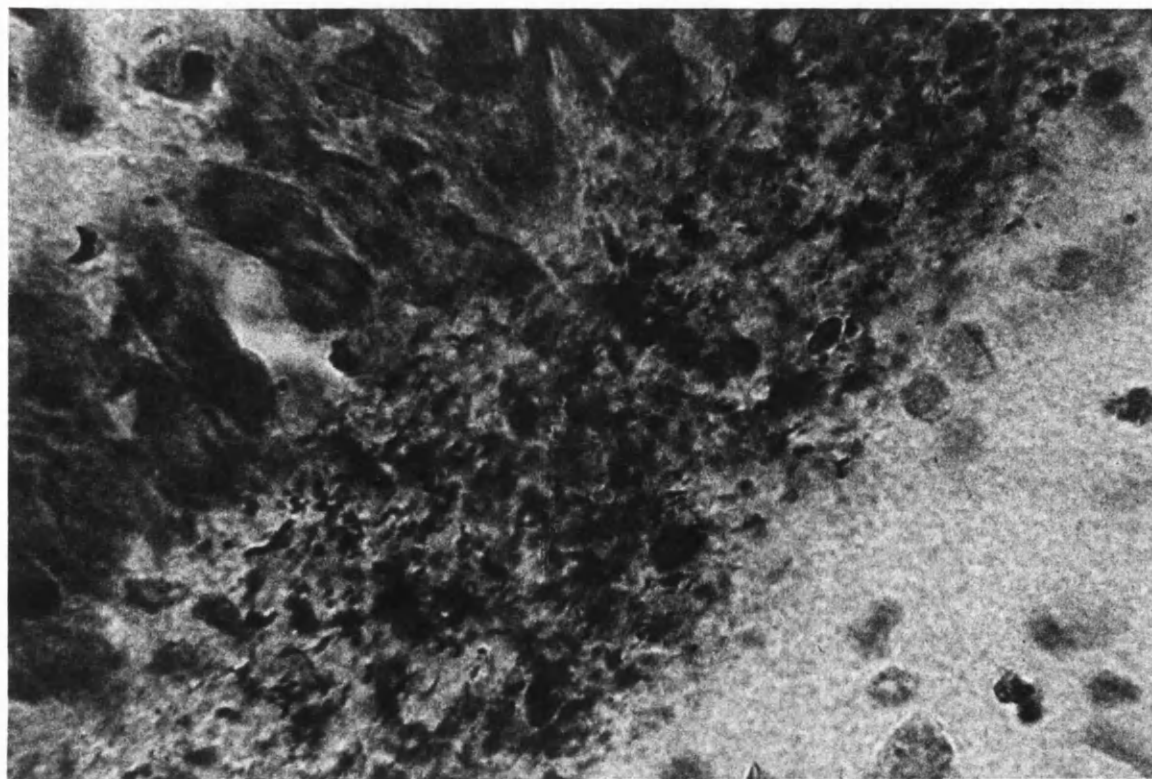
projection, although it must be noted that the injection site covered the lateral part of the suprapyramidal blade and did not encompass granule cells around the crest of the dentate gyrus, whereas a number of these cells were included within the uptake sites of the three rhodamine injections. Secondly, the change in trajectory of the projection in proximal CA3 was more marked than for the other injections, and the longitudinal component was found to be substantially narrower in this instance. The most striking difference, however, was manifested in the transverse component. Unlike the rhodamine injections, in which this component was found to be of approximately uniform width across its length, considerable variation in the amount of CA3 field covered in the temporal direction was noted across the length of this component, with maximal coverage (approximately 2mm of the septotemporal extent) occurring in the part of distal CA3 lying deep to the lateral aspect of the suprapyramidal blade of the dentate gyrus. There was progressively less temporal coverage in more proximal parts of CA3 up to the transition point in the projection trajectory, lending a neck-like appearance to the junction of the two projection components. As in the rhodamine injections, the projection exhibited only negligible coverage of the CA3 field septal to the injection site.

30um

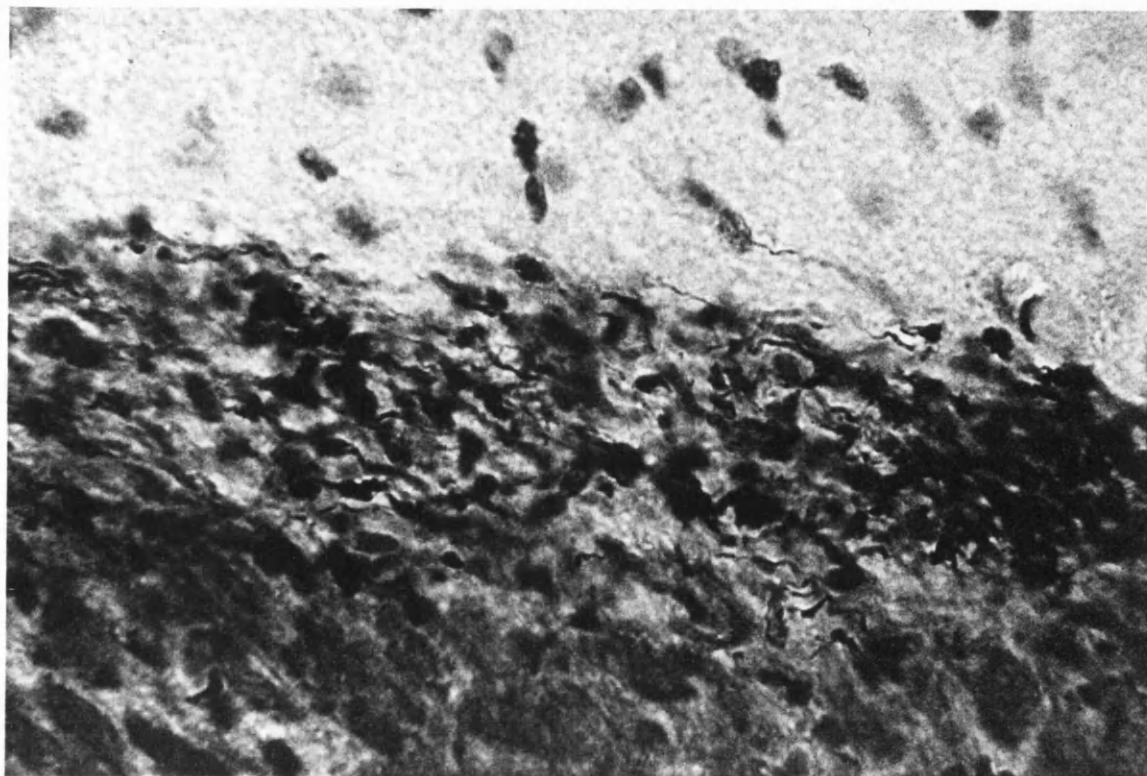


Biocytin labelling showing the longitudinally-directed component of the projection in proximal CA3. *Above* At low power      *Below* At high power

um



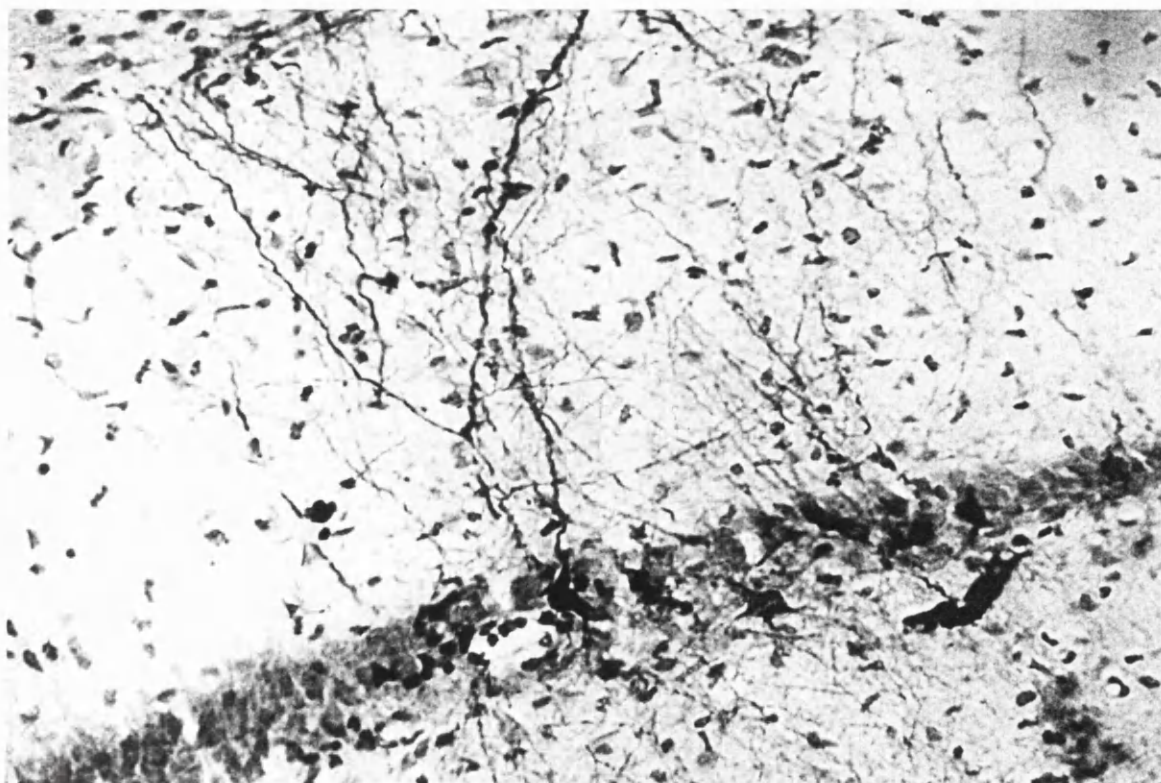
20µm



*Above* Biocytin labelling of mossy fibre terminals in mid-CA3

*Below* Sparse filling of CA1 pyramidal cell bodies and basal dendrites

80µm



## **Fine structure of the projection**

The mossy fibres are seen to run together in a discrete bundle which traverses the most proximal part of the stratum radiatum of CA3 (the stratum lucidum). Large outgrowths, corresponding to the giant synaptic boutons, are given off at intervals along the fibres, to which they appear to be attached by a short "neck". The average diameter of these boutons is at least one order of magnitude greater than that of the parent mossy fibres. Observation with high power objectives shows that some mossy fibres run *within* the stratum pyramidale, and it is assumed that these fibres, by virtue of their giant boutons which are similarly contained within the pyramidal cell layer, synapse on the proximal dendrites of neurons located deeper in the CA3 field.

### **III A double-labelling study of the projections from the entorhinal cortex to the hippocampus**

The organization of the projections from the entorhinal cortex to the CA3 and CA1 fields of the hippocampus, and the degree of overlap in these projections with regard to cells of origin, were assessed in a double-labelling retrograde study, in which the fluorescent dyes Fast Blue and rhodamine microspheres were injected into the hippocampus. In each operation similar quantities of the two dyes were injected separately into locations in the CA3 and the CA1 fields in the ipsilateral hippocampus. Given that the strata moleculare of the two fields (the main field of termination for projecting entorhinal fibres) are juxtaposed, especial care was taken to ensure satisfactory localization of these injections. As mentioned previously in Experiment Iiiiii, the CA3 injection merited particular attention on account of the possibility of the backtracking of dye along the pipette/electrode path into the dendritic field of CA1.

14 animals were used in this study, of which nine had injections of sufficient specificity for data analysis. The results are summarised on pages 185-189. The patterns of labelling are shown using models of the medial and lateral aspects of the posterior cerebral cortex, covering the extent of the entorhinal cortex from its caudal pole to its border with the piriform cortex at the rostral end. Alongside each set of results an unfolded map of the ipsilateral hippocampus is provided showing the injection locations in the CA3 and CA1 fields. In addition, the labelling in three of these injections (into septal, midseptotemporal and temporal) is shown in full on pages 191-193 using a more detailed representation of the entorhinal cortex, with the distribution of labelling being shown in 12 out of 25 coronal sections spanning the entorhinal cortex (sections 1 and 23 representing respectively the caudal and rostral limits).

## **A note on the cytoarchitectonic parcellation of the entorhinal cortex as used in this study**

In the anatomical review provided at the beginning of this dissertation, the entorhinal cortex was split into lateral and medial areas (LEA and MEA), in accordance with a widely accepted method of subdivision. Since this experiment was aimed at studying the topographic organization of the entorhinal projections to Ammon's horn, a decision was made to adopt the same classification and nomenclature of the various subdivisions of the entorhinal cortex as was used by Ruth *et al.* (1982, 1988) in their studies of the topographical relationship of the entorhinal projection to the dentate gyrus. Given the similarities between these latter studies and this experiment, such standardisation of classification facilitates the comparison of the inputs from the entorhinal cortex to all three fields of the hippocampus.

The entorhinal cortex (Brodmann area 28) is subdivided using cytoarchitectonic and hodological criteria into medial (area 28m), intermediate (area 28i) and lateral (area 28l) regions, as appreciated in the works of Lorente de No (1933, 1934), Blackstad (1956) and Steward (1976). Areas 28m and 28i are not subdivided further. In accordance with the cytoarchitectonic differences highlighted by Krettek and Price (1977), area 28l is parcellated into dorsolateral (dl), ventrolateral (vl) and ventromedial (vm) subdivisions. On the basis of a hodological distinction - a specific dopaminergic innervation (Collier and Routtenberg 1977) - the rostromedial area TR was also included in the lateral entorhinal cortex by Ruth *et al.* (1988).

In this study, the rostrocaudal, mediolateral and dorsoventral axes are used to represent the three-dimensional shape of the entorhinal cortex. For the sake of brevity, the term "transverse" is used in place of "ventromedial-dorsolateral" in those instances where a description through a given coronal section through the cortex is required.

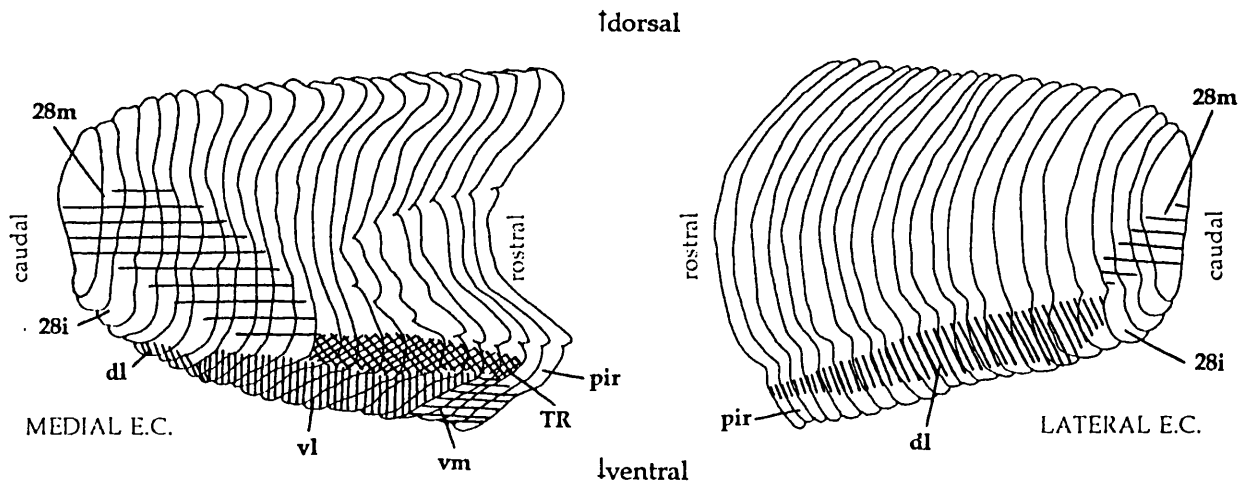
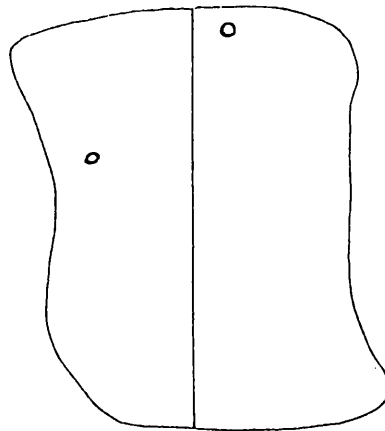


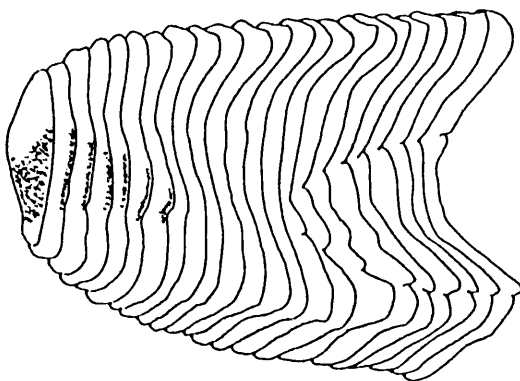
**Fig.8 Above** The various cytoarchitectonic subdivisions of the entorhinal cortex as seen on medial and lateral representations of the posterior cerebral cortex.

T129

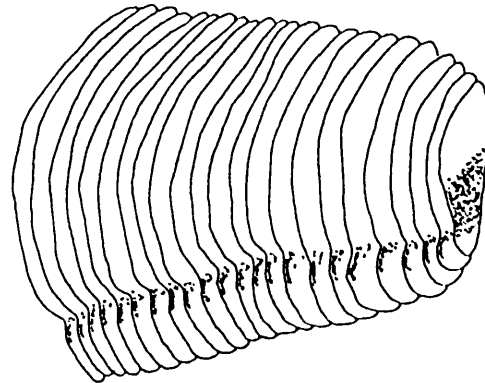


CA1

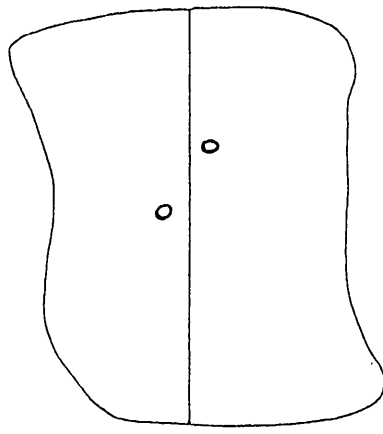
CA3



193

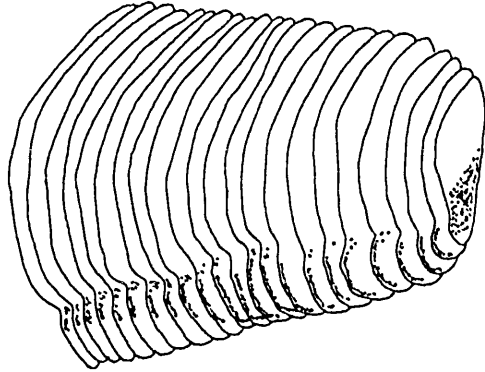
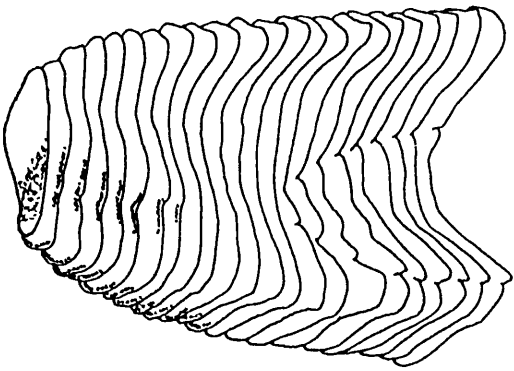


T131

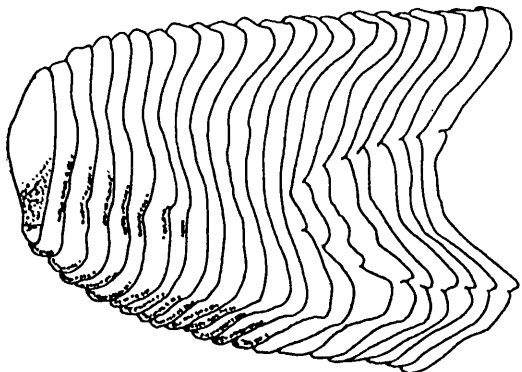
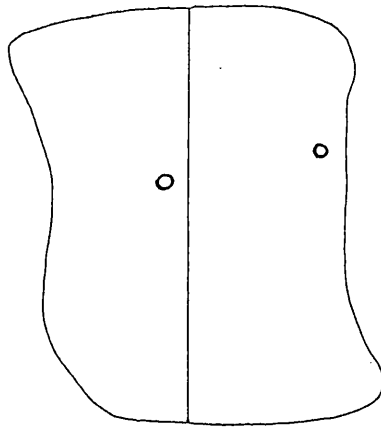


CA1

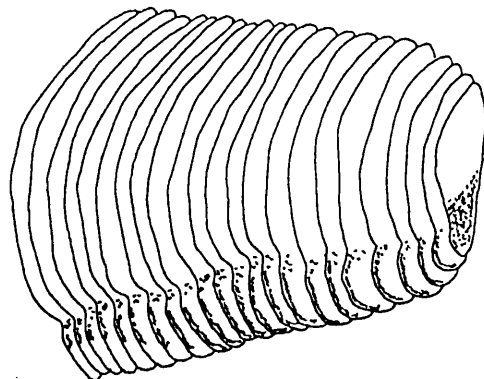
CA3



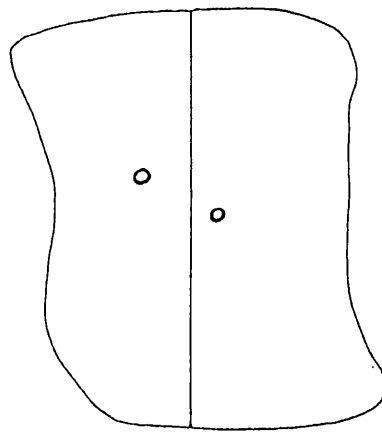
T159



194

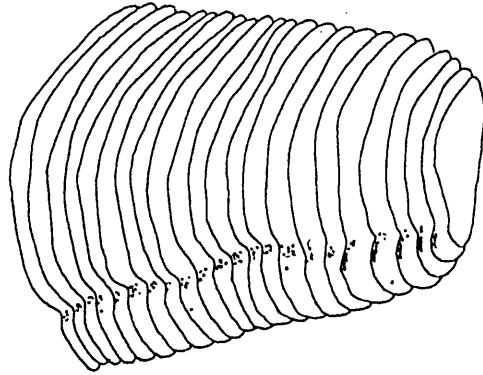
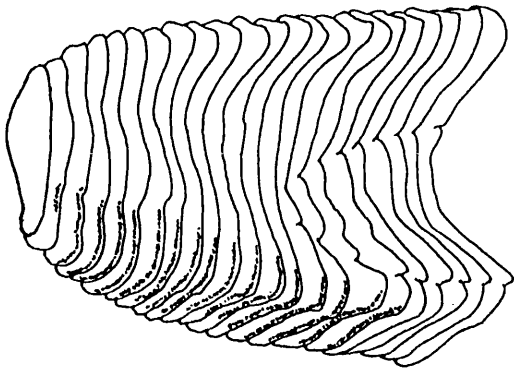


T113

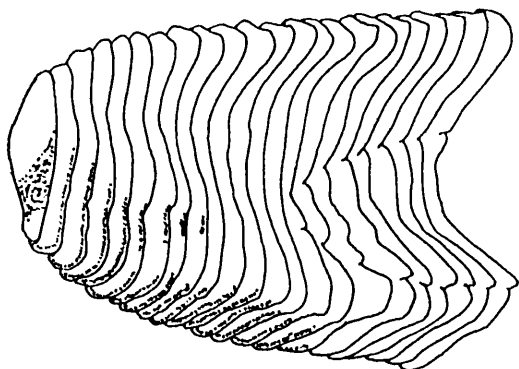
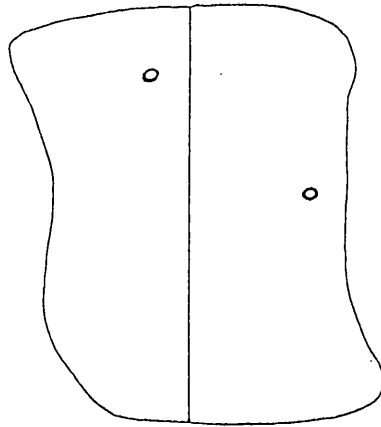


CA1

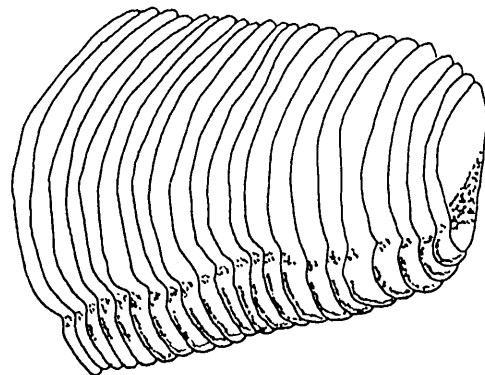
CA3



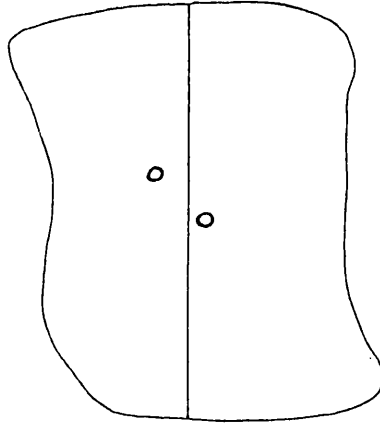
T161



195

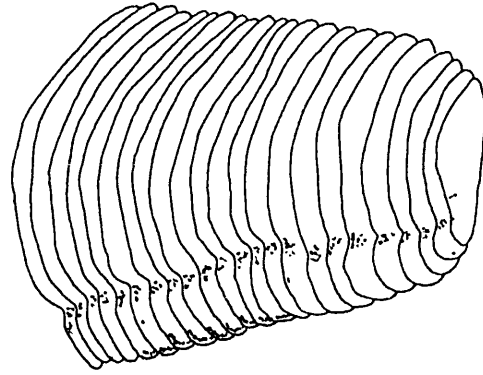
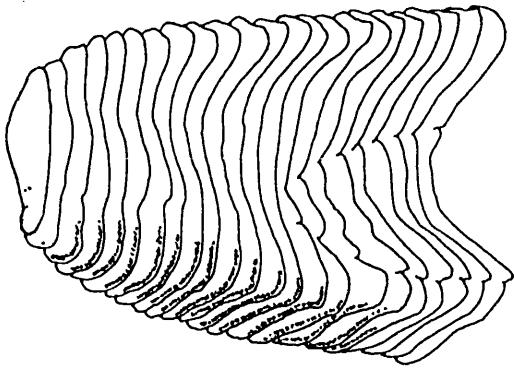


T133

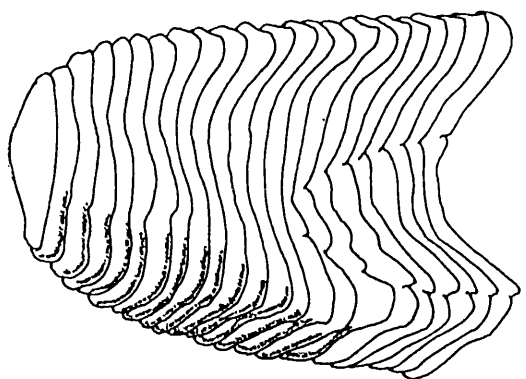
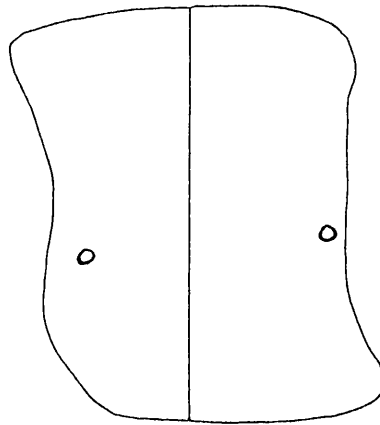


CA1

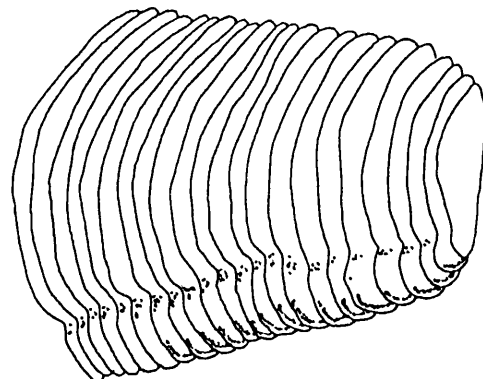
CA3



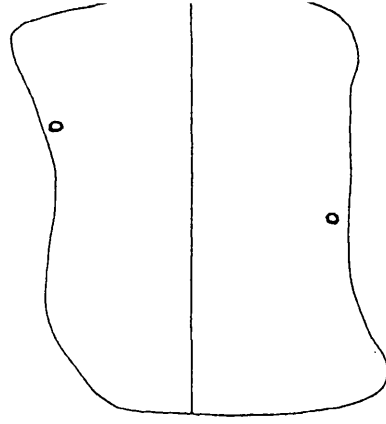
T148



196

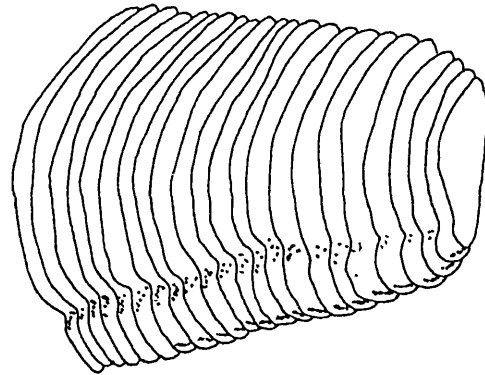
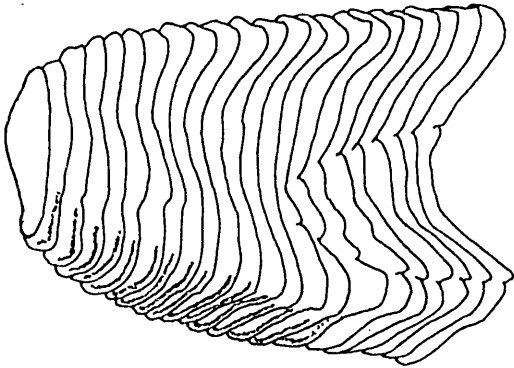


T157

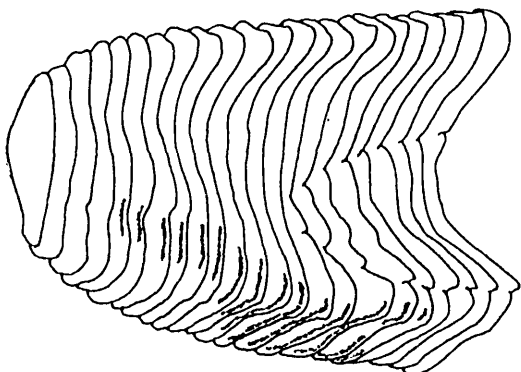
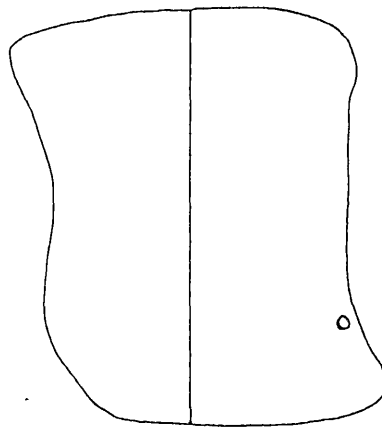


CA1

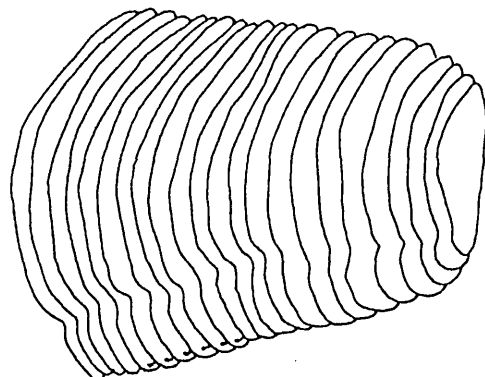
CA3



T153

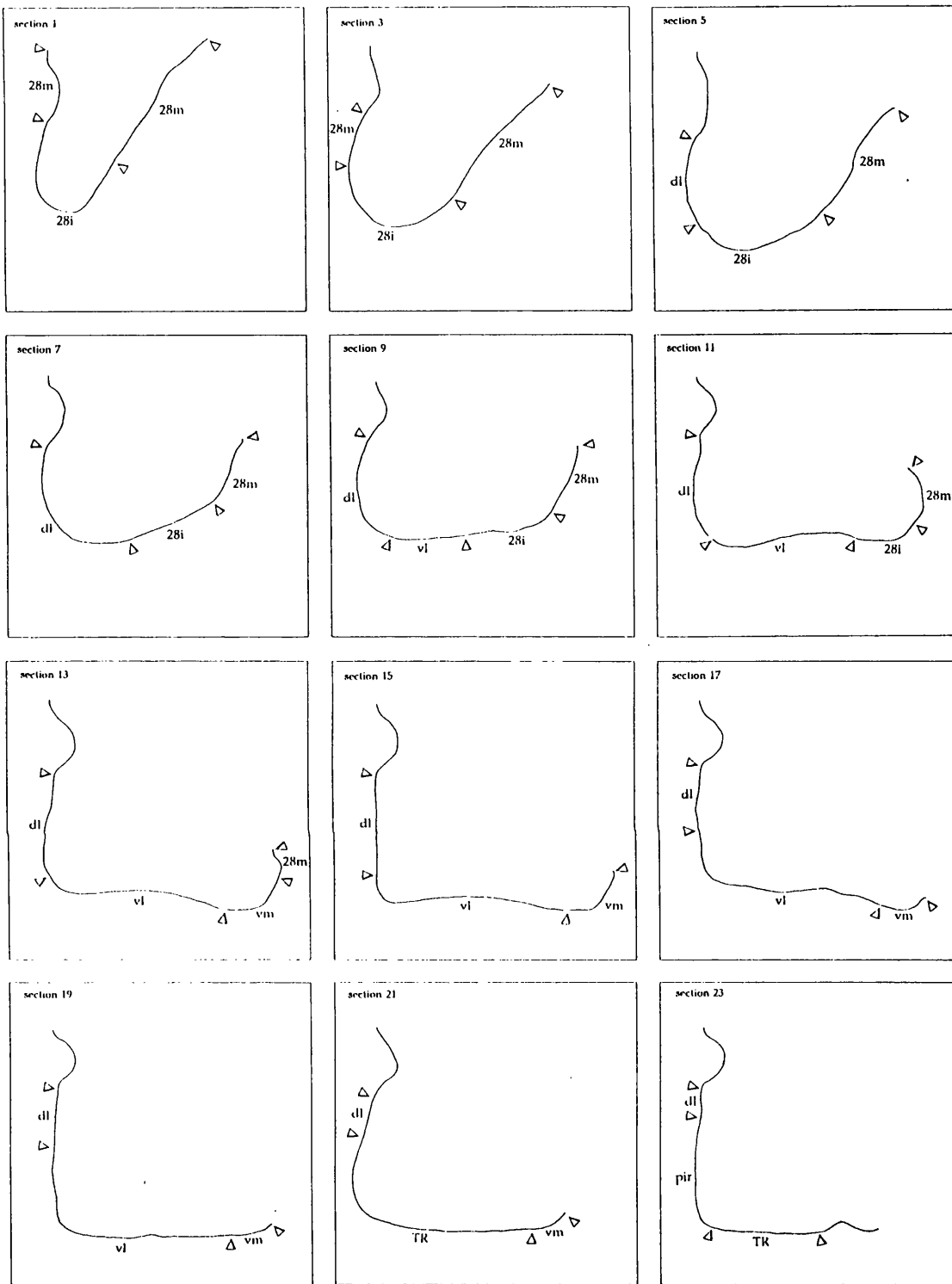


197

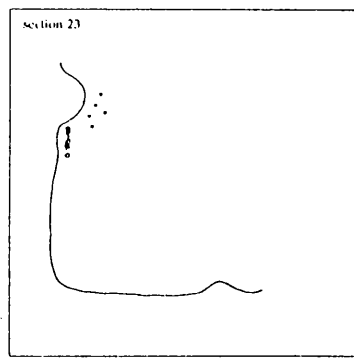
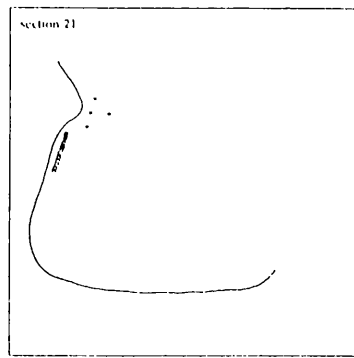
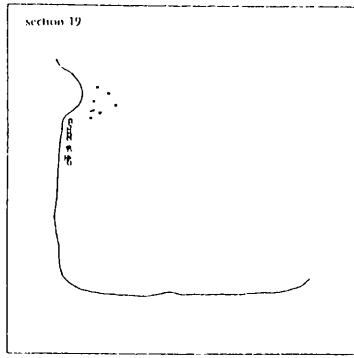
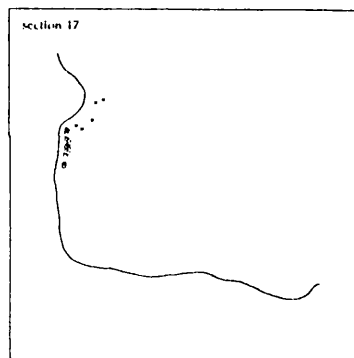
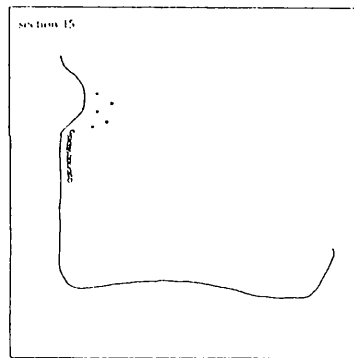
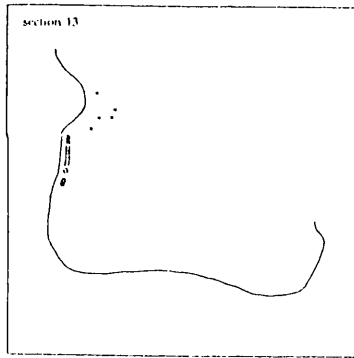
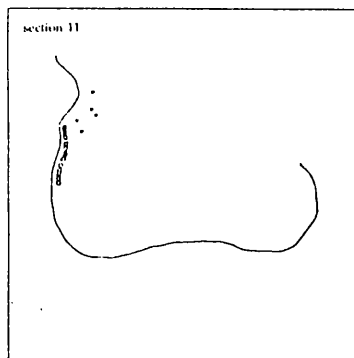
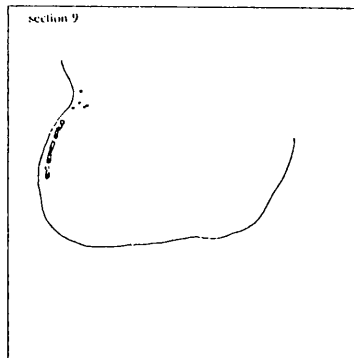
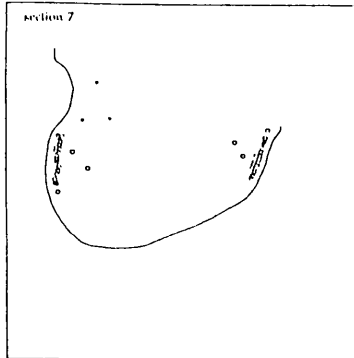
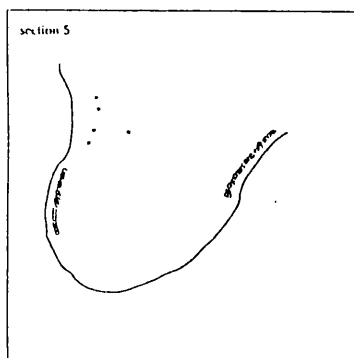
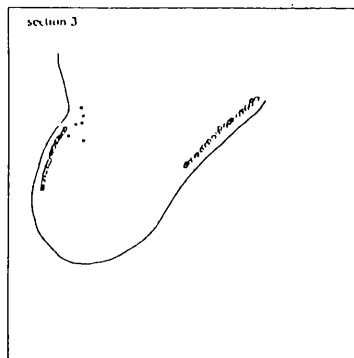
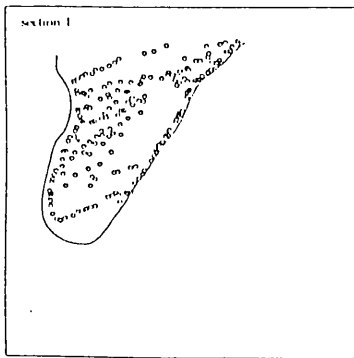


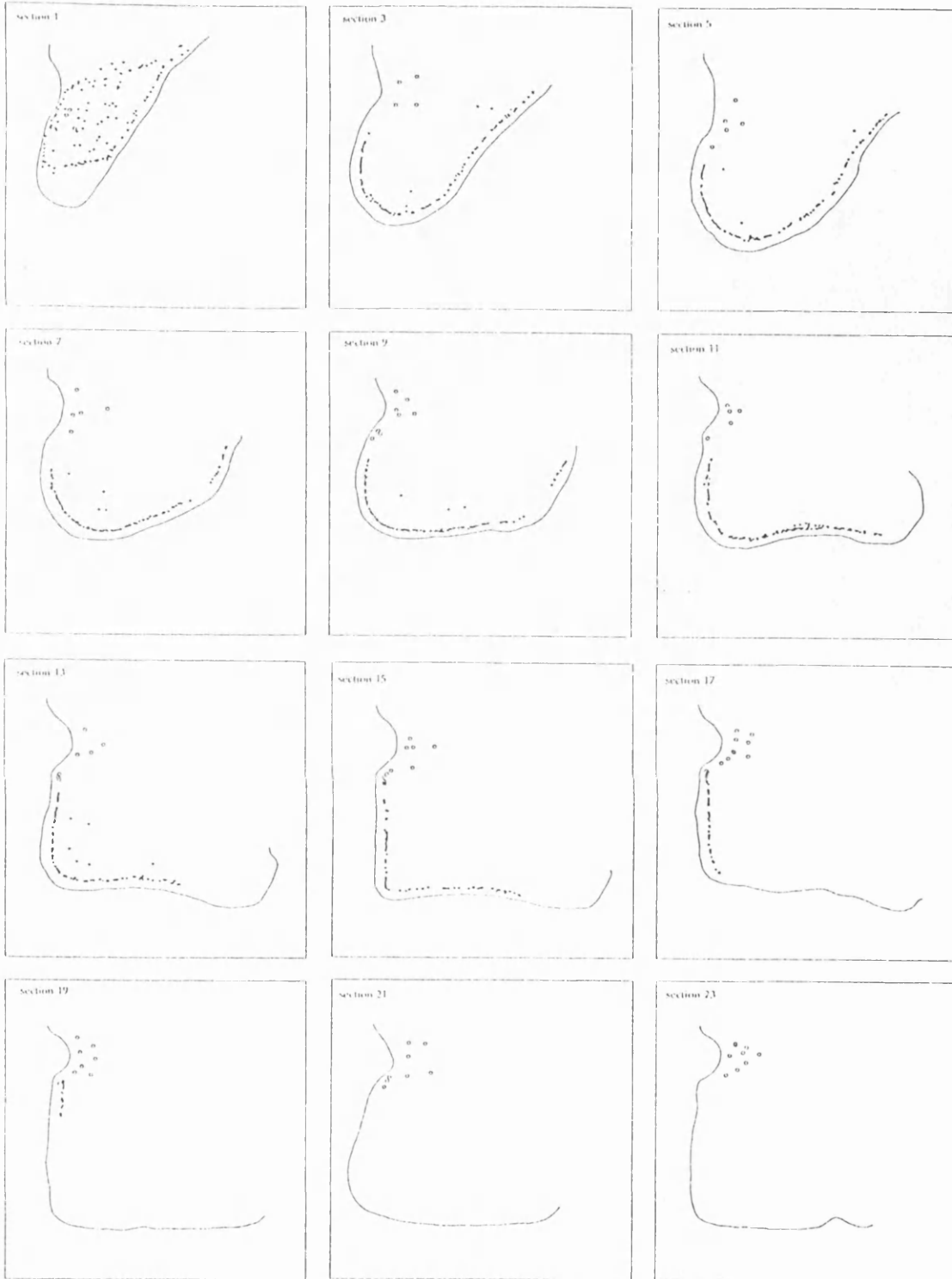
←lateral medial→

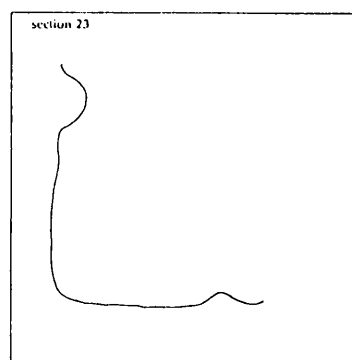
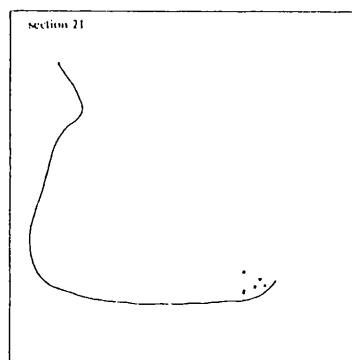
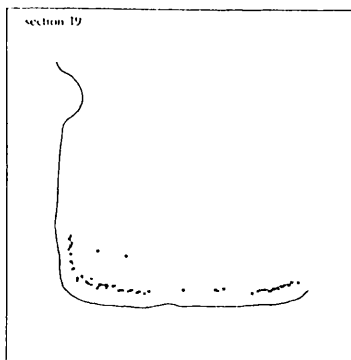
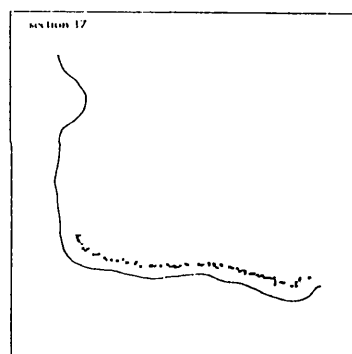
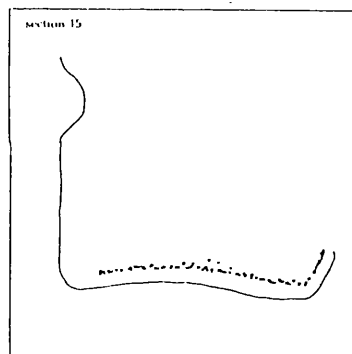
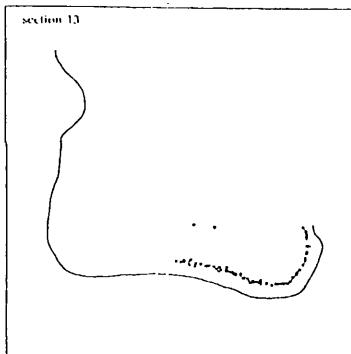
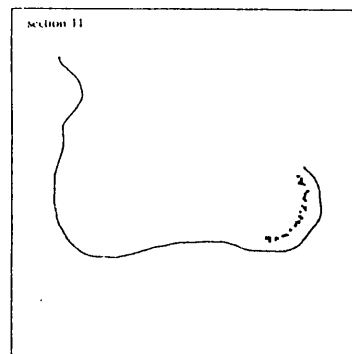
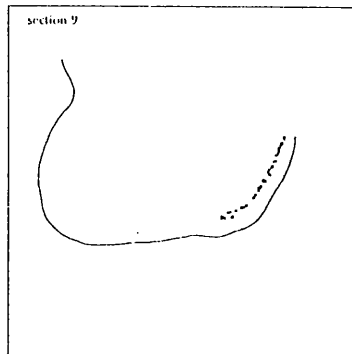
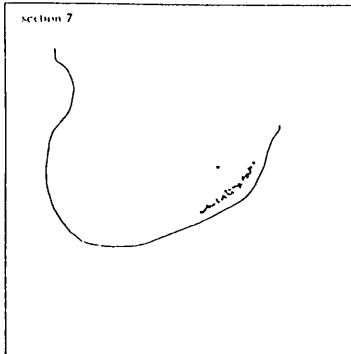
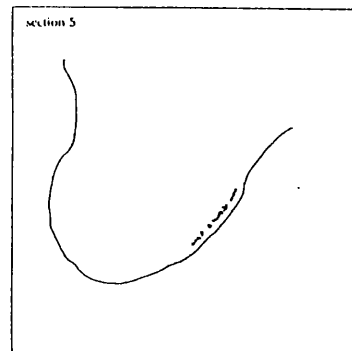
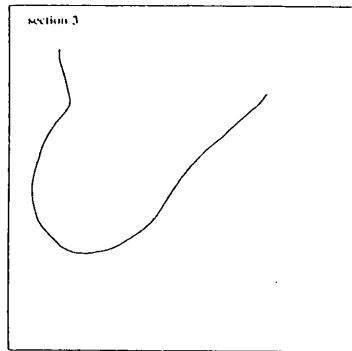
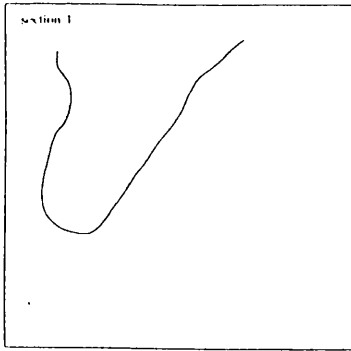
↑dorsal  
↓ventral



**Fig.9** The following sections through the entorhinal cortex were drawn using camera lucida from a Nissl-stained control brain. The various subdivisions of the entorhinal cortex are specified according to cytoarchitectonic criteria. Section 1 (*top left*) and Section 23 (*bottom right*) represent respectively the caudal and rostral extremes of the entorhinal cortex. Section separation (as above) is 400 $\mu$ m. pir = piriform cortex







## **The distribution of labelling: CA3 injections**

### *A note on injection specificity*

Given that injections into distal CA3 necessarily penetrated the molecular layer of the dentate gyrus ( a major recipient of perforant path fibres), data was taken only from subjects in which the dye was localized within the CA3 dendritic fields. Since the latter also abuts onto the hilus, it is likely that the uptake sites in these injections encompassed hilar neurons (such as the mossy cells and basket cells) which are also believed to receive an input from the entorhinal cortex, and while the number of affected hilar cells is small in comparison with the cells in proximal CA3, any interpretation of these results is therefore subject to some qualification on this score.

A further point must be made about the specificity of these injections. Since efforts were made to localize the injections within CA3 and CA1, placement of dye in the strata moleculare of CA3 and CA1 was avoided. It is therefore accepted that injections were not placed in the optimal sites for disruption of incoming entorhinal fibres.

## **The organization of the entorhinal-CA3 projection**

Before the topographical organization in this pathway is considered in detail, some general comments on the results of these injections can be made. In all cases, the labelling was observed over a substantial portion of the entorhinal cortex, with extensive coverage both in the rostrocaudal and transverse directions, with a negligible fraction of labelling noted outside this region, in the form of individually-filled cells scattered across the entorhinal cortex. In any given coronal section, the labelling therefore took the form of a strip of cells covering a fraction of the transverse length

of the entorhinal area. As a final point, it is interesting to note that the continuity in the distribution of labelling is also seen in those injections giving rise to labelling along the medial, as well as the lateral, wall of the entorhinal cortex since in these cases the backfilling which extends across the caudal pole of the entorhinal cortex serves to unite the two groups of labelled cells.

The vast majority of labelled cells were located in layer II, regardless of the location within the entorhinal cortex. In the lateral entorhinal area, where layer II is split into superficial and deep sublayers, the labelling is found predominantly in the superficial sublayer. In addition, a small number of cells was also noted in layer III and, in a few cases, a few cells were observed in the deep layers of the entorhinal cortex. In both instances these cells were found to lie deep to a region of heavy labelling in layer II.

Sections cut at the caudal end of the cerebral cortex are orientated parallel to, rather than perpendicular to, the cortical laminae. It was therefore difficult to apportion the labelled cells to the various laminae at this point, and it is assumed that the labelling represented a continuation of the backfilling of layer II cells at the caudal pole of the entorhinal cortex.

### *Septal injections*

Of the four injections aimed at the septal pole of CA3, only one (T136) was localized within the apical dendritic field of CA3. In this injection, labelling was found in the caudal part of area 28m, with the majority of cells being located along the dorsal half of its medial wall. Additional labelling was observed along the narrow dorsoventral extent of its lateral wall, where it was contiguous with labelling in the lateral part of area 28i. In both areas labelling was restricted to the caudal 1700 $\mu$ m.

In area 28l, labelling was confined to area dl, and was located adjacent to the ventral lip of the rhinal fissure across its rostrocaudal length. This labelling therefore represents dorsal filling at the caudal end of area dl, at which point the subfield has a substantial dorsoventral spread, but this specificity cannot easily be discerned at the rostral limit of area dl, on account of the restricted dorsoventral range.

### *Mid-septotemporal injections*

Data was collected from 7 injections located across the middle region of CA3. In general, the labelling in areas 28m and 28i extended further in the rostral direction than in the case of the septal injection, whereas in area 28l, labelling was found in area vl, in addition to that in area dl. For example, in injection T161 labelling was located in the ventral portion of area 28m and extended 1700 $\mu$ m from its caudal limit, with labelling absent from the rostral portion of the field. In area 28i, labelling extended across its rostrocaudal length, and was distributed along most of the transverse extent of the field. At its rostral end, the labelling became contiguous with that in the caudal part of area vl.

In area 28l, labelling extended across all but the most rostral part of area dl, with the backfilled cells in the caudal half of the field being restricted to its ventromedial portion. Labelled cells were also distributed across much of the transverse extent in the caudal half of area vl, with the labelling in the rostral direction becoming increasingly restricted to the lateral part of the field. No labelling was noted in area vm.

A comparison of the patterns of labelling in the 7 midseptotemporal injections shows that the extent of labelling in 28m and 28i in the rostral direction, as well as the relative proportions of the labelling in areas dl and vl, are dependent on the septotemporal position of the injection site in the CA3 field, such that injections located

more temporally produce progressively greater amounts of labelling in rostral 28m and 28i, and give rise to greater backfilling in area vl, at the expense of labelling in area dl. Note that in injection T157, the most temporally placed of this series of injections, labelling in area 28m and 28i was shifted rostrally to such an extent that filled cells were entirely absent from the caudal pole of the entorhinal cortex, and that in area dl the labelling was restricted to its most caudoventral part.

Of these midseptotemporal injections, two pairs (T131 & T159, T133 & T148) were located at approximately the same septotemporal level but at different ends of the proximodistal length of CA3. In addition, the injections were all of comparable size, with an uptake diameter of approximately 500 $\mu$ m. While the data available is obviously too restricted to formulate any conclusive statements concerning the differences in the entorhinal projection to proximal and distal parts of the CA3 field, it is perhaps worth noting that, in the above cases, while the overall patterns of labelling were similar, the density of labelling following proximal injections was greater (by approximately 50%) than the corresponding distal injections. In addition, in the case of the proximal injections, there was a slightly increased coverage of the entorhinal cortex, both in rostrocaudal and transverse directions.

### *Temporal injections*

Data was collected from one injection (T153) in the temporal part of the CA3 field. The trends in the organization of this projection, noticed initially in the comparison of septal and midseptotemporal injections, are also apparent in this example. In area 28m, labelling was entirely absent from the the caudalmost 500 $\mu$ m of the field, and at its rostral end the cells were confined to its ventral portion. In area 28i,

labelling was present only in its most rostromedial part, where it was contiguous with the backfilling both in area 28m and in area vl.

The labelling in the lateral entorhinal area was located mainly in area vl, with area dl being free of backfilled cells. Labelling was exhibited across much of the transverse extent of area vl in the rostral half of the field, with additional labelling being found in the caudalmost portion of area vm. Backfilled cells were not found either in area TR, or in the transition zone between the entorhinal and piriform cortices.

### **The topography of the entorhinal-CA3 projection**

On the basis of the organization found in these results, the entorhinal cortex can be split into two subdivisions. The first subdivision, comprising areas 28m and 28i, shows a topographic organization in the projection to CA3 such that progressively more rostral regions provide an input to more temporal parts of the CA3 field. In addition to this rostrocaudal gradient, there is an associated dorsoventral organization such that cells located dorsally in this area project to septal parts of CA3, whereas ventrally-located cells project to cells in temporal CA3.

The second subdivision, consisting of the various regions of the lateral entorhinal area, displays a topographical organization of a different type. There exists a rostrocaudal organization similar in nature to that described above, but it appears to be less marked, with resultant labelling in this area often found to extend across the entire rostrocaudal extent of the lateral entorhinal area. The pattern of organization of the "lateral" pathway is most noticeable in the transverse axis: cells located along the dorsolateral border of the entorhinal cortex (within area dl) project to septal CA3, whereas cells located more ventromedially (with an increasing involvement of area vl and then area vm) project to progressively more temporal parts of the CA3 field. This

gradient is coupled with the "weaker" rostrocaudal gradient such that projections to septal CA3 arise primarily (though not exclusively) from the caudal part of the lateral entorhinal area, whereas the main population of cells projecting to temporal CA3 are located in the rostral part of the entorhinal cortex. Although this experiment failed to demonstrate labelling in the rostrally-located area TR, it must also be noted that this experiment did not include an injection placed at the extreme temporal end of the CA3 field. It therefore remains to be seen whether this region can be included within the definition of the lateral entorhinal area on the basis of this particular projection.

## The distribution of labelling: CA1 injections

In all cases labelling was found around the medial and ventral banks of the rhinal fissure, adjacent to the dorsolateral edge of the entorhinal cortex. Unlike the labelling from CA3 injections, injections in CA1, regardless of the position of the injection within the CA1 field, produced scant backfilling, with an average of 6 neurons being labelled in any given coronal section of 35 $\mu$ m thickness. Furthermore, the location and quantity of labelled cells were not found to vary with rostrocaudal position; injections invariably gave rise to a sparsely-labelled strip of cells running adjacent to the rhinal fissure across the entire length of the entorhinal cortex.

In six cases a small number of scattered cells was found along the ventral lip of the rhinal fissure at the extreme edge of area dl. Unlike the labelling described above, this labelling was scattered irregularly throughout the rostrocaudal length of the entorhinal cortex, with a greater incidence of labelled cells towards the rostral end. In addition to this, cells were occasionally labelled in more ventral parts of area dl, in area vl, and in rare instances an isolated cell was observed in area 28i or area 28m.

The great majority of cells labelled around the rhinal fissure were located in layer III, with cells occasionally being noted in layer II adjacent to the plexiform layer. In contrast, the labelling at the dorsal edge of area dl was almost invariably found in the superficial sublayer of layer II, with a minority of cells being found in the superficial portion of layer III. Of the small population of cells noted in other parts of the entorhinal cortex, all were found in the superficial part of layer III. In no instances were cells found in the deep cortical layers.

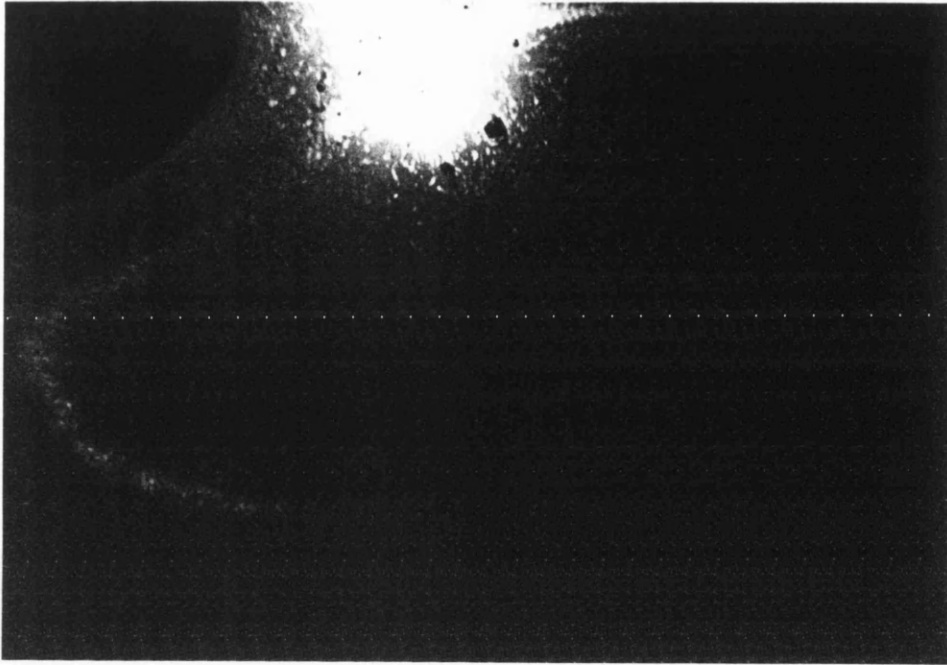
## **The incidence of double-labelling within the entorhinal cortex**

These results show that the populations of labelled cells following injections into CA3 and CA1, regardless of the location of the injections in their respective fields, appear to be largely distinct, both in terms of laminar organization and in distribution within the posterior cerebral cortex. While CA3 injections never gave rise to labelling in the region around the rhinal fissure beyond the dorsolateral limit of the entorhinal cortex, injections in CA1 often produced sparse labelling at the dorsal edge of area dl which overlapped (in terms of regional coverage) with heavier labelling resultant from the corresponding CA3 injections. Although these "CA1" cells were often found embedded in a densely-labelled cluster of "CA3" cells, closer inspection failed to reveal any evidence of double-labelling. This absence was similarly noted for the small number of "CA1" cells located in more ventral, and medial, parts of the entorhinal cortex.

The photographs on pages 210-211 illustrate the segregation in the populations of projection cells in injection T161. Double exposures were taken in order to demonstrate both Fast Blue and rhodamine-labelled cells. Note that there are no instances of double-labelling, in spite of an overlap in the distribution of the two groups of cells projecting to the hippocampus.

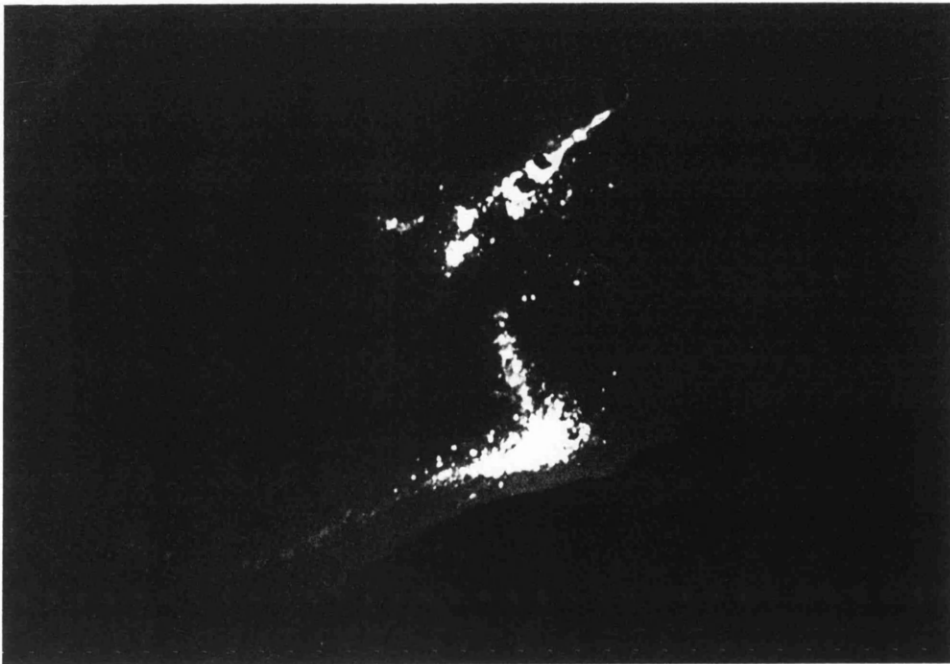
Two additional photographs on page 212 are included which depict rare situations in which backfilled cells are observed in laminae other than that normally associated with the projection.

200um  
↔

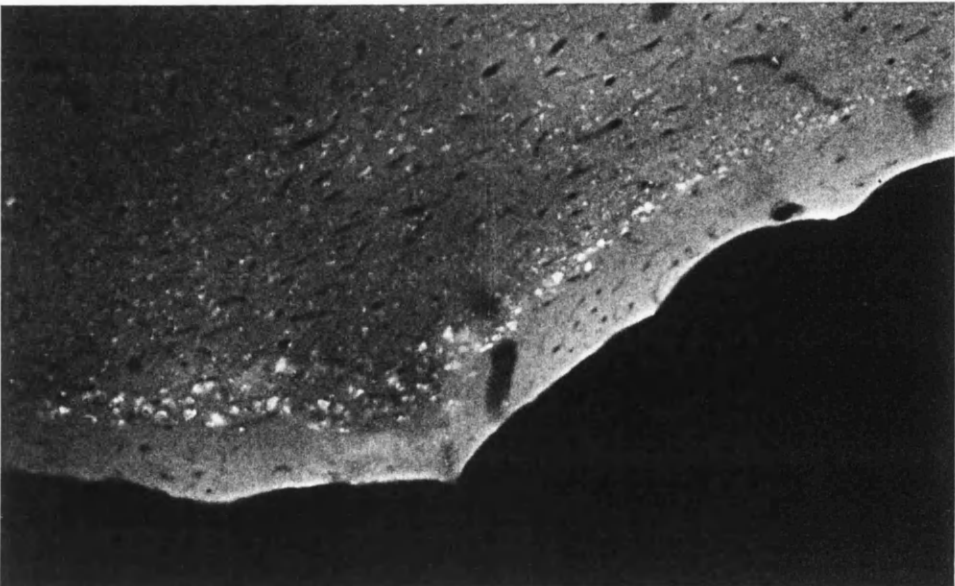
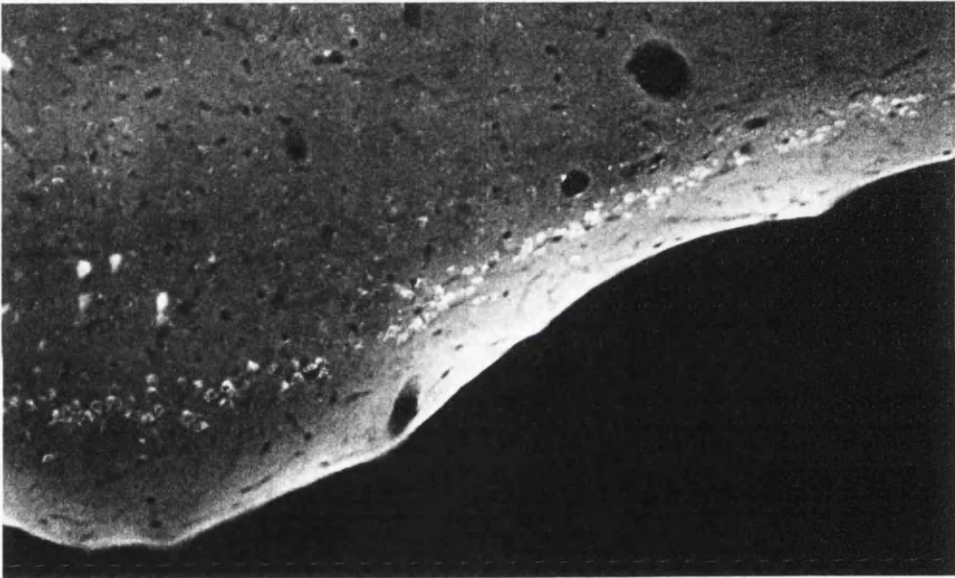
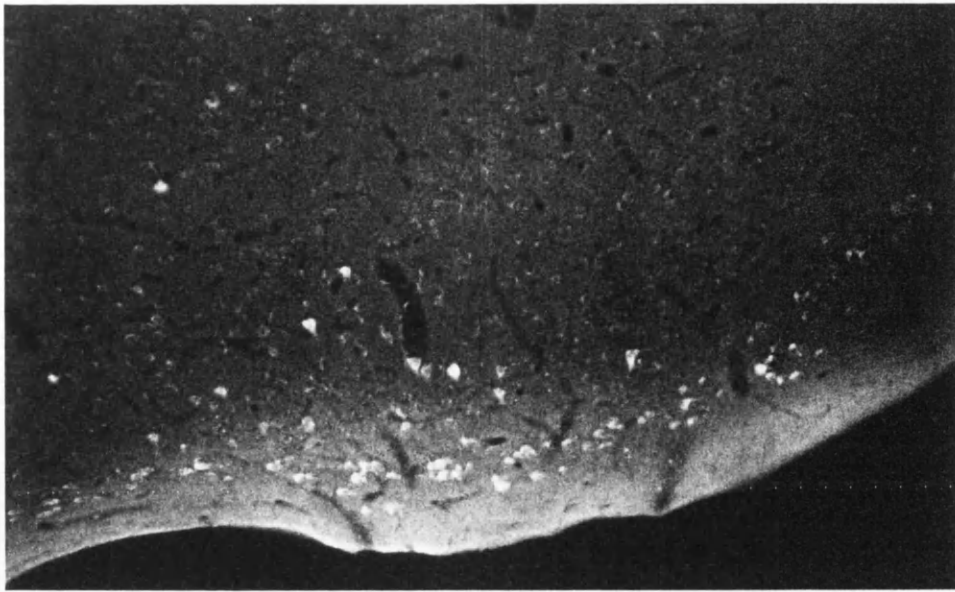


*Above* (T161) Fast Blue injection site into the CA1 field

*Below* (T161) Rhodamine injection site into the CA3 field



120um



(T161) A series of dual exposure photographs of the labelling at various levels of the entorhinal cortex adjacent to the rhinal fissure. Note the complete absence of double-labelled cells and the laminar organization of the labelling.

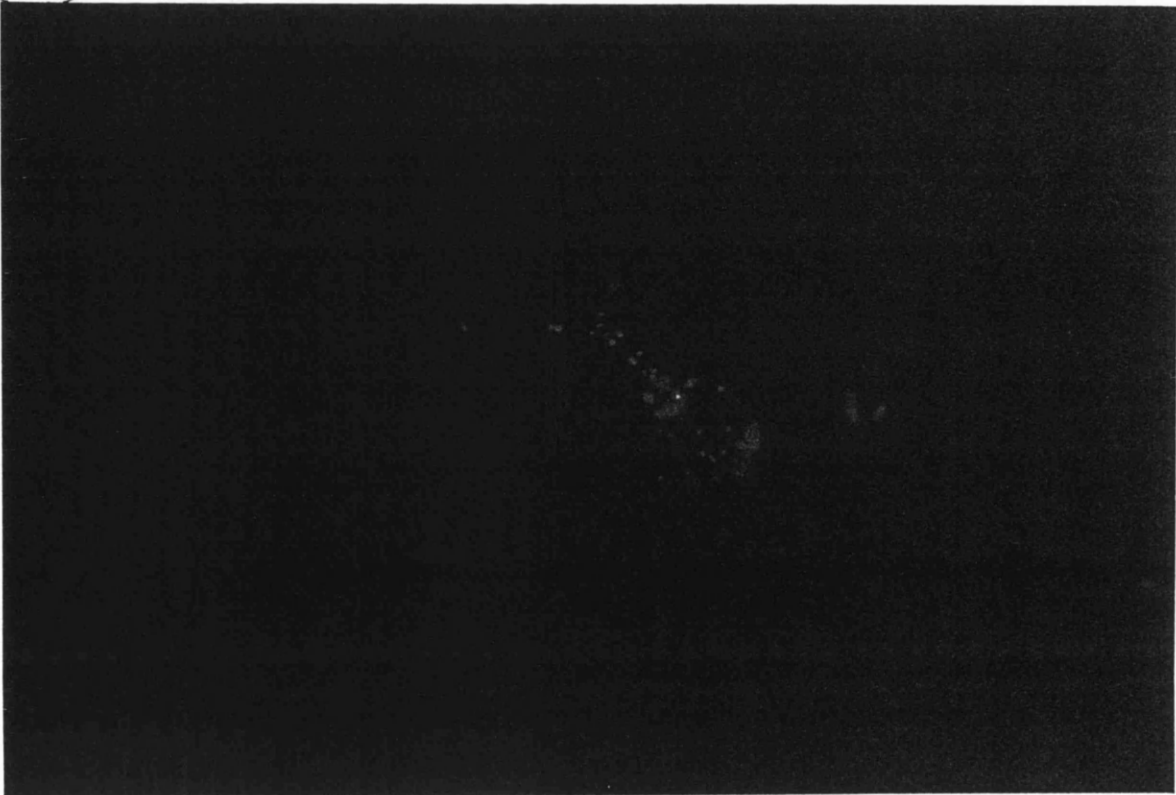
Top at 1.8mm from the caudal pole Middle at 3mm Bottom at 4mm



*Above* Two CA1-backfilled entorhinal neurons cells in superficial layer II

*Below* A single CA3-backfilled entorhinal neuron in layer III

6um



## DISCUSSION

### 1.1. The bilateral organization of the CA3-CA1 projection

Two main findings arise from these results: firstly, the similarity of the labelling in the two CA3 fields following a single injection in CA1 indicates that the ipsilateral Schaffer collateral pathway is functionally indistinguishable from the contralateral pathway, and secondly, the identical patterns of labelling with the two dyes resulting from injections into homologous regions in the two CA1 fields suggests that homologous parts of CA1 receive the same information from the CA3 field.

The issue of bilateral organization within this pathway (as one component of the intrahippocampal circuitry) has been addressed in earlier studies: using autoradiographic techniques, Gottlieb and Cowan (1973) studied the nature of the ipsi- and contralateral projections within the hippocampus and concluded that each field that provides a commissural projection also gives rise to an ipsilateral projection that terminates in the same region and on the same part of the dendritic tree. The work of Swanson *et al.* (1978) using similar techniques, while upholding this precept, concluded additionally that the contralateral hippocampal pathways were invariably less extensive than their ipsilateral counterparts, both in terms of cell numbers and of the septotemporal divergence of the projections, although these differences were observed to be less marked in the case of the CA3-CA1 projection. In contrast, Laurberg (1979) used the Fink-Heimer method and the HRP staining technique to show that the ipsi- and contralateral projections of CA3 were very similar in terms of extent.

The retrograde tracing technique used in this study, by virtue of backfilling cell bodies, adds a further dimension to the analysis of the bilateral organization which is absent in the latter study, namely the ability to define the population of projecting cells

in CA3, and as such these results both support the findings of Laurberg (1979) and demonstrate in addition a correspondence in the numbers of projecting cells in the two CA3 fields. As with the latter study, the bilateral symmetry of the projection was similarly found to hold true across the extent of the hippocampus.

## 1.2. Developmental implications of bilateral symmetry in the projection

Following the observation that the contralateral intrahippocampal pathways were less extensive than their ipsilateral counterparts, Swanson *et al.* (1978) concluded that the formation of connections was governed at least in part by spatiotemporal considerations, such that a greater number of connections are made by ipsilateral fibres, on account of an earlier arrival at the destination site, when compared with the increased distance required for the contralateral fibres to traverse.

Our findings, and those of Laurberg (1979), do not support this theory. Instead, the bilateral symmetry of the projection suggests that the final pattern of connectivity is independent of any such considerations. At this point it is worth recalling the "neurogenetic hypothesis" underlying connection specification as introduced by Bayer and Altman (1987). From their data, and from that of a number of other studies on neocortical connectivity (Wise *et al.* 1979; Innocenti 1981; Reh and Kalil 1982; Stanfield *et al.* 1982; Bates and Killacky 1984), a two-stage process of connection formation is described: stage one, involving axon outgrowth, describes a state of nonspecific axonal termination; stage two, involving the selective elimination of axon collaterals, determines the final pattern of connectivity, which reflects the time of neuronal origin.

Other work on neuronal development has shown that different cell populations express different antigens on their cell surfaces (McKay *et al.* 1983; Pfenninger 1984), which have been shown in invertebrates to play a part in directing the trajectory of

axon growth, while in vertebrates some evidence exists to suggest that surface antigens, known as recognition molecules, might code for synaptic contact rather than for axon trajectory (Altman 1982). The expression of surface antigens is believed to be temporally dependent (McKay *et al.* 1983).

The bilateral symmetry found in the CA3-CA1 projection would therefore appear to agree with the above findings. Given that the two hippocampi develop simultaneously, then homologous cells in the two CA1 fields, expressing similar recognition molecules, would be expected to receive collaterals from the same cells in CA3. Similarly, if the retention of axon collaterals is a function of the time of neuronal origin, then the ipsilateral and contralateral projections, arising as they do from cells originating simultaneously on both sides of the brain, would be expected to be equivalent in size and in extent.

## THE SCHAFFER COLLATERAL PATHWAY

### 2.1.1. The organization within the CA3-CA1 projection

The results in this retrograde tracing study correspond well with those of earlier anatomical experiments on the CA3-CA1 pathway. Studies such as those of Hjorth-Simonsen (1973), Swanson *et al.* (1978) and Laurberg (1979) provide ample evidence of septotemporal divergence in the pathway, while the detailed investigation conducted by Ishizuka *et al.* (1990) utilized the properties of the anterograde tracers PHA-L and HRP to give accurate descriptions of the organization of the projection in three dimensions. The septotemporal and transverse gradients of the projection observed in our results correspond to those noted in the latter study. In short, the projection is topographically organized such that, in the septotemporal plane, cells in septal and temporal parts of the CA3 field project predominantly to septal and temporal regions of CA1 respectively, whereas in the transverse plane, CA3 cells located proximally and distally with respect to the dentate gyrus provide inputs to correspondingly distal and proximal parts of the CA1 field *at the same septotemporal level*. Note that this transverse organization does not hold true across the length of the hippocampus: given its diagonal configuration, inputs to any given region in CA1 from CA3 cells located at more septal levels originate closer to the CA2 border than those from cells in temporal CA3.

Regions in CA1 of similar size receive information from approximately the same fraction (in terms of the total surface area) of the CA3 field, regardless of the positions of the regions in the CA1 field. Given that the pyramidal cell density is non-uniform across the septotemporal extent of the CA3 field, with a three- to four-fold increase in cell density at the temporal end (Gaarskjaer 1978a), then the implication is that a region

in temporal CA1 receives three to four times the number of projections obtained by a region of equivalent size in septal CA1. Data regarding the variation in pyramidal cell density in the CA1 field is still lacking, and it remains to be seen if temporally-located CA1 cells are indeed the beneficiaries of a greater amount of incoming information (in the case of uniform cell density across the length of the CA1 field), or if there is homogeneity - in quantitative terms - in the transfer of information across Ammon's horn (as a result of similarities in the variations of cell density in the CA3 and CA1 fields).

### 2.1.2. Segregation of the pathway into diagonal lamellae

While the retrograde tracing technique was not used to provide information on the third dimension of the projection, which outlines the pattern of termination of the Schaffer collaterals in the radial plane spanning the dendritic fields of CA1, this method can instead be employed to evaluate the projection in another fashion. Following the completion of a substantial number of injections into the CA1 field, with subsequent analysis of the patterns of labelling, the distribution of backfilled cells in CA3 was compared *across* injections. It was discovered that CA1 injections arrayed along an axis angled acutely to the septotemporal axis gave rise to similar patterns of labelling in CA3.

Further inspection revealed that the degree of correspondence observed in the patterns of backfilling was a function of the angular relationship of the injections to this "CA1 axis", such that the degree of overlap in the distribution of labelled cells decreased in proportion to the angular separation of the injections from the CA1 axis, with minimal overlap occurring at the point where the injection sites were aligned perpendicular to the CA1 axis.

T129R  
T126B  
T126R

T148B  
T93B  
T169B

T150B  
T153B

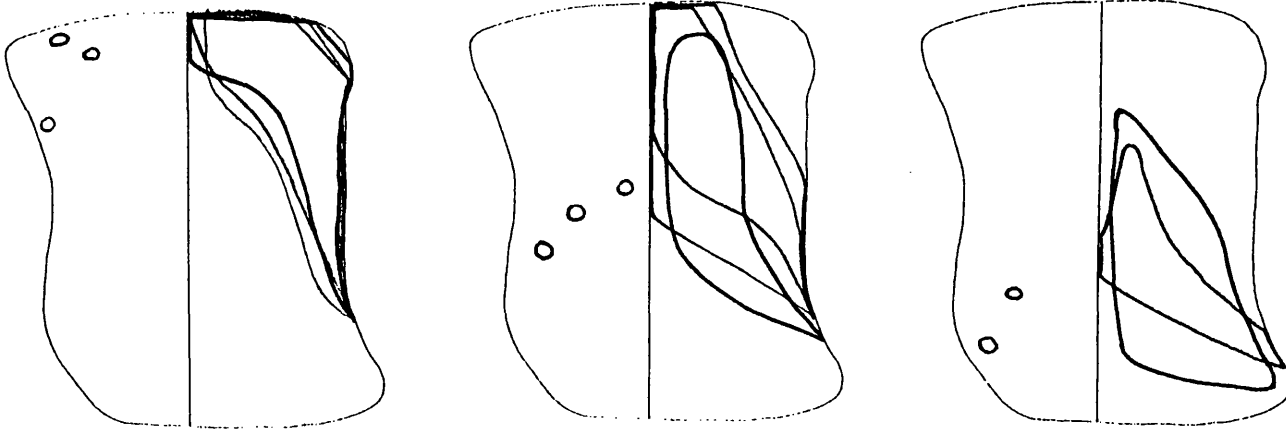


Fig.9 Three examples of the similarity in labelling produced by injections arranged along a diagonal axis in the CA1 field. Note that this pattern is observed across the septotemporal length of CA1.

The angle subtended by the "CA1 axis" to the septotemporal axis of the hippocampus is similar to that subtended by the long axis of the bands of labelling in CA3 to the same septotemporal axis, such that in the unfolded representation of the septotemporal length of the intervening CA2 field (see Figure 11, below). While this

T170B  
T93R

T171B  
T170R

T171B  
T168R

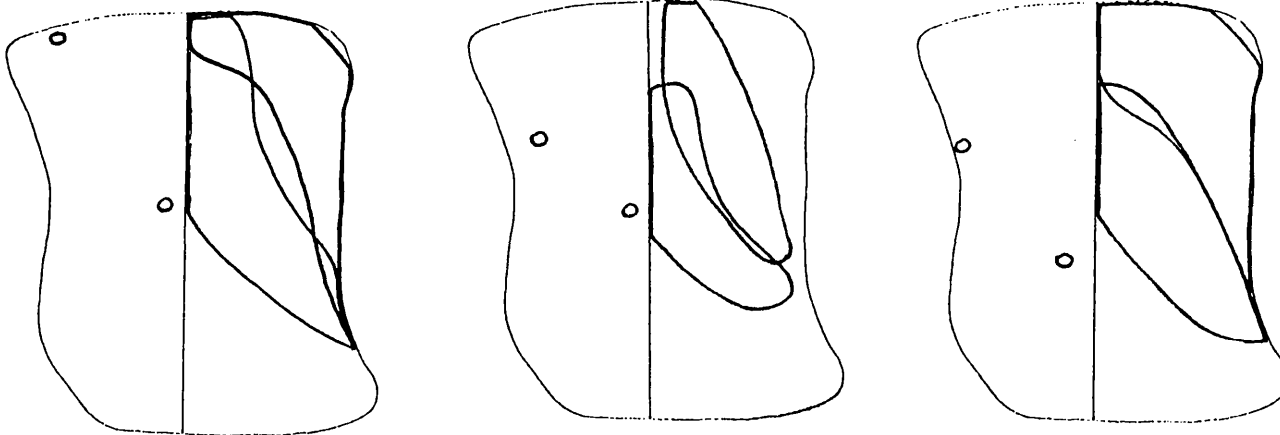


Fig.10 Injections arranged perpendicular to the "CA1 axis" produce labelling with minimal overlap

relationship would appear to be of unclear significance in the unfolded model of the hippocampus, the implications of such organization become more apparent when considered in a more accurate model which incorporates the bend of the hippocampus. Viewed in this respect, the CA1 axis is approximately superimposed on the CA3 axis and is similarly orientated, which leads to the conclusion that they represent the same axis.

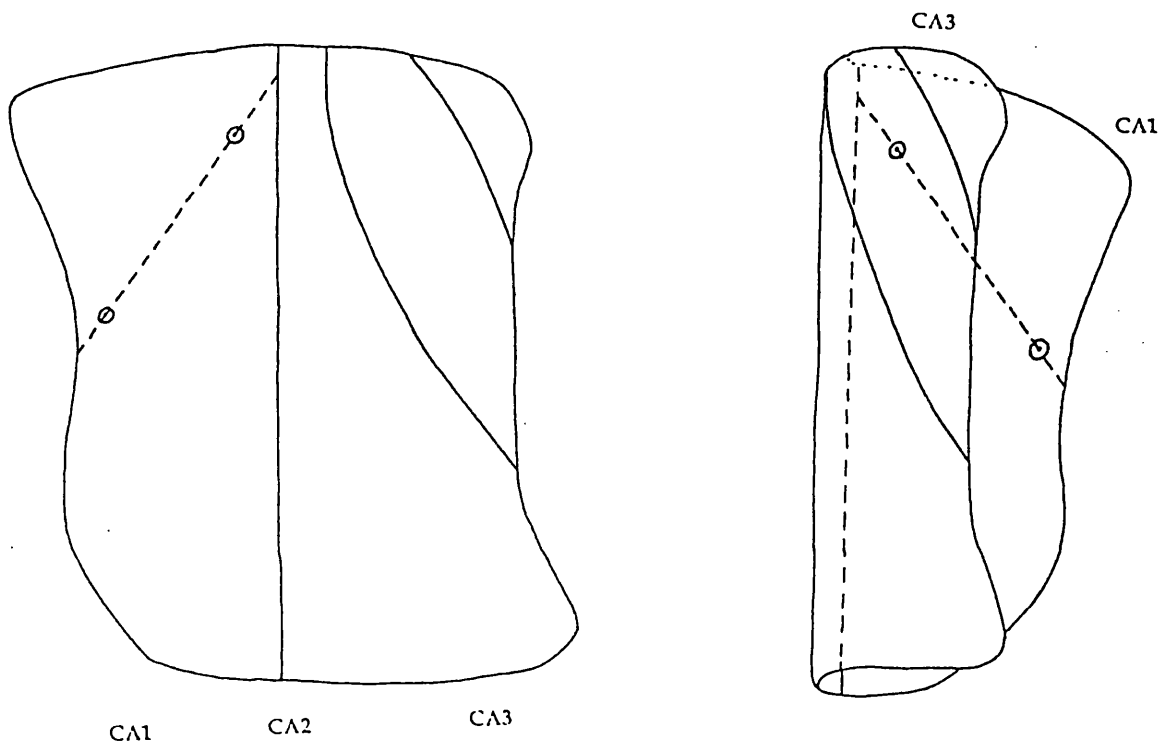


Fig.11 An example of the similarity in the distribution of projecting cells in CA3 and that of the recipient cells in CA1 in terms of the orientation with respect to the septotemporal axis, as seen in unfolded and folded representations of the hippocampus. The injections displayed above are T158B (in distal CA1) and T161B (in proximal CA1), which give rise to similarly-positioned bands of labelling.

The implication of this is that the Schaffer collaterals traverse the comparatively short distance separating the CA3 and CA1 fields. Indeed, the possibility exists that the curvature of Ammon's horn, serving as it does to superimpose the CA1 field upon the

CA3 field, represents a means of facilitating connectivity between the two fields. The projection is thus best described in three dimensions, with the specification of an additional dimension, oriented perpendicular both to the septotemporal and to the transverse dimensions, which is used to represent the passage of fibres across the CA3-CA1 gap. This dimension therefore bears a resemblance to the radial dimension specified by Ishizuka *et al.* in their evaluation of the intrahippocampal CA3 pathways, in which the pattern of termination of CA3 collaterals in the dendritic fields of CA3 and CA1 is evaluated.

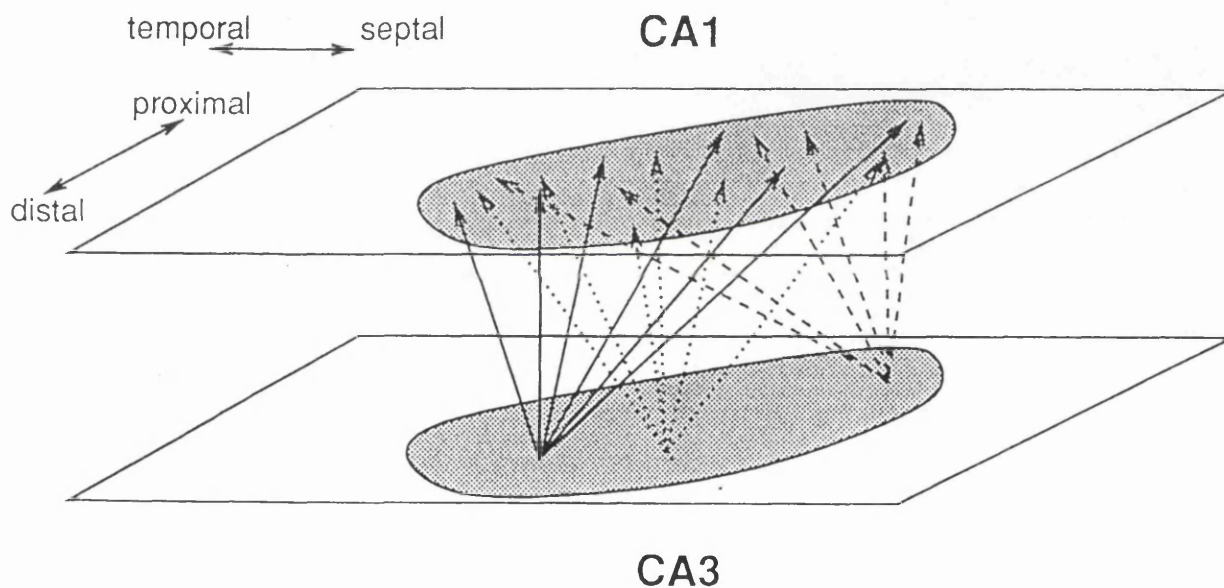


Fig.12 The superimposition of CA1 upon CA3 in the "normal" folded hippocampus serves to minimise the distance traversed by the Schaffer collaterals. The above diagram depicts the connectivity in a lamella of the pathway.

It is worth recalling that earlier anatomical studies such as those cited at the beginning of this section, while furnishing considerable evidence against the lamellar hypothesis as an accurate model of hippocampal connectivity, declined to offer an

alternative hypothesis in its place. The recent anterograde studies (Ishizuka *et al.* 1990; Tamamaki and Nojyo 1991a) showed a diagonal pattern within the projection, but the inability of the anterograde tracing technique to provide information on the distribution of the cells in CA3 which projected in such a fashion prevented further comment on the nature of the projection. The results from this study not only complement the observations made in the above anterograde studies but also highlight a form of diagonal organization both in the distribution of projecting CA3 cells and in that of the recipient CA1 cells. The implications of this organization will be examined later following a discussion of the organization of the other intrahippocampal pathways.

One final point which merits discussion in view of the organization of the CA3-CA1 projection concerns the "radial dimension" of the projection, which was described by Ishizuka *et al.* (1990). As noted on pages 34-35, it was demonstrated that the zone of termination of the Schaffer collaterals within the dendritic field of CA1 varied according to the location of the projecting cells within the CA3 field. While the technique of retrograde labelling is less suited than the anterograde technique to assessing the radial organization of the projection, it is accepted that the present study, in which injections into CA1 were restricted to the stratum radiatum, could be expanded to accommodate a number of injections into the stratum oriens of CA1 in an attempt to provide further data on the radial dimension of the CA3-CA1 projection.

### **2.1.3. The relationship between anatomical and functional connectivity**

Extracellular injection techniques such as that used in this study yield data on the distribution of projection neurons which send fibres to specified regions, and as such give an idea as to the *potential* source of information to those regions. However,

in the light of electrophysiological studies which show that a strong control is exercised over hippocampal activity by inhibitory interneurons (Miles and Wong 1983, 1986, 1987), it seems likely that, for the CA3-CA1 projection, only a fraction of the CA3 cells in a band will be active at any one time and hence able to transmit information to the recipient band of neurons in CA1. In a similar fashion, the inhibitory control in CA1 will in turn place a restriction on the number of "actively recipient" CA1 neurons.

Estimates of the number of inhibitory interneurons in the hippocampus indicate that they are outnumbered by the projection neurons by a factor of 100 to 1. Given this paucity, it seems reasonable to surmise that their powerful inhibitory control is exercised by means of extensive axonal ramifications within the hippocampal cell field, and that the pattern of these ramifications determines the distribution of active projection neurons. The studies on the basket cell (Ramon y Cajal 1911; Lorente de No 1934) demonstrate a local ramification of the axonal plexus around the pyramidal cell somata, such that the feedforward or feedback inhibition mediated by these cells results in a local suppression of activity (Andersen *et al.* 1964; Knowles and Schwartzkroin 1981). Assuming that the basket cells are uniformly scattered throughout the hippocampus, such that there is homogeneity of inhibitory control, then an efferent volley would result in the activation of a fraction of cells similarly scattered within a lamella, with each cell active within a surrounding region of inhibited cells. A similar model can be described for the effect of other interneurons, such as the oriens/alvear cells documented by Lacaille *et al.* (1987), although in these cases the lack of information regarding their axonal arborizations prevents a better understanding of the exact pattern of inhibition.

Miles and Wong (1983) have shown that activity in a single CA3 pyramidal cell may result in the synchronous discharge of a large neuronal population under conditions in which inhibition is suppressed. Not only does this demonstrate that the

local excitatory connections, or "recurrent synapses", in CA3 are divergent in nature, but there is the added implication that these connections are sufficiently powerful to induce activity in a large number of postsynaptic neurons. In such a model, one might expect that activity in the initial CA3 cell would lead to a wave of cascade activity which spreads in accordance with the pattern of associational connections. Given the organization of the CA3-CA3 pathway, this would entail excitation of all the cells within the longitudinally-arranged strip in CA3 containing the initially-active cell, with little activity in other parts of the CA3 field. Furthermore, these cells might reasonably be expected to generate activity in an equally large population of CA1 cells occupying the appropriate diagonal strips of the CA3-CA1 projection.

One obvious consequence of the topographical organization within the CA3-CA1 pathway is that the cells occupying the same diagonal strip in CA1 are privy to the same information as transferred from the CA3 field. (A similar conclusion can be drawn for the CA3 cells, in view of the organization of the mossy fibre and CA3 associational systems as outlined in this dissertation and elsewhere). It is therefore intriguing to find that multi-unit recording studies have *failed* to demonstrate that neighbouring pyramidal cells possess similar patterns of firing within the environment (O'Keefe and Speakman 1987; Muller and Kubie 1987). Instead it is suggested that, in terms of the spatial mapping theory of hippocampal function (O'Keefe and Nadel 1987), the environment is represented by activity in a small subset of the total number of place cells - about 20% of the pyramidal cell population, according to Thompson and Best (1989) - which are distributed throughout the hippocampus. Our results, while confirming the absence of point-to-point topography in hippocampal connectivity (with its implications for hippocampal function), also suggest that there are constraints upon the distributed nature of the environmental representation within the hippocampus, in that "active subsets" of place cells are likely to be confined within specific regions of the

hippocampus, as a result of the segregation of information along the intrahippocampal pathways. Finally, it is postulated that the distributed pattern of place cell activity occurs as a result of control by interneurons, which serve to restrict the generation of recurrent excitation.

## THE CA3 ASSOCIATION PATHWAY

### 2.2.1. Specificity of labelling following CA3 injections

Current anatomical thinking states that the granule cells of the dentate gyrus and the various hilar neurons (with the exception of the pyramidal basket cells) do not receive inputs from the pyramidal cells of CA3, and as such the inclusion of these regions within the injection site was not held to affect the resultant backfilling in CA3. Labelling within the hilus, however, was seen following these injections, but the filled cells appeared different in size and morphology (so far as could be discerned under fluorescent microscopy) and probably represented mossy cells, since these labelled cells were noted at some distance from the injection site. While this offers the intriguing possibility that mossy cells are innervated by the pyramidal cells of CA3, the injections into CA3 as employed in this study are nevertheless considered to be of satisfactory specificity.

### 2.2.2. The organization of the CA3 association projection

Injections into CA3 produced patterns of labelling in CA3 which are oriented parallel to the septotemporal axis, indicating that the cells of origin of the pathway are organized in longitudinal strips across the field. Furthermore, the fact that labelling tended to occur in the part of the transverse extent of CA3 where the injection was located strongly suggests that the projection is mainly directed at cells in the same longitudinal strip. This specificity was found to be invariant across the CA3 field.

Another feature of the association pathway is the equal involvement of projection cells septal and temporal to the region of recipient cells. Injections resulted

in labelling which extended for approximately equal distances in the two directions, so that the septotemporal level at which the injection site was located corresponded approximately with the midpoint of the strip of labelling.

This longitudinally-arranged projection correlates with the description given by Lorente de No (1934), in which it is written that the CA3 pyramidal cells give rise to collaterals which run above the cell layer in the stratum radiatum, parallel to the long axis of the hippocampus, to innervate other parts of CA3. However, it was believed that these collaterals arose mainly from cells in distal CA3 (subfield CA3<sub>d</sub>). While the reports of Swanson *et al.* (1978), Tamamaki and Nojyo (1991a) agree as to the longitudinal nature of the association pathway, the results of Ishizuka *et al.* (1990) suggest a different organization: instead of running parallel to the septotemporal axis, the projection is held to be organized in a diagonal manner across the CA3 field, with septally-directed collaterals terminating in proximal CA3 (adjacent to the hilar border) and temporally-directed fibres projecting to distal CA3, abutting the CA2 border. In an unfolded representation of the hippocampus, the CA3-CA3 pathway is therefore be arranged in an opposite sense to the CA3-CA1 pathway, since the diagonal nature of the latter is oriented such that Schaffer collaterals coursing septally terminate in distal CA1, whereas temporally-directed fibres project to proximal parts of the CA1 field. Applying the same principle as in Section 2.2.2. of this Discussion, it is clear that the orientation of the CA3-CA3 projection *in the folded hippocampus* mirrors that of the CA3-CA1 projection.

The implications for the pattern of information transfer across the hippocampus are substantial. If, as is widely accepted, the CA3 and CA1 fields process information which is transmitted from the entorhinal cortex by way of the dentate gyrus, then the highly restricted pattern (in the septotemporal plane) of the mossy fibre projection indicates that any mixing of information (assuming that the information arriving from

the entorhinal cortex is heterogeneous in nature) must necessarily occur by means of the CA3 association pathway. Hence, on the one hand, if the CA3 association pathway is organized parallel to the septotemporal axis of the hippocampus, as suggested in this dissertation and in the works of Lorente de No (1934), Swanson *et al.* (1978), as well as the recent study of Tamamaki and Nojyo (1991a), then the projection allows the processing of information across a broad sweep of CA3 cells which transcends the diagonal nature of the CA3-CA1 pathway, with the result that cells in CA1 are recipients of information which has already undergone extensive mixing across the septotemporal length of the CA3 field. On the other hand, the findings of Ishizuka *et al.* (1990) indicate that the two pathways are orientated in the same fashion, which implies that information processing in the CA3 field is confined within the same group of cells that project in turn to CA1, with the latter consequently receiving inputs of a more restricted nature. The information processing performed by the CA1 field is thus clearly dependent upon the configuration of the CA3 association pathway.

As a final point, the observations of Ishizuka *et al.* (1990), implicitly demonstrating that the CA3-CA3 and CA3-CA1 pathways are similarly organized, would appear to offer greater support for the concept of functional segregation within the hippocampus.

### **2.2.3. The relationship between the CA3-CA1 and the CA3-CA3 projections**

The issue of heterogeneity in the distribution of cells in the CA3 field giving rise to the Schaffer collateral system and to the association pathway was first voiced by Lorente de No (1934). It was his belief that cells in proximal CA3 (subfield CA3<sub>1</sub>) contributed mostly to the former pathway, whereas at the other end of CA3 (subfield

CA3<sub>a</sub>) few cells projected to CA1 but instead gave rise to the CA3 association pathway. Cells in the middle of the transverse extent of CA3 were understood to contribute in equal proportions to the two pathways.

Later studies have disputed this division of the CA3 projection cells. While confirming the existence of collaterals from CA3 cells which ran both septally and temporally along the longitudinal axis, Swanson *et al.* (1978) found that cells from all parts of CA3 gave rise to collaterals which terminated in CA1. At the same time, it was acknowledged that the co-mingling of the fibres of the two projection systems caused great difficulty in the distinction of the two systems.

A similar problem was noted by Hjorth-Simonsen (1973) and by Ishizuka *et al.* (1990). On the basis of similar termination zones in the stratum radiatum and stratum oriens of CA3 and CA1, and on the observation that both pathways were found to originate in proximal CA3, Hjorth-Simonsen (1973) argued against the division of the collaterals of the CA3 cells into two distinct pathways. The intracellular studies of Ishizuka *et al.* (1990), in which the ramifications of the various primary collaterals were observed throughout the hippocampus, arrived at the same conclusion.

Our results agree with both of the above studies with regard to the similarity in the septotemporal extent of the two pathways, and as such refute the claim of Lorente de No (1934) that the Schaffer collateral system served to link the hippocampal fields at the same transverse level whereas the longitudinal association pathway served to join parts of the hippocampus at different septotemporal levels. However, the marked directionality noted in each pathway provides an alternative case for the consideration of the two systems as separate entities. A similar point was conceded by Hjorth-Simonsen (1973), following the observation that the fields of termination in CA3 and CA1 diverged in temporal parts of the hippocampus. (This finding was also observed in the present study, and is attributed to the diagonal nature of the CA3-CA1

projection which shifts away from the CA2 field in the temporal direction).

It appears that cells in all parts of the CA3 field contribute to both pathways, and thus act as components within two distinct functioning strips within these pathways. Evidence for the existence of multiple collateral projections within CA3, and for the homogeneity of these projections across the CA3 field, is also presented in the multiple retrograde labelling study conducted by Swanson *et al.* (1981), which provides alternative proof of the contribution of CA3 cells to a number of separate pathways.

## THE MOSSY FIBRE PATHWAY

### 2.3.1. The organization of the mossy fibre projection

The pattern of the mossy fibre projection from the dentate gyrus to CA3 as shown in this experiment correlates well with the various anatomical and electrophysiological reports of this pathway (Blackstad *et al.* 1970; Lømo 1971; Swanson *et al.* 1978; Gaarskjaer 1981a,b, 1986) in that the projection is organized in a transverse fashion across the CA3 field. In addition to this transverse projection, the results from these injections showed that, on approaching the CA2 region, the mossy fibres changed direction to course parallel to the longitudinal axis of CA3 towards the temporal pole of CA3, echoing the observations made in a number of earlier studies (Ramon y Cajal 1911; Lorente de No 1934; McLardy 1963). Blackstad *et al.* (1970) have suggested that the change in direction of the mossy fibres in proximal CA3 towards the temporal pole is due to a lack of synaptic termination sites at the septotemporal level of the injection (and at more septal levels), such that the fibres alter their trajectory in search of available sites temporal to the injection. Gaarskjaer (1986) reinforces this argument by citing the numerical ratios of recipient CA3 pyramidal cells to granule cells - greater in temporal regions - which would favour such a modification of fibre direction. A related factor underlying the abrupt shift in direction is the lack of innervation of the CA1 field.

While the three rhodamine injections uniformly displayed the trajectory pattern described above, the biocytin injection (T117) was notable for some additional temporally-directed labelling in proximal CA3. This pattern of labelling bears a distinct similarity to that observed by Swanson *et al.* (1978) for the "infrapyramidal bundle" of mossy fibres, which was found to be largely confined to the septal third of the CA3

field, within which the fibres ran the entire transverse length of the field. Temporal to the region, the infrapyramidal bundle was seen only to innervate parts of CA3 adjacent to the hilus, although in the midseptotemporal region there was an additional tongue-shape projection into the CA3 field adjacent to the CA2 border.

The most interesting aspect of this similarity lies in the fact that the labelling in T117 is clearly confined to the so-called "suprapyramidal" bundle. The argument against the segregation of the mossy fibre projection into supra- and infrapyramidal bundles has already been put forward in Section 3.2.2. of the first part of this dissertation, and in fact Swanson *et al.* (1978) themselves conceded the point that the two bundles were not easily distinguished, and that the fibres of the infrapyramidal bundle probably merged with those of the suprapyramidal bundle beyond the hilar region. As far as injection T117 is concerned, the fact that the temporal spread of labelling in proximal CA3 is found to lie directly beneath the zone of disruption of the superficial blade of the dentate gyrus corresponding to the injection site suggests that this apparently anomalous pattern of projection is in fact a result of the inclusion of a sizeable fraction of the septotemporal extent of the dentate gyrus in the injection site. An initial appraisal of the sizes of the injections employed in the study of Swanson *et al.* (1978) hints at a similar explanation for the pattern of projection.

With regards to the fine structure of the projection, the results of the biocytin injection correspond with those of ultrastructural studies (Blackstad and Kjarheim 1961; Hamlyn 1962; Amaral and Dent 1981; Gaarskjaer *et al.* 1982) which have shown that the mossy fibres are thin, unmyelinated axons 0.1-0.7 $\mu$ m in diameter, along which giant synaptic boutons (up to 10 $\mu$ m in diameter) are distributed, with an average inter-bouton distance along a single mossy fibre of 250-450 $\mu$ m (Blackstad and Kjaerheim 1961).

In summary the mossy fibre projection, in accordance with numerous other

reports, is topographically organized such that septal and temporal parts of the dentate gyrus project across the transverse length of the CA3 field to septal and temporal parts of CA3 respectively. Furthermore, the transversely-directed nature of the projection indicates that the pathway is organized in the form of individually-functioning units which are oriented orthogonal to the septotemporal axis of the hippocampus, the functional importance of which is underlined by the notable absence of associational or commissural connections between granule cells. Finally, it is acknowledged that this theory is upheld in spite of the evidence for a longitudinally-directed component of the projection in the proximal part of the CA3 field. The functional implications of this aspect of the projection has yet to be understood, and as such it has yet to be incorporated into models of the dentate gyrus-CA3 relationship. It may well be that due consideration of this component will lead to a reappraisal of the pathway, to the effect that the concept of transverse organization is redefined accordingly to incorporate the longitudinal component in proximal CA3.

### **2.3.2. The confinement of anterograde labelling to the mossy fibre system**

In all four examples anterograde labelling was restricted to the mossy fibre system. Given that the three rhodamine injections were targeted - successfully - at the proximal end of the CA3 field, anterograde labelling of the efferent pathways of CA3 might reasonably be expected. In the case of the biocytin injection, the injection site encompassed within its considerable extent a sizeable portion of the proximal CA3 field, such that substantial anterograde labelling within CA3 and CA1 might again be envisioned. The absence of labelling in all but the mossy fibre system is suggestive of a feature specific to that system, with a possible clue as to the nature of this feature

being noted following consideration of the nature of the rhodamine labelling. In these cases, anterogradely-transported rhodamine microspheres appear to be accumulated at the mossy fibre terminals. Light microscopic observation using high power objective lenses suggests that the transported microspheres are uniform in size, in comparison with the wide range of sizes noted in the retrogradely-transported microspheres. This uniformity in size might reflect the mechanism of transport, in which microspheres within a given size range are taken up into vesicles by pinocytosis, and are thus transported to the presynaptic terminals of the mossy fibres.

The confinement of the biocytin labelling to this projection offers no ready explanation. Unlike the microspheres, biocytin is an anterograde tracer which has been used to label a number of neuronal systems, although at present its usage within the hippocampus has not been widely documented. Given the mode of its delivery - as a solute in vehicle - its uptake by fibre systems would seem to be easily achieved.

It is suggested that the peculiar ability of the mossy fibres to allow anterograde transport in both cases might be a reflection of a difference in the intracellular transport system of these fibres. Although there exists no direct evidence for such a difference, the possibility is suggested by the study conducted by Goldschmidt and Steward (1980) on the effect of colchicine on the hippocampus, which resulted in near-total destruction of granule cells and mossy fibres, with negligible damage to other hippocampal structures and pathways. The authors concluded that colchicine, as an inhibitor of microtubule assembly, might target the dentate gyrus on account of some as-yet-undiagnosed difference in its cellular structure. A pilot study conducted by the present author, in which another inhibitor of microtubule assembly, namely vinblastine, was injected into the hippocampus, resulted in a similar pattern of destruction to that achieved by colchicine. On the basis of these findings, it is proposed that the mossy fibres might employ a particular mechanism of axonal transport, involving microtubule-

associated proteins specific to the fibres, which facilitates anterograde transport of dyes along the lengths of the mossy fibres, and which confers a unique susceptibility to the effects of microtubule inhibitors such as colchicine and vinblastine.

# AN OVERALL CONSIDERATION OF THE INTRAHIPPOCAMPAL PATHWAYS

The stream of mossy fibres running transversely across the CA3 fields intersects that of the Schaffer collaterals which are directed diagonally across CA3 and CA1. Crossing both of these systems is the CA3 associational projection which is oriented parallel to the septotemporal axis and is therefore arranged at an acute angle to the Schaffer collaterals and at right angles to the mossy fibre projection. The crossing pattern of these fibres is shown below in Figure 13 using an unfolded representation

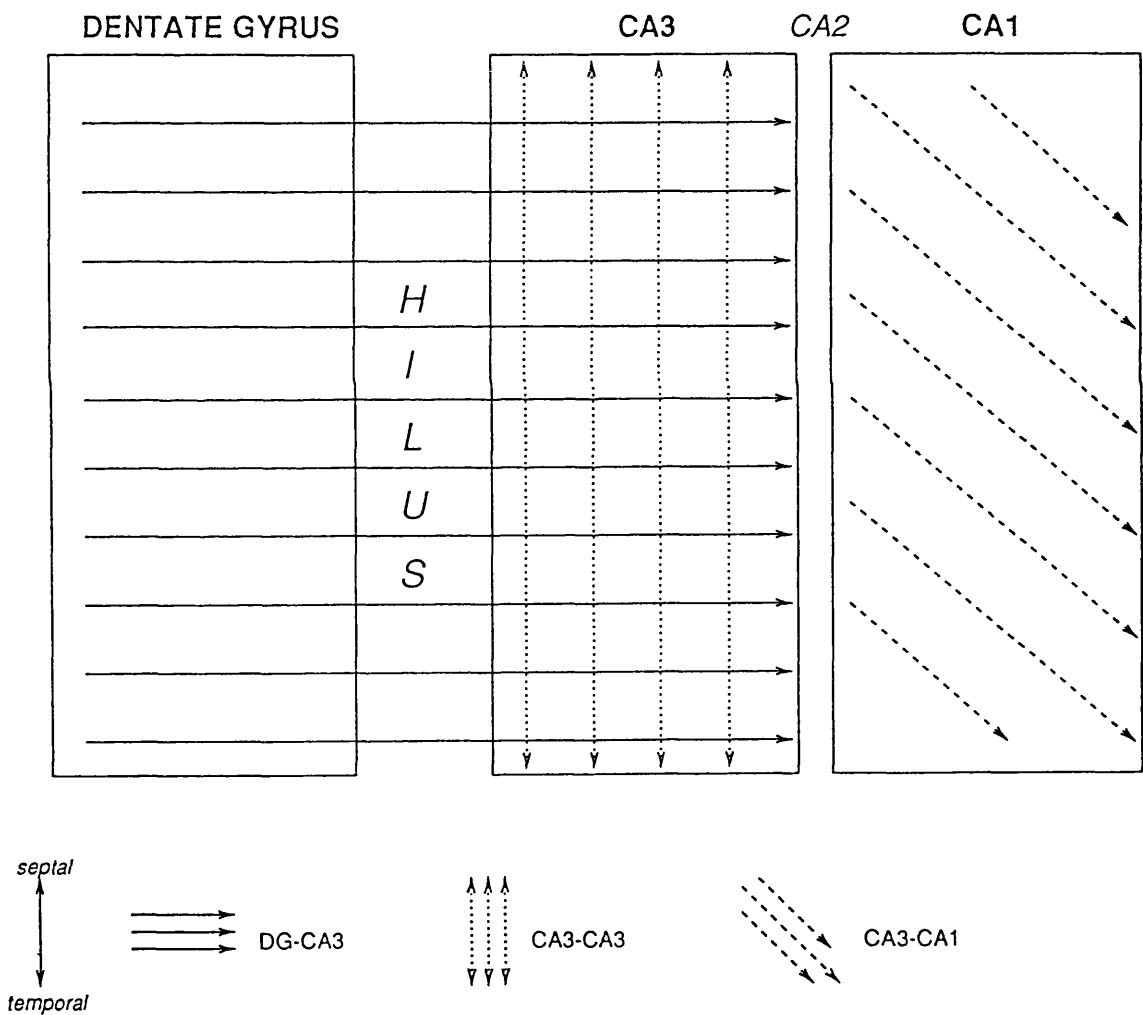


Fig.13 The orientation of the various intrahippocampal pathways as shown in an unfolded representation of the hippocampus.

of the hippocampus. While the direction of the projection from the CA1 field to the subicular complex was not explored in this dissertation, the subject has received attention from Tamamaki and Nojyo (1990) and was also found to possess a lamellar organization such that the alvear fibres are oriented in much the same way as the bands of CA1 cells which constitute part of the lamella of the Schaffer collateral pathway.

In Section 2.1.2. of this Discussion the concept of a radial dimension within the CA3-CA1 projection was introduced. This dimension can also be incorporated so as to provide a three-dimensional model of the intrahippocampal pathways. Unlike the Schaffer collateral projection, neither the mossy fibre system nor the CA3 association pathway have a component in this dimension, so that the three fibre systems show marked differences in terms of their arrangements in the three dimensions.

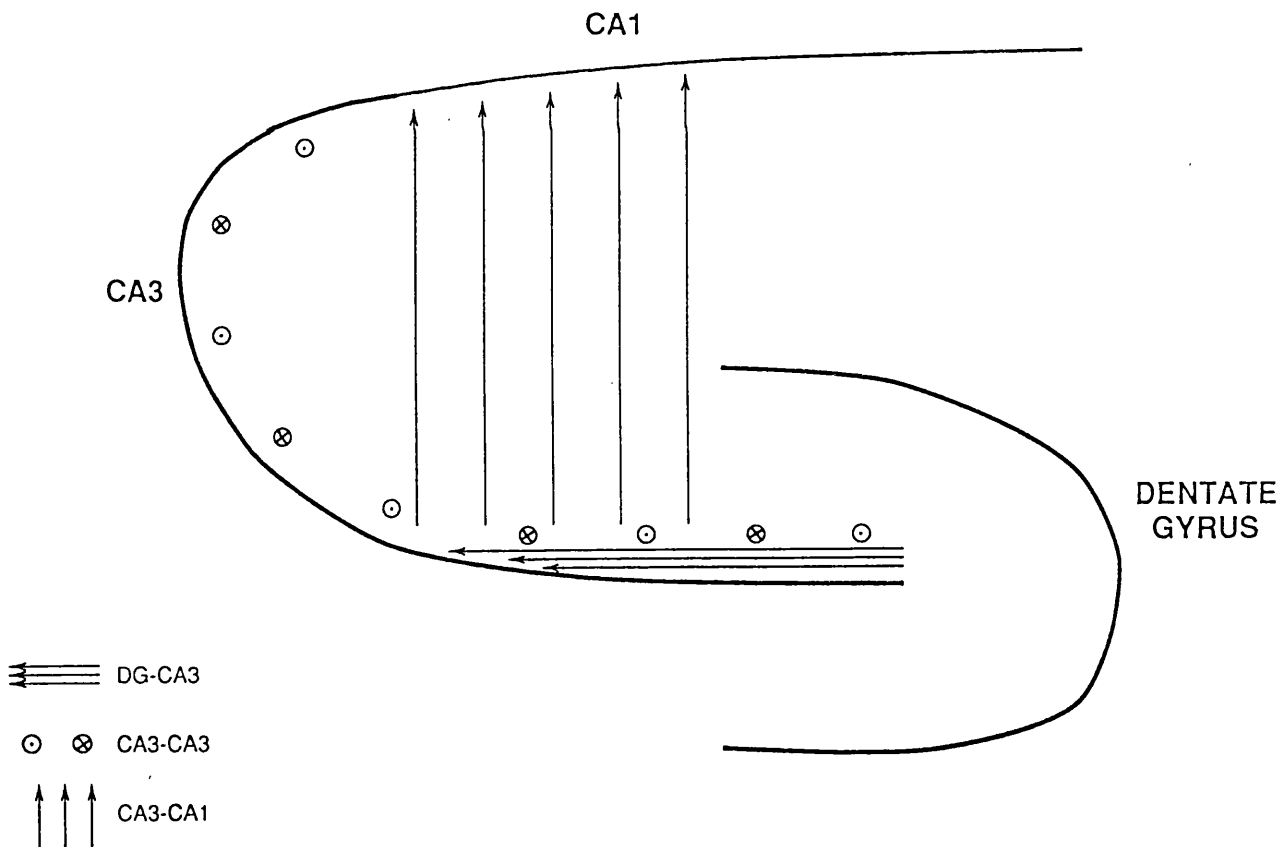


Fig.14 The orientation of the various intrahippocampal pathways as shown in a transverse section through the extended hippocampus.

The data accumulated in this experiment show a marked correspondence with the results of the study conducted by Tamamaki and Nojyo (1991a). This correspondence is perhaps the more striking in view of the differences between the two studies, with the latter report employing electron microscopic techniques to assess the trajectories of single hippocampal neurons following intracellular injections with the anterograde HRP tracer.

Far from suggesting that the intrahippocampal pathways are organized in such a way as to ensure the segregation of information within the hippocampus, as depicted in the lamellar hypothesis of Andersen *et al.* (1971), this arrangement implies instead that they are designed to allow substantial divergence and "mixing" of information throughout the hippocampus. Further work needs to be done before the implications of separate organization within each pathway can be assessed.

### **3. THE PROJECTION FROM THE ENTORHINAL CORTEX TO THE HIPPOCAMPUS**

#### **3.1 Afferents to the CA3 field**

##### **3.1.1. The functional subdivision of the projection**

Two distinct gradients in the pattern of labelled entorhinal cells were observed following injections which spanned the septotemporal extent of the CA3 field. The first of these corresponds to the organization of the projection from cells located in the lateral reaches of the entorhinal cortex, in which a dorsolateral-ventromedial axis in the transverse plane corresponds to the septotemporal axis of the recipient CA3 cells. The second gradient was observed in more medial parts of the entorhinal cortex and, unlike the first gradient, manifested itself in both the longitudinal (rostrocaudal) and transverse planes, with cells in caudodorsal and rostroventral regions projecting to septal and temporal parts of CA3 respectively.

These findings clearly indicate that there are two separate components to the entorhinal-CA3 projection, corresponding to the medial and lateral pathways quoted in a number of studies (Hjorth-Simonsen 1972; McNaughton 1980; Witter 1989), and as such conflict with the belief that there exist three subdivisions to the projection (representing the lateral, intermediate and medial parts of the entorhinal cortex) which is upheld by Steward (1976) and Wyss (1981), since our results demonstrate that the efferents from the latter two regions are organized in a similar fashion.

### 3.1.2. Projection axes within the entorhinal cortex

A description of the entorhinal cortex in three dimensions was provided on page 184. If the medial and lateral projections to the hippocampus are assessed in a similar fashion, it becomes apparent that each is organized along two out of the three axes of the entorhinal cortex: the medial pathway is organized along the dorsoventral and mediolateral axes, with relatively little involvement in the rostrocaudal plane, whereas the lateral pathway displays organization in the mediolateral and dorsoventral axes and has a relatively restricted representation in the mediolateral plane.

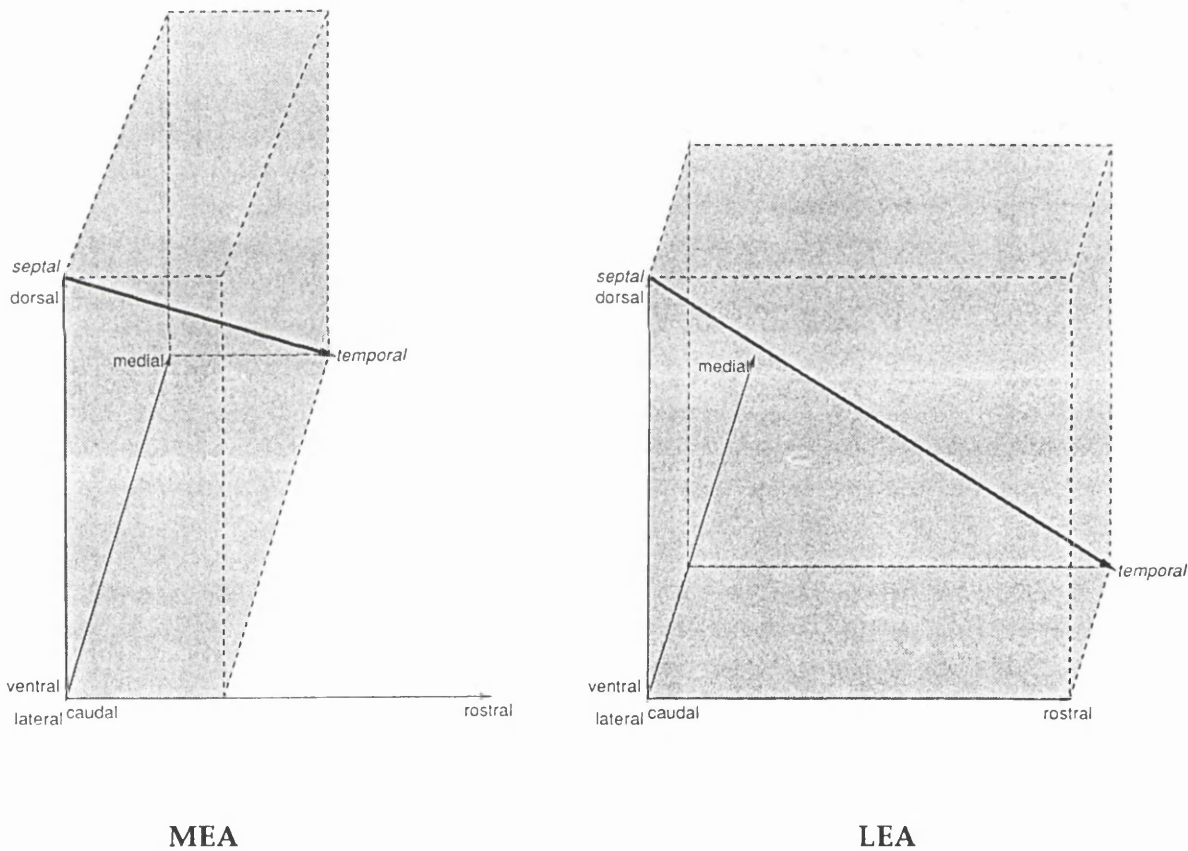


Fig.15 A representation of the extents within the entorhinal cortex of the medial (*left*) and lateral (*right*) projections to the CA3 field. A bold arrow is used to depict the axis in each projection which corresponds with the septotemporal axis of CA3.

As shown in Figure 15 above, the gradient of the projection to the CA3 field can be represented in each case by a diagonal axis, depicted above as a bold arrow, such

that cells in septal CA3 are innervated by the region of the entorhinal cortex corresponding to the origin of the arrow, whereas temporally-located cells receive projections from the region represented by the head of the arrow.

As well as demonstrating an axis within each of the projections from the entorhinal cortex to the hippocampus which corresponds to the septotemporal axis of the latter, the marked difference between the two axes suggests different gradients of development in the medial and lateral portions of the entorhinal cortex. Conceivably, if the patterns of projection in the entorhinal cortex are also determined according to temporal parameters (see pages 213-214 of this *Discussion*) then one might surmise that cells at the caudodorsolateral end of the entorhinal cortex were linked in terms of development with cells in the septal part of the hippocampus, while cells located in progressively more temporal parts of the hippocampus receive inputs from cells in medial and lateral parts of the entorhinal cortex which are located progressively further away from the caudodorsolateral limit (as well as from each other), in accordance with the developmental gradients which are represented in turn by the direction of the arrows in Figure 15.

As a final consideration, the fact that the medial and lateral pathways are organized almost at right angles to each other - in spite of the demonstration that they represent differing aspects of the same projection rather than being entirely separate entities - may be indicative of a difference in the manner in which information is transferred to the hippocampus. Some authors (O'Keefe 1989) have suggested that the entorhinal projection conveys information concerning the three-dimensional (Cartesian) nature of the environment and, in light of this theory, it is tempting to regard the two pathways as conveying complementary features of this environmental data. If this bears out, then the different patterns of termination of the two pathways in the hippocampus implies a form of functional heterogeneity, with different regions in CA3 receiving

varying amounts of environmental information.

### 3.1.3. A comparison of the projections to the dentate gyrus and to the CA3 field

In the initial description of this experiment on page 184 of the Results section, it was emphasised that the method of subdivision of the entorhinal cortex would be the same as that used by Ruth *et al.* (1982, 1988), in order that the projections to the dentate gyrus and to CA3 might readily be compared. While the argument against this method of subdivision in terms of functional relevance was presented in the preceding section, the original intention has been maintained.

In short, it appears that the two projections are virtually identical in terms of topographical organization. Given that the projection to CA3 arises predominantly from cells in layer II, with a negligible contribution observed from layer III and the deep layers, echoing the laminar organization already established for the projection to the dentate gyrus, it seems reasonable to suggest that the two projections are in fact components of the same efferent system, such that granule cells and CA3 pyramidal cells located at the same septotemporal level receiving information from the same population of neurons in the entorhinal cortex. In view of the scant amount of data from our results which demonstrates that the entorhinal projections to cells located at different ends of the transverse extent of CA3 at the same septotemporal level are similarly organized, it becomes possible to depict the trajectory of the efferent system of the entorhinal cortex within the hippocampus proper. It appears that the fibres change course to run in a transverse fashion through the hippocampus, innervating both granule cells and pyramidal cells, in parallel with the mossy fibre system. The similarity with the latter pathway continues with respect to the CA1 field: given that the projection from the entorhinal cortex to CA1 is organized in an entirely different

fashion to that of the projection to the dentate gyrus-CA3, the latter pathway - like the mossy fibre system - is excluded *in toto* from the CA1 field. In a recently-published abstract, Tamamaki and Nojyo (1991b) presented preliminary evidence which suggested that spinous neurons of layer II of the entorhinal cortex projected in a "sheet-like" manner across the hippocampus, providing innervation to the supra- and infrapyramidal blades of the dentate gyrus and to fields CA3 and CA2 of Ammon's horn. Mention of the CA1 field in terms of this projection was conspicuous by its absence.

## **3.2. Afferents to the CA1 field**

### **3.2.1. The pattern of projection**

The most striking aspect of the findings in this experiment is the exclusivity in the distribution in the cells of origin of this pathway. In all cases these cells were located around the edges of the rhinal fissure, at the dorsolateral limit of the entorhinal cortex, although isolated cells were occasionally labelled in more ventral, and medial, regions. In direct contrast to the specificity in the transverse plane, the cells of origin of this pathway were distributed uniformly across the entire rostrocaudal extent of the entorhinal cortex. With regard to the laminar organization of the projection, these results confirm the observations of Steward and Scoville (1976) that the projecting cells were located in layer III, although examples of projection cells in layer II were also noted in the present study. Within layer III, cells were invariably found to be scattered across its extent, with no indication for a preferential projection from superficial or deep portions of the layer, or for the segregation of the cells of origin into discrete

groups. No cells from layers IV-VI were found to contribute to the projection.

Studies which have devoted attention to the entorhinal-CA1 projection in the rat lie thin on the ground. Apart from the seminal work of Steward and Scoville (1976), the only other report of note is the publication of Witter *et al.* (1988), in which the projections to the dentate gyrus and to the CA1 field were compared following injections of the anterograde tracer PHA-L into the entorhinal cortex. The results indicate a degree of heterogeneity within the entorhinal cortex, such that the projection to the dentate gyrus arose mainly from caudomedial regions, while progressively more rostrocaudal parts of the entorhinal cortex projected preferentially to CA1. Cells located at the rostrocaudal extreme gave rise to fibres which terminated solely within the CA1 field.

It is clear that the pattern of projection to CA1, as evinced by Witter *et al.* (1988), differs markedly from that demonstrated in the present study. At the same time, their observations on the nature of the projection to the dentate gyrus are also at variance with those from other reports concerning this pathway, most notably those of Ruth *et al.* (1982, 1988), in which the projection is seen to arise from cells located across the rostrocaudal and mediolateral extents of the entorhinal cortex. Another curious discrepancy in the report of Witter *et al.* (1988) lies in the lack of anterograde labelling in the CA3 field, which has been widely recognised as a major recipient of fibres from the entorhinal cortex (Blackstad 1956; Steward 1976; Steward and Scoville 1976; Witter 1989). Given the quoted similarity in the patterns of projection from the entorhinal cortex to the dentate gyrus and to the CA3 field (Witter *et al.* 1989; Tamamaki and Nojyo 1991b), one would expect a distribution of labelling in the stratum moleculare of CA3 similar to that noted in the molecular layer of the dentate gyrus.

This is not to say that the present study is devoid of limitations. Since the issue of "false" labelling as a result of damage to fibres of passage (a problem which

presumably is also encountered by Witter *et al.* 1988) has already been dealt with, the main concern revolves around the placement of injections. In the experiment, emphasis was placed on ensuring the localization of the injection site within the CA1 field, and as a result of this it was conceded that the primary region of termination within CA1 of entorhinal fibres, namely the stratum moleculare, may not necessarily be included within the uptake site of the injection, which could lead to a reduced estimation of the projection. Even with this caveat in mind, the consistency in labelling across injections, both in terms of the number of projection cells and in their distribution within the posterior cerebral cortex nevertheless remains highly suggestive of separate projection to CA1. One possibility is that there exists a specific projection from the perirhinal cortex, the axons of which terminate in the stratum radiatum (and possibly the stratum oriens) of CA1. This projection would therefore be considered as a separate entity to the projection to CA1 from the entorhinal cortex, which is more extensive and displays topographical organization across the septotemporal length of CA1 (Steward 1976; Steward and Scoville 1976; Witter *et al.* 1988). Given the absence of labelling within the entorhinal cortex following injections into the stratum radiatum of CA1, it might be assumed that the axons of the entorhinal-CA1 pathway terminate specifically in the stratum moleculare of CA1 and were thus not included within the injection sites.

### **3.3. Implications for the transfer of information to the hippocampus**

Several studies in the rat have demonstrated that the lateral part of the entorhinal cortex is the recipient of different inputs from the remainder of the entorhinal cortex. For example, the agranular insular and retrosplenial cortices have been shown to project preferentially to the ventral bank of the rhinal fissure and to

adjacent parts of the entorhinal cortex (Deacon *et al.* 1983; Markowitsch and Guldin 1983), while inputs from temporal and medial prefrontal cortices terminate specifically in the perirhinal cortex and the adjacent parts of the entorhinal cortex (Deacon *et al.* 1983; Reep *et al.* 1987). Furthermore, the projection to the entorhinal cortex from the dorsolateral region of the frontal lobe is directed at its lateral portion.

In summary, the specific innervation to the CA1 field from cells in the perirhinal cortex and in the adjacent dorsolateral part of the entorhinal cortex may serve to relay selective information to that region which might manifest itself as a difference in the behavioural and functional correlates of pyramidal cell activity in the CA1 and CA3 fields, given that cells in the latter field are not privy to this information. This contrasts strongly with the projections from the entorhinal cortex to the dentate gyrus and to CA3: the fact that these two fields appear to "share" the incoming information serves instead to question anew the functional significance of the dentate gyrus. This observation is of additional interest in the light of the electrophysiological studies of McNaughton *et al.* (1989), the results of which suggest that the direct entorhinal-CA3 pathway is sufficient to maintain place field activity in CA3, in spite of the removal of the disynaptic entorhinal-dentate-CA3 circuit following selective colchicine-induced destruction of the dentate gyrus. By demonstrating the size and distribution of the entorhinal-CA3 projection, the results of this experiment also refute the notion of the dentate gyrus as a central, indispensable link in the pattern of information processing, as depicted in the concept of the trisynaptic circuit. The importance of the direct projections from the entorhinal cortex to the CA3 and CA1 fields in future models of intrinsic hippocampal connectivity remains to be seen.

1. Alonso, A. and C. Kohler. 1984. A study of the reciprocal connections between the septum and the entorhinal area using anterograde and retrograde axonal transport methods in the rat brain. *J. Comp. Neurol.* 225:327-343.
2. Altman, J. 1982. Morphological development of the rat cerebellum and some of its mechanisms. In *The Cerebellum - New Vistas*. S. Palay and V. Chan-Palay, editors. Springer, Berlin. 8-49.
3. Amaral, D.G. 1978. A Golgi study of cell types in the hilar region of the hippocampus in the rat. *J. Comp. Neurol.* 182:851-914.
4. Amaral, D.G., W. M. Cowan, and R. Insausti. 1987. The entorhinal cortex of the monkey. 1. Cytoarchitectonic organization. *J. Comp. Neurol.* 264:326-355.
5. Amaral, D.G. and J. A. Dent. 1981. Development of the mossy fibres of the dentate gyrus: I. A light and electron microscopic study of the mossy fibres and their expansions. *J. Comp. Neurol.* 195:51-86.
6. Amaral, D.G., C. Dolorfo, and P. Alvarez-Royo. 1991. Organization of CA1 projections to the subiculum: a PHA-L analysis in the rat. *Hippocampus* 1:415-436.
7. Amaral, D.G., R. Insausti, and W. M. Cowan. 1984. The commissural connections of the monkey hippocampal formation. *J. Comp. Neurol.* 224:307-336.
8. Amaral, D.G., N. Ishizuka, and B. Claiborne. 1990. Neurons, numbers and the

hippocampal network. In *Progress in Brain Research*, Vol.83. J. Storm-Mathisen, J. Zimmer, and O. P. Ottersen, editors. Elsevier Science B.V. (Biomedical Division),

9. Amaral, D.G. and J. Kurz. 1985. An analysis of the origins of the cholinergic and noncholinergic septal projections to the hippocampal formation of the rat. *J. Comp. Neurol.* 240:37-59.

10. Amaral, D.G. and M. P. Witter. 1989. The three-dimensional organization of the hippocampal formation: a review of anatomical data. *Neuroscience* 31 (3):571-591.

11. Andersen, P., T. V. P. Bliss, and K. K. Skrede. 1971. Lamellar organization of hippocampal excitatory pathways. *Exp. Brain Res.* 13:222-238.

12. Andersen, P., J. C. Eccles, and Y. Loynning. 1964. Location of postsynaptic inhibitory synapses on hippocampal pyramids. *J. Neurophysiol.* 27:592-607.

13. Andreasen, M., J. D. C. Lambert, and M. S. Jensen. 1989. Effects of new non-N-methyl-D-aspartate antagonists on synaptic transmission in the in vitro rat hippocampus. *J. Physiol.* 414:317-336.

14. Angevine, J.B. 1965. Time of neuron origin in the hippocampal region, an autoradiographic study in the mouse. *Exp. Neurol. Suppl.* 2:1-70.

15. Assaf, S.Y., V. Crunelli, and J. S. Kelley. 1981. Action of 5-hydroxytryptamine on granule cells in the rat hippocampal slice. *J. Physiol. (Paris)* 77:377-380.

16. Azmitia, E.C. 1978. The serotonin-producing neurons in the midbrain median and dorsal raphe nuclei. In *Handbook of Psychopharmacology: Vol. 9. Chemical Pathways in the Brain*. L. L. Iversen, S. D. Iversen, and S. H. Snyder, editors. Plenum Press, New York. 233-304.

17. Bakst, I., J. H. Morrison, and D. G. Amaral. 1985. The distribution of somatostatin-like immunoreactivity in the monkey hippocampal formation. *J. Comp. Neurol.* 236:423-442.

18. Bates, C.A. and H. P. Killacky. 1984. The emergence of a discretely distributed pattern of corticospinal projecting neurons. *Dev. Brain Res.* 13:265-273.

19. Bayer, S.A. and J. Altman. 1974. Hippocampal development in the rat:cytogenesis and morphogenesis examined with autoradiography and low-level X-irradiation. *J. Comp. Neurol.* 158:55-80.

20. Bayer, S.A. and J. Altman. 1987. Directions in neurogenetic gradients and patterns of anatomical connections in the telecephalon. *Prog. Neurobiol.* 29:57-106.

21. Bech, S.G., W. P. Clark, and J. Goldfarb. 1985. Spiperone differentiates multiple 5-hydroxytryptamine responses in rat hippocampal slices in vitro. *Eur. J. Pharmacol.* 116:195-197.

22. Beckstead, R.M. 1978. Afferent connections of the entorhinal area in the rat as

- demonstrated by retrograde cell-labelling with horseradish peroxidase. *Brain Res.* 152:249-264.
23. Bilkey, D.K. and G. V. Goddard. 1987. Septohippocampal and commissural pathways antagonistically control inhibitory interneurons in the dentate gyrus. *Brain Res.* 405:320-325.
24. Bilkey, D.K. and P. A. Schwartzkroin. 1990. Variation in electrophysiology and morphology of hippocampal CA3 pyramidal cells. *Brain Res.* 514:77-83.
25. Blackstad, T.W. 1956. Commissural connections of the hippocampal region in the rat, with special reference to their mode of termination. *J. Comp. Neurol.* 105:417.
26. Blackstad, T.W., K. Brink, J. Hem, and B. Jeune. 1970. Distribution of hippocampal mossy fibres in the rat. An experimental study with silver impregnation methods. *J. Comp. Neurol.* 138:433-450.
27. Blackstad, T.W., K. Fuxe, and T. Hokfelt. 1967. Noradrenaline nerve terminals in the hippocampal region of the rat and guinea pig. *Z. Zellforsch.* 78:463-473.
28. Bolam, J.P. and Y. Smith. 1990. The GABA and substance P input to dopaminergic neurones in the substantia nigra of the rat. *Brain Res.* 529:57-78.
29. Boss, B.D., G. M. Peterson, and W. M. Cowan. 1985. On the number of neurons in the dentate gyrus of the rat. *Brain Res.* 338:144-150.

30. Brashear, H.R., L. Zaborsky, and L. Heimer. 1986. Distribution of GABAergic and cholinergic neurons in the rat diagonal band. *Neuroscience* 17:439-451.
31. Brodmann, K. 1909. Vergleichende Lokalisationslehre der Grosshirnrinde in ihren Prinzipien dargestellt auf Grund des Zellenbaues. J.A.Barth, Leipzig.
32. Buzsaki, G. 1984. Feed-forward inhibition in the hippocampal formation. *Prog. Neurobiol.* 22:131-153.
33. Buzsaki, G. and E. Eidelberg. 1981. Commissural projection to the dentate gyrus of the rat: evidence for feedforward inhibition. *Brain Res.* 230:346-350.
34. Cecetto, D.F. and C. B. Saper. 1987. Evidence for a viscerotopic sensory representation in the cortex and thalamus in the rat. *J. Comp. Neurol.* 262:27-45.
35. Chavkin, C., W. J. Shoemaker, J. F. McGinty, A. Bayon, and F. E. Bloom. 1985. Characterization of the prodynorphin and proenkephalin neuropeptide system in rat hippocampus. *J. Neurosci.* 5:808-816.
36. Christian, E.P. and F. E. Dudek. 1988. Electrophysiological evidence from glutamate microapplications for local excitatory circuits in the CA1 area of rat hippocampal slices. *J. Neurophysiol.* 59 (1):110-123.
37. Chronister, R.B. and J. F. DeFrance. 1979. Organization of projection neurons of the

hippocampus. *Exp. Neurol.* 66:502-523.

38. Claiborne, B.J., D. G. Amaral, and W. M. Cowan. 1986. A light and electron microscopic analysis of the mossy fibers of the rat dentate gyrus. *J. Comp. Neurol.* 246:435-458.

39. Collier, T.J. and A. Routtenberg. 1977. Entorhinal cortex: Catecholamine fluorescence and Nissl staining of identical Vibratome sections. *Brain Res.* 128:354-360.

40. Collingridge, G.L., S. J. Kehl, and H. McLennan. 1983. Excitatory amino acids in synaptic transmission in the Schaffer collateral-commissural pathway of the rat hippocampus. *J. Physiol.* 334:33-46.

41. Conde, F. 1987. Further studies on the use of the fluorescent tracers Fast Blue and Diamidino Yellow: effective uptake area and cellular storage sites. *J. Neurosci. Meth.* 21:31-43.

42. Conrad, L.C.A., C. M. Leonard, and D. W. Pfaff. 1974. Connections of the median and dorsal raphe nuclei in the rat: an autoradiographic and degeneration study. *J. Comp. Neurol.* 156:179-206.

43. Cotman, C.W., J. A. Flatman, A. H. Ganong, and M. N. Perkins. 1986. Effects of excitatory amino acids antagonists on evoked and spontaneous excitatory potentials in guinea-pig hippocampus. *J. Physiol.* 378:403-415.

44. Cragg, B.G. and L. H. Hamlyn. 1957. Some commissural and septal connections of the hippocampus in the rabbit. A combined histological and electrical study. *J. Physiol.* 133:460-485.
45. Crawford, I.L. and J. D. Connor. 1972. Localization and release of glutamic acid in relation to the hippocampal mossy fibre pathway. *Nature* 244:442-443.
46. Dahl, D., W. H. Bailey, and J. Winson. 1983. Effect of norepinephrine depletion of hippocampus on neuronal transmission from perforant pathway through dentate gyrus. *J. Neurophysiol.* 49:123-133.
47. Daitz, H.M. and T. P. S. Powell. 1954. Studies of the connexions of the fornix system. *J. Neurol. Neurosurg. Psychiat.* 17:75-82.
48. Davies, S. and C. Kohler. 1985. The substance P innervation of the rat hippocampal region. *Anat. Embryol.* 173:45-52.
49. Deacon, T.W., H. Eichenbaum, P. Rosenberg, and K. W. Eckmann. 1983. Afferent connections of the perirhinal cortex in the rat. *J. Comp. Neurol.* 220:168-190.
50. Deadwyler, S.A., J. R. West, C. W. Cotman, and G. S. Lynch. 1974. A neurophysiological analysis of the commissural projection to the dentate gyrus of the rat. *J. Neurophysiol.* 38:167-184.
51. DeFrance, J.F., S. T. Kitai, and T. Shimono. 1973. Electrophysiological analysis of

the hippocampal-septal projections. I. Response and topographical characteristics. *Exp.*

*Brain Res.* 17:447-462.

52. DeFrance, J.F. and H. Yoshihara. 1975. Fimbria input to the nucleus accumbens septi. *Brain Res.* 90:159-163.

53. Desmond, N.L. and W. B. Levy. 1982. A quantitative anatomical study of the granule cell dendritic fields of the rat dentate gyrus using a novel probabilistic method. *J. Comp. Neurol.* 212:131-145.

54. Donovan, M.K. and J. M. Wyss. 1983. Evidence for some collateralization between cortical and diencephalic efferent axons of the rat subicular cortex. *Brain Res.* 259:181-192.

55. Finch, D.M., E. L. Derian, and T. L. Babb. 1983. Demonstration of axonal projections of neurons in the rat hippocampus and subiculum by intracellular injection of HRP. *Brain Res.* 271:201-216.

56. Finch, D.M., E. E. Wong, E. L. Derian, and T. L. Babb. 1986. Neurophysiology of limbic system pathways in the rat: projections from the subicular complex and hippocampus to the entorhinal cortex. *Brain Res.* 397:205-213.

57. Frotscher, M. 1985. Mossy fibres form synapses with identified pyramidal basket cells in the CA3 region of the guinea pig hippocampus: a combined Golgi-electron microscope study. *J. Neurocytol.* 14:245-259.

58. Frotscher, M., C. S. Leranth, K. Lubbers, and W. H. Oertel. 1984. Commissural afferents innervate glutamate decarboxylase immunoreactive non-pyramidal neurons in the guinea pig hippocampus. *Neurosci. Lett.* 46:137-143.

59. Fuxe, K. 1965. Evidence for the existence of monoamine neurons in the central nervous system. IV. The distribution of monoamine nerve terminals in the central nervous system. *Acta Physiol. Scand.* 64:37-85.

60. Gaarskjaer, F.B. 1978. Organization of the mossy fibre system of the rat studied in extended hippocampi. I. Terminal area related to number of granule and pyramidal cells. *J. Comp. Neurol.* 178:49-72.

61. Gaarskjaer, F.B. 1978. Organization of the mossy fibre system of the rat studied in extended hippocampi. II. Experimental analysis of fibre distribution with silver impregnation methods. *J. Comp. Neurol.* 178:73-89.

62. Gaarskjaer, F.B. 1981. The hippocampal mossy fibre system of the rat studied with retrograde tracing techniques. Correlation between topographic organization and neurogenetic gradients. *J. Comp. Neurol.* 203:717-735.

63. Gaarskjaer, F.B. 1986. The organization and development of the hippocampal mossy fiber system. *Brain Res. Rev.* 11:335-357.

64. Gage, F.H., A. Bjorklund, U. Stenevi, S. B. Dunnett, and P. A. T. Kelly. 1984.

Intrahippocampal septal grafts ameliorate learning impairments in aged rats. *Science* 225:533-536.

65. Gall, C., L. M. Berry, and L. A. Hodgson. 1986. Cholecystinin in the mouse hippocampus: localization in the mossy fiber and dentate commissural systems. *Exp. Brain Res.* 62:431-437.

66. Gall, C., N. Brecha, K-I. Chang, and H. J. Karten. 1984. Ontogeny of enkephalin-like immunoreactivity in the rat hippocampus. *Neuroscience* 11:359-380.

67. Gall, C., N. Brecha, H. J. Karten, and K-I. Chang. 1981. Localization of enkephalin-like immunoreactivity to identified axonal and neuronal populations of the rat hippocampus. *J. Comp. Neurol.* 198:225-250.

68. Germroth, P., W. K. Schwerdtfeger, and E. H. Buhl. 1989. Morphology of identified entorhinal neurons projecting to the hippocampus: a light microscopical study combining retrograde tracing and intracellular injection. *Neuroscience* 30:683-691.

69. Germroth, P., W. K. Schwerdtfeger, and E. H. Buhl. 1991. Ultrastructure and aspects of functional organization of pyramidal and nonpyramidal entorhinal projection neurons contributing to the perforant path. *J. Comp. Neurol.* 305:215-231.

70. Golgi, C. 1886. Sulla fina anatomia degli organi centrali sistema nervoso. U. Hoepli, Milano.

71. Gottlieb, D.I. and W. M. Cowan. 1972. Evidence for a temporal factor in the occupation of available synaptic sites during the development of the dentate gyrus. *Brain Res.* 41:452-456.
72. Gottlieb, D.I. and W. M. Cowan. 1973. Autoradiographic studies of the commissural and ipsilateral association connections of the hippocampus and the dentate gyrus. I. The commissural connections. *J. Comp. Neurol.* 149:393-422.
73. Graybiel, A.M. 1983. Compartmental organization of the mammalian striatum. In *Molecular and Cellular Mechanisms Underlying Higher Brain Functions, Progress in Brain Research Vol. 58.* J-P. Changeux, M. Imbert, and F. E. Bloom, editors. Elsevier, Amsterdam. 247-256.
74. Greenwood, R.S., S. Godar, T. A. Reaves, and I. N. Haywood. 1982. Cholecystokinin in hippocampal pathways. *J. Comp. Neurol.* 198:335-350.
75. Groenewegen, H.J. and H. W. M. Steinbusch. 1984. Serotonergic and non-serotonergic projections from the interpeduncular nucleus to the ventral hippocampus in the rat. *Neurosci. Lett.* 51:19-24.
76. Haglund, L., L. W. Swanson, and C. Kohler. 1984. The projections of the supramammillary nucleus to the hippocampal formation: an immunohistochemical and anterograde transport study with the lectin PHA-L in the rat. *J. Comp. Neurol.* 229:171-185.

77. Hamlyn, L.H. 1962. The fine structure of the mossy fibre endings in the hippocampus of the rabbit. *J. Anat.* 96:112-120.
78. Haug, F.M.S. 1976. Sulphide silver pattern and cytoarchitectonics of parahippocampal areas in the rat. *Adv. Anat. Embryol. Cell Biol.* 52:1-73.
79. Herkenham, M. 1978. The connections of the nucleus reuniens thalami: evidence for a direct thalamo-hippocampal pathway in the rat. *J. Comp. Neurol.* 177:589-610.
80. Hjorth-Simonsen, A. 1973. Some intrinsic connections of the hippocampus in the rat: an experimental analysis. *J. Comp. Neurol.* 147:145-161.
81. Hjorth-Simonsen, A. and B. Jeune. 1972. Origin and termination of the hippocampal perforant path in the rat studied by silver impregnation. *J. Comp. Neurol.* 144:215-232.
82. Hjorth-Simonsen, A. and S. Laurberg. 1977. Commissural connections of the dentate area of the rat. *J. Comp. Neurol.* 174:591-606.
83. Hjorth-Simonsen, A. and J. Zimmer. 1975. Crossed pathways from the entorhinal area to the fascia dentata. *J. Comp. Neurol.* 161:57-70.
84. Hokfelt, T., A. Ljungdahl, K. Fuxe, and O. Johansson. 1974. Pharmacohistochemical evidence of the existence of dopamine nerve terminals in the limbic cortex. *Eur. J. Pharmacol.* 25:108-112.

85. Houser, C.R., G. D. Crawford, R. P. Barber, P. M. Salvaterra, and J. E. Vaughn. 1983. Organization and morphological characteristics of cholinergic neurons: An immunocytochemical study with a monoclonal antibody to choline acetyltransferase. *Brain Res.* 226:97-119.
86. Innis, R.B., F. M. A. Correa, G. R. Uhl, B. Schneider, and S. H. Snyder. 1979. Cholecystokinin octapeptide immunoreactivity. Histochemical localization in rat brain. *Proc. Natl. Acad. Sci. USA* 76:521-525.
87. Innocenti, G.M. 1981. Growth and reshaping of axons in the establishment of visual callosal connections. *Science* 212:824-827.
88. Insausti, R., D. G. Amaral, and W. M. Cowan. 1987. The entorhinal cortex of the monkey. 3. Subcortical afferents. In . 396-408.
89. Ishizuka, N., J. Weber, and D. G. Amaral. 1990. Organization of intrahippocampal projections originating from CA3 pyramidal cells in the rat. *J. Comp. Neurol.* 295:580-623.
90. Izzo, P.N. 1991. A note on the use of biocytin in anterograde tracing studies in the central nervous system: application at both light and electron microscopic level. *J. Neurosci. Meth.* 36:155-166.
91. Jones, E.G. and T. P. S. Powell. 1970. An anatomical study of converging sensory pathways within the cerebral cortex of the monkey. *Brain* 3:793-820.

92. Kandel, E.R. and W. A. Spencer. 1961. Electrophysiology of hippocampal neurons. II. After-potentials and repetitive firing. *J. Neurophysiol.* 24:243-259.
93. Katz, L.C., A. Burkhalter, and W. J. Dreyer. 1984. Fluorescent latex microspheres as a retrograde neuronal marker for in vivo and in vitro studies of visual cortex. *Nature* 310:498-500.
94. Kelley, A.E. and V. B. Domesick. 1982. The distribution of the projections from the hippocampal formation to the nucleus accumbens in the rat: an anterograde and retrograde HRP study. *Neuroscience* 7:2321-2335.
95. King, M.A., P. M. Louis, B. E. Hunter, and D. W. Walker. 1989. Biocytin: a versatile anterograde neuroanatomical tract-tracing alternative. *Brain Res.* 497:361-367.
96. Kjarheim, A. and T. W. Blackstad. 1961. Special axo-dendritic synapses in the hippocampal cortex: electron and light microscopic studies on the layer of mossy fibres. *J. Comp. Neurol.* 117:133-159.
97. Knowles, W.D. and P. A. Schwartzkroin. 1981. Local circuit synaptic interactions in hippocampal brain slices. *J. Neurosci.* 1:318-322.
98. Koch, E. and T. Poggio. 1982. A theoretical analysis of electrical properties of spines. *Proc. R. Soc.* 218:455-477.

99. Koelliker, A. 1896. Handbuch der Gewebelehre des Menschen. Vol.2 Nervensystem des Menschen und der Tiere. Wilhelm Engelman, Leipzig.
100. Kohler, C. 1985. Intrinsic projections of the retrohippocampal region in the rat brain. 1. The subicular complex. *J. Comp. Neurol.* 236:504-522.
101. Kohler, C. 1986. Intrinsic connections of the retrohippocampal region in the rat brain. II. The medial entorhinal area. *J. Comp. Neurol.* 246:149-169.
102. Kohler, C. 1988. Intrinsic connections of the retrohippocampal region in the rat brain. III. The lateral entorhinal area. *J. Comp. Neurol.* 271:208-228.
103. Kohler, C. and V. Chan-Palay. 1982. Somatostatin-like immunoreactive neurons in the hippocampus: An immunocytochemical study in the rat. *Neurosci. Lett.* 34:259-264.
104. Kohler, C., V. Chan-Palay, and J-Y. Wu. 1984. Septal neurons containing glutamic acid decarboxylase immunoreactivity project to the hippocampal region in the rat brain. *Anat. Embryol.* 169:41-44.
105. Kohler, C., L. Eriksson, S. Davies, and V. Chan-Palay. 1986. Neuropeptide Y innervation of the hippocampal region in the rat and monkey brain. *J. Comp. Neurol.* 244:384-400.
106. Kohler, C., M. T. Shipley, B. Srebro, and W. Harkmark. 1978. Some retrohippocampal afferents to the entorhinal cortex. Cells of origin as studied by the

HRP method in the rat and mouse. *Neurosci. Lett.* 10:115-120.

107. Kohler, C. and H. Steinbusch. 1982. Identification of serotonin and non-serotonin-containing neurons of the midbrain raphe projecting to the entorhinal area and the hippocampal formation. A combined immunohistochemical and fluorescent retrograde tracing study in the rat brain. *Neuroscience* 7:951-975.

108. Kohler, C. and H. Steinbusch. 1982. Identification of serotonin and non-serotonin-containing neurons of the midbrain raphe projecting to the entorhinal area and the hippocampal formation. A combined immunohistochemical and fluorescent retrograde tracing study in the rat brain. *Neuroscience* 7:951-975.

109. Kosel, K.C., G. W. Van Hoesen, and D. L. Rosene. 1982. Non-hippocampal cortical projections from the entorhinal cortex in the rat and Rhesus monkey. *Brain Res.* 244:201-213.

110. Krettek, J.E. and J. L. Price. 1977. Projections from the amygdaloid complex and adjacent olfactory structures to the entorhinal cortex and to the subiculum in the rat and cat. *J. Comp. Neurol.* 172:723-752.

111. Krettek, J.E. and J. L. Price. 1978. Amygdaloid projections to subcortical structures within the basal forebrain and the brainstem in the rat and cat. *J. Comp. Neurol.* 178:225-254.

112. Kunkel, D.D., A. Hendrickson, J-Y. Wu, and P. A. Schwartzkroin. 1986. Glutamic

acid decarboxylase (GAD) immunocytochemistry of developing rabbit hippocampus.

*J. Neurosci.* 6:541-552.

113. Laatsch, R.H. and W. M. Cowan. 1966. Electron microscopic studies of the dentate gyrus of the rat. I. Normal structure with special reference to synaptic organization. *J. Comp. Neurol.* 128:359-396.

114. Lacaille, J-C., A. L. Mueller, P. P. Kundel, and P. A. Schwartzkroin. 1987. Local circuit interactions between oriens/alveus interneurons and CA1 pyramidal cells in hippocampal slices: electrophysiology and morphology. *J. Neurosci.* 7:1974-1993.

115. Laurberg, S. 1979. Commissural and intrinsic connections of the rat hippocampus. *J. Comp. Neurol.* 184:685-708.

116. Lebovitz, R.M., M. Dichter, and W. A. Spencer. 1971. Recurrent excitation in the CA3 region of cat hippocampus. *Int. J. Neurosci.* 2:99-108.

117. Lewis, P.R. and C. C. D. Shute. 1967. The cholinergic limbic system: projections to hippocampal formation, medial cortex, nuclei of the ascending cholinergic reticular system, and the subfornical organ and supra-optic crest. *Brain Res.* 90:521-540.

118. Lingenhohl, K. and D. M. Finch. 1991. Morphological characterization of rat entorhinal neurons in vivo: soma-dendritic structure and axonal domains. *Exp. Brain Res.* 84:57-75.

119. Loren, I., P. C. Emson, I. Fahrenkrug, A. Bjorklund, I. Alumets, R. Hakansson, and F. Sundler. 1979. Distribution of vasoactive intestinal peptide in rat and mouse brain. An immunocytochemical study. *Neuroscience* 4:1953-1976.
120. Lorente de No, R. 1933. Studies on the structure of the cerebral cortex. I. The area entorhinalis. *J. Psychol. Neurol.* 45.6:381-438.
121. Lorente de No, R. 1934. Studies on the structure of the cerebral cortex. II. Continuation of the study of the ammonic system. *J. Psychol. Neurol. (Leipzig)* 46:113-177.
122. Loy, R., D. A. Koziell, J. D. Lindsey, and R. Y. Moore. 1980. Noradrenergic innervation of the adult rat hippocampal formation. *J. Comp. Neurol.* 189:699-710.
123. Markowitsch, H.J. and W. O. Guldin. 1983. Heterotopic interhemispheric cortical connections in the rat. *Brain Res. Bull.* 10:805-810.
124. Masukawa, L.M., L. S. Benards, and D. A. Prince. 1982. Variations in electrophysiological properties of hippocampal neurons in different subfields. *Brain Res.* 242:341-344.
125. McGinty, J.F., S. J. Hendrickson, A. Goldstein, L. Terenius, and F. E. Bloom. 1983. Dynorpin is contained within hippocampal mossy fibres: immunohistochemical alterations after kainic acid administration and colchicine-induced neurotoxicity. *Proc. Natl. Acad. Sci. USA* 80:589-593.

126. McKay, R.D.G., S. Hockfield, J. Johansen, I. Thompson, and K. Frederickson. 1983. Surface molecules identify groups of growing axons. *Science* 222:788-794.
127. McNaughton, B.L. 1980. Evidence for two physiologically distinct perforant pathways to the fascia dentata. *Brain Res.* 199:1-19.
128. McNaughton, B.L. 1989. Neuronal mechanisms for spatial computation and information storage. In *Neural connections and mental computations*. L. Nadel, L. A. Cooper, P. Culicover, and R. M. Harnish, editors. MIT Press, Cambridge, Massachusetts. 285-350.
129. McNaughton, B.L., C. A. Barnes, and P. Andersen. 1981. Synaptic efficacy and EPSP summation in granule cells of rat fascia dentata studied in vitro. *J. Neurophysiol.* 46 (5):952-966.
130. McNaughton, B.L., C. A. Barnes, J. Meltzer, and R. J. Sutherland. 1989. Hippocampal granule cells are necessary for normal spatial learning but not for spatially-selective pyramidal cell discharge. *Exp. Brain Res.* 76:485-496.
131. Meibach, R.C. and A. Siegel. 1975. The origin of fornix fibres which project to the mammillary bodies in the rat: a horseradish peroxidase study. *Brain Res.* 88:508-512.
132. Meibach, R.C. and A. Siegel. 1977. Efferent connections of the septal area in the rat: an analysis utilizing retrograde and anterograde transport methods. *Brain Res.* 119:1-20.

133. Meibach, R.C. and A. Siegel. 1977. Efferent connections of the hippocampal formation in the rat. *Brain Res.* 124:197-224.
134. Melander, T., W. A. Staines, T. Hokfelt, A. Rokaeus, F. Eckerstein, P. M. Salvaterra, and B. M. Wainer. 1985. Galanin-like immunoreactivity in cholinergic neurons of the setum-basal forebrain complex projecting to the hippocampus of the rat. *Brain Res.* 360:130-138.
135. Mellgren, S.I. and B. Srebro. 1973. Changes in acetylcholinesterase and distribution of degenerating fibres in the hippocampal region after septal lesions in the rat. *Brain Res.* 52:19-36.
136. Merrill, E.G. and A. Ainsworth. 1972. Glass-coated platinum-plated tungsten microelectrodes. *Med. Biol. Eng. Comput.* 10:662-672.
137. Miles, R. and R. K. S. Wong. 1983. Single neurons can initiate synchronized population discharge in the hippocampus. *Nature* 306:371-373.
138. Miles, R. and R. K. S. Wong. 1984. Unitary inhibitory synaptic potentials in the guinea-pig hippocampus in vitro. *J. Physiol.* 356:97-113.
139. Miles, R. and R. K. S. Wong. 1986. Excitatory synaptic interactions between CA3 neurones in the guinea-pig hippocampus. *J. Physiol.* 373:397-418.

140. Miller, J.P., W. Rall, and J. Rinzel. 1985. Synaptic amplification by active membrane in dendritic spines. *Brain Res.* 325:320-325.
141. Milner, T.A. and D. G. Amaral. 1984. Evidence for a ventral septal projection to the hippocampal formation of the rat. *Exp. Brain Res.* 55:579-585.
142. Milner, T.A., R. Loy, and D. G. Amaral. 1983. An anatomical study of the development of the septo-hippocampal projection in the rat. *Dev. Brain Res.* 8:343-371.
143. Miyakawa, H. and H. Kato. 1986. Active properties of dendritic membrane examined by current source density analysis in hippocampal CA1 pyramidal neurons. *Brain Res.* 399:303-309.
144. Monmaur, P. and M. A. Thomson. 1983. Topographic organization of septal cells innervating the dorsal hippocampal formation of the rat: special reference to both the CA1 and dentate theta generators. *Exp. Neurol.* 82:366-378.
145. Moore, R.Y. and A. E. Halaris. 1975. Hippocampal innervation by serotonin neurons of the midbrain raphe in the rat. *J. Comp. Neurol.* 164:171-184.
146. Morrison, J.H., R. Benoit, P. J. Magistretti, N. Ling, and F. Bloom. 1982. Immunohistochemical distribution of prosomatostatin-related peptides in hippocampus. *Neurosci. Lett.* 34:137-142.
147. Mountcastle, V.B. 1957. Modality and topographic properties of single neurons of

cat's somatic sensory cortex. *J. Neurophysiol.* 20:408-434.

148. Muller, R.U. and J. L. Kubie. 1987. The effects of changes in the environment on the spatial firing of hippocampal complex-spike cells. *J. Neurosci.* 7 (7):1951-1968.

149. Nadler, J.V., K. W. Vaca, W. F. White, G. S. Lynch, and C. W. Cotman. 1976. Aspartate and glutamate as possible transmitters of excitatory hippocampal afferents. *Nature* 260:538-540.

150. Nafstad, P.H.J. 1967. An electron microscopic study on the termination of the perforant path fibres in the hippocampus and the fascia dentata. *Z. Zellforsch.* 76:532-542.

151. Nauta, W.J.H. 1956. An experimental study of the fornix system in the rat. *J. Comp. Neurol.* 104:247-251.

152. O'Keefe, J. 1988. Computations the hippocampus might perform. In *Neural connections and mental computations*. L. Nadel, L. A. Cooper, P. Culicover, and R. M. Harnish, editors. MIT Press, Cambridge, Massachusetts. 225-284.

153. O'Keefe, J. and L. Nadel. 1978. *The hippocampus as a cognitive map*. Clarendon Press, Oxford.

154. O'Keefe, J. and A. Speakman. 1987. Single unit activity in the rat hippocampus during a spatial memory task. *Exp. Brain Res.* 68:1-27.

155. Ottersen, O.P. and J. Storm-Mathisen. 1985. Different neuronal localization of aspartate-like and glutamate-like immunoreactivities in the hippocampus of rat, guinea-pig and Senegalese baboon (*Papio papio*), with a note on the distribution of gamma-aminobutyrate. *Neuroscience* 16:589-606.
156. Pandya, D.N. and B. Seltzer. 1982. Association areas of the cerebral cortex. *Trends Neurosci.* 5:386-392.
157. Pandya, D.N. and E. H. Yeterian. 1984. Architecture and connections of cortical association areas. In *Cerebral Cortex, Association and Auditory Cortices*, Vol. 4. A. Peters and E. G. Jones, editors. Plenum Press, New York. 3-61.
158. Pasquier, D.A. and F. Reinoso-Suarez. 1976. Direct projections from hypothalamus to hippocampus in the rat demonstrated by retrograde transport of horseradish peroxidase. *Brain Res.* 108:165-169.
159. Paxinos, G. and C. Watson. 1986. *The Rat Brain in Stereotaxic Coordinates*. Academic Press, Sydney.
160. Pfenninger, K.H., M. F. Malie-Pfenninger, L. B. Friedman, and P. Simkowitz. 1984. Lectin labelling of sprouting neurons. III. Type-specific glycoconjugates on growth cones of different origin. *Dev. Biol.* 106:97-108.
161. Phillipson, O.T. and A. C. Griffiths. 1985. The topographic order of inputs to the

nucleus accumbens in the rat. *Neuroscience* 16:275-296.

162. Raisman, G. 1966. The connexions of the septum. *Brain* 89:317-348.

163. Raisman, G., W. M. Cowan, and T. P. S. Powell. 1965. The extrinsic afferent, commissural and association fibres of the hippocampus. *Brain* 88:963-995.

164. Raisman, G., W. M. Cowan, and T. P. S. Powell. 1966. An experimental analysis of the efferent projection of the hippocampus. *Brain* 89:83-108.

165. Ramon y Cajal, S. 1893. Estructura del asta de Ammon y fascia dentata. *Ann. Soc. Esp. Hist. Nat.* 22:

166. Ramon y Cajal, S. 1901. Studien uber die Hirnrinde des Menschen. J.A.Barth, Leipzig.

167. Ramon y Cajal, S. 1911. Histologie de Systeme Nerveux de l'Homme et des Vertebres. Maloine, Paris.

168. Reep, R.L., J. V. Corwin, A. Hashimoto, and R. T. Watson. 1987. Efferent connections of the rostral portion of medial agranular cortex in rats. *Brain Res. Bull.* 19:203-221.

169. Reh, T. and K. Kalil. 1982. Development of the pyramidal tract in the hamster. II. An electron microscope study. *J. Comp. Neurol.* 205:77-88.

170. Ribak, C.E. and L. Seress. 1983. Five types of basket cell in the hippocampal dentate gyrus: a combined Golgi and electron microscopic study. *J. Neurocytol.* 12:577-597.
171. Ribak, C.E., L. Seress, and D. G. Amaral. 1985. The development, ultrastructure and synaptic connections of the mossy cells of the dentate gyrus. *J. Neurocytol.* 14:835-857.
172. Richter-Levin, G. and M. Segal. 1988. Serotonin releasers modulate reactivity of the rat hippocampus to afferent stimulation. *Neurosci. Lett.* 94:173-176.
173. Rockland, K.S. and D. N. Pandya. 1979. Laminar origins and terminations of cortical connections of the occipital lobe in the rhesus monkey. *Brain Res.* 179:3-20.
174. Room, P. and H. J. Groenewegen. 1986. Connections of the parahippocampal cortex in the cat. I. Cortical afferents. *J. Comp. Neurol.* 251:451-473.
175. Rose, A.M., T. Hattori, and H. C. Fibiger. 1976. Analysis of the septohippocampal pathway by light and electron microscopic autoradiography. *Brain Res.* 108:170-174.
176. Rose, J.E. and C. N. Woolsey. 1948. Structure and relations of limbic cortex and anterior thalamic nuclei in rabbit and cat. *J. Comp. Neurol.* 89:279-347.
177. Rose, M. 1927. Der Allocortex bei Tier und Mensch. *J. Psychol. Neurol.* 34:1-111.

178. Ruth, R. 1982. Kainic acid lesions of the hippocampus produced iontophoretically: the problem of distant damage. *Exp. Neurol.* 76:508-527.
179. Ruth, R.E., T. J. Collier, and A. Routtenberg. 1988. Topographical relationship between the entorhinal cortex and the septotemporal axis of the dentate gyrus in rats. 2. Cells projecting from lateral entorhinal subdivisions. *J. Comp. Neurol.* 270:506-516.
180. Sandler, R. and A. D. Smith. 1991. Coexistence of GABA and glutamate in mossy fiber terminals of the primate hippocampus: An ultrastructural study. *J. Comp. Neurol.* 303:177-192.
181. Saper, C.B. 1982. Convergence of autonomic and limbic connections in the insular cortex of the rat. *J. Comp. Neurol.* 210:163-173.
182. Saper, C.B. 1984. Organization of cerebral cortical afferent systems in the rat. II. Magnocellular basal nucleus. *J. Comp. Neurol.* 222:313-342.
183. Sayer, R.J., M. J. Friedlander, and S. J. Redman. 1990. The time course and amplitude of EPSPs evoked at synapses between pairs of CA3/CA1 neurons in the hippocampal slice. *J. Neurosci.* 10 (3):826-836.
184. Scatton, B., H. Simon, M. LeMoal, and S. Bischoff. 1980. Origin of dopaminergic innervation of the rat hippocampal formation. *Neurosci. Lett.* 18:125-131.

185. Schaffer, K. 1892. Beitrag zur histologie der ammonshorn formation. *Arch. Mikrosk. Anat.* 39:611-632.
186. Scharfman, H.E. 1991. Dentate hilar cells with dendrites in the molecular layer have lower thresholds for synaptic activation than granule cells. *J. Neurosci.* 11:1660-1674.
187. Scharfman, H.E., D. D. Kunkel, and P. A. Schwartzkroin. 1990. Synaptic connections of dentate granule cells and hilar neurons: results of paired intracellular recordings and intracellular horseradish peroxidase injections. *Neuroscience* 37:693-707.
188. Scharfman, H.E. and P. A. Schwartzkroin. 1988. Electrophysiology of morphologically identified mossy cells recorded in the dentate hilus in guinea pig hippocampal slices. *J. Neurosci.* 8:3812-3821.
189. Schwartzkroin, P.A. and D. D. Kunkel. 1985. Morphology of identified interneurons in the CA1 regions of guinea pig hippocampus. *J. Comp. Neurol.* 232:205-218.
190. Schwartzkroin, P.A. and L. H. Mathers. 1978. Physiological and morphological identification of a nonpyramidal hippocampal cell type. *Brain Res.* 157:1-10.
191. Schwerdtfeger, W.K. and E. Buhl. 1986. Various types of hippocampal non-pyramidal neurons project to the septum and contralateral hippocampus. *Brain Res.* 386:146-154.

192. Scoville, W.B. and B. Milner. 1957. Loss of recent memory after bilateral hippocampal lesions. *J. Neurol. Neurosurg. Psychiat.* 20:11-21.
193. Segal, M. 1979. A potent inhibitory monosynaptic hypothalamo-hippocampal connection. *Brain Res.* 162:137-141.
194. Segal, M. 1980. The action of serotonin in the rat hippocampal slice preparation. *J. Physiol. (Lond. )* 303:423-439.
195. Segal, M. and S. Landis. 1974. Afferents to the hippocampus of the rat studied with the method of retrograde transport of horseradish peroxidase. *Brain Res.* 78:1-15.
196. Seress, L. and C. E. Ribak. 1983. GABAergic cells in the dentate gyrus appear to be local circuit and projection neurons. *Exp. Brain Res.* 50:173-182.
197. Seress, L. and C. E. Ribak. 1984. Direct commissural connections to the basket cells of the hippocampal dentate gyrus: anatomical evidence for feedforward inhibition. *J. Neurocytol.* 13:215-225.
198. Shipley, M.T. 1975. The topographical and laminar organization of the presubiculum's projection to the ipsilateral and contralateral entorhinal cortex in the guinea pig. *J. Comp. Neurol.* 160:127-146.
199. Shu, S., G. Ju, and L. Fan. 1988. The glucose oxidase-DAB-nickel method in

peroxidase histochemistry of the nervous system. *Neurosci. Lett.* 85:169-171.

200. Sloviter, R.S. and G. Nilaver. 1987. Immunocytochemical localization of GABA-, cholecystokinin-, vasoactive intestinal polypeptide and somatostatin-like immunoreactivity in the area dentata and hippocampus of the rat. *J. Comp. Neurol.* 256:42-61.

201. Somogyi, P., A. J. Hodgson, A. D. Smith, M. G. Nunzi, A. Gorio, and J. Y. Wu. 1984. Different populations of GABAergic neurons in the visual cortex and hippocampus of cat contain somatostatin- or cholecystokinin-immunoreactive material. *J. Neurosci.* 4:2590-2603.

202. Sorensen, K.E. 1985. Projections of the entorhinal area to the striatum, nucleus accumbens, and cerebral cortex in the guinea pig. *J. Comp. Neurol.* 238:308-322.

203. Sorensen, K.E. and M. T. Shipley. 1979. Projections from the subiculum to the deep layers of the ipsilateral presubicular and entorhinal cortices in the guinea pig. *J. Comp. Neurol.* 188:313-334.

204. Sorensen, K.E. and M. P. Witter. 1983. Entorhinal efferents reach the caudato-putamen. *Neurosci. Lett.* 35:259-264.

205. Soriano, E., A. Cobas, C. Lopez, and P. Berbel. 1983. Morphology of mossy fibre collaterals in the hilus of the rat. *Neurosci. Lett. Supplement* 14:S352.

206. Stanfield, B.B. and W. M. Cowan. 1984. An EM autoradiographic study of the hypothalamo-hippocampal projection. *Brain Res.* 309:299-307.
207. Stanfield, B.B., D. D. M. O'Leary, and C. Fricks. 1982. Selective collateral elimination in early postnatal development restricts cortical distribution of rat pyramidal tract neurons. *Nature* 298:371-373.
208. Stengaard-Pedersen, K., K. Fredens, and L-I. Larsson. 1983. Comparative localization of enkephalin and cholecystokinin immunoreactivities and heavy metals in the hippocampus. *Brain Res.* 273:81-96.
209. Steward, O. 1976. Topographic organization of the projections from the entorhinal area to the hippocampal formation of the rat. *J. Comp. Neurol.* 167:285-314.
210. Steward, O. and S. A. Scoville. 1976. Cells of origin of entorhinal cortical afferents to the hippocampus and fascia dentata of the rat. *J. Comp. Neurol.* 169:347-370.
211. Storm-Mathisen, J. 1977. Glutamic acid and excitatory nerve endings: reduction of glutamic acid uptake after axotomy. *Brain Res.* 120:379-386.
212. Storm-Mathisen, J., A. K. Leknes, A. T. Bore, J. L. Vaaland, P. Edminson, F. M. S. Haug, and O. P. Ottersen. 1983. First visualisation of glutamate and GABA in neurones by immunocytochemistry. *Nature* 301:517-520.
213. Storm-Mathisen, J. and M. W. Opsahl. 1978. Aspartate and/or glutamate may be

- transmitters in hippocampal efferents to septum and hypothalamus. *Neurosci. Lett.* 9:65-70.
214. Suzuki, W.A. and D. G. Amaral. 1990. Cortical inputs to the CA1 field of the monkey hippocampus originate from the perirhinal and parahippocampal cortex but not from area TE. *Neurosci. Lett.* 115: 43-48.
215. Swanson, L.W. 1981. A direct projection from Ammon's horn to prefrontal cortex in the rat. *Brain Res.* 217:150-154.
216. Swanson, L.W. 1983. Neuropeptides - new vistas on synaptic transmission. *Trends Neurosci.* 6:294-295.
217. Swanson, L.W. and W. M. Cowan. 1976. Autoradiographic studies of the development and connections of the septal area in the rat. In *The Septal Nuclei: Advances in Behavioral Biology*, Vol. 20. J. F. DeFrance, editor. Plenum Press, New York. 37-64.
218. Swanson, L.W. and W. M. Cowan. 1977. An autoradiographic study of the organization of the efferent connections of the hippocampal formation in the rat. *J. Comp. Neurol.* 172:49-84.
219. Swanson, L.W. and W. M. Cowan. 1979. The connections of the septal region in the rat. *J. Comp. Neurol.* 186:621-655.

220. Swanson, L.W. and B. K. Hartman. 1975. The central adrenergic system. An immunofluorescence study of the location of cell bodies and their efferent connections in the rat utilizing dopamine-B-hydroxylase as a marker. *J. Comp. Neurol.* 163:467-506.
221. Swanson, L.W. and C. Kohler. 1986. Anatomical evidence for direct projections from the entorhinal area to the entire cortical mantle in the rat. *J. Neurosci.* 6:3010-3023.
222. Swanson, L.W., P. E. Sawchenko, and W. M. Cowan. 1980. Evidence for collateral projections by neurons in Ammon's horn, the dentate gyrus and the subiculum: a multiple retrograde labeling study in the rat. *J. Neurosci.* 1(5):548-559.
223. Swanson, L.W., P. E. Sawchenko, and W. M. Cowan. 1981. Evidence for collateral projections by neurons in Ammon's horn, the dentate gyrus, and the subiculum: a multiple retrograde labeling study in the rat. *J. Neurosci.* 1:548-559.
224. Swanson, L.W., J. M. Wyss, and W. M. Cowan. 1978. An autoradiographic study of the organization of intrahippocampal association pathways in the rat. *J. Comp. Neurol.* 181:681-715.
225. Tamamaki, N., K. Abe, and Y. Nojyo. 1987. Columnar organization in the subiculum formed by axon branches originating from single CA1 pyramidal neurons in the rat hippocampus. *Brain Res.* 412:156-160.
226. Tamamaki, N. and Y. Nojyo. 1990. Disposition of the slab-like modules formed by axon branches originating from single CA1 pyramidal neurons in the rat hippocampus.

*J. Comp. Neurol.* 291:509-519.

227. Tamamaki, N. and Y. Nojyo. 1991. Crossing fiber arrays in the rat hippocampus as demonstrated by three-dimensional reconstruction. *J. Comp. Neurol.* 303:435-442.

228. Taube, J.S., R. U. Muller, and J. B. Ranck. 1990. Head-direction cells recorded from the postsubiculum in freely moving rats. II. Effects of environmental manipulations. *J. Neurosci.* 10 (2):436-447.

229. Taube, J.S., R. U. Muller, and J. B. (Jr.) Ranck. 1990. Head-direction cells recorded from the postsubiculum in freely moving rats. I. Description and quantitative analysis. *J. Neurosci.* 10(2):420-435.

230. Thompson, L.T. and P. J. Best. 1989. Place cells and silent cells in the hippocampus of freely- behaving rats. *J. Neurosci.* 9:2382-2390.

231. Thomson, A.M. and S. Radpour. 1991. Excitatory connections between CA1 pyramidal cells revealed by spike triggered averaging in slices of rat hippocampus are partially NMDA receptor mediated. *Eur. J. Neurosci.* 3:587.

232. Totterdell, S. and A. D. Smith. 1986. Cholecystokinin-immunoreactive boutons in synaptic contact with hippocampal pyramidal neurons that project to the nucleus accumbens. *Neuroscience* 19:181-192.

233. Traub, R.D. and R. Llinas. 1979. Hippocampal pyramidal cells: significance of

- dendritic ionic conductances for neuronal function and epileptogenesis. *J. Neurophysiol.* 42:476-496.
234. Turner, D.A. 1984. Conductance transients onto dendritic spines in a segmental cable model of hippocampal neurons. *Biophys. J.* 46:85-96.
235. Turner, D.A. 1988. Waveform and amplitude characteristics of evoked responses to dendritic stimulation of CA1 guinea-pig pyramidal cells. *J. Physiol. (Lond. )* 395:419-439.
236. Van Groen, T. and F. H. Lopes da Silva. 1986. The organization of the reciprocal connections between the subiculum and the entorhinal cortex in the cat. II. An electrophysiological study. *J. Comp. Neurol.* 251:111-120.
237. Van Groen, T., F. J. van Haren, M. P. Witter, and H. J. Groenewegen. 1986. The organization of the reciprocal connections between the subiculum and the entorhinal cortex in the cat: I. A neuroanatomical tracing study. *J. Comp. Neurol.* 250:485-497.
238. Van Groen, T. and J. M. Wyss. 1988. Species differences in hippocampal commissural connections: Studies in rat, guinea pig, rabbit and cat. *J. Comp. Neurol.* 267:322-334.
239. Van Groen, T. and J. M. Wyss. 1990. Extrinsic projections from area CA1 of the rat hippocampus: olfactory, cortical, subcortical and bilateral hippocampal formation projections. *J. Comp. Neurol.* 302:515-528.

240. Van Hoesen, G.W. 1981. The differential distribution, diversity and sprouting of cortical projections to the amygdala in the Rhesus monkey. In *The Amygdaloid Complex*. Y. Ben-Ari, editor. Elsevier/North-Holland Biomedical Press, Amsterdam.
241. Van Hoesen, G.W. and D. N. Pandya. 1975. Some connections of the entorhinal (area 28) and perirhinal (area 35) cortices of the Rhesus monkey. I. Temporal lobe afferents. *Brain Res.* 95:1-24.
242. Vogt, B.A. and M. W. Miller. 1983. Cortical connections between rat cingulate cortex and visual, motor, and postsubicular cortices. *J. Comp. Neurol.* 216:192-210.
243. Vogt, C. and O. Vogt. 1919. Allgemeinere Ergebnisse unserer Hirnforschung. *J. Psychol. u. Neur.* 25:
244. Walaas, I. and F. Fonnum. 1980. Biochemical evidence for glutamate as a transmitter in hippocampal efferents to the basal forebrain and hypothalamus in the rat brain. *Neuroscience* 5:1691-1698.
245. West, M.J. and A. H. Andersen. 1980. An allometric study of the area dentata in the rat and mouse. *Brain Res. Rev.* 2:317-348.
246. Wilhite, B.L., T. J. Teyler, and C. Hendricks. 1986. Functional relations of the rodent claustral-entorhinal-hippocampal system. *Brain Res.* 365:54-60.

247. Winson, J. and C. Abzug. 1977. Gating of neuronal transmission in the hippocampus: efficacy of transmission varies with behavioral state. *Science* 196:1223-1225.
248. Winson, J. and C. Abzug. 1978. Dependence upon behaviour of neuronal transmission from perforant pathway through entorhinal cortex. *Brain Res.* 147:422-427.
249. Wise, S.P., E. A. Murray, and J. D. Coulter. 1979. Somatotopic organization of corticospinal and corticotrigeminal neurons in the rat. *Neuroscience* 4:65-78.
250. Witter, M.P. and D. G. Amaral. 1991. Entorhinal cortex of the monkey: V. Projections to the dentate gyrus, hippocampus and subicular complex. *J. Comp. Neurol.* 307:437-459.
251. Witter, M.P., D. G. Amaral, and G. W. Van Hoesen. 1989. The entorhinal-dentate projection in the macaque monkey: topographical organization along the longitudinal axis of the hippocampus. *J. Neurosci.* 9:216-228.
252. Witter, M.P. and H. J. Groenewegen. 1984. Laminar origin and septotemporal distribution of entorhinal and perirhinal projections to the hippocampus in the cat. *J. Comp. Neurol.* 224:371-385.
253. Witter, M.P. and H. J. Groenewegen. 1990. The subiculum: cytoarchitectonically a simple structure, but hodologically complex. In *Understanding the brain through the hippocampus*. J. Storm-Mathisen, J. Zimmer, and O. P. Ottersen, editors. Elsevier,

Amsterdam. 47-58.

254. Witter, M.P., H. J. Groenewegen, F. H. Lopes da Silva, and A. H. M. Lohman. 1989. Functional organization of the extrinsic and intrinsic circuitry of the parahippocampal region. *Prog. Neurobiol.* 33(3):161-253.

255. Witter, M.P., R. Holtrop, and A. A. Van de Loosdrecht. 1988. Direct projections from the periallocortical subicular complex to the fascia dentata in the rat. An anatomical tracing study using Phaseolus vulgaris-leucoagglutinin. *Neurosci. Res. Comm.* 2:61-68.

256. Witter, M.P., P. Room, H. J. Groenewegen, and A. H. M. Lohman. 1986. Connections of the parahippocampal cortex in the cat. V. Intrinsic connections: comments on input/output connections with the hippocampus. *J. Comp. Neurol.* 252:78-94.

257. Wong, R.K.S. and D. A. Prince. 1979. Dendritic mechanisms underlying penicillin induced epileptiform activity. *Science* 204:1228-1230.

258. Wyss, J.M. 1981. An autoradiographic study of the efferent connections of the entorhinal cortex in the rat. *J. Comp. Neurol.* 199:495-512.

259. Wyss, J.M., L. W. Swanson, and W. M. Cowan. 1979. A study of subcortical afferents to the hippocampal formation in the rat. *Neuroscience* 4:463-476.

260. Yamamoto, C. 1972. Activation of hippocampal neurons by mossy fibre stimulation in thin brain sections in vitro. *Exp. Brain Res.* 14:423-435.
261. Yanagihara, M., K. Niimi, and K. Ono. 1987. Thalamic projections to the hippocampal and entorhinal areas in the cat. *J. Comp. Neurol.* 266:122-141.
262. Yang, C.R. and G. J. Mogensen. 1984. Electrophysiological responses of neurones in the nucleus accumbens to hippocampal stimulation and the attenuation of the excitatory responses by the mesolimbic dopaminergic system. *Brain Res.* 324:69-84.
263. Yang, C.R. and G. J. Mogensen. 1985. An electrophysiological study of the neural projections from the hippocampus to the ventral pallidum and the subpallidal areas by way of the nucleus accumbens. *Neuroscience* 15:1015-1024.
264. Yeckel, M.F. and T. W. Berger. 1990. Feedforward excitation of the hippocampus by afferents from the entorhinal cortex: Redefinition of the role of the trisynaptic pathway. *Proc. Natl. Acad. Sci. USA* 87:5832-5836.
265. Zipp, F., R. Nitsch, E. Soriano, and M. Frotscher. 1989. Entorhinal fibres form synaptic contacts on parvalbumin-immunoreactive neurons in the rat fascia dentata. *Brain Res.* 495:161-166.